UNIVERSITY OF SOUTHAMPTON

INSTITUTE OF SOUND AND VIBRATION RESEARCH
FACULTY OF ENGINEERING, SCIENCE AND MATHEMATICS

NONLINEAR TRANSIENT STRUCTURAL RESPONSE ANALYSIS

by

Mirko Schaedlich

Thesis submitted for the degree of
Doctor of Philosophy

- January 2007 -

UNIVERSITY OF SOUTHAMPTON

ABSTRACT

FACULTY OF ENGINEERING, SCIENCE AND MATHEMATICS
INSTITUTE OF SOUND AND VIBRATION RESEARCH

DOCTOR OF PHILOSOPHY

NONLINEAR TRANSIENT STRUCTURAL RESPONSE ANALYSIS

by Mirko Schaedlich

This work presents various aspect of the analysis of nonlinear dynamical single-degree-of-freedom (SDOF) systems possessing two example polynomial-type restoring forces. The first is a lesser known purely nonlinear, single-term expression containing both the signum function and absolute-value function, thus possessing the property of becoming non-Lipschizian at specific system equilibrium points if the real but positive polynomial exponent is set to values smaller than one. The second restoring force corresponds to the well-known Duffing-type. For both autonomous conservative systems extreme values of the response and oscillation frequency are obtained in terms of exact analytical expressions. Solutions for the phenomena of multiple harmonic frequency components are given, and nonlinear shock response spectra readily applicable to accurate response prediction in practice are presented.

Time-varying exact closed-form solutions for both autonomous systems, either single or multiple term, are derived. Employing the concept of differential transformation (DT) a set of algebraic equations is obtained that models the generalised dissipative nonautonomous time domain response behaviour. The results obtained from both analytical approximate methods, single/multiple term solutions and DT, are compared to direct numerical integration Runge-Kutta routines. It is shown that excellent agreement exists for both sets of results and that the newly derived methods are capable of even exceeding accuracy and computational performance of various commonly used Runge-Kutta algorithms. Solution expressions for the transient nonconservative SDOF systems are readily applicable to multi-degree-of-freedom (MDOF) systems. A rigorous uniqueness and stability analysis carried out for the oscillatory models considered in this work ensures that all of the obtained solutions are valid and feasible within their respective domain of definition.

Do not look back and ask why,
look forward and ask, why not.

— H.L. Becker

Acknowledgements

As with any large undertaking there are a number of people on whose shoulders we stand. No doubt, this is certainly the case for me in this thesis and the particular shoulders on which I stand are those of my teachers and my family. I owe an immense debt of gratitude to my supervisors Dr. Neil Ferguson and Mr. Stuart Dyne for their guidance and unconditional support of my work here at the ISVR, their endless patience and constant availability which gave me the chance for countless and invaluable discussions. Sincere appreciation goes to Prof. Mike Brennan and Dr. Tim Waters for their kind help and constructive reviewing of this work and for providing me with the chance of working in such an inspiring and amicable research environment in the first place. I would also like to acknowledge the financial support from DSTL Fort Halsted who have enabled this project to exist.

Special thanks go to Prof. Gary Koopmann and Prof. George Lesieutre for their warm welcome to the Center for Acoustics and Vibration at Penn State University. I would like to thank them and the people from the WUN alliance for making my visit to the CAV possible and so productive. I am also indebted to Prof. Joe Cusumano for his insight and guidance through numerous problems of nonlinear system analysis. And last but not least, a big 'thank you' goes to my fellow PhD students and friends at Penn State for making my stay such an enjoyable time.

I feel very much obliged to Prof. Peter Ruge from the Institute for Structural Dynamics, Dresden University, one of my first teachers of the subject, for giving me the curiosity about dynamical systems. I have benefitted immensely from his extensive knowledge and excellent teaching skills.

My work would have been incomparable harder without the constant support and exceptional assistance from researcher, engineers and staff of ISVR, ICS, and the university's Information System Services. In no specific order I would like to express my gratitude to the following people: our secretaries Anne-Marie McDonnell and Diane Farrenden for keeping my outside-world communication in sync, John Fithian and Glen Barber for their support in arranging the set up of various experiments, Ivan Wolton and his colleagues from ISS for providing me access to the university's high performance computing facilities and their kind and prompt assistance in all my Unix shell mistakes, John Haughton and Richard Cross from the ISVR computer support for their invaluable help in data rescue and backup. And of course, what would all this time in my office have been without the presence of my dear colleagues and friends from the ISVR ICS and Dynamics Group.

Finally, but most importantly, special thanks go to my family. Words are certainly not enough to express the gratitude I owe to my parents for their constant support and encouragement throughout my studies. And last but not least, finishing this work would have been impossible without the help and truly welcoming kindness of Cèline, Marjorie, Rob and their family.

CONTENTS

LIST OF FIGURES

LIST OF TABLES

NOTATION

The following lists are intended to give a brief overview of almost all of the variables and symbols used. In the rare case of symbols omitted in the tables below, their mathematical denotation becomes clear from the context of usage. It should be noted that a general agreement made is that small **bold** face Latin and Greek letters designate vectors enclosed by curly brackets $\{...\}$, whereas capital **bold** letters refer to matrices confined in square brackets $[...]$. A brief description of various special functions used in this work is given in appendix B.

Parameters and Variables

D_s		Polynomial discriminant	n/a
$\mathbf{H}$		Hessian matrix	n/a
$\mathbf{I}$		Identity matrix	n/a
$\mathbf{J}$		Jacobian matrix of first-order partial derivatives	n/a
$P(t)$	$= p_0\, p_t(t)$	External forcing function	N
T		General oscillation period	s
T_δ		Oscill. period - impulse excitation	s
${}_{\mathrm{f}_1}T_\delta$		Oscill. period - impulse, $f_1(u)$ system	s
${}_{\mathrm{f}_2}T_\delta$		Oscill. period - impulse, $f_2(u)$ system	s
T_{H}		Oscillation period - step excitation	s
${}_{\mathrm{f}_1}T_{\mathrm{H}}$		Oscill. period - step, $f_1(u)$ system	s
${}_{\mathrm{f}_2}T_{\mathrm{H}}$		Oscill. period - step, $f_2(u)$ system	s
$V(\mathbf{u})$		System total energy function	Nm
$V_{\mathrm{kin}}(\mathbf{u})$		Kinetic energy	Nm

$V_{\mathrm{pot}}(\mathbf{u})$		Potential energy	Nm
b		Nonlinear stiffness function exponent	–
$f(u)$		General nonlinear restoring forces	N
$f_1(u), f_2(u)$		Example nonlinear restoring forces	N
f_n		Natural oscillation frequency of linear system	Hz
f_{NL}		Oscillation frequency of nonlinear system	Hz
f_{norm}	$= \frac{f_{\mathsf{NL}}}{f_{\mathrm{n}}}$	Normalised natural nonlinear oscillation frequency	–
k_α		Linear stiffness coefficient	N/m
k_β		Nonlinear stiffness coefficient	$\mathsf{N/m^b}$
k_γ	$= \frac{k_\beta}{k_\alpha}$	Nonlinear stiffness ratio	$\mathsf{1/m^{b-1}}$
m		SDOF system mass	kg
$\overline{m}_\delta$		Mass scaling factor - impulse excitation	1/kg
$\overline{m}_{\mathrm{H}}$		Mass scaling factor - step excitation	1/kg
$p_t(t)$		Time-dependent part of forcing function	–
p_0		Force magnitude magnitude for step excitation	N
p_δ		Force magnitude for impulse excitation	N
$\widehat{p}_0, \widehat{p_\delta}$	$= \frac{p_0}{m}, \frac{p_\delta}{m}$	Mass-normalised step, impulse magnitude	N/kg
t		Time	s
$u(t)$		Displacement function	m
u_{min}		Minimum displacement	m
u_{max}		Maximum displacement	m
u_{Ex}	$= \{u_{\mathsf{min}}, u_{\mathsf{max}}\}$	Set of extreme displacement response values	m
u_{eq}		Displacement equilibrium point	m
$u_{\mathsf{stat,lin}}$		Static displacement of linear system	m
u_{norm}	$= \frac{u_{\mathsf{Ex}}}{u_{\mathsf{stat,lin}}}$	Normalised extreme displacement	–
$\overline{u}_{\mathsf{Ex,m}}$		Mass normalised extreme displacement	m/kg
$\overline{u}_{\mathsf{Ex,m,s}}$		Mass and linear static displacement normalised extreme displacement	1/kg
$\mathbf{u}(t)$		State space vector	m, m/s
$\dot{u}(t),\ v(t)$	$= \frac{\mathrm{d}}{\mathrm{d}t}u(t)$	Velocity	m/s
$\dot{u}_{\mathsf{min}}$		Minimum velocity	m/s
$\dot{u}_{\mathsf{max}}$		Maximum velocity	m/s
$\dot{u}_{\mathsf{Ex}}$	$= \{\dot{u}_{\mathsf{min}}, \dot{u}_{\mathsf{max}}\}$	Set of extreme velocity response values	m/s
$\dot{\mathbf{u}}(t)$		First derivative of state vector	$\mathsf{m/s, m/s^2}$

$\ddot{u}(t),\ a(t)$	$= \frac{\mathrm{d}^2}{\mathrm{d}t^2}u(t)$	Acceleration	$\mathsf{m/s^2}$
$\ddot{u}_{\mathsf{min}}$		Minimum acceleration	$\mathsf{m/s^2}$
$\ddot{u}_{\mathsf{max}}$		Maximum acceleration	$\mathsf{m/s^2}$
$\ddot{u}_{\mathsf{Ex}}$	$= \{\ddot{u}_{\mathsf{min}}, \ddot{u}_{\mathsf{max}}\}$	Set of extreme acceleration response values	$\mathsf{m/s^2}$
$\mathbf{x}_i$		Matrix eigenvector	n/a
$\mathbf{y}(t)$		Unique solution vector to differential system	n/a
$\mathbf{z}$		Parameter vector	various
λ_i		Matrix eigenvalue	n/a
ω_{n}	$= 2\pi f_{\mathrm{n}}$	Linear oscillation frequency	$\mathsf{rad/s}$
ω_{NL}	$= 2\pi f_{\mathsf{NL}}$	Nonlinear oscillation frequency	$\mathsf{rad/s}$
$\omega_\alpha^2,\ \omega_\beta^2$	$= \frac{k_\alpha}{m},\ \frac{k_\beta}{m}$	Nonlinear oscillation frequency squared	$(\mathsf{rad/s})^2$
			$\frac{\mathsf{rad}}{(\mathsf{s}^2\mathsf{m}^{b-1})}$
$\xi,\ \chi$		Sets of polynomial roots	n/a

Special Symbols and Transformations

$C^r(S)$	Continuity classification: set of r-times continuously differentiable functions defined on the set S
`const`	Constant scalar or function value
D	Domain of the phase or configuration space with dimension n
$D - \{\mathbf{x}_0\}$	Set or field of points defined in D except $\mathbf{x}_0$
$\mathcal{D}_{\mathbf{F}}$	Lie or orbital derivative
$\mathrm{dist}\,(\mathbf{x}, S) = \inf_{\mathbf{y}\in S} \|\mathbf{x} - \mathbf{y}\|$	Minimum distance between two vectors, $\mathbf{x}$ is not in the set S, $\mathbf{y}$ is
$\mathbf{div}\,,\ \nabla\cdot$	Divergence of vector field
$\det(\mathbf{X})$	Determinant of a (square) matrix
$\mathbb{e}$	Exponential function
$\mathbf{F}$	Nonlinear vector field or map (discrete time systems)
$G : \mathbb{R}^n \to \mathbb{R}^m$	Function or map definition; G maps the real-valued vector space of dimension n into the real m-dimensional space
Γ_c	Closed orbit in 2D state space

$\mathbf{grad}$, ∇		Gradient of scalar field
i	$=\sqrt{-1}$	Imaginary unit
$\Im\{z\}$		Imaginary part of the complex number z
$\inf(S)$		Infimum of set S (greatest lower bound)
$\Re\{z\}$		Real part of z
$\mathbb{R}^n$		Real-valued vector space of dimension n
$\{.\}^{\mathrm{T}}$, $[.]^{\mathrm{T}}$		Vector or matrix transposition
$\mathrm{tr}\,(\mathbf{X})$		Trace of a (square) matrix
$\|\mathbf{x}\|$	$=\sum_{i=1}^{n}\|x_i\|$	Vector norm
$\|\mathbf{X}\|$	$=\sum_{i,j=1}^{n}\|x_{i,j}\|$	Matrix norm
$\forall$, $\in$, $\ni$		For all, element of, not element of
$\cap$, $\cup$		Intersection, union (of sets)

Special Functions

$\|u\|$	$=u\,\mathrm{sgn}(u)$	Absolute value function
$\delta\,(t)$		Dirac delta impulse function
$\mathsf{E}\,(\psi,\kappa)$		Incomplete elliptic integral of the second kind with argument ψ and modulus κ
$\mathsf{E}(\kappa)$		Complete elliptic integral of the second kind
$\mathsf{F}(\psi,\kappa)$		Incomplete elliptic integral of the first kind
$\mathsf{F}_\xi\,(\psi,\kappa)$		Incomplete elliptic integral of the first kind resulting from integration of polynomial function with root set ξ
${}_2\mathsf{F}_1(...)$		Gauss's hypergeometric function
$\Gamma\,(...)$		Complete Gamma function
$H\,(t)$		Heaviside step function
$L\,(\mathbf{u})$		Lyapunov function
$\mathsf{K}(\kappa)$		Complete elliptic integral of first kind, modulus κ
$\mathrm{pq}\,(\psi,\kappa)$		Jacobian elliptic function where the term pq stands for one of the combinations given in appendix B.3
$\mathrm{sgn}(u)$		Signum function (-1, 0, $+1$ for $u<0$, $u=0$, $u>0$, resp.)

Number Sets or Fields

$\mathbb{N}$	Set of non-negative integer numbers (natural numbers)
$\mathbb{Z}$	Set of integer numbers
$\mathbb{R}$	Field of real numbers
$\mathbb{R}_+$	Field of positive real numbers
$\mathbb{C}$	Field of complex numbers

CHAPTER 1

INTRODUCTION

1.1 Dynamical systems

The mathematical investigation of dynamical systems prior to Poincaré's studies in the 1880s mainly concentrated on obtaining analytical solutions to the governing difference, differential or integro-differential equations. Many great names in analysis are associated with these studies - Leibnitz, Newton, Euler, Gauss, Lagrange, Jacobi, Laplace, Lie and, of course, Poincaré, amongst numerous others. With dynamics being originally a branch of physics, the subject began in the 17th century when Leibnitz and Newton formed a coherent concept of calculus and, subsequently, Newton solved the two-body problem.[1)] Following generations of mathematicians and physicists tried to extend the analytical methods of Newton to the three-body problem but after decades of effort Bruns proved in 1887 that the problem was essentially impossible to solve in terms of obtaining closed-form, analytical expressions for the motion of the three bodies. In 1898 Painlevé extended Bruns' theorem to n-bodies and at this point, if not even before, it became utterly clear that solving all dynamical systems in terms of indefinite integrals involving elementary functions and uniformly valid power series was not possible. This fundamental discovery led to the conclusion that other approaches must be developed to understand the secrets hidden within the dynamic equations. These first two hundred years of scientific philosophy, from Newton, Leibnitz and Euler through to Hamilton and Maxwell produced with great success many brilliant formulations of "the rules of the world", but only very limited results in finding their solutions.

The breakthrough came with the work of Poincaré, who introduced an entirely new point of view that emphasised the extraction of qualitative rather than quantitative information out of the governing equations. Many of his ideas were subsequently refined and amplified by others but

[1)]The problem of calculating the motion of the earth around the sun, given the inverse square law of gravitation between them.

the genius of his imagination and insight can hardly be overstated[2)] Mathematicians extended his concepts to such areas as topology, dimension theory, asymptotic series, and bifurcation theory, to name a few. Many great names associated with the area of system dynamics built on the wealth of his ideas and produced a variety of new concepts. Amongst them in the first half of the 20th century were van der Pol, Duffing, Andronov, Littlewood, Cartwright, Levinson and Smale, pioneers in the invention of new mathematical techniques for the analysis of nonlinear oscillators in radio and radar technologies. Meanwhile, in a separate development, the geometric methods of Poincaré were being extended to yield a much deeper insight into classical mechanics, led by the work of Birkhoff, Kolmogorov, Bogoliubov, Krylov, Mitropolsky ('Averaging Method of Perturbation Theory'), Arnol'd and Moser who studied the complex behaviour of Hamilton systems. With the digital computer in the 1950's a new tool of analysis came on to the scene and the semi-numerical studies of lattice dynamics by Fermi, Pasta and Ulam are probably the most well-known of this time. Many excellent ideas still heavily in use today originate from this decade, amongst them Hopf bifurcation and the KAM theory (Komolgorov-Arnol'd-Moser). The 1960's and 70's relied more and more on the use of computers enabling scientist to perform in-depth studies of the nature of selected dynamical systems using numerical simulation. Although predicted by Poincaré in his investigation of the famous three-body problem, Lorenz delivered the first direct proof of deterministic chaotic behaviour for a simple nonlinear system. This was taken further by Mandelbrot and others to form the theory of fractal structures. From the late 70's to the late 90's a whole new range of concepts emerged ranging from strange attractors, self-organisation of matter, solitons, homoclinic bifurcation sequences in chaotic systems to cellular automata (Conway, Wolfram).

In the same context with the work of Poincaré, the stability concept of Lyapunov must be mentioned. Problems of stability appear for the first time in mechanics during investigation of an equilibrium state of a dynamical system. Although various approaches to the problem have been introduced as early as in the 17th century by Torricelli and were later considerably extended by Lagrange (1788), the publication of Lyapunov's thesis in 1892 marks a watershed so that scientists today divide the history of motion stability into pre-Lyapunov and post-Lyapunov periods. Earlier contributions to the subject by Maxwell (1868), Vyshnegradsky (1878), Routh (1877-84) and others were significant and a few concepts are still important today. But the main shortcoming of the researchers of those times was that in their analysis of perturbed dynamical systems they considered only the linearised equations of the perturbed motion and did not take into account the influence of higher order, nonlinear terms. As will be seen in subsequent chapters of this work, systems with identical linear but different nonlinear components do not share a single grain of common property with respect to motion stability, even if the value of the nonlinear term is very small compared to the linear, and the motion of the nonlinear system differs only insignificantly from the motion of its linear counterpart. It is impossible to summarise all the ideas Lyapunov

[2)] Poincaré was also the first person to glimpse the possibility of chaos, in which a deterministic system exhibits aperiodic behaviour that depends sensitively on the initial conditions thereby making long-term response prediction extremely difficult. However, this must not be confused with random systems or stochastic processes. The entire future of a deterministic-chaotic systems can still be calculated, although for almost all cases by means of direct numerical integration.

introduced into the theory of motion stability, but two fundamental results are important to point out since they are essential for understanding the very basics of the entire approach. First, Lyapunov provided a rigorous definition of motion stability. Although this seems plain and simple, the absence of such a definition had often caused severe misunderstanding since the motion of a system can be stable in one sense but unstable in the other. Secondly, he suggested two main methods for analysing stability problems of motion, of which the second of these methods, also called 'The Direct Lyapunov Method', is today known as a standard procedure due to its simplicity and efficiency.

As with the ideas of Poincaré, Lyapunov's theory was developed in various directions by following generations of researchers. Further analysis methods were investigated and original results obtained by Lyapunov were determined more precisely. The theory of motion stability is far from complete at this time and current research is concerned with effects of large perturbations of initial conditions, time-dependent perturbations, as well as perturbation in finite time intervals and under random forces. Both concepts of Poincaré and Lyapunov together with the contribution of so many others throughout the last century are now the very foundation of dynamical systems science and until today nonlinear dynamics with its numerous different branches such as chaos theory, nonlinear control, neural network dynamics, etc., has not lost any of its early attractions and ongoing research is more vital than ever.

1.2 Basic concepts

One of the aims of this work is to make it also accessible to the interested reader who is not particular familiar with the subject of nonlinear dynamical system analysis and it is therefore essential to express the quite complex matter as simple as possible. This rather elementary objective is not easily achieved, and before describing the content of the thesis a few fundamental concepts of the mathematical theory behind the analysis of dynamical systems must be explained.

A dynamical system is made of two basic components: a rule or "dynamic", specifying how the system evolves, therefore sometimes called 'evolution equation', and an initial condition or "state" from which the systems starts. In mathematical terms this is referred to as 'initial value problem', or IVP.[3)] By far the most successful class of rules for describing real-world phenomena are differential[4)] or difference equations. The term 'differential' refers to evolution equations of systems having a continuously defined independent variable whereas difference equations, also known as iterated maps, arise in problems where the independent variable takes on discrete values. The work described herein solely investigates nonlinear explicit ordinary differential equations (ODE) with time as the independent variable. In this context, by definition, 'ordinary' refers to

[3)] In contrast to boundary value problems (BVP), where the state of the (not necessarily dynamic) system at the boundary of the independent variable domain of definition is partially known.

[4)] This includes differential-algebraic equations (DAE) which are a more general form of explicit ordinary differential equations (ODE). Both DAE and ODE belong to the group of implicit differential equations. Sometimes the use of implicit and explicit is not consistent and the term ODE refers to both. However, there is a strict mathematical distinction to partial differential equations known as PDE.

equations with only one independent variable. It is worth pointing out that the term 'nonlinear' or 'nonlinear dynamical system' is not uniformly used throughout literature. For example, linear parametric equations are frequently included in studies of nonlinear oscillators, whereas nonlinear equations which are known to be linearisable by transformation, e.g. 'quasilinear' partial differential equations, are sometimes considered to be linear. In order to avoid any misunderstanding, a linear operator $\mathcal{L}\big[\mathbf{x}(t)\big]$ for the vector functions $\mathbf{x}(t)$ and $\mathbf{y}(t)$ is defined such that linear superposition for any two constants c_1 and c_2 holds

$$\mathcal{L}\big[c_1\,\mathbf{x}(t) + c_2\,\mathbf{y}(t)\big] = c_1\,\mathcal{L}\big[\mathbf{x}(t)\big] + c_2\,\mathcal{L}\big[\mathbf{y}(t)\big]\,, \qquad t, c_1, c_2 \in \mathbb{R};\ \mathbf{x}(t), \mathbf{y}(t) \in \mathbb{R}^n\,,$$

given $\mathbf{x}(t)$ and $\mathbf{y}(t)$ satisfy the appropriate regularity properties.[5] By virtue, a nonlinear operator $\mathcal{N}\big[\mathbf{x}(t)\big]$ is then defined to be any operator which does not satisfy the above equation for some constants c_1, c_2 or some functions $\mathbf{x}(t)$, $\mathbf{y}(t) \in C^r$. The order r of the operator defines the order of the differential system.

The classical theory of ordinary differential equations has a long and traditional history in mathematical science. Fundamental relations of this theory make it possible to study all evolutionary processes that exhibit the properties of determinacy, finite-dimensionality and differentiability. To be more precise, a process is called deterministic if its entire past and its complete future course are uniquely determined by its present state.[6] The solution $\mathbf{x}(t)$ of a differential equation can be thought of as a time-parameterised, continuous curve starting at the initial values $\mathbf{x}\,(t \equiv t_0)$ embedded in an n-dimensional vector space $\mathbb{R}^n$, the so-called phase space. Depending on the specific context, this path of evolution is also called integral curve, orbit or trajectory. In other words, the phase space is the set of all states of the process. Contrary, the real-world physical space of the dynamical system is frequently referred to as the configuration space.[7] In the work presented here the phase space has the form of an Euclidian space $\mathbf{E}^n$ of dimension n, thus, the associated distance between any two points is expressed by the Euclidian norm or metric

$$\mathrm{d}\,(\mathbf{x}, \mathbf{y}) = \sqrt{\sum_{j=1}^{n} (x_j - y_j)^2}\,.$$

A process is called finite-dimensional if its phase space is finite dimensional, i.e. if the number of parameters needed to describe its states of evolution is finite.[8] In recent years it became practice to refer to all other variables apart from time t and the solution $\mathbf{x}(t)$ itself as control variables. Logically, the m-dimensional set of control variables is the control space.

[5] If $\mathcal{L}\big[\mathbf{x}(t)\big]$ is a differential operator of order r, then both functions need to be C^r-continuous, i.e. r-times differentiable.

[6] A semi-deterministic process is the propagation of heat since its future is determined by its present but the past is not. Nondeterministic processes are usually ascribed to quantum mechanics, but recent publications have shown that exactly the same phenomena can occur in classical mechanics. See chapter 2 for details.

[7] Clearly, depending on the mechanical system under consideration this space can be one-dimensional (straight line), two-dimensional (planar) or three-dimensional (spatial).

[8] Obviously, this is not the case for space-continuous systems such as vibrating strings, beams and membranes or the motion of fluids. Such systems require PDEs for a complete (but simple) mathematical description of their physical behaviour.

A process is called differentiable if its phase space has the structure of a differentiable manifold, and the change of state of the dynamical system with time is described by differentiable functions. Colloquially speaking, a manifold is a collection of patches sewed together in some smooth way. Each patch is represented by a parametric equation and the smoothness of the sewing means that there are no cusps, corners, sharp edges or self-crossings.[9] The differentiability of the manifold ensures that no global coordinate system is needed for exercising calculus. More specifically, the differentiable manifold allows the definition of a globally differentiable tangent space and thus makes it possible to introduce differentiable functions and differentiable vector fields, which are frequently termed as the 'flow' of the dynamical system.

If time appears explicitly in the dynamics or flow of the system then the oscillator is termed nonautonomous, otherwise it is called autonomous. Despite the fact that it is possible to rewrite any nonautonomous system defined in $\mathbb{R}^n$ as an autonomous system in $\mathbb{R}^{n+1}$, this mathematical trick has not been used in here. Although an 'extended phase space' of dimension $n+1$ seems all too natural for nonautonomous systems, the method ignores the physical distinction of the time variables.[10]

Building on these basic concepts of dynamic system analysis many more definitions will be introduced in the following chapters of the thesis. However, it is fair to assume that familiarity with the above ideas should make it significantly easier to understand them.

1.3 Thesis outline

Chapter 2 of the thesis gives a comprehensive but by no means complete review of previous work in the field of nonlinear dynamic systems analysis, mainly related to structural mechanics. It covers not only topics to which contribution is made in here, such as extreme response or time domain analysis of nonlinear systems as discussed in section 2.2, the chapter also aims to shed some light on rather fundamental problems of the field. Section 2.3 for instance addresses the important aspects of existence and uniqueness of nonlinear solutions and thereby incorporating the latest findings on identifying nondeterministic, chaotic systems. However, the main emphasis of the literature review is placed on the most controversial branch of nonlinear system dynamics: the search for explicit, analytical exact or analytical-approximate time domain solutions. It is section 2.4 which reviews the efficiency and accuracy of various methods introduced throughout the last 50 years, and attempts to relate them to a new and recently developed approach which has been successfully expanded.

Significant progress has been made since the late 1960s when first expressions for extreme value response of a few nonlinear single-degree-of-freedom (SDOF) systems were given. Chapter 3 builds on these early contributions but derives new and far more general expressions, which

[9] A one-dimensional manifold is, for example, an infinite straight line, a circle or an ellipse. The surfaces of an infinite cylinder or the unbounded real plane are examples of two-dimensional manifolds, likewise are the surface of a sphere or a torus.

[10] The method provides a very effective way of rewriting a harmonically forced, linear second-order oscillator as a nonlinear, autonomous, three-dimensional first order system. Thus, it becomes possible to associate certain properties of forced linear systems to autonomous nonlinear systems.

makes it possible to incorporate a much broader range of autonomous oscillators under several different conditions. However, an essential part of the chapter deals with the rather difficult task of establishing existence and uniqueness of a non-Lipschitzian oscillatory system.[11] It will be shown how both Lyapunov's second theorem and Morse theory can be applied to prove that the nonconservative system is stable in the entire phase plane.

Building on the these extreme value response solutions, chapter 4 is devoted to the time domain analysis of autonomous non-dissipative systems. Exact analytical expressions for the Duffing oscillator are presented in section 4.2 supposing the freely vibrating system is subjected to general initial conditions. Explicit ranges of feasibility for each analytical solution are given which have been obtained in conjunction with the motion stability analysis of chapter 3. For the step excited SDOF system possessing one of the two nonlinear restoring forces considered in this work, various single-term analytical-approximate solutions are derived in section 4.3. Accuracy and efficiency of each expression heavily depends upon the system control parameters and a detailed comparison is included in the analysis. Section 4.4 significantly extends the approach to multi-term analytical approximation solutions. In particular, a modified and enhanced Bubnov-Galerkin procedure is presented together with a Picard integral iteration scheme. Both methods are compared to commonly available Runge-Kutta direct numerical integration algorithms.

Chapter 5 introduces a significant transition to nonautonomous oscillators and builds on the results of a recently published analytical-approximate solution algorithm called Taylor Differential Transformation (TDT). The approach is highly versatile and applicable to all types of linear and nonlinear systems. Two versions of the method are presented in section 5.2, together with appendix C, and both are compared to exact analytical results from chapter 4 as well as Runge-Kutta procedures. This initial evaluation of the method's suitability for highly nonlinear and transient systems makes it possible to obtain analytical-approximate solutions for nonconservative SDOF oscillators subjected to blast excitation.

A brief summary and evaluation of the thesis results are given in the last chapter. It emphasises the improvement and progress of existing methods and newly derived solutions in this work. But equally important, it clearly indicates various restrictions of the novel methods and makes an attempt to point out important questions and yet unsolved problems which require significant future research effort.

1.4 Thesis objectives and contribution

It is an agreed fact throughout modern science that almost all real-world phenomena are nonlinear. Moreover, it has been acknowledged since the days of Newton and Euler that even very simple processes in nature cannot satisfactorily be characterised by the linear law of superposition. In the past, the description of these processes using linear differential equations has been viewed as sufficient in the majority of circumstances, but with the increasingly rapid advances in sciences and technology, these simplified mathematical models appear more and more inadequate in capturing and understanding complex real-world problems. It is therefore the most logical step to leave

[11] A precise definition of the term is given in section 3.2.

behind the realm of linear analysis and start focussing on the rich and sheer endless possibilities offered by a world of nonlinear dynamical analysis.

It can be seen as the foremost objective of this thesis to add a small contribution towards this transitions by publishing solutions which can be readily put to work for investigating the response behaviour of a large family of geometrically nonlinear oscillators. But the thesis provides a little more than that. Not only does it show how these novel results must be classed compared to past and present research, it also tries to put them on a sound basis using both celebrated and lesser well-known nonlinear analysis methods developed by numerous researchers in the past. Several of these methods have never been applied before to any of the systems discussed here. Some required little adjustment, for others substantial modifications were necessary in order to make them fully suitable to the problems considered.

Although this work is essentially concerned with the investigation of two geometrically nonlinear SDOF systems having both polynomial-type restoring stiffness forces, the majority of newly derived expressions and subsequently obtained response results are applicable to an entire family of nonlinear systems. Moreover, the fundamental contributions towards obtaining analytical-approximate time domain solutions for highly transient, nonlinear oscillators has been presented in such a form that enables immediate application to multiple-degree-of-freedom (MDOF) systems. In particular, this work contributes in the following areas:

- Based on an energy conservation approach for Hamiltonian systems the methods for calculating single nonlinear response values have been expanded, thus explicit analytical expressions are derived for extreme[12)] displacement, velocity and acceleration under generalised autonomous excitation. Whereas previously only nonzero initial values *or* impulse/step excitation were permitted, it is now possible to predict the SDOF system behaviour when the oscillator is subjected to both conditions simultaneously. This makes it easy to obtain nonlinear response spectra for precise and effective prediction of system behaviour in practice.

- Using these new results a second integration of the planar system trajectory with respect to time leads to closed-form expressions for the nonlinear oscillation frequency of the periodical system. These expressions have been successfully solved in terms of Jacobian elliptic functions. Moreover, a detailed analysis of the domain of definition of the independent time variable reveals the existence of multiple oscillation frequency components which are in perfect agreement with previously predicted results from numerical Fourier transformation reported elsewhere.

- In analogy to the association of a hyperbola with the canonical form of a planar Hamilton system in the (linearised) vicinity of an unstable equilibrium point, it is proved that the eigenvectors of the linearised system at a degenerate or non-degenerate but stable fixed point are identical to the slope of the diameters of an ellipse representing the invariant integral manifold of the system.

[12)] In the sense of minimum and maximum.

- Two separate methods are introduced for establishing the existence and uniqueness of a non-Lipschitzian, nonlinear, polynomial-type restoring stiffness force. The first one is based on a combination of Picard iteration and recently published results for terminal systems. Significantly, instead of employing the Lipschitz conditions for the j-th state-space derivative of the nonlinear flow, it is suggested that Peano's theorem can be used for the more complex cases where the j-th derivative does not satisfy the Lipschitz criteria. The second method is based on the application of the Brauer-Sternberger theorem and takes advantage of the fact that for the system under consideration the Hamiltonian can be chosen as stability function which makes the procedure very effective.

- Significant contribution is made in this work towards establishing analytical and analytical-approximate time-domain solutions for a large family of nonlinear oscillators. These previously unpublished results include expressions for autonomous and nonautonomous, nonconservative SDOF systems. In comparison to widely employed but purely numerical solution methods, all of the new approaches show great versatility and considerably increased accuracy.

To summarise, the thesis builds on a variety of established results, some are well-known others have been published very recently, extends these methods further and derives a number of new applications immediately accessible to researchers and engineers alike.

CHAPTER 2

REVIEW OF PREVIOUS RESEARCH

2.1 Introduction

Although the study of nonlinear oscillation received its first scientific and engineering attention slightly more than a hundred years ago, the amount of publications on this truly multidisciplinary subject is immense. Several reasons can be identified. Firstly, time varying nonlinear systems are of interest to a large research community spreading from the most fundamental discipline of all, mathematics, to all kinds of subjects in science and engineering. In fact, one of the first reasons for deriving a mathematical theory for nonlinear systems were unsolved problems in celestial mechanics, formulated, but not satisfactorily solved by scientists throughout the last centuries. Secondly, with the significant advances in physics, chemistry and engineering in the 19th and 20th century, even more complicated nonlinear dynamics problems arose. Thirdly, with the emergence of circuit and systems theory in electrical engineering in the 1950's, the generation of nonlinear oscillation problems seemed endless. However, it was this very advance which brought the nonlinear research community one of their most valued tools: the digital computer.[1)] This suddenly enabled scientists to make use of highly appreciated numerical algorithms developed more than half a century earlier but previously not suitable for hand-calculations [1,2]. A fourth reason lies clearly within the amount of phenomena discovered in nonlinear systems in a rather short amount of time compared to other disciplines. These include amplitude dependent frequencies, multiple frequency response, solution bifurcation, etc., just to name a few. Most worthy to mention is the much celebrated recent discovery of deterministic chaos. Causes for the many of these events are not yet fully explored and research is far from completely characterising any of the phenomena, although some have been revealed over the last fifty years. Finally, as the fifth and last reason in this incomplete se-

[1)] In the 1940's and 1950's numerical computations were performed on analog computers.

lection, there is the constant discovery of new aspects of nonlinear behaviour across all scientific fields. The recent occurrence of the so-called 'terminal systems' is a good example.

The literature review presented in this chapter focuses mainly on vibration in structural systems. Since the thesis examines strongly nonlinear oscillations of conservative and nonconservative systems due to free vibration and external forcing, the majority of the cited references deal with this subject. The following section 2.2 details some publications which mainly focus on methods predicting minimum and maximum values of displacement and velocity for nonlinear systems, a few even account for calculating the true nonlinear oscillation frequency. It is worth mentioning that these concepts have been the first application of nonlinear oscillation theory in mechanical engineering. Section 2.3 presents recently published results for a special type on nonlinear oscillator, so-called terminal systems. These will become important for establishing the uniqueness of analytical solutions in chapter 3, where the differential equations of the oscillator under consideration do not satisfy commonly used but strict uniqueness conditions. In the last two decades most of the publications deal with schemes to derive the nonlinear response time-history even if the system is highly nonlinear. Since these approaches are usually based on modified established methods for quasi-linear or weakly nonlinear systems, section 2.4 lists papers briefly describing these much celebrated conventional methods before starting to explain and reference important changes. However, the nature of dynamical response makes it necessary to differentiate between steady-state and truly transient system behaviour.

It is important to point out that none of these lists of references regarding any of the topics in section 2.2 to 2.4 claims to be exhaustive. Each one should merely be seen as a selection of publications specifically chosen for each individual topic under study in later chapters of this work. Listing all available references is certainly beyond the scope of this work and hence some specific selection has taken place.

2.2 Extreme response values of nonlinear systems

With its unique properties of accumulating, preserving and redistributing all externally ascribed energy in a strict linear manner, conservative dynamical systems can be analysed in various ways in order to extract closed-form solutions for essential response parameters even in case of highly nonlinear restoring force characteristics. In the special case of autonomous SDOF oscillators explicit analytical results for extreme values of displacement, velocity and acceleration can be derived utilizing this energy approach. Furthermore, due to the constant vibration amplitude if no explicitly time-varying forces are present in the system, nonlinear oscillation period and frequency can be obtained from first-integral type equations for the system representing the total energy at all time. Although the approach appears to be quite simple in its fundamental concept, difficulties soon arise in solving complex integral expressions even for well-known and clearly structured restoring forces such as the nonlinear pendulum [3] or Duffing-type equations [4]. This made it necessary for previous researchers to introduce certain assumptions, more or less consistent with the physical situation at hand, in order to confine the complexity of the problem and the governing equations, reducing them to types more easily accessible and solvable. The most obvious approach for sim-

plifying complicated real-world problems is, without any doubt, linearisation. Although for many physical models this is a stark idealisation, the solution is obtained by superimposing the results of all of its individually analysed (linear) parts, a method inapplicable for the original nonlinear problem in question.

One of the first approaches aimed towards such simplification was introduced by Ergin [5], who approximated the nonlinear force-displacement function by a bilinear characteristics under the condition of minimising the mean-square error between both. Thomson [6] solved a special case of Ergin's general formulation with constant stiffness coefficients for specific ranges of displacement of the linearised system. In [7] Bapat *et al* obtained force and stiffness normalised maximum displacement values for Duffing-type conservative oscillators subjected to constant force magnitude excitation using the method in [5]. The authors correctly point out that these results can also be applied to the same system subjected to other pulse excitation shapes, but only if the pulse duration is shorter than the time required for the system to reach its first peak displacement. This seriously limits the usability of the approach in [5] for producing shock spectra for a wide range of nonlinear systems. As will be derived later in chapter 3, knowing only the mass and stiffness parameters together with the magnitude of the applied force one *cannot* predict the oscillation frequency of the nonlinear system *a priori* . Hence, shock spectra presented in [7] have to be used with caution if applied to time varying impulses as suggested by the authors. Analysis of various polynomial nonlinear restoring forces, amongst them the hardening Duffing stiffness type [4], the same authors presented extreme displacement solutions obtained from a truly nonlinear analysis by evaluating the governing differential equations [8,9]. Unfortunately, results can only be applied to systems with zero initial values, and hence, system response due to impulse excitation or free vibrations remain unknown. Furthermore, no stability considerations are derived and it is therefore difficult or nearly impossible to estimate the range of system parameters feasible for the results given.

Using the so-called direct linearisation method, a modification of [5] introduced by Panovko [10], Bapat *et al* [11] yield approximate expressions for maximum response values of periodic systems. Together with a superposition method [12] the authors obtained nonlinear oscillation frequency approximations for freely vibrating SDOF systems with hardening stiffness type characteristics. An attempt to approximate the response of nonconservative systems, results of [8, 9] were extended in [13], allowing for the prediction of maximum displacement values of linear viscously damped systems having Coulomb friction. Approximation for the nonlinear oscillation frequencies were repeatedly obtained using [10]. However, the oscillator must possess zero initial conditions and results are only applicable for hardening-type stiffness functions since the total energy of the system remains unbounded by the proposed scheme and hence stability for the majority of nonlinear oscillators cannot be assured. Timoshenko *et al* [3] briefly gave solutions for the free vibration of polynomial-type restoring forces with integer value exponents. Hundal [14] presented maximum displacement and acceleration ratios for systems with quadratic damping subjected to rectangular impulses of finite duration. Solution of the nonlinear problem is a two-stage process. First, the author obtained response values during the pulse loading using numerical integration. The subsequent free vibration of the system was obtained using various analytical-approximate

methods listed above.

Obtaining an analytical solution for the autonomous, freely vibrating Duffing oscillator by Fourier expansion, Tamura and Matsuda [15] considered the influence of the relative error accumulation in single and double precision computation. The authors proposed suitable combinations of numerical computation algorithms together with approximation formulae in order to calculate the exact solutions to the nonlinear problem with the most reasonable accuracy under a variety of parameter conditions. Tamura and Li [16] used a very similar method to obtain approximate analytical solutions[2)] for the free vibration of a quadratic-type hardening spring. The Fourier coefficients are obtained numerically bearing in mind the error considerations from [15]. In two subsequent papers [17,18] Tamura *et al* derived approximate analytical expressions converging to the (yet unknown) exact solutions of a single-term cubic stiffness oscillator [17] and the complete Duffing-type stiffness system [18] having all polynomial terms (zero to 3rd order) present. This was achieved by rewriting the original governing differential equation in forms for which solutions haven been previously obtained [15,16] utilising a bilinear transformation specially suitable for the specific nonlinear system under study. Approximations were given as a Fourier series in terms of periodic trigonometric and hyperbolic functions where only uneven elements are retained. However, as will be shown in this work, the above problem does not exhibit multiple oscillations frequencies if expressed using Jacobian elliptic functions. In [19] the author Lin considerably improved previously presented results for approximation of the oscillation frequency by He [20–22] for a Duffing-type stiffness equation which features the linear and a fifth-order polynomial term in the displacement. Whereas He used linearised or parameterised perturbation techniques and a variational iteration method, respectively, Lin employed a new parameter iteration method for showing that, even if the nonlinearity in the governing equation is non-small, the approximating expression of the oscillation period of the system converges asymptotically to the exact solution, contrary to He, where the frequency approaches a constant depending on the amplitude of oscillation and the nonlinear stiffness ratio, independent of the number of performed iterations. In a subsequent series of publications [23–29] He presented a variety of methods applicable to both weak and strong nonlinear systems. The larger part of these newly derived approaches were actually modifications or combinations of established concepts of nonlinear analysis tailored to cope with non-universal requirements of specific problems. Similar to [30] where the author applied the method of harmonic balance (HBM) [31] to the energy equation of a Hamiltonian system, rather than to its governing equation of motion.

A number of these techniques have also been applied to multiple-degree-of-freedom (MDOF) or space continuous systems using diverse spatial discretisation methods. For example, Ribeiro and Petyt use the HBM in connection with finite elements to analyse internal resonance phenomena of uniform beams [32] and isotropic [33–35] as well as laminated plates [36–38].

[2)] It seems to be common practice in numerous articles to term newly derived solutions as 'exact' although they are expressed in various forms of series approximations. It is true that these approximations resemble the exact solution for an *infinite* number of series elements. However, as is easily understood, this is impossible for the application to real physical problems where for computational reasons a series expansion must be *finite*. Hence, a small error is introduced and the solutions can no longer be referred to as exact. Surprisingly, the vast majority of articles easily interchanging the terminology for 'exact' and 'approximate' do present such error estimations for their obtained results.

The majority of recently published papers dealing with extreme value response also include approximation techniques for modelling time domain behaviour of the nonlinear system under consideration. Tiwari *et al* [39] gives frequency-amplitude relations for the Duffing-harmonic oscillator introduced by Mickens [40], assuming a single-term solution and utilising the Ritz procedure for the nonlinear oscillator [41]. Phase space plots show significantly increased accuracy for the time history solution compared to [40, 42]. Cveticanin [43] analysed the energy function of a system with linear and quadratic stiffness terms giving limits for the initial energy and extreme response values. By examining a modified perturbation technique presented in [44, 45];[3] Sanchez [47] can prove, contrary to the author's statement in the original articles, that the error in the method becomes unacceptable for large values of the nonlinear stiffness coefficients. In fact, solving the same problems with the well-established method of multiple scales leads to similar results.

The above list of recent publications from [39] to [47] is by no means exhaustive. Numerous other authors essentially contributed to this field of nonlinear dynamics. Since time domain solutions and extreme value results are not always clearly separated in more contemporary reportings, the majority of these researchers will be mentioned in section 2.4 of this chapter.

2.3 The problem of existence and uniqueness of solutions

Occurrence of one of the most exciting phenomena in nonlinear system response, chaos, had already been anticipated at the beginning of the last century. The first true experiment on chaos was the numerical investigation of the famous Lorenz system [48], used for modelling thermal convection in the earth's atmosphere in order to improve weather prediction. Although the system of three first-order ordinary differential equations is rather simple, Lorenz discovered exponential divergence of the solution evolution over time despite nearby initial conditions. Since then chaos theory became a new field in science and engineering [49]. The amount of publications investigating the simple system Lorenz first described in 1963 is tremendous, let alone the countless number of journal articles, proceedings and books dealing with chaotic system dynamics across all fields. However, it has only been in the recent decade that a new type of chaotic system behaviour, so-called terminal dynamics [50–55], has been brought to the attention of a growing number of researchers.

Lorenz-type behaviour in the chaotic parameter regime is characterised by the inherent nonlinearity of the system, which spreads any initial uncertainty across the entire range of the strange attractor. Colloquially speaking, this can be seen as a global property of the oscillating system whereas locally the dynamical uncertainty in the phase space is related only to the uncertainty of the variables in the configuration space. In contrast, piecewise deterministic or terminal dynamical systems are forced into nondeterministic chaos by local instabilities of the governing differential equations. Furthermore, terminal systems feature short-times predictability, essentially between singularities, a phenomenon completely unknown in deterministic chaos, where exponential divergence of initially close solutions is often expressed by dynamical phase space measures, e.g.

[3] The method of He [45] was found to be inapplicable to nonlinear damped systems, see Rajendran *et al* [46].

Lyapunov exponents[4] [56]. This accounts for what is probably the most striking difference between both systems. Despite being chaotic, the Lorenz-type oscillator is fully deterministic. Contrary, the singularity in a terminal system transforms the otherwise deterministic solution trajectory into a complete stochastic and irreversible process, thus loosing all previously defined information [50, 54]. Each singularity in a terminal dynamics-type system has an associated probability distribution uniquely defined by the properties of the given system. This in turn implies that qualitative methods such as Lyapunov exponents become obsolete [57]. Another equally important difference between both classes of chaotic oscillators emerges when comparing relaxation times. Whereas regular non-chaotic and deterministic chaotic oscillators reach their singular points in infinite time, terminal systems approach the non-deterministic singularity, which not necessarily needs to be an equilibrium point, in finite time, thus completing the stochastic process at least once. The only two properties shared by both types of chaotic oscillators are complete deterministic equations of motion and long-term non-predictability of solutions.

Non-deterministic chaotic or terminal behaviour generated by the influence of tiny disturbances such as noise in the experimental setup or round-off errors in the numerical simulation is possible for the most simple systems. Using a basic coordinate transformation for the harmonic oscillator[5] Dixon *et al* [53] showed that the new nonlinear system exhibits non-deterministic behaviour at the origin of the cartesian coordinate system. The mathematical reasons for such qualitative mutation were clearly identified as being either discontinuity[6] [59] or violation of the Lipschitz criterion[7] [60] of the vector field. By definition, the first one implies the latter [61]. The simple example in [53] and many others [57, 62–65] explicitly show the importance of ruling out non-deterministic chaotic behaviour for terminal-type systems.

The pioneering work of Filippov [66] who developed and proved theorems of existence and uniqueness, including dependence of the solution on the initial conditions, for differential equations with discontinuous right-hand side is seen today as the first rigorous approach towards the problem.[8] At around the same time Hartman proposed in [68] existence of a vector-valued function in $\mathbb{R}^n$ which is only continuous rather than Lipschitz in a given interval can be established by constructing a sequence of Lipschitz continuous approximations. Unfortunately, this applies to non-autonomous systems only and does not include uniqueness. However, with Filippov's work laying the cornerstone various extensions and improvements to his original framework were pub-

[4] The Lyapunov exponent ρ_L characterises the mean exponential rate of divergence of two initially close trajectories and is given as $\rho_L = \lim_{t\to\infty} \ln(c/c_0)/t$ with c being the distance between trajectories at time t, and c_0 the initial distance between these trajectories at $t = t_0$.

[5] In general, efforts are made in nonlinear system analysis to transform nonlinear systems into linear or quasi-linear ones. However, this approach works in both directions. The same is true for often used transformation into cylindrical or spherical coordinate systems.

[6] A real-valued function $g(x)$ defined in a subset $S \subset \mathbb{R}$ is continuous at x_a if for any $\epsilon > 0$ there exists a δ such that for all $x \in S$ with $|x - x_a| < \delta$ the inequality $|g(x) - g(x_a)| < \epsilon$ is satisfied (Cauchy $\delta - \epsilon$ definition) [58]. This should not be confused with smoothness, which is a more restrictive mathematical concept since it involves differentiability.

[7] See chapter 3 for details.

[8] It is worth mentioning that theorems which relax the rather strict Lipschitz conditions have been established before Flippov by Osgood (1898), Montel (1926), and Nagumo (1926), to name a few, but do not allow for local discontinuity or non-smoothness of the vector field. See [67] for details.

lished [69–72].

Towards the the middle of the 1990's solutions to a new class of problems emerged. It has been noticed that a wide range of real-world processes cannot be modelled with the traditional deterministic Laplacian view of dynamics. The time evolution of numerous differential systems in classical mechanics, circuit theory and physics in general, are not uniquely defined by the initial conditions and past behaviour, although completely describable in terms of deterministic equations [50, 73–75]. This led to a new classification of systems, so-called non-deterministic chaotic or terminal oscillators as described above, which are implicitly defined by non-Lipschitz vector fields. Current research is mainly focused on two branches of non-Lipschitz oscillatory systems. First, although the flow-constructing differential equations are non-smooth,[9] associated Lyapunov function candidates generally satisfy the Lipschitz condition and it is then possible to derive theorems for the unique solutions of the vector field using properties of the smooth non-negative semi-definite Lyapunov stability function [65, 77]. However, in the second category of terminal systems belong those oscillators which do not even possess a Lipschitz continuous Lyapunov function [78,79]. As pointed out before, research is currently still ongoing since considerable large classes of previously not treatable systems [80, 81] are presently under examination and the rather small list of selected references herein is by no means exhaustive. The example encountered in this work falls into the first category of non-Lipschitz systems having a defined and $\dot{C}^1$-continuous Lyapunov function in the interval of the essential singularity.

2.4 Time-domain solution

At the beginning of the second half of the last century simple approximation methods emerged for predicting extreme response values of weakly nonlinear SDOF systems [5–7, 12]. Some of them were soon replaced by approaches giving the exact maximum response displacement and oscillation frequency [8, 9, 13]. Since these new exact methods were only applicable to a few nonlinear systems with very specific properties, more general approximation methods were sought which were suitable for a wider range of oscillators [14, 22, 23, 82, 83]. Details of this still ongoing development were given in section 2.2. The majority of the novel methods did not only allow for the exact or approximate prediction of maximum amplitudes and oscillation periods of the solutions for the nonlinear system, they literally 'suggested' time domain expressions for the nonlinear autonomous system due to their very nature of approximation [84, 85].

However, most of these approaches are only valid for autonomous or periodically excited nonlinear systems. Additionally, for a large number of methods the system under study must be energy conserving. Under such special circumstances the response of the system is termed steady-state and section 2.4.1 of this chapter gives an up-to-date review of methods developed with respect to the specific nature of systems examined here. For many decades almost all of these methods were only applicable to quasi-linear or weakly nonlinear systems, where the coefficient of the linear term is at least one order of magnitude larger than the nonlinear coefficient. Fairly recently

[9] There are several denotation associated with the term 'smooth' [58, 76]. In this work a function $f(x)$ is said to be smooth over an interval $I = \left\{ x \in \mathbb{R} \middle| a \leq x \leq b \right\}$ if and only if $f(x)$ is defined and at least C^1-continuous in I.

significant improvements have been made to well-established perturbation and averaging methods to allow for the solution of systems dominated by the nonlinear terms. However, despite such earlier restrictions on autonomous excitation, non-dissipation and weak nonlinearity a vast number of real-world processes can be modelled satisfactorily [86,87]. In the majority of cases results show good agreement with experimentally obtained data [88, 89].

For nonlinear nonautonomous oscillators the application of analytical techniques is much more problematic. In the case of complex time-varying excitation functions there are numerous examples for linear systems where an explicit closed-form solution is not obtainable, since the integral expressions originating from the Laplace formalism [58, 90] are too difficult to be solved. For nonlinear systems the situation is analogous. Although no explicit integral expressions can be derived due to the invalidity of concepts similar to Laplace, nonlinear algebraic equations, which arise after insertion of potential trial functions, are too complex to yield unique explicit solutions. This already makes it very difficult to find closed-form solutions for nonlinear systems with a constant excitation magnitude, apart from some very special cases [91]. To the author's knowledge there exist so far no general analytical solution for a nonlinear SDOF system taking non-periodic time-varying external forcing into account. A summary of previous research regarding steady-state and transient system behaviour is given in the following two sections.

2.4.1 Nonlinear steady-state response[10)]

In his classical book [31] Nafeyh gives a state-of-the art summary of more than forty years of approximate analytical methods for analysing nonlinear systems of autonomous differential equations. In a subsequent publication [85] these methods are updated and expanded where necessary and new findings are presented. The majority of approaches given either in [31, 85] or other well-known sources [92, 93] deal with weakly nonlinear systems, i.e. the constant coefficient of the linear part in the governing equation is orders of magnitudes larger than all coefficients for the nonlinear parts. Only in the last two decades approximation methods appeared allowing for equally valued coefficients or so-called strongly nonlinear systems, where the linear part can be neglected or completely omitted during the analysis.

Variational approach versus perturbation method

In what can be regarded as a brief summary of contemporarily applied, approximate nonlinear analysis methods, Szulkin *et al* [94] list two approaches heavily utilised at this time: the perturbation method with some of its variants, referring to the original texts (in Russian) of Krylov, Bogolyubov and Mitropolski; and the work of Ritz and Galerkin, originally developed and adopted for the solution of boundary value problems [95]. Largely modified variants of these original perturbation methods are still indispensable today in finding time-domain solutions for nonlinear systems. Analogous for Ritz-Galerkin procedures, which are today classified as variational methods

[10)] It should be noted that the term steady-state response as used in this work is independent of the system excitation. Steady-state response can originate from free vibration, constant value excitation (step loading), or periodic excitation with a well-defined frequency ω_P.

underlining similarities to other weighted-residual procedures [96, 97]. Szulkin *et al* clearly point out the disadvantages of perturbation theory such as weak nonlinearity of the governing equation and high divergence of the solution outside the small approximation interval. The results for the freely vibrating, hardening-type Duffing oscillator are much improved using the Ritz-Galerkin method. In [98] Klotter and Cobb discussed the shortcomings of approximating nonlinear SDOF system response using trigonometric functions in conjunction with the Ritz method. Even for various weakly nonlinear systems a large number of terms in the trial function are needed, in order to model the time-displacement relationship within acceptable error bounds. Since the resulting nonlinear algebraic equations must be solved numerically, this significantly increased the computational work in the early days of digital computing despite the simpleness of a SDOF systems. The authors introduced a specially problem-tailored shape function valid within the the interval of one oscillation cycle to account for differences between the approximate-exact (numerical integration) and the Ritz solution and therefore minimise the overall error. Another successful application of the Ritz method is given by Reif [99], who examined a freely vibrating, hardening-type Duffing SDOF system subjected to the condition all dynamical motion starts from an uncompressed spring position and not, as usually, from the static equilibrium. The newly derived oscillator consist of a complete third-order polynomial stiffness term and all coefficients of both, a two-term and four-term trial function approximation are obtained from an analog computer. Ueda and Matsuzaki [100] employed the Galerkin finite element method as a special case of the weighted residual approach for discretisation of the time domain in order to yield approximate results for the radial displacement of an infinite long cylinder using trigonometric trial functions. Although only a two-term trial solution was chosen, results show remarkable convergence to exact analytical and numerical integration data. Furthermore, no limitations such as weak nonlinearity or small amplitude vibration must be obeyed.

Some of the approximation methods described previously are also suitable for analysing multiple-degree-of-freedom (MDOF) systems, although the increasing number of perturbation parameters significantly increases the complexity of the resulting algebraic equations, which in turn can render the methods incapable of obtaining approximations beyond first order. Huang [101] uses a regular perturbation technique [31] for a weakly nonlinear coupled, linear anchored[1)] and viscously damped two-degree-of-freedom (TDOF) system. However, in a subsequent discussion of these results [102] the author acknowledged that a much simpler iteration method, although mathematically poorly founded compared to perturbation schemes, gives results of higher accuracy. Furthermore, the method can be employed for weakly coupled MDOF systems where the regular perturbation in [101] clearly becomes unsuitable. By using a symmetrical potential energy function Vito [103] derived frequency-amplitude relations for a TDOF system employing a single-term approximation. However, serious drawbacks of the methods arise from assuming small vibration amplitudes and weakly nonlinear coupling and anchoring forces. This implies that the actual mode shapes of the nonlinear oscillator are independent of amplitude, which is clearly not the case for general nonlinear systems [104]. Bailey [105] applied the Ritz method to the double

[1)]The anchoring spring connects the MDOF systems to a rigid base.

pendulum with large amplitude vibrations and Scharle [106] examined the relationship between different approximation methods dwelling on the difference in concept of the approximation and the approximation technique itself.

Bal [107] gives a time-history approximate solution for the harmonically excited Duffing equation using the least-square method together with a unique weighting function derived from the cross-correlation between excitation and system response. Due to the fact that the trial solution is a one-term trigonometric function, results do not compare well to numerical integration. Using a three-term testing function Groves [108] solved the same problem of a harmonically excited softening-type Duffing system using algebraic manipulation software to obtain explicit expressions for the algebraic nonlinear equations for determining the solution approximation coefficients. However, he could only establish a proof-of-concept, not a proof of the suggested method itself since he assumed that the system response frequency and excitation frequency were identical.

Classical methods and ultraspherical polynomials

Using ultraspherical polynomials[12)] (UP) introduced by Denman *et al* [110,111] and others [112–114], Sinha and Srinivasan [115] examined two freely vibrating SDOF systems, one with cubic and quintic nonlinear restoring force terms and one with linear damping and quadratic and cubic stiffness terms. For certain parameters in the UP trial functions the approach is identical to the well-known and commonly used Krylov-Bogolyubov-Mitropolski method (KBMM) [85]. Although a time-displacement analysis was presented, only amplitude values and oscillation period were obtained and results compare rather poorly against numerical integration for high amplitudes of oscillation. Having shown that the ultraspherical polynomial approximation method (UPAM) is a generalisation of KBMM, Rangacharyulu and Srinivasan [116] introduced modifications which allow for interpretation of the UPAM as a Galerkin procedure. For the free vibration of a weakly nonlinear two-degree-of-freedom system (TDOF) with viscous linear damping Rangacharyulu *et al* [117] obtained approximate time-displacement solutions using the UPAM together with harmonic trial function of a single frequency, hence the method breaks down near internal resonant points. The same authors used for a similar TDOF system [118] with no damping but a weakly nonlinear, hardening Duffing-type coupling spring the KBMM to obtain equations for amplitude and phase. They identified that UPAM does not lead to any closed form solutions, since it simply transforms the oscillator's governing equations into a coupled Ricattian system [68, 76] for which no general simplification is known. A general examination of a transformation technique partially used in [118] for rewriting nonlinearly damped systems as linear systems is given in [119, 120]. However, results with acceptable accuracy can only be established for a specific class of nonlinear damped oscillators having linear stiffness terms. Srirangarajan and Srinivasan [121] use UP for solving third-order, homogeneous, weakly nonlinear equations. For a linear viscously damped TDOF system subjected to unidirectional blast-type loading (exponential

[12)] Also named Gegenbauer polynomials. Ultraspherical polynomials are orthogonal with respect to a specific weighting factor defined in the interval $[-1, 1]$. For certain discrete parameter values they reduce to Chebyshev or Legendre polynomials [58, 109].

decay and cosine function half-period) with linear anchoring but nonlinear coupling spring Rangacharyulu [122] applied a coordinate transformation to obtain the governing differential equation in a form suitable for the KBMM and UP trial functions. However, the same disadvantages of the method as mentioned above, weakly nonlinearity, small response amplitudes, etc., make it unfeasible for the problems considered herein.

Improved algorithms for classical methods

Tamura *et al* correctly pointed out in [123] that most of the perturbation methods above are confined to approximate the fundamental harmonic of the nonlinear system and tend to cause serious problems or even break down if one attempts to obtain higher-order harmonic components, which are clearly contained in the nonlinear system [92, 124, 125]; hence their inclusion into the approximate solution would therefore be highly beneficial to the overall accuracy of the method. Based on the work of Hayashi [126] and others, the authors derived a multi-harmonic balance method for selected, weakly nonlinear systems, which allows for the simultaneous calculation of all desired higher harmonic terms. Although the computational effort grows significantly, accuracy is clearly improved.

It is important to mention that despite numerous disadvantages of the above perturbation methods (KBMM, Linsted-Poincaré, WKB, MMS, etc.), see [31, 85, 127] for details, most of the schemes which allow for the analytical approximation of solutions can be used to determine its existence, uniqueness, stability and reliance on parametric values. For example, Awrejcewicz [128] used the HB method and developed for both, the perturbation parameter and the vibration amplitude (which was assumed to be small), a series approximation for analysing Hopf bifurcation in Mathieu-Duffing oscillators [92]. The author obtained expressions for the parameter-frequency-amplitude relations in the case of forced systems close to and far from resonance.

Having developed such useful tools as these perturbation methods, it comes as no surprise that tremendous efforts have been made to overcome the above restrictions of small amplitude vibrations or strictly linear viscous damping, but most of all the confinement to small system nonlinearities including the inability of all approaches to derive from the perturbation itself the feasible range of the nonlinear terms in the governing equations.

Classical methods using elliptic functions and augmented systems

Bravo Yuste *et al* [129–131] presented an enhancement of the KBMM where Jacobian elliptic functions are used instead of the commonly accepted trigonometric ones and called it an extended KBMM (EKBMM). Although the derived averaging integral expressions are more difficult to solve analytically, the restriction to quasi-linear systems as required for the KBMM is no longer necessary, hence the new method is applicable to free vibration of a vast range of nonlinear systems. In a series of papers Bravo Yuste and Diaz Bejarano [132], Garcia-Margallo and Diaz Bejarano [133], Mickens [134], Diaz Bejarano [135], Garcia-Margallo *et al* [136], Diaz Bejarano and Martin Sanchez [124], and Garcia-Margallo and Diaz Bejarano [137] derived a generalisation

of the well-established HBM to account for improved convergence and a wider range of applicable nonlinear systems. Based on the Fourier expansion of elliptic functions they introduced approximate analytical solutions for freely vibrating Duffing and Van-der-Pol systems where the nonlinear coefficients do not necessarily need to be small. Chen *et al* [138] introduced Jacobian elliptic functions into the HBM analysis of second order polynomial-type systems.

Combining the method of multiple scales (MMS) with a so-called δ-expansion, Bender *et al* [139] could transform the classical MMS to a new method suitable for calculating approximate results for strongly nonlinear unforced Duffing oscillator with a satisfying error level. A combination of the MMS with elliptic functions has been shown by Belhaq and Lakrad [140] for a similar class of autonomous systems.

Senator and Bapat [141] used the work of Jones [142], Mickens [134], Rahman and Burton [83], and Eminhizer *et al* [143] to extend the Lindstedt-Poincaré small nonlinearity based perturbation method by adding the characteristics of a physically non-existent neighboring linear oscillator in order to derive time-history solutions for strongly nonlinear, conservative and freely vibrating systems. Further modifications were presented by Chen and Cheung [144] and Yang *et al* [145] using Jacobian elliptic functions.

Sotiropoulou and Panayotounakos [146] introduced a transformation method which reduces second-order nonlinear ordinary differential equations to integro-differential and Abel's classes of equations. More importantly, the authors proved that there exists no analytical, closed-form solution to the harmonically excited, conservative Duffing oscillator. In a series of papers Cveticanin [147–154] presented different approaches for the approximate exact solution of TDOF strongly nonlinear systems which possess complex coefficients.

Analytical-numerical solution methods

Numerical integration methods are regarded as the most suitable approach for strongly nonlinear system due to their flexibility and independence from specific generating solutions of the system or its initial conditions [1, 2, 155–159]. However, serious problems arise in handling unstable solutions and convergence rates are extremely low near solution bifurcation points, sometimes convergence cannot be achieved at all. Furthermore, no definite statements about existence, uniqueness or stability can be made. Depending on the size of the problem, determining parameter regions of interest and stability can be computationally very expensive. By combining a classical perturbation scheme with an numerical iterative method similar to the Newton-Rhapson algorithm [160], Chan *et al* [161, 162] treated freely vibrating Duffing and Van-der-Pol systems reaching good agreement with numerical data for moderate and strong nonlinear oscillators. A similar approach presented by Lau and Cheung [163] and Lau and Yuen [164] established an incremental HBM. However, the scheme requires certain *a priori* knowledge of the nonlinear system under study and is therefore less versatile. Very recently these approaches have been simplified by Chung *et al* [165]. Wu and Lim [166] generalised an approach introduced in [167, 168] which is based on the combination of the linearisation of the governing equation with the HBM, this omits sets of equations with complex nonlinearities as required in the classical HBM [85]. The method

is simple and delivers accurate results for strongly nonlinearities when applied to homogeneous conservative systems.

Employing a special time-transformation method Qaisi [169] reformulated the governing equation of the harmonically excited, conservative and hardening-type Duffing oscillator in such a way to make it accessible for the power series method. Although the approach can be applied to other nonlinear systems, convergence of the solution is only guaranteed under vaguely specified conditions. Li and Wu [170] present a generalisation of Micken's iteration procedure [171] by analysing free vibration of a SDOF system where the strongly nonlinear restoring force does not necessarily be an odd function. Maccari [172] analysed the transient and steady-state response of a general nonlinear oscillator containing third-order stiffness and damping terms, including respective cross-products, which is subjected to a multi-harmonic excitation function using the asymptotic perturbation method. An interesting approach is shown by Cai *et al* in [173]. The authors used the least square numerical method to transform general nonlinear homogeneous ODEs into Duffing-type equations for which exact analytical solutions are available. Although the scheme is applicable to a small number of differential systems only, problems involving nonconservative strongly nonlinear oscillators can be solved.

Using a newly derived expansion method such that strongly nonlinear systems are transformed into weakly nonlinear systems, Ge and Ku [174] employed the less well-known Melnikov approach for small nonlinearities [175,176]. Obtaining parameters for a time depending trial solution from a conventional perturbation scheme, Mandal [177] presented poor results in an attempt to model the time history of the harmonically forced Duffing oscillator.

Evaluating the afore mentioned shortcomings of classical small-parameter perturbation techniques, He [178] presented a detailed overview of recently developed methods, mainly by the author himself based on the work of many other researchers, which are not restricted to weak nonlinearities or small amplitude vibrations. This includes, amongst others, a variational iteration method using Lagrange multipliers [22], homotopy, parameterised and linearised perturbation methods[13] [23, 44, 181], a modified Linstedt-Poincaré approach and a modified Adomian decomposition method [182,183].

Solutions for equivalent system configurations

All of the papers mentioned so far deal with a variety of different systems, since quite regularly the authors apply specially tailored methods for specific classes of nonlinear oscillators such as Duffing or Van-der-Pol type characteristics, which have received much attention in literature. In chapter 3 of this work a strongly nonlinear polynomial type restoring force f_1 will be introduced which has only been referenced sparsely. However, some publications do exist, including a number of papers examining similar stiffness-type forces. Lipscomb and Mickens [184] gave an exact analytical solution for a second-order differential equation containing the signum function term. Dividing the system into different regions of stability enabled the authors to derive solutions for

[13]The term 'homotopy perturbation method' stands for the methodological and mathematical coupling of the theory of homotopic topological spaces and perturbation theory. A homotopy is a continuous transformation from one function to another [179, 180].

piecewise linear equations. Potti and Sarma [185] proposed a Fourier series approximation for the solution of the problem, although the authors do not explain how to expand the signum function with respect to time without knowing the solution of the differential equation beforehand. Instead of using trigonometric functions in Fourier series, and thus avoiding unnecessary error sources due to the Gibbs phenomenon [186], Pilipchuk [187] employed a saw-tooth time transformation (STTT) [188] and obtained the exact solution to the problem [185]. Furthermore, for a similar but more complex nonlinear restoring force an approximate result is given. The restoring force under consideration in Awrejcewicz and Andrianov [189] has the same mathematical structure as f_1. However, the authors only derived reasonably accurate time-displacement solutions for free vibration with a restricted set of initial conditions (zero initial displacement) and very small values of the nonlinear stiffness term.

The above summary of publications listing numerous analytical approximate methods for weak and strong nonlinear systems outlines advantages and disadvantages of almost all approaches available today. However, this review is by no means complete. It is intended to give a selected overview of schemes appropriate for the nonlinear problems encountered in later chapters of this work.

2.4.2 *Nonlinear transient response*

Classical perturbation theory

Some of the results [190–194] arguably belong to the previous section since they resemble steady-state response behaviour of the nonlinear system under consideration. However, most of the systems examined by Ariaratnam and Bauer are subjected to time-varying impulses. Unfortunately, the Lighthill-Lindstedt-Poincaré perturbation method [31, 85] employed can only account for weakly nonlinear systems and produces large errors if the nonlinear coefficients reach the same magnitude as the largest linear one. Furthermore, the approach can only deal with unidirectional excitation and the force magnitude must change smoothly over time. Srirangarajan and Srinivasan [195] presented a modified approach which allows for the inclusion of linearly damped systems. Applying the solution of the linear problem as a transformation function gives the original nonlinear problem in a form for which Anderson's UP [114] can be used. Results are derived for cosine and exponentially decaying impulses, but compare poorly to numerical data (Runge-Kutta) for dominant nonlinear parameters and excitation magnitudes. In [196] Sinha and Srinivasan proposed time-displacement history approximations for moderately nonlinear systems with non-small response amplitude and weakly nonlinear damping subjected to step excitation by employing UP. For special sets of parameters, results of the amplitude attenuation curves compare well to numerical integration data. However, comparison between single oscillation cycles shows much less similarity.

Extended perturbation theory

White [197] discussed the problem of nonlinearity occurrence in transient analysis experimental data and the importance to know whether the nonlinear distortion is caused by genuine system behaviour or simply errors in the experimental setup and data capture. Although the intention of the paper lies in rasing awareness of the effects of nonlinearity, rather than presenting a comprehensive analysis procedure, the overall approach remains questionable due to repeated application of linear convolution techniques only justified by the fact that all nonlinear terms in the systems under study are 4 to 5 orders of magnitude smaller than the largest linear term.

Similar to [196], Anderson [198] used his previously introduced UP for weakly damped SDOF systems subjected to step function excitation. Although the method gives results with small overall error, it is restricted to moderate nonlinearity and small excitation amplitudes. Beshai and Dokainish [199] can prove that Bauer's approximation [191–194] is valid only for very short time intervals. By splitting the anticipated solution of the weak nonlinear stiffness-type oscillator into a homogeneous and a particular integral part as used for linear systems, the authors obtain reasonable results for weakly nonconservative, step excited systems.

Integral transformations

Based on a Volterra integral series [200], Sato and Asada [201] applied a multidimensional Laplace transform to obtain a frequency domain transfer function for the moderate nonlinear system. However, apart from the questionable fact of repetitive use of the linear transformation kernel,[14] definitely not applicable to non-weak nonlinear systems, the two main problems of the suggested approach are due to association of variables in the complex transformation process (in fact, the examples presented by the authors were based only on a two-term approximation due to complications in variable identification), and the inverse transformation from complex Laplace to real-valued time domain, which largely relies on a numerical algorithm developed by Hosono [202]. Nevertheless, for half-sine wave external force application to small nonlinearity-amplitude oscillators results compare well to Runge-Kutta data.

A similar approach was pursued by Chandra Shekar *et al* [203], where the authors employed a regular perturbation technique to separate approximation terms of the same order and separately Laplace transform each linear differential equation. Results were obtained for SDOF systems weakly nonlinear in both damping and stiffness terms and subjected to transient unidirectional loading functions of various shapes. Although damping was allowed to reach moderate levels (critical damping ratio up to 0.1), stiffness nonlinearity must be small. For a wide range of parameters results compare well to numerical data but the method breaks down near resonance points, i.e. when excitation and response contain identical harmonic components of the same order.

[14] In general, the kernel of the Laplace transformation as a linear integral operation is the Dirac-impulse response of the linear system.

Differential transformation technique

An entirely different approach was employed by Abbasov *et al* [204]. In order to avoid difficulties arising from the usage of integral transforms (Laplace, Fourier) for nonlinear problems;[15] a differential approach is suggested based on the Taylor series expansion and therefore termed Taylor Differential Method or Taylor Differential Transform (TDT). The origin of the TDT remains somewhat obscure until today. Most researchers in the western hemisphere claim Zhou [205] introduced the method first. However, the Ukrainian scientist and engineer Pukhov published as early as 1978 articles clearly laying out the fundamentals of the method [206–208]. There has been much discussion about this issue in the past [204].

Although the method is relatively new, it is used across numerous fields in engineering; there are several reasons for this. Firstly, due to its flexibility it allows for application to nearly all known problems in nonlinear system analysis ranging from simple freely vibrating SDOF oscillators showing well-studied, analytically formulated steady-state response pattern, to nonlinear-dissipative nonautonomous systems with complex, explicitly time-varying excitation force resulting in highly transient response behaviour. Secondly, application of the TDT scheme is not limited to SDOF oscillators only. In fact, although resulting algebraic equations become rather complex, MDOF systems with many degrees of freedom can be treated likewise. Generally speaking, TDT can be applied to any linear or nonlinear system regardless of whether differential, differential-difference or integro-differential equations are involved. Thirdly, compared to many other methods listed above, convergence of TDT is generally very good since it is an exact series approximation, thus in case of poor convergence, including more terms of the series guarantees that the approximate solution reaches the exact unique solution of the system. This is a mathematically justified inherit feature of the approach, not common for some of the schemes introduced above. Fourthly, the ability to obtain both numerical (spectra) and analytic (power series or functional series) solutions of the differential equations under study is one the most important advantages of the TDT. Despite these excellent qualities of the method together with the fact that it can be employed for solving a great diversity of problems, TDT has been used sparsely only in the past by a relative small group of researchers. However, awareness of the method is continuously increasing in recent years. Suitable examples are given in Chen and Ho [209] who used TDT to obtain nearly exact eigenvalues for the classical Sturm-Liuoville problem, Bert [210] and Yu *et al* [211] who analysed the steady-state heat conduction in tapered fins and Chen and Ju [212] who solved transient advective-dispersive transport problems employing differential transformation.

The analysis of strongly nonlinear dissipative second-order IVP using a single time step was given in [212, 213]. This must be seen as very basic approach and acceptable results are only obtained if either a large number of terms in the approximation series are included or the time horizon of interest is made small. Failure to do so leads to significant errors which have been unnoticed by Chen and Wu [214] if compared to the exact analytical solutions available for the Duffing system or measured against results obtained using other well-established numerical routines. However,

[15] Usually, non-real valued integrals of the inverse transform are too difficult to be solved analytically.

accuracy can be significantly increased by dividing the time domain of interest into an arbitrary number of fixed-size sub-domains as shown in [215–217] for similar systems. In addition, computational efficiency is considerably improved by introducing an adaptive stepping algorithm rather than constant time steps and ensuring the local error in each step does not exceed a given tolerance. Successful implementations of this idea for autonomous differential systems have been introduced by Jang *et al* [218] and Kurnaz *et al* [219].

Utilising the well-known fact that every higher-order differential equation can be written as a coupled system of first-order equations Hassan [217] and Chen *et al* [220] obtained highly accurate results for strongly nonlinear, harmonically excited dissipative systems having up to four coupled differential equations. Although the error is significantly minimised compared to generally employed embedded Runge-Kutta algorithms, the method is computational more expensive due to a constant time-stepping. The idea of an adaptive TDT routine for first-order autonomous systems has been brought forward to by Jang *et al* [218] and Kurnaz *et al* [219].

Current research is concerned generalising the TDT to n-dimensional partial differential equation problems [221] and the possibility of employing polynomial transformation in order to increase accuracy of the Taylor approximation around a given point and thus significantly improving computational efficiency of the TDT algorithm for large time domain intervals [222–225].

2.5 Summary

The literature review presented in this chapter is quite comprehensive. Although by no means exhaustive, the different aspects of nonlinear system dynamics covered in the thesis make it necessary to incorporate such a vast range of publications. The study of the nonlinear SDOF system is in itself a large subject and source of published work and methodologies, such as the Harmonic Balance Method, the method of Multiple Time Scales, etc. Novel expressions for extreme value response will be given in the next chapter, partially building on the results introduced in section 2.2. In order to ensure existence and uniqueness of these new solutions for the non-Lipschitzian f restoring force system the terminal behaviour as discussed in 2.3 must be ruled out. This is essential as otherwise one cannot defend the solutions obtained as being the only ones possible. Finally, chapters 4 and 5 investigate explicit time-domain response expressions for nonlinear steady-state and transient systems, thus referring strongly to publications listed in section 2.4. In particular, the novel use of the Taylor Differential Transformation allows an algebraic set of equations to replace the integration of a set of differential equations.

CHAPTER 3

NONLINEAR AUTONOMOUS SDOF SYSTEMS EXTREME VALUES OF THE TRANSIENT RESPONSE

3.1 Introduction

In this chapter the theoretical framework will be derived for obtaining particular single-valued response parameters of nonlinear, conservative and autonomous single-degree-of-freedom systems (SDOF). These include extreme (minimum/maximum) solutions for displacement, velocity and acceleration as well as the fundamental oscillation frequency together with its higher harmonics for representation in terms of trigonometric functions, where possible. There are no restrictions regarding the nature of the non-dissipative nonlinear restoring force such as association to certain classes of fundamental functions [226, 227]. The second-order differential system can have arbitrary initial conditions, contrary to [3], and the excitation force does not have to be unidirectional [7]. All results presented are in closed form, but cannot always be given explicitly. Furthermore, the well-known solutions for the linear oscillator are incorporated as special cases and can easily be obtained by setting the appropriate nonlinear terms to zero.

The following section 3.2 describes the second-order, ordinary differential equation of motion of the general system under study. Well-known elements of the established theory of local and global stability analysis for nonlinear systems will be introduced, which are relevant for the specific types of oscillators considered in this chapter. This includes various theorems assuring the existence and stability of closed orbits and associated fixed points as well as their interrelation. It will be shown that for the specific autonomous system in question local stability analysis does not give conclusive results and the theory of Lyapunov must therefore be used in order to facilitate a global analysis. However, due to the very special nature of feasible Lyapunov function candidates for the problem, LaSalle's Invariant Principle becomes necessary to finally dispel remaining ambi-

guity with respect to unstable domains in the phase plane of the planar system. Additionally, Morse theory will be employed to prove orbital stability of the solution originating from the Hamiltonian of the oscillator. Although large parts of section 3.2 contain a fair amount of formalism and might be difficult to understand or to follow for the inexperienced reader, they are absolutely necessary prerequisites for a complete analytical solution analysis of specific nonlinear examples presented in section 3.4.

Novel closed-form expressions valid for autonomous conservative systems with arbitrary restoring force are derived in section 3.3. A simplification of these general results ultimately leads to solutions for special cases presented before elsewhere [3,7–9,11,41,228].

Subsequently, these new solutions are verified in section 3.4 by examining two examples of typical polynomial-type nonlinear restoring forces previously adopted and described in the literature. The nonlinear term $f_1(u) = k_\beta \operatorname{sgn}(u)\ |u|^b$ has mainly been investigated by Timoshenko *et al* [3] and Bapat *et al* [8], but solutions were confined to either free vibration, zero initial conditions or specially selected parameter values for the nonlinear function f_1. However, the results presented in what follows are not tied to such restrictions and have therefore a much wider range of application. Due to the mathematical nature of f_1, i.e. it fails to satisfy the important Lipschitz condition, large emphasis is placed on establishing alternative theorems in section 3.4.1, which clearly guarantee uniqueness of solutions for the nonlinear problem.

The second nonlinear force $f_2(u) = k_\alpha\, u + k_\beta\, u^3$ considered in 3.4 is the well-known and extensively studied Duffing oscillator [4,15,18–21,39,40,82,83,169,229]. Due to the parameters involved, there are three possible variations of $f_2(u)$ all having different response characteristics and stability domains. Basic results for some versions of the Duffing system regarding existence, uniqueness and phase plane stability can be found in [61,92,230], for example. Section 3.4.2 extends these results and gives precise criteria of stability for all three types for the most general case of the conservative, autonomous second-order differential problem: non-zero initial values and a constant right-hand side forcing term. To the author's knowledge, such generalised results have not been published previously.

Furthermore, based on enhanced solutions of Bapat *et al* [8] derived herein, expressions for the phenomenon of multiple oscillation frequencies for certain system parameter combinations of both restoring forces are obtained. Similar predictions are stated elsewhere in connection with analytical approximation schemes such as the method of harmonic balance, the method of Krylov-Bogolyubov-Mitropolski or general perturbation techniques [15,17,139,142]. However, the results presented in this work clearly prove that this multiplicity in terms of trigonometric functions is an inherit feature of the nonlinear system itself, obtainable via the exact analytical solution using special tabulated functions.

Finally, section 3.5 offers a brief summary and overview of all newly derived results and attempts to show how these will be used in subsequent chapters.

3.2 The equation of motion and stability considerations

The nonlinear equation of motion of a non-autonomous, dissipative SDOF system is given as an initial value problem (IVP) of the form [231]

$$m\ddot{u}(t) + f\big(t, \dot{u}(t), u(t)\big) = P(t) \qquad f,\ m,\ P,\ t,\ u,\ \dot{u},\ \ddot{u} \in \mathbb{R}, \quad t \geq 0 \tag{3.1}$$

where m is the oscillating mass, $u(t)$, $\dot{u}(t)$, $\ddot{u}(t)$ denote displacement, velocity and acceleration, respectively, and $f\,(t, \dot{u}, u)$ represents the nonlinear restoring force due to any kind of damping and elastic or nonelastic/plastic stiffness mechanism occurring in the system. The expression on the right hand side can in its most simplest form be written as $P(t) = p_0 \times p_t(t)$ where p_0 is the constant force amplitude and $p_t(t)$ is a pure time-varying function. If the excitation is constant with time then Eq.(3.1) reduces to the equation of motion for an autonomous system

$$m\ddot{u}(t) + f\big(\dot{u}(t), u(t)\big) = p_0\,. \tag{3.2}$$

Furthermore, letting f be independent of $\dot{u}(t)$, i.e. $f = f(u)$ is a function of the displacement only, gives the equation of motion for an autonomous energy conserving system as

$$m\ddot{u}(t) + f(u) = p_0\,, \tag{3.3a}$$

subjected to arbitrary initial conditions

$$u(t=0) = u_0 \qquad \text{and} \qquad \dot{u}(t=0) = \dot{u}_0\,. \tag{3.3b}$$

Using the substitutions $u_1 = u$ and $u_2 = \dot{u}$ one can rewrite the second-order differential equation (3.3) as a general first order system [92]

$$\dot{\mathbf{u}} = \mathbf{F}\,(\mathbf{u}\,;\,\mathbf{z}) \qquad \text{with} \qquad \mathbf{u}\,(t=0) = \mathbf{u}_0 \tag{3.4}$$

where $\mathbf{u} = \{u_1\ u_2\ \ldots\ u_m\}^{\mathrm{T}}$ is the finite, m-dimensional state vector defined in $\mathbf{u} \in \mathbb{R}^m$, $\mathbf{z}$ the vector of control or auxiliary parameters with dimension n, $\mathbf{z} \in \mathbb{R}^n$, $\mathbf{F}$ the nonlinear vector field, and $\mathbf{u}_0$ the vector of initial conditions. With respect to (3.3a) it follows that $\mathbf{u} \in \mathbb{R}^2$. It is important to point out that in some cases the differential equation cannot be written as in (3.4). Instead, the more general implicit form

$$\mathbf{F}\,(\mathbf{u}, \dot{\mathbf{u}}; \mathbf{z}) = 0 \tag{3.5}$$

must be given since it is not always possible to solve (3.5) in terms of $\dot{\mathbf{u}}$. However, derivation of definitions, theorems and results presented in this and following chapters assumes that the dynamical problem under consideration can be explicitly stated as in (3.4). Customising these findings to the more general system in (3.5) can be a complex task [232].

For autonomous systems the vector field $\mathbf{F}$ is a map in the state space such that

$$\mathbf{F} : \mathbb{R}^m \times \mathbb{R}^n \rightarrow \mathbb{R}^m \,, \tag{3.6}$$

and a solution $\mathbf{u}(t)$ of (3.4) is referred to in this work as a continuously differentiable function of time t satisfying [233]

$$\mathbf{u}(t) = \mathbf{u}_0 + \int_0^t \mathbf{F}\big(\mathbf{u}(\tau)\big)\, \mathrm{d}\tau \,. \tag{3.7}$$

Equation (3.7), often referred to in literature as integral form of the solution of the IVP (3.4) or solution in the sense of Carathéodory [234], clearly ensures dependency on the initial conditions $\mathbf{u}_0$. It is easy to see that (3.7) is derived from (3.4) by integration, hence both equations are equivalent. Intuitively, if (3.4) is a $\mathcal{C}^r$-continuous vector function, any solution $\mathbf{u}(t)$ of the given vector field $\mathbf{F}$ satisfying (3.7) is in general $\mathcal{C}^{r+1}$ continuous. This statement is put on a rigourous mathematical basis by the theorem of regularity [235].

An important property of an autonomous system is monotony of its solution. Since the field in Eq.(3.4) consists of parallel vectors tangent to the solution (3.7) for all t because $\mathbf{F}(t, ...) \equiv \mathbf{F}(...)$, it is easily understood that for two solutions of (3.4) with

$$\|\mathbf{u}_1(t_0)\| < \|\mathbf{u}_2(t_0)\| \qquad \text{this implies} \qquad \|\mathbf{u}_1(t)\| < \|\mathbf{u}_2(t)\| \quad \forall\, t \,. \tag{3.8}$$

3.2.1 *Existence and uniqueness of equilibrium solutions and closed orbits*

In order to derive the results presented in sections 3.3 of this chapter, a number of definitions and assumptions for the general system in (3.4) have to be made, which are given in what follows. First, because of (3.6), the oscillator (3.4) is invariant to shifts in the time origin and, due to the translation property [230], if $\mathbf{u}(t)$ is a solution, then $\mathbf{u}(t + t_1)$ is also a solution of (3.4) for any arbitrary t_1. Furthermore, (3.4) is assumed to have a nontrivial[1)] periodic solution $\mathbf{u}(t)$ of least finite period $T > 0$ such that

$$\mathbf{u}(t_0) = \mathbf{u}(t_0 + T) \tag{3.9}$$

where $\mathbf{u}(t_0 + t) \neq \mathbf{u}(t_0)$ for $0 < t < T$. Equation (3.9) as solution of (3.4) represents a closed orbit Γ_c in the state space $\mathbb{R}^m$ [92]. Whether such periodic solutions do not exist for any given oscillatory system in the two-dimensional state space $\mathbb{R}^2$ is established using Bendixson's criterion [236], which states that the divergence

$$\nabla \cdot \mathbf{F}(\mathbf{u}, \mathbf{z}) \tag{3.10}$$

[1)] The term *nontrivial* is employed to exclude constant solutions corresponding to stationary points. Such solutions satisfy (3.9) but do not describe oscillation.

of the field in (3.4) must change sign or stay equal zero if the trajectory of (3.4) is a periodic orbit in the simply connected region[2] $D \subset \mathbb{R}^2$. Bendixson's criterion is a special case of Dulac's criterion [61] where the real-valued C^1-continuous Dulac function $G(\mathbf{u})$ is equal to 1. If

$$\nabla\Big(G(\mathbf{u})\ \mathbf{F}(\mathbf{u},\mathbf{z})\Big) \tag{3.11}$$

is of constant sign and not identically zero in D, then (3.4) has no periodic orbit lying entirely in the simply connected domain D. The proof for both theorems (3.10) and (3.11) is straightforward since it simply bases on Green's rule [58, 186]. Similar to finding a Lyapunov function for direct stability analysis, see section 3.2.3 below, no general method exists for determining an appropriate $G(\mathbf{u})$ for a given two-dimensional set of differential equations. Examples where Eq.(3.10) is insufficient to exclude the existence of periodic orbits and (3.11) must be used instead are presented in [92].

It is important to note that both criteria in (3.10) and (3.11) are only necessary but not sufficient for the existence of closed orbits Γ_c. Even if a given system fails to satisfy either of the two conditions, one or more Γ_c can still exist. This incompleteness can be overcome by using one of the key theoretical results[3] in nonlinear dynamics, the Poincaré-Bendixson theorem. A variety of different formulations of the theorem can be found in literature but the essence is summarised as follows

> **Theorem 1 (Poincaré-Bendixson).** *Let $R \subset \mathbb{R}^2$ be a compact, positively invariant set for the flow $\mathbf{F}(\mathbf{u},\mathbf{z})$ of the continuous time (no map), autonomous and planar dynamical system* (3.4) *and assume that r is a bounded orbit. Then, if R contains only ordinary points (no equilibrium points), $\omega(r)$ is a closed orbit of* (3.4).

Informally, a region, domain or set is positively (negatively) invariant if trajectories beginning in it are confined to it for all positive (negative) times. Furthermore, all compact sets in $\mathbb{R}^n$ are closed[4] and bounded[5] sets [238], and hence, the ω-limit set (or cycle) $\omega(r)$ of the orbit r is not empty, i.e. at least one orbit exists. The idea of the Poincaré-Bendixson theorem is intuitively clear, its proof, however, is rather complicated because of the topological statements involved [76]. There are some remarks to be made considering the above presented formalism.

First, the simple example of the linear oscillator [239] emphasises the fact that Poincaré-Bendixson assures the existence of a periodic orbit but not its uniqueness. In fact, a slightly modified version [231] concludes that the number of both critical points and periodic orbits in the compact invariant set R remains unknown. Second, since the invariant region or set as well as

[2] A domain D is simply connected if, for every simple closed curve C in D, the inner region of C is also a subset of D. A simply connected region or domain can be smoothly contracted to a point [58]. Colloquially speaking, simply connected means there are no 'holes' or 'separate parts' within D.

[3] The theorem rules out *deterministic* chaotic behaviour of continuous time planar (2-dimensional) system by limiting the possibilities of motion in the phase plane. In higher-order systems $n \geq 3$ Poincaré-Bendixson no longer applies and chaos can emerge, see the Lorentz system [237] for example. However, for discrete time systems (maps) chaotic behaviour is possible even in one dimension [238]. Furthermore, theorem 1 does not account for terminal or non-deterministic chaotic systems, which do not satisfy the Lipschitz condition (3.12).

[4] A set $S \subset \mathbb{R}^n$ is closed if and only if every convergent sequence $\{u_k\}$ with elements in S converges to a point in S [58]. An example in $\mathbb{R}^1$: the closed interval of real numbers $[a,b]$.

[5] A set S is bounded (above and below) if there is a $c > 0$ such that $\|u\| \leq c\ \forall\, u \in S$.

the orbit may be large, Poincaré-Bendixson is not a localised theorem although there might be several sets R_i with $i = 1, 2, ..., \infty$ containing closed orbits in the entire phase space $\mathbb{R}^2$. Third, Bendixson's/Dulac's criterion and the Poincaré-Bendixson theorem only apply to generic two-dimensional systems ($n = 2$) as considered in this work. A generalisation to higher-order systems $n > 2$ is not realisable mainly due to the fact that the proof for the theorem relies on the Jordan curve lemma[6] [230]. More reasons why Poincaré-Bendixson is not easily proven for higher-order spaces $\mathbb{R}^n$ are given in [240] for C^1 flows in $\mathbb{R}^3$ and C^∞ flows in $\mathbb{R}^4$. Fourth, neither Bendixson/Dulac nor Poincaré-Bendixson can predict the existence of limit cycles[7] (isolated periodic solutions), rather than that of closed orbits, which becomes important in later chapters in the discussion of nonconservative systems. The fifth and last remark is concerned with the interrelation of closed orbits and critical points as employed in the equilibrium counting of the index theory [242]. In short, the theory says that for every periodic orbit there exists at least one equilibrium point. Depending on the nature of the equilibrium (saddle, node, centre, etc.), as will be established in the following section 3.2.2, the orbit surrounding it is associated with a real number, the so-called Poincaré index[8].

In order to analyse the stability of stationary points at the centre of Γ_c, and hence the closed orbit itself, it must be guaranteed solution (3.9) does exist for every set of initial conditions $\mathbf{u}_0 = \{u_0, \dot{u}_0\}^T$ and all feasible ranges of the parameters contained in the auxiliary vector $\mathbf{z}$ in (3.4). Furthermore, the obtained solution has to be unique, i.e. it needs to be ensured (3.9) is the only solution[9] of (3.4) for any given set of $\mathbf{u}_0$ and $\mathbf{z}$, which is not guaranteed by any of the above given theorems.

As a first step it is supposed $\mathbf{F}(\mathbf{u}, \mathbf{z})$ is continuous in $\mathbf{u}$, from which it immediately follows that $\mathbf{u}(t)$ is continuous due to the requirement in (3.7). Moreover, if $\mathbf{F}$ is a C^r function of all three quantities t, $\mathbf{u}$ and $\mathbf{z}$, then the associated solution $\mathbf{u}(t)$ of system (3.4) is also at least a C^r function of t and $\mathbf{z}$ [230], but in most cases $\mathbf{u}(t)$ is even C^{r+1}. Usually, one would define $\mathbf{F}(t, \mathbf{u}, \mathbf{z})$ continuous in $\mathbf{u}$ but piecewise continuous in t where any solution $\mathbf{u}(t)$ could only be piecewise differentiable with respect to t [231]. This assumption for nonautonomous systems, which makes it possible to include piecewise continuous time-varying input forces with multiply occurring step-like properties, such as a (rectangular) impulse train, is examined in chapter 5. However, returning back to the autonomous system in equation (3.4) it is easy to find an example which proves that continuity alone does not guarantee a unique solution.[10] In fact, continuity of $\mathbf{F}(\mathbf{u}, \mathbf{z})$ in its arguments solely ensures that there exist at least one solution $\mathbf{u}(t)$ such that (3.7) is satisfied [76]. Therefore, another condition must be imposed on (3.4), which can be found in

[6] The theorem states that a closed curve in $\mathbb{R}^2$ which does not intersect itself separates $\mathbb{R}^2$ into two connected components, one bounded and one unbounded [58].

[7] Every limit cycle is a closed orbit. The converse is, however, not true [241].

[8] If a critical point is classified as either a node, focus or centre is has the index $+1$.

[9] Uniqueness of solutions of the flow (3.4) ensures that the vector field $\mathbf{F}$ is sufficiently smooth and different trajectories never intersect.

[10] A much cited example in literature, which is somewhat similar to the nonlinear restoring forces used in this work, is the continuous scalar system $\dot{u} = u^{\frac{1}{2}}$ in $\mathbb{R}^1$ with the initial condition u_0. It has for the special case of $u_0 = 0$ the two non-unique solutions $u_1(t) \equiv 0$ and $u_2(t) = \frac{1}{4}t^2$.

the Lipschitz theorem [230]. A vector-valued function[11] is said to be Lipschitz(-continuous) in its arguments, if

$$\|\mathbf{F}(\mathbf{u}) - \mathbf{F}(\mathbf{y})\| \leq l \|\mathbf{u} - \mathbf{y}\| , \qquad l \in \mathbb{R}, \quad l < \infty \tag{3.12}$$

where l is the Lipschitz constant. If the field $\mathbf{F}$ with scalar $\mathcal{C}^1$ components is continuously differentiable in $\mathbf{u}$ and $\partial\mathbf{F}/\partial\mathbf{u}$ exists for all $\mathbf{u} \in D$ where $D \subset \mathbb{R}^m$ as assumed above, then the left hand side of (3.12) divided by the right for $\Delta\mathbf{u} = \mathbf{u} - \mathbf{y}$ with $\Delta\mathbf{u} \to 0$ represents the first derivative of the vector field with respect to the $\mathbb{R}^m$-dimensional state space and can be rewritten as

$$\|\mathbf{J}\,\mathbf{F}(\mathbf{u})\| \leq l \qquad \text{with} \qquad l \geq 0 , \tag{3.13}$$

where $\mathbf{J}$ is the Jacobian matrix of first partial derivatives [58]. In other words, for the second-order system (3.3), in a phase plot of the field $\mathbf{F}$ versus its solution $\mathbf{u}(t)$, a straight line connecting any two points[12] of $\mathbf{F}$ must have a slope whose absolute value is smaller than, or equal to l. A simple proof of Eq.(3.12) can be found in [61]. It is worth mentioning that Lipschitz continuity (3.12) is a special case of the Hölder condition [243] for $\alpha \equiv 1$. This is utilised for the derivation of uniqueness theorems for differential systems which fail (3.12) in certain intervals of $\mathbf{u}$.

Since equation (3.13) does not necessarily hold uniformly for all functions in the entire domain $D \subset \mathbb{R}^m$, it is advantageous to define local and global Lipschitz conditions[13]. The field (3.4) is locally Lipschitz in the sub-domain $D_{\text{loc}} \subset D$ if both, $\mathbf{F}$ and its first derivative $\|\mathbf{J}\,\mathbf{F}(\mathbf{u})\|$ are continuous on $D_{\text{loc}} \subset D$. If $\mathbf{F}$ and $\|\mathbf{J}\,\mathbf{F}(\mathbf{u})\|$ are continuous on $D_{\text{glob}} \subset D$ then $\mathbf{F}$ is globally Lipschitz if and only if $\|\mathbf{J}\,\mathbf{F}(\mathbf{u})\|$ is uniformly bounded in D_{glob} [242]. Although the Lipschitz condition is weaker than continuous differentiability [58], but stronger than continuity, meaningful examples modelling real physical processes can be constructed, which are not globally Lipschitz but do have unique global solutions [61, 92]. Given this restrictive nature of the global Lipschitz condition, a theorem can be established requiring (3.4) to be only locally Lipschitz, but on the expense that one can assure there exists a compact[14] subset S of the domain $D \subset \mathbb{R}^n$, $\mathbf{u}_0 = \mathbf{u}(t_0) \in S$, such that every solution $\mathbf{u}_s(t)$ of (3.4) never leaves S for all $t \geq t_0$ [244].

According to Peano's theorem [245], existence of a solution $\mathbf{u}(t)$ of (3.4) is ensured by simply requiring the vector field $\mathbf{F}(\mathbf{u})$ to be continuous in the closed set

$$D_+ = \left\{ t \in \mathbb{R} : t_0 \leq t \leq t_0 + a ;\ \mathbf{u} \in \mathbb{R}^n : \|\mathbf{u} - \mathbf{u}_0\| \leq b \right\} \tag{3.14}$$

with $\mathbf{u}(t_0) \equiv \mathbf{u}_0 \in D_+$. However, it is generally preferred in literature to guarantee local/global existence by using the local/global Lipschitz criteria presented above, together with a basic application of the contraction mapping theorem, see [68, 246], to prove both existence and uniqueness

[11] The same applies to 'ordinary' functions, which are vector functions of dimension $n = 1$.
[12] It is assumed the field $\mathbf{F}$ is sufficiently smooth.
[13] Even if l exists for all points $\mathbf{u}_l \in D$, it is not guaranteed it is uniform, i.e. has the same value across D.
[14] Every closed and bounded set in $\mathbb{R}^n$ is a compact set.

altogether. This sometimes obscures the fact that Peano's existence theorem also holds for non-Lipschitz vector fields, for which the proof of uniqueness fails using (3.13) as will be seen in section 3.4 of this chapter.

3.2.2 *Stability in first approximation - the linearised system*

For the equation of motion formulated in (3.3) the associated first-order system is

$$\begin{Bmatrix} \dot{u}_1 \\ \dot{u}_2 \end{Bmatrix} = \begin{Bmatrix} u_2 \\ \frac{1}{m}\left(p_0 - f\left(u_1\right)\right) \end{Bmatrix} \qquad \text{with} \qquad \mathbf{u_0} = \begin{Bmatrix} u_{01} \\ u_{02} \end{Bmatrix} = \begin{Bmatrix} u_0 \\ \dot{u}_0 \end{Bmatrix} \tag{3.15}$$

as vector of the initial conditions (3.3b). The stationary points of the nonlinear system, if (3.15) has unique solutions, are obtained by setting $\dot{\mathbf{u}} = 0$ [92], hence

$$\mathbf{0} = \mathbf{F}\left(\mathbf{u}; \mathbf{z}\right) = \begin{Bmatrix} u_2 \\ \frac{1}{m}\left(p_0 - f\left(u_1\right)\right) \end{Bmatrix} . \tag{3.16}$$

The set of vectors $\mathbf{u}_{\mathrm{Eq},i}$ with $i = 1, 2, ..., n$ satisfying (3.16) are also called equilibrium or critical points. Retaining only the linear terms of a Taylor series expansion of (3.4) around $\mathbf{u}_{\mathrm{Eq},i}$ leads to the linearised system[15] [230]

$$\dot{\mathbf{y}} = \mathbf{JF}\,\mathbf{y} \tag{3.17a}$$

where the matrix product

$$\mathbf{JF} = \begin{bmatrix} 0 & 1 \\ -\frac{1}{m}\frac{\partial}{\partial u_1} f\left(u_1\right) & 0 \end{bmatrix} \tag{3.17b}$$

is derived using the Jacobian matrix $\mathbf{J}$ of first partial derivatives [58]. Together with its two eigenvalues λ_1, λ_2

$$\lambda_i = \pm\sqrt{-\frac{1}{m}\frac{\partial}{\partial u_1} f\left(u_1\right)} , \qquad i = 1, 2 \tag{3.17c}$$

obtained from the characteristic equation

$$\lambda^2 - \mathrm{tr}\left(\mathbf{JF}\right) + \det\left(\mathbf{JF}\right) = 0 , \tag{3.17d}$$

the eigenvectors $\mathbf{x_1}, \mathbf{x_2}$ of the matrix $\mathbf{JF}$ in (3.17b) are such that the algebraic equation

$$\left(\mathbf{JF} - \lambda_i \mathbf{I}\right)\mathbf{x}_i = 0 \tag{3.17e}$$

[15] In order to simplify notation, it is sometimes practice in literature to shift the equilibrium points to the origin of the phase space by a simple coordinate transformation $\overline{\mathbf{y}} = \mathbf{y} - \mathbf{u}_{\mathrm{Eq},i}$. This is regarded as being of non-essential nature for the Taylor approximation and has therefore not been followed in this work.

is satisfied for each λ_i [58]

$$\mathbf{x_1} = \begin{Bmatrix} x_1 \\ \lambda_1 \end{Bmatrix} = \begin{Bmatrix} 1 \\ \sqrt{-\frac{1}{m}\frac{\partial}{\partial u_1} f(u_1)} \end{Bmatrix}, \quad \mathbf{x_2} = \begin{Bmatrix} x_1 \\ \lambda_2 \end{Bmatrix} = \begin{Bmatrix} 1 \\ -\sqrt{-\frac{1}{m}\frac{\partial}{\partial u_1} f(u_1)} \end{Bmatrix}. \tag{3.17f}$$

Assuming a positive mass m, the sign of the first derivative of the nonlinear restoring force $f(u_1)$ is crucial for the local stability of the system around its equilibrium points. For a negative $\partial f_1 / \partial u_1$ both λ_i are real and of opposite sign, therefore the associated equilibrium point is hyperbolic (all λ_i have nonzero real parts), in particular: a saddle [230]. If $\partial f_1 / \partial u_1 > 0$, all λ_i and $\mathbf{x_i}$ are complex with zero real part and $\mathbf{u}_{\mathrm{Eq}}$ is non-hyperbolic stationary point termed centre [230]. Linear matrix algebra suggests that if $f(u_1) = \mathtt{const}$ at $u_1 \equiv \mathbf{u}_{\mathrm{Eq}}$, equation (3.17c) yields $\lambda_{1/2} = 0$ and therefore

$$\mathbf{x_1} = \begin{Bmatrix} 1 \\ 0 \end{Bmatrix}, \qquad \mathbf{x_2} = \mathbf{0}. \tag{3.18}$$

Since the eigenvectors $\mathbf{x_i}$ of (3.17a) correspond to eigenspaces of the linear system which are invariant under the flow of the linear differential equation, so-called subspaces,[16] solution (3.18) creates a one-dimensional vector space along the u_1-axis. This implies that in the vicinity of an equilibrium point $\mathbf{u}_{\mathrm{Eq},i}$ rendering equation (3.17c) equal to zero, in this case called a degenerate fixed point, the linear system spans an equilibrium subspace rather than a single equilibrium point [247]. It becomes immediately apparent that in such a case the linear analysis of system (3.4) cannot decide on the stability of the nonlinear system and is therefore of limited use only.

The first rigorous approach towards defining stability in a general sense is due to Lyapunov and his now famous definition [248], that any arbitrary point $\mathbf{u}$ is stable if the flow $\mathbf{F}(\mathbf{u}, t)$ starting at $\mathbf{u}(t_0)$ stays sufficiently close to $\mathbf{u}$ for all time $t \geq t_0$ as $t \to \infty$. The point $\mathbf{u}$ is then said to be Lyapunov-stable. If this stability for the flow $\mathbf{F}$ also holds for negative time $t \leq t_0$ as $t \to -\infty$, and hence is therefore in fact independent of t, the point $\mathbf{u}$ is called uniformly Lyapunov stable. Furthermore, a point $\mathbf{u}$ in the vicinity of a stable equilibrium point $\mathbf{u}_{\mathrm{Eq}}$ is said to be quasi-asymptotic stable, if the flow $\mathbf{F}(\mathbf{u}, t)$ of $\mathbf{u}$ tends towards $\mathbf{u}_{\mathrm{Eq}}$ as t approaches infinity.[17] And finally, any point $\mathbf{u}$ in the phase space is called asymptotic stable if, and only if it is both Lyapunov stable and quasi-asymptotic stable. It should be noted that all three definitions are easily applicable in higher dimensions ($n > 3$). For the purpose of this work it is sufficient to consider the essence of the theorems as given above. However, their proper mathematical definitions are given in [249] for example. A last remark worth mentioning is that stability concerning fixed points of either the nonlinear system or the linearised system is frequently called in literature as 'stability in the sense of Lyapunov' [237].

For attracting sets such as periodic orbits or limit cycles introduced earlier in this chapter, the concept of Lyapunov stability as defined above must be modified, since two nearby points may

[16] Eigensubspaces are the linear equivalent of invariant manifolds described in section 3.2.4 of this chapter.

[17] For this definition it is only important what happens in the limit as $t \to \infty$. There is no need for $\mathbf{u}$ to 'stay close' to $\mathbf{u}_{\mathrm{Eq}}$ as $t_0 \leq t < \infty$.

move apart due to phase lagging, where the angular velocity varies with the distance from the periodic orbit[18] [247]. Nevertheless, Lyapunov orbital stability, quasi-asymptotic and asymptotic orbital stability can be defined [236] similar to the description above for single points in the phase space. For this intent a manifold[19] Υ on a hyper-surface ($n-1$ dimensional subspace in an n dimensional phase space) is introduced, which is nowhere tangent to the orbit but intersected by it transversely through the point $\mathbf{u}_\Upsilon$. Then for any point $\mathbf{u} \in \Upsilon$ sufficiently near $\mathbf{u}_\Upsilon$, the solution of the flow $\mathbf{F}$ from (3.4) through $\mathbf{u}$ at the arbitrarily chosen reference time $t_0 = 0$, will cross Υ again at $t_0 + T$ at a point $\Pi(\mathbf{u})$ near $\mathbf{u}_\Upsilon$. This mapping $\mathbf{u} \rightarrow \Pi(\mathbf{u})$ of the phase flow solution into the manifold Υ is called a return-map, or more well-known, a Poincaré-map [250] and plays, apart from orbital stability considerations, an important role in analysing chaos [251–253]. Due to the fact that from the stability analysis in the vicinity of a single point of an reduced-order dimensional phase space conclusions are drawn whether the entire nonlinear system is stable makes the Poincaré approach a linear analysis as well. The theorems concerning the stability of periodic solutions, such as closed orbits or limit cycles, is frequently termed in literature as 'stability in the sense of Poincaré' [237].[20]

Numerous theorems in literature state precisely what influence the fixed-point stability solution of the linearised system (3.17a) has on the stability of critical points of the nonlinear system in (3.15). For hyperbolic equilibrium points there are two important principles, the stable manifold theorem [240] and Hartman-Grobman's theorem [249], whereas the Shoshitaishvili theorem applies to non-hyperbolic critical points [125,247]. From these it follows that fixed-points $\mathbf{u}_{\mathrm{Eq}}$ of the nonlinear system are locally stable or unstable (in a sufficient neighbourhood of $\mathbf{u}_{\mathrm{Eq}}$) if the critical points of the corresponding linear system are asymptotically stable or unstable. For the hyperbolic equilibrium point the stable manifold theorem proves that at $\mathbf{u}_{\mathrm{Eq}}$ the nonlinear system has stable and unstable manifolds tangent to the stable and unstable eigenvector subspaces of the linear system. Since this is not necessarily sufficient to prove asymptotic stability (or instability), Hartman-Grobman is required to demonstrate that there exist a homeomorphism between open sets in the vicinity of the equilibrium point $\mathbf{u}_{\mathrm{Eq}}$ such that the nonlinear system (3.4) at $\mathbf{u}_{\mathrm{Eq}}$ is topologically equivalent to the linear system defined in (3.17a). It should be noted that it is possible, in some circumstances, to explicitly derive the stable manifold of the nonlinear system, if, for example, the exact analytical solution of (3.4) is known or can be approximated using Picard's method of successive approximation, which is based for initial value problems, as treated in this chapter, on the fact that every solution of (3.4) is only a solution if it satisfies (3.7), see [76,255] for example.

Unfortunately, for non-hyperbolic fixed points[21] the qualitative behaviour of the nonlinear

[18] This obviously excludes linear systems where the frequency of oscillation is independent of the amplitude and hence of the radius of the closed orbit in the phase space.

[19] A n-dimensional manifold has a precise and rigid mathematical definition, see [243] for example. Roughly speaking, it behaves 'locally' like a vector space, but 'globally' like a curved surface. Examples in lower-order dimensions are the unit circle as a one dimensional manifold in $\mathbb{R}^2$ and the unit sphere as 2D manifold in a 3D phase space.

[20] An equally important but less frequently encountered stability concept is due to Lagrange [254], which deals with the boundedness of solutions.

[21] Non-hyperbolic critical points are sometimes in literature referred to as 'equilibrium points where the linear system has all eigenvalues on imaginary axes', hence the real parts of all λ_i are identical zero.

state equation (3.4) near the equilibrium point can be quite different from that of the linearised equation. This is easily understood in view of the results due to perturbation of the linearised system (3.17a) as shown in [68] for example, which classifies saddle fixed points as structurally stable and centre points as structurally unstable since they do not persist even under small perturbations.[22] Hence, for non-hyperbolic points the linearised analysis cannot determine the character of neutrally stable fixed points (centres) of the nonlinear system. Most commonly, it requires either the presence of some kind of symmetry[23] within the nonlinear field $\mathbf{F}$ from equation (3.4), see [247], or the existence of an energy conserving-type function as will be shown in the next section, to prove that a non-hyperbolic point remains structurally stable[24] under perturbation of the nonlinear system, and stable in the sense of Lyapunov and Poincaré as introduced in this section.

3.2.3 *Global stability - Lyapunov function*

In terms of direct stability[25] it is assumed in this work, if not stated otherwise, that there exists a function $V(u_1, u_2)$ for the system in equation (3.4), which is at least $\mathcal{C}^2$-continuous, with the properties of a first integral, such that the system can be represented by a Hamilton equation [96]

$$\dot{u}_1 = \frac{\partial}{\partial u_2} V(u_1, u_2) \;, \qquad \dot{u}_2 = -\frac{\partial}{\partial u_1} V(u_1, u_2) \;. \tag{3.19}$$

That a function V with such properties must exist for the system given in (3.15) is easily proven by differentiating each equation in (3.19) with respect to the complementary variable

$$\frac{\partial}{\partial u_1 \, \partial u_2} V(u_1, u_2) \equiv \frac{\partial \dot{u}_1}{\partial u_1} = -\frac{\partial \dot{u}_2}{\partial u_2} \,, \tag{3.20}$$

which is together with (3.16) equal to zero. Hence, (3.20) is valid for all $\mathbf{u} = \{u_1 \,, u_2\}^{\mathrm{T}}$ with $\mathbf{u} \in \mathbb{R}$. Equation (3.19) for the definition of the Hamiltonian is fulfilled if $V(u_1, u_2) \equiv V(\mathbf{u})$ is chosen as the system's energy function

$$V(\mathbf{u}) = \frac{1}{2} u_2^2 + \frac{1}{m} \left[\int_{u_1} f(\xi) \, \mathrm{d}\xi - p_0 \, u_1 \right] \,, \tag{3.21a}$$

together with a scalar value of the system's initial energy $V_0(\mathbf{u}_0)$ as introduced by the vector $\mathbf{u}_0$ from equation (3.3b)

$$V_0(\mathbf{u}_0) = \frac{1}{2} \dot{u}_0^2 + \frac{1}{m} \left[\int_{u_0} f(\xi) \, \mathrm{d}\xi - p_0 \, u_0 \right] \,. \tag{3.21b}$$

[22] Even an infinitesimal small perturbation can render a centre to an unstable node.

[23] As in the nonlinear example in section 3.4.2.

[24] Unlike Lyapunov and Poincaré definitions of stability the term 'structural stability' has as underlying idea the (small) changes (perturbations) of the defining differential system equations, which applies immediately to the bifurcation of critical point solutions for the nonlinear system, see section 3.4. For example, nodes, foci and saddle equilibrium points are said to be structurally stable since their qualitatively behaviour stays preserved under infinitesimal perturbations, whereas centre fixed-points are not structurally stable.

[25] The expression *direct stability* refers to the method of Lyapunov's second theorem, since it is possible to analyse the nonlinear system directly, i.e. without the necessity of a foregoing linearisation as in the previous section.

The second stability theorem of Lyapunov[26] states precisely the conditions which make an equilibrium point $\mathbf{u}_{\mathrm{Eq}}$ of the nonlinear system (3.4) stable [230]

Theorem 2 (Lyapunov Stability Theorem). *Let* $\mathbf{u}_{\mathrm{Eq}} = 0$ *be an equilibrium point of the nonlinear system* (3.4) *with the* $m \times n$ *dimensional map* $\mathbf{F}$ *as defined in* (3.6) *and let* $L(\mathbf{u})$ *be a scalar function of* $\mathbf{u}$ *defined in some neighborhood* D *of* $\mathbf{u}_{\mathrm{Eq}}$, *which is at least* C^1*-continuous such that*

(i) $L(\mathbf{u}_{\mathrm{Eq}}) = 0$,

(ii) $L(\mathbf{u}) > 0 \quad in \quad D - \{\mathbf{u}_{\mathrm{Eq}}\} \quad$ *(positive definite)*

(iii) $\mathcal{D}_{\mathbf{F}} L(\mathbf{u}) \leq 0 \quad in \quad D - \{\mathbf{u}_{\mathrm{Eq}}\} \quad$ *(negative semi-definite)*

then $\mathbf{u}_{\mathrm{Eq}} = 0$ *is a stable fixed point.*

For the sake of convenience and simplicity of notation it is commonly assumed the equilibrium under study is the origin $\mathbf{u}_{\mathrm{Eq}} = 0$. As mentioned earlier already, there is no loss of generality in doing so since for any critical point $\mathbf{u}_{\mathrm{Eq}} \neq 0$ a simple coordinate transformation renders a new system with $\mathbf{u}_{\mathrm{Eq}} = 0$, see [238] for example. The term $\mathcal{D}_{\mathbf{F}}$ is a differential operator called the orbital derivative[27]

$$\mathcal{D}_{\mathbf{F}} L(\mathbf{u}) = \nabla L(\mathbf{u}) \cdot \mathbf{F}(\mathbf{u}) = \frac{\partial L(\mathbf{u})}{\partial \mathbf{u}} \mathbf{F}(\mathbf{u}) = \frac{\partial L(\mathbf{u})}{\partial \mathbf{u}} \frac{\mathrm{d}\mathbf{u}}{\mathrm{d}t} = \dot{L}(\mathbf{u}) \tag{3.22}$$

which is identical to the time derivative of the Lyapunov function along a solution $\mathbf{u}(t)$ of (3.4). Or in other words, as apparent from the term $\nabla L(\mathbf{u}) \cdot \mathbf{F}(\mathbf{u})$ in (3.22), the orbital derivative is the gradient projection of the Lyapunov function onto the vector field of the flow $\mathbf{F}$. If in the above theorem the third condition *(iii)* is replaced by

$$\mathcal{D}_{\mathbf{F}} L(\mathbf{u}) < 0 \qquad \text{(negative definite)}, \tag{3.23}$$

then $\mathbf{u}_{\mathrm{Eq}} = 0$ is asymptotically stable [230]. This will be used in section 3.4 to estimate the region of attraction of a nonlinear system.

The major disadvantage of the otherwise ingenious stability approach by Lyapunov is the fact that no general method exists to analytically construct a suitable function $L(\mathbf{u})$. Although various theorems have been established addressing the existence of L, see [256] for example, and some procedures were developed deriving L for a few special systems[28] [244], it largely remains a trial-and-error process. For structural dynamical systems it is often suggested to use the energy function as Lyapunov, although there are examples where this leads not necessarily to a function with the desired properties as given in theorem 2 above [257]. It is clear to see that a vast range of potential functions can be chosen to satisfy points *(i)* and *(ii)* since $L(\mathbf{u})$ is independent of

[26] The theorems presented in the previous section 3.2.2 regarding the stability of arbitrary points of the flow $\mathbf{F}$ are generally referred to in literature as Lyapunov's first theorems [241].

[27] In more recently dated literature $\mathcal{D}_{\mathbf{F}}$ is referred to as Lie derivative [243]. It has a different notation for autonomous systems.

[28] A frequently used and quite successful method for autonomous systems is known as the 'variable gradient method'.

the actual dynamical system under consideration. The difficult part is to find one specific function amongst the range of feasible ones which satisfy condition *(iii)*. This last condition, explicitly defined in (3.22), clearly depends in an essential manner upon the system under study. However, in the fortunate circumstance of a Hamiltonian oscillator the energy function not only can be used to derive the equation of motion of the system [258], as seen in (3.19), it also serves for the purpose of being utilised as Lyapunov function

$$L(\mathbf{u}) \equiv V(\mathbf{u}) \; . \tag{3.24}$$

Two important remarks with respect to the above stability definitions are worth mentioning. First, it is important to note that Lyapunov's second theorem as given in the form above can only be applied to a global domain of interest since the proof for the theorem relies on the fact that both points *(ii)* and *(iii)* hold only on a compact domain (closed and bounded) of the phase space [242]. Secondly, it provides only sufficient but no necessary conditions for stability as can easily be verified by applying theorem 2 to a simple viscously damped SDOF oscillator.[29] The first point is addressed by adding a fourth condition to theorem 2, see [254], hence limiting the range of feasible functions, which requires $L(\mathbf{u})$ to be radially unbounded [58] such that

$$L(\mathbf{u}) \rightarrow \infty \qquad \text{as} \qquad \|\mathbf{u}\| \rightarrow \infty \, . \tag{3.25}$$

Applying jointly theorem 2 and equation (3.25) the Lyapunov function becomes globally stable, or, with the more stringent third point from (3.23), globally asymptotically stable. The second remark concerning the conditions of theorem 2 being sufficient but not strictly necessary is resolved by an extension of Lyapunov's theorem due to the Invariance Principle of LaSalle [238,259]

Theorem 3 (LaSalle's Theorem). *Let* $\Omega_c = \{\mathbf{u} \in \mathbb{R}^n \mid L(\mathbf{u}) \leq C\}$ *be a compact set that is positively invariant*[30] *with respect to the solution* $\mathbf{u}(t)$ *of* (3.4) *and suppose that* $L(\mathbf{u})$ *is a continuously differentiable function* $L(\mathbf{u}) : \mathbb{R}^n \rightarrow \mathbb{R}$ *such that* $\mathcal{D}_{\mathbf{F}} L(\mathbf{u}) \leq 0$ *in* Ω_c. *Further, define* $\Omega_0 \subset \Omega_c$ *such that* $\Omega_0 = \{\mathbf{u} \in \Omega_c \mid \mathcal{D}_{\mathbf{F}} L(\mathbf{u}) = 0\}$, *that is* Ω_0 *is the set of all points in* Ω_c *where* $\mathcal{D}_{\mathbf{F}} L(\mathbf{u}) = 0$, *and let* Ω_L *be the largest invariant set in* Ω_0. *Then every solution starting in* Ω_c *approaches* Ω_L *as* $t \rightarrow \infty$.

In order to show that every solution $\mathbf{u}(t)$ of (3.4) approaches the origin as time tends to infinity, it is necessary to prove that the largest invariant set $\Omega_L \subset \Omega_0$ is the origin itself. This can be accomplished by showing that no other solution than the trivial one $\mathbf{u}(t) \equiv 0$ can stay in Ω_0. A rigorous proof of the theorem is given in [242]. The two important amendments of LaSalle to the theorem of Lyapunov are the relaxation of conditions imposed on $L(\mathbf{u})$. First, the Lyapunov function is no longer required to be positive definite, only continuously differentiable. Secondly,

[29] Failure of a Lyapunov function candidate (trial function) to satisfy theorem 2 does not necessarily imply instability of the oscillating system under consideration. It is merely a sign of an ill-chosen trial function and must always be verified by further investigation using more precise theorems, such as LaSalle and/or the stable manifold theorem, or explicit phase plane plots.

[30] A set $S \subset \mathbb{R}^n$ is said to be invariant with respect to the flow $\mathbf{F}(\mathbf{u}, t)$ if any solution $\mathbf{u}(t = 0) \in S$ of $\mathbf{F}$ is $\mathbf{u}(t) \in S$, for all $t \neq 0$, $t \in \mathbb{R}$ [260]. In other words, if a solution belongs to S at some time instant (not necessarily $t \equiv 0$), then it stays in S for all negative and positive time t. If this is only true for $t \geq 0$ then S is positively invariant.

the fact that theorem 3 is applicable to more general dynamic events other than (but including) equilibrium points, such as closed orbits or limit cycles, makes it far more reliable. Two special cases of LaSalle's theorem[31] can be formulated concerning the stability of the origin. The first one, devised by Barbashin [262], clearly proves that if $L(\mathbf{u})$ from theorem 3 is positive definite, then the origin $\mathbf{u} = 0$ is asymptotically stable. The second theorem, due to Krasovskii [256], slightly extends this proof by assuming $L(\mathbf{u})$ is radially unbounded and therefore affirming the origin of being globally asymptotically stable if, and only if it is locally asymptotic stable.

3.2.4 *Integral manifolds and Morse theory*

For scleronomic[32] mechanical systems with a velocity-independent potential energy function as given in (3.21) the Hamiltonian represents the total energy of the system. Since it can be derived by a one-time integration of the equation of motion (3.3), it is also referred to as 'first integral' of the system in (3.4). With the definition of the orbital derivative from above, equation (3.21a) leads directly to

$$\mathcal{D}_{\mathbf{F}} V(\mathbf{u}) = 0\,, \tag{3.26}$$

and thus, the projection of the first integral along a solution $\mathbf{u}(t)$ of the flow $\mathbf{F}$ is zero, or in other words, the Hamiltonian along $\mathbf{u}(t)$ is a constant. The fact that $V(\mathbf{u}) = \mathtt{const}$ defines so-called level sets of the first integral (3.21) which constitutes of bundles of closed orbits termed integral manifolds [260]. In the case of an autonomous system, they exist for all past and future times $(-\infty < t < \infty)$ and therefore are referred to as invariant sets. Utilising the theorem of Liouville [241], which simply states that the phase flow $\mathbf{F}(\mathbf{u})$ of (3.4) is volume preserving[33] if $V(\mathbf{u})$ in (3.21) exists, the immediate consequence for Hamiltonian systems is that these cannot be asymptotically stable in terms of the theorems given above.

Although the analysis of level sets for first-integral systems is in general not simple, even in the two-dimensional case, their local behaviour in the vicinity of non-degenerate critical points can be investigated using the Morse Lemma [242]. It follows either from (3.26), or from the Liouville theorem in conjunction with (3.21), that the Hamiltonian oscillator has critical points $\mathbf{u}_{\mathrm{cr},i}$ given by the solution of

$$\mathbf{grad}\, V(\mathbf{u}_{\mathrm{cr}}) = \nabla V(u_{1,\mathrm{cr}}, u_{2,\mathrm{cr}}) = \begin{Bmatrix} \frac{1}{m}\big(f(u_1) - p_0\big) \\ u_2 \end{Bmatrix} = 0\,. \tag{3.27}$$

Any of these points is called non-degenerate if it satisfies

$$\|\mathbf{H}\, V(u_{1,\mathrm{cr}}, u_{2,\mathrm{cr}})\| \neq 0 \tag{3.28a}$$

[31] Both theorems have been established as specific cases and where proved before LaSalle formulated the Invariance Principle. See [261] for details.

[32] Time-independent constraints, see [263] for example.

[33] In the sense of non-dissipative.

with $\mathbf{H}$ being the Hessian matrix of second order partial derivatives given as [58]

$$\frac{\partial^2}{\partial u_i \, \partial u_j}, \qquad \text{with} \quad i,j = 1,2 \tag{3.28b}$$

in the case of planar oscillators. Hence, for the system in (3.15) equation (3.28a) becomes

$$\frac{1}{m}\frac{\partial}{\partial u_1} f(u_1)\Big|_{u_{1,\mathrm{cr}}} \neq 0 \tag{3.29}$$

with the value of $V(u_{1,\mathrm{cr}}, 0)$ at $\mathbf{u}_{\mathrm{cr},i} = \{u_{1,\mathrm{cr}}; 0\}^{\mathrm{T}}$ called critical value. Therefore, any equilibrium point $\mathbf{u}_{\mathrm{Eq}}$ obtained from (3.4) fulfilling (3.29) is either a saddle if

$$\|\mathbf{H}\, V\| < 0\,, \tag{3.30a}$$

or a centre, if

$$\|\mathbf{H}\, V\| > 0\,. \tag{3.30b}$$

and therefore a locally isolated critical point [257]. Since both criteria in Eq.(3.30) are derived from the Morse lemma,[34] they correspond in their informational character to results obtained in the linearised stability analysis in section 3.2.2 of this chapter. However, the fundamental advantage of the Morse function concept compared to section 3.2.2 lies in the fact that fulfilling equation (3.28) automatically guarantees the existence of the associated dynamical patterns, either centre or saddle, in the nonlinear system. Contrary, in the linearised analysis all hyperbolic equilibrium points are required to be asymptotically stable in order to exist in the nonlinear system, which is, see the Liouville theorem above, not possible for first-integral systems.

However, for equilibrium points not satisfying Eq.(3.28), so called degenerate fixed points, the Morse function theory is not applicable. In general, for n-dimensional systems with periodical solutions this can be overcome by starting off with the stable manifold theorem for periodic orbits [68], which links stable, unstable and centre subspaces of the periodic orbit Γ_c to a certain number of associated stable, unstable and centre manifolds of dimension $(n-1)$. In a second step, the centre manifold theorem [264] is used to establish a one-to-one relation between the flow $\mathbf{F}$ and the centre manifold as function of the orbit Γ_c, termed $W^c(\Gamma_c)$. The stable manifold of a periodic solution (orbit or limit cycle) is associated with the Floquet multipliers[35] with modulus smaller than one,[36] whereas the centre manifold directly connects to the one characteristic multiplier with modulus equal to one [234], or in the autonomous planar case, both multipliers equal to one. It is

[34] The associated Morse function of the nonlinear system from (3.4) is derived via Taylor expansion in the neighborhood of the non-degenerate critical point $\mathbf{u}_{\mathrm{cr}}$ from (3.29), and can therefore be only locally accurate.

[35] Floquet theory deals with linear differential systems having time-varying coefficients [239]. In nonlinear analysis it is utilised as an explicit method, similar to equilibrium linearisation in section 3.2.2, for the approximation of perturbed periodic solutions. The Floquet multipliers are the eigenvalues of the so-called monodromy matrix [265,266], which is, roughly speaking, a transformation matrix that maps the solution vector $\mathbf{u}(t)$ of (3.4) at time $t = 0$ to another vector at $t = T$, where T is the least period of the nonlinear system (3.4). See chapter 4 for details.

[36] For planar autonomous systems the modulus of one of the two eigenvalues of the monodromy matrix is always equal to one [179].

important to differentiate between stable/unstable manifold concepts for fixed-point and periodic solutions. Although very similar from a technical point of view, they are targeting fundamentally different topological phenomena of differential dynamical system. For fixed points the manifolds of the nonlinear system are derived from stability considerations of the eigenspaces of the locally linearised system. For periodic solutions the manifolds of the nonlinear oscillator originate from the analysis of a time-varying linear system along the orbit of the original nonlinear system and is therefore implemented using Floquet-theory.

A special case of the manifold theorems for the planar phase space ($n = 2$) and certainly the most basic tool for studying the stability (and bifurcation) of periodic orbits and limit cycles is the Poincaré-map already mentioned in section 3.2.2 above. Further details are given in [230,237,249] for example. In the same section it has been noted that Lyapunov's concept of stability, originally designated for fixed-point solutions, can be expanded to be used for periodic solutions alike. In some special circumstances such as Hamiltonian or gradient systems it is not always necessary to prove Lyapunov stability using Poincaré-mapping or the stable manifold theorem. A precise definition of an invariant[37] set for a periodic solution of (3.4) can be employed showing that if the orbit of such a solution satisfies the criteria of the invariant set, it is (asymptotically) stable or unstable, and hence the nontrivial periodic solution of (3.4) is (asymptotically) orbitally stable or unstable. Such a definition can be given as follows, see [257] or [267, 268] for example.

Definition 1. *Considering the autonomous system in equation* (3.4) *where the flow* $\mathbf{F}$ *is a* $\mathcal{C}$ *differentiable map* $\mathbf{F} : S \to \mathbb{R}^m$ *according to* (3.6), *let* $U \subset S$ *be a closed invariant set of* (3.4) *and define an* ϵ*-neighbourhood of* U *by* $N_\epsilon = \left\{\mathbf{u} \in \mathbb{R}^m \middle| \operatorname{dist}(\mathbf{u}, U) < \epsilon\right\}$. *Then* U *is stable if*

$$\mathbf{u}(t_0) \in N_\delta \qquad \textit{implies that} \qquad \mathbf{u}(t) \in N_\epsilon\,, \qquad \forall\, t \geq t_0\,, \tag{3.31}$$

that is, for each $\epsilon > 0$ *there is a* $\delta > 0$ *such that any solution* $\mathbf{u}(t)$ *starting in the neighborhood* N_δ *of* U *at* $t = t_0$ *stays in* N_ϵ *for all* t. *The set* U *is called unstable if it is not stable. The set* U *is defined asymptotically stable, if* $\mathbf{u}(t_0) \in N_\delta$ *implies that* $\lim_{t\to\infty} \operatorname{dist}(\mathbf{u}(t), U) = 0$.

There are some remarks to make regarding the above stability definition. First, the domain S is equivalent to the union of the state space with dimension $\mathbb{R}^m$ and the control vector space $\mathbb{R}^n$. Secondly, the term $\operatorname{dist}(\mathbf{u}, U)$ represents the minimum distance from a given point in the solution trajectory $\mathbf{u}(t)$ of the flow to a point in the set U. Thirdly, it becomes immediately apparent that the concept of δ and ϵ neighborhoods bases on Lyapunov's stability theory for fixed points since definition 1 above reduces to Lyapunov's first stability theorem [248] if U is a fixed point.

For the specific case of the invariant set U being the closed orbit Γ_c of a nontrivial periodic solution $\mathbf{u}_\mathrm{p}(t)$ defined as

$$\Gamma_c = \left\{\mathbf{u} \in \mathbb{R}^m \middle| \mathbf{u} = \mathbf{u}_\mathrm{p}(t),\, 0 \leq t \leq T_c\right\}\,, \tag{3.32}$$

[37] As has been explained earlier, the term 'invariant set' is equally used for all dynamical entities encountered in the phase space which are constant in positive and negative time.

where T_c is the period, then the orbit is either stable or unstable in the sense of Lyapunov by the criteria given in definition 1. This leads finally to the definition of orbital stability [268]

Definition 2. *A nontrivial periodic solution $\mathbf{u}_{\mathrm{p}}(t)$ of the system in (3.4) is orbitally stable if the closed orbit Γ_c in (3.32) generated by $\mathbf{u}_{\mathrm{p}}(t)$ is stable. The solution $\mathbf{u}_{\mathrm{p}}(t)$ is asymptotically orbitally stable if Γ_c is asymptotically stable.*

Equation (3.21) describing the Hamilton's system energy at all time can be rewritten for a planar system as

$$V(\mathbf{u}) = V_{\mathrm{kin}}(u_2) + V_{\mathrm{pot}}(u_1) \tag{3.33}$$

with the kinetic energy being a function of velocity only

$$V_{\mathrm{kin}}(u_2) = \frac{m}{2} u_2^2 \tag{3.34a}$$

and the potential energy solely depending upon the displacement of the SDOF

$$V_{\mathrm{pot}}(u_1) = \int_{u_1} f(\xi)\, \mathrm{d}\xi - p_0\, u_1 \,. \tag{3.34b}$$

A closer examination of Eq.(3.33) reveals certain characteristics of the nonlinear flow $\mathbf{F}(\mathbf{u})$ of the Hamiltonian oscillator around its equilibrium points $\mathbf{u}_{\mathrm{Eq},i}$, irrespective of the fact whether the system has any degenerate or non-degenerate critical points. It is easy to see from (3.16) that any system with an energy function given in (3.21) has fixed points at $\mathbf{u}_{\mathrm{Eq},i} = \{u_{\mathsf{eq}}, 0\}^{\mathrm{T}}$ with the total energy

$$V(\mathbf{u}_{\mathrm{Eq}}) \equiv V_{\mathrm{pot}}(u_{\mathsf{eq}}) \tag{3.35}$$

since V_{kin} is equal zero at $\mathbf{u}_{\mathrm{Eq}}$. Liouville's theorem together with (3.26) implies that if the point $\mathbf{u}_{\mathrm{Eq}}$ is an equilibrium point, the first derivative of (3.35) must be zero, hence

$$\left.\frac{\partial V(\mathbf{u})}{\partial u_1}\right|_{\mathbf{u}_{\mathrm{Eq}}} = \left.\frac{\partial V_{\mathrm{pot}}(u_1)}{\partial u_1}\right|_{u_{\mathsf{eq}}} = 0\,. \tag{3.36}$$

Without explicitly knowing the exact structure of the potential energy function, V_{pot} can be approximated in a neighborhood of the fixed point $\mathbf{u}_{\mathrm{Eq}}$ using a Taylor series

$$\widetilde{V}_{\mathrm{pot}}(u_1) = V_{\mathrm{pot}}(u_{\mathsf{eq}}) + \left.\frac{\partial V_{\mathrm{pot}}(u_1)}{\partial u_1}\right|_{u_{\mathsf{eq}}} (u_1 - u_{\mathsf{eq}}) + \frac{1}{2} \left.\frac{\partial^2 V_{\mathrm{pot}}(u_1)}{\partial u_1^2}\right|_{u_{\mathsf{eq}}} (u_1 - u_{\mathsf{eq}})^2 + \dots \tag{3.37}$$

Subsequent combination of both equations (3.33) and (3.37) together with the conditions from (3.35) and (3.36) yields an explicit expression for the integral manifolds in the vicinity of the fixed

point $\mathbf{u}_{\mathrm{Eq},i}$

$$V(\mathbf{u}_0,\, p_0) - V_{\mathrm{pot}}(u_{\mathsf{eq}}) = \frac{1}{2}\, m\, u_2^2 + \sum_{q=2}^{N\to\infty} \frac{1}{q!} \left.\frac{\partial^{(q)} V_{\mathrm{pot}}}{\partial u_1^{(q)}}\right|_{u_{\mathsf{eq}}} (u_1 - u_{\mathsf{eq}})^q \tag{3.38}$$

where the value of the otherwise independent function $V(\mathbf{u})$ is predetermined by initial conditions $\mathbf{u}_0$ and the applied force magnitude p_0, hence $V(\mathbf{u}) \equiv V_0(\mathbf{u}_0)$ from Eq.(3.21b). The nature of the extreme solution at the fixed point is determined by the first term in the series approximation of (3.38), thus for $\partial^2 V_{\mathrm{pot}}/\partial u_1^2 > 0$ the energy function $V(\mathbf{u})$ has a stable (local) minimum at $\mathbf{u}_{\mathrm{Eq},i}$, and for $\partial^2 V_{\mathrm{pot}}/\partial u_1^2 < 0$ an unstable (local) maximum. It is worth pointing out that the left-hand side of (3.38) is a constant reflecting the difference in energy input into the system by initial conditions and applied load and the energy required by the system to sustain periodic motion at the equilibrium point $\mathbf{u}_{\mathrm{Eq},i} = \{u_{\mathsf{eq}}, 0\}^{\mathrm{T}}$. In general, equation (3.38) is an algebraic curve of order N. Depending on the value of N each curve has a specified name [58, 180]. For $N = 3, 4$ or 5, for example, equation (3.38) becomes a cubic, quartic or quintic curve, respectively. As will be seen later on in this chapter, section 3.4.2, a family of quartic curves, so-called Cassini Ovals, becomes of special interest since they describe the integral manifolds of the conservative Duffing-type oscillator. However, for certain restoring forces $f(u_1)$ where higher-order derivatives are small compared to the function values in an closed interval I_{Eq} where

$$I_{\mathrm{Eq}} = \Big[(1-\epsilon)u_{\mathsf{eq}},\, (1+\epsilon)u_{\mathsf{eq}}\Big]\,, \qquad \epsilon \ll 1 \tag{3.39}$$

around the equilibrium point $u_1 \equiv u_{\mathsf{eq}}$, e.g.

$$\left|\left.\frac{\mathrm{d}^{(n)} f(u_1)}{\mathrm{d}u_1^{(n)}}\right|_{I_{\mathrm{Eq}}}\right| \ll |f(u_1)|\,, \tag{3.40}$$

terms with $q > 2$ can be ignored in the approximation of $V_{\mathrm{pot}}(\mathbf{u})$ in (3.38), thus giving

$$C_0 = m\, u_2^2 + \left.\frac{\partial^2 V_{\mathrm{pot}}}{\partial u_1^2}\right|_{u_{\mathsf{eq}}} (u_1 - u_{\mathsf{eq}})^2\,, \tag{3.41}$$

with the specific constant $C_0 = 2\big(V(\mathbf{u}_0,\, p_0) - V_{\mathrm{pot}}(u_{\mathsf{eq}})\big)$. It is easy to prove that for a local minimum of (3.34b), $\partial^2 V_{\mathrm{pot}}/\partial u_1^2 > 0$, and $C_0 > 0$ equation (3.41) becomes an ellipse, but shrinks for $C_0 = 0$ to the stationary point itself. For the case $C_0 < 0$ no oscillation is possible. Contrary, in case of an unstable local maximum of the potential energy function with

$$\partial^2 V_{\mathrm{pot}}/\partial u_1^2 < 0\,,$$

Eq.(3.41) represents for $C_0 > 0$ a hyperbola with the major axis parallel to the u_2-axis running through the point $u_1 \equiv u_{\mathsf{eq}}$, and for $C_0 < 0$ the major axis coincides with the u_1-axis. For $C_0 = 0$ equation (3.41) gives two straight lines crossing the u_1-axis at u_{eq}. These are identical with the asymptotes of the hyperbola for the two cases where $C_0 \neq 0$. It is interesting to note that, assuming

a linearisation of (3.33) around $\mathbf{u}_{\mathrm{Eq},i}$, these two straight lines correspond to the eigenvectors of the linear system. This can be shown as follows. Differentiating (3.34b) twice leads to

$$\frac{\partial^2 V_{\mathrm{pot}}}{\partial u_1^2} \equiv \frac{\partial f(u_1)}{\partial u_1} < 0 \,. \tag{3.42a}$$

Rewriting (3.41) in its canonical form [186] and setting without loss of generality $C_0 = 1$ gives

$$-\frac{(u_1 - u_{\mathrm{eq}})^2}{a^2} + \frac{u_2^2}{b^2} = 1 \,, \qquad \text{thus} \qquad a = \sqrt{\frac{1}{\frac{\partial f(u_1)}{\partial u_1}}} \quad \text{and} \quad b = \sqrt{\frac{1}{m}} \,, \tag{3.42b}$$

which results after comparison with (3.17f) for the eigenvectors $\mathbf{x_1}$, $\mathbf{x_2}$ of the linearised system in

$$\mathbf{x}_{1,2} = \left\{ \begin{array}{c} 1 \\ \pm\frac{b}{a} \end{array} \right\} \tag{3.42c}$$

and can be written as an linear function of u_1 only valid in the vicinity of $\mathbf{u}_{\mathrm{Eq}} = \{u_{\mathrm{eq}}, 0\}^{\mathrm{T}}$

$$u_2(u_1) = \frac{\pm b}{a} (u_1 - u_{\mathrm{eq}}) \,. \tag{3.42d}$$

For $u_{\mathrm{eq}} = 0$ Eq.(3.42d) is perfectly identical to the equation for the asymptotes of the hyperbola in its canonical form as given in (3.42b), see [58] for example.

In analogy, similar results are obtained for the ellipse if $\partial f(u_1)/\partial u_1 > 0$ and $C_0 > 0$. Hence,

$$\frac{(u_1 - u_{\mathrm{eq}})^2}{a^2} + \frac{u_2^2}{b^2} = 1 \qquad \text{with} \qquad a = \sqrt{-\frac{1}{\frac{\partial f(u_1)}{\partial u_1}}} \tag{3.43a}$$

and b according to (3.42b) leading to complex eigenvalues and eigenvectors of the linearised system

$$\mathbf{x}_{1,2} = \left\{ \begin{array}{c} 1 \\ \pm\mathrm{i}\,\frac{b}{a} \end{array} \right\} \,, \tag{3.43b}$$

giving

$$u_2(u_1) = \pm\mathrm{i}\,\frac{b}{a} (u_1 - u_{\mathrm{eq}}) \,. \tag{3.43c}$$

Any chord through the center of an ellipse specifies a family of parallel chords that includes the tangents of the same slope. In fact, the mid-points of all these chords define another chord that is the diameter conjugate to the first chord, see [269] for more details. The slopes of these two lines, e_1 and e_2, respectively, crossing each other and the major axis of the ellipse at u_{eq} are determined

by [160]

$$-e_1 e_2 = \left(\frac{b}{a}\right)^2 , \tag{3.43d}$$

which can be rewritten as

$$\pm \mathrm{i}\sqrt{e_1 e_2} = \frac{b}{a} \qquad \text{leading to} \qquad \sqrt{e_1 e_2} = \pm \mathrm{i}\frac{b}{a} . \tag{3.43e}$$

Thus, in case of an non-hyperbolic equilibrium point of the linearised Hamiltonian system from Eq.(3.17), the eigenvectors of the linear system in the vicinity of a degenerated or non-degenerated fixed point are identical to the slope of diameters of the invariant integral manifold ellipse in second order approximation.[38)]

An important fact worth mentioning for the step excited system with $p \neq 0$ in (3.15) is the phenomenon that despite predicted periodical solution the actual orbit of the SDOF shrinks to the fixed-point solution obtained from the system's equilibrium equation (3.16). This emerges, apart from the trivial case $p_0 = 0$, $\mathbf{u}_0 = 0$, only if the initial energy $V_0(\mathbf{u}_0)$ in (3.21b) is equal to

$$V(\mathbf{u}) + V_0(\mathbf{u}_0) \tag{3.44}$$

from Eq.(3.21a), thus $V(\mathbf{u}) = 0$. Under these circumstance the phase space hyperplane is tangent to the ellipsoid $V(\mathbf{u})$ from (3.21a) at its one and only global minimum. This can be the case, for example, if the initial conditions are set such that

$$\mathbf{u}_0 = \mathbf{u}_{\mathrm{Eq}} , \tag{3.45}$$

where $\mathbf{u}_{\mathrm{Eq}}$ is obtained from Eq.(3.16) with $p_0 \neq 0$. The critical point $\mathbf{u}_{\mathrm{Eq}}$ in the state space corresponds to the new static equilibrium due to the constant force p_0 from (3.63). For the condition in (3.45) the system in Eq.(3.15) does not oscillate. The restoring force $f(u)$ in (3.3) does not necessarily need to be nonlinear. In fact, using the linear SDOF system the phenomenon can be explained by employing the exact analytical solution due to step excitation easily obtained using Laplace transformation [270]

$$u(t) = u_0 \cos(\omega_{\mathrm{n}} t) + \frac{p_0}{k_\beta}\left(1 - \cos(\omega_{\mathrm{n}} t)\right) \tag{3.46}$$

with $u_{\mathrm{eq}} = p_0/k_\beta$ as equilibrium solution and p_0, k_β, $\omega_{\mathrm{n}}^2 = k_\beta/m$ as step excitation magnitude, linear stiffness coefficient, and natural frequency, respectively. For the special case of $u_0 \equiv u_{\mathrm{eq}}$ no oscillation takes place in equation (3.46) and the linear system stays at rest at its new equilibrium position u_{eq}.

[38)] Since only terms with $q \leq 2$ in (3.38) have been retained.

3.3 Response parameters of conservative systems

Obtaining universal expressions for extreme values of displacement and velocity is not straightforward for the majority of restoring force-displacement relationships in the general differential equation (3.2). A first integration with respect to $u(t)$ reflects the energy balance of the conservative system (3.3) as derived in section 3.2.3, which stays constant in the interval $t_0 \leq t \leq \infty$. Assuming that the velocity $\dot{u}(t)$ is equal to zero when the oscillator reaches its minimum or maximum displacement position u_{min}, u_{max}, respectively, this leads to an algebraic equation, which in certain cases can be transformed into a closed-form analytical expression for the extreme displacement $u_{\mathsf{Ex}} = \{u_{\mathsf{min}}, u_{\mathsf{max}}\}$. Separation of variables and a subsequent second integration with respect to time and displacement on either side leads to an explicit expression for the oscillation period of the periodically vibrating SDOF. In general, for arbitrary initial conditions, this gives complex integral equations, but for a few particular cases of nonlinear restoring forces these expressions can be solved by means of special tabulated functions. A further simplification of initial conditions allows for the reduction of these special functions to basic algebraic expressions.

3.3.1 *Free vibration and impulse excitation*

In case of $p_0 = 0$ for the right-hand side of Eq.(3.3) the system undergoes free vibration. Contrary, an idealised impulse excitation for an SDOF oscillator is given by the Dirac delta distribution defined as [271]

$$\delta(t - t_0) = \begin{cases} \infty & \text{if} \quad t = t_0 \\ 0 & \text{if} \quad t \neq t_0 \end{cases} \qquad \text{together with} \qquad \int_{-\infty}^{\infty} \delta(t - t_0)\,\mathrm{d}t = 1\,. \tag{3.47}$$

Assuming only one single impulse during the response time interval under consideration, the time of input $t = t_0$ can always be set such that $t_0 = 0$. Introducing an amplitude magnification factor p_δ, the right-hand side of Eq.(3.3a) becomes $p_\delta\,\delta(t)$ which together with (3.47) simply reads p_δ. Standard textbooks [227] show for linear systems with $f(u) = k_\alpha\,u(t)$ free vibration and unit impulse excitation possess the same equation of motion

$$m\ddot{u}(t) + f(u) = 0\,, \tag{3.48}$$

but with distinct initial velocities. In case of $p_0 = 0$, Eq.(3.48) is subjected to (3.3b), whereas for $p_\delta\,\delta(t) = p_\delta$ the new initial velocity becomes $p_\delta/m + \dot{u}_0$. The concept in [227] is easily extended to restoring forces other than linear, since

$$\lim_{\Delta t \to 0} \int_0^{\Delta t} f(u)\,\mathrm{d}t = 0 \tag{3.49}$$

holds even if $\mathrm{d}f(u)/\mathrm{d}u \neq \mathtt{const}$, i.e $f(u)$ is nonlinear [270]. Therefore, viewing the impulse excited system as the more general case of both types of oscillation, all expression derived in what follows incorporate solutions for the freely vibrating system and can be obtained by setting p_δ

equal to zero in the appropriate equations.

Integration of Eq.(3.48) with respect to $u(t)$ using [3]

$$\frac{\mathrm{d}}{\mathrm{d}t}\dot{u}(t) = \frac{1}{2}\frac{\mathrm{d}}{\mathrm{d}u}\left(\frac{\mathrm{d}u(t)}{\mathrm{d}t}\right)^2 \tag{3.50}$$

leads to an expression for the system's total energy in terms of kinetic and potential energy similar to Eq.(3.21a) for the first-order system,

$$\frac{m}{2}\dot{u}^2 + \int_u f(u)\,\mathrm{d}u - C_1 = 0 \tag{3.51a}$$

with the integration constant C_1 obtained from Eq.(3.51a) at $t = 0$

$$C_1 = \frac{m}{2}\left(\frac{p_\delta}{m} + \dot{u}_0\right)^2 + \int_u f(u)\,\mathrm{d}u\Big|_{u=u_0} . \tag{3.51b}$$

The periodically shifting of total energy between kinetic and potential in Eq.(3.51a) as $t \to \infty$ dictates zero velocity at values of extreme displacement and $u_{\mathsf{Ex}} = \{u_{\mathsf{min}},\, u_{\mathsf{max}}\}$ can be obtained from Eq.(3.51a) together with (3.51b)

$$\int_u f(u)\,\mathrm{d}u\Big|_{u=u_{\mathsf{Ex}}} = \frac{m}{2}\left(\frac{p_\delta}{m} + \dot{u}_0\right)^2 + \int_u f(u)\,\mathrm{d}u\Big|_{u=u_0} . \tag{3.52}$$

Contrary, as will be seen in section 3.3.2, minimum and/or maximum values of velocity, i.e.,

$$\dot{u}_{\mathsf{Ex}} = \{\dot{u}_{\mathsf{min}},\, \dot{u}_{\mathsf{max}}\} , \tag{3.53}$$

do not generally occur at positions of zero displacement. If one supposes for the moment $\dot{u}_{\mathsf{max}}$ occurs at an arbitrary point of elongation, say u_{arb} with $u_{\mathsf{arb}} \in u_{\mathsf{Ex}}$, that is u_{arb} lies within the interval $(u_{\mathsf{min}}, u_{\mathsf{max}})$, rearranging (3.51a) gives the velocity $\dot{u}$ as a function of the time dependent displacement $u(t)$

$$\dot{u}^2(u) = \frac{2}{m}\left(\int_u f(u)\,\mathrm{d}u\Big|_{u=u_0} + \frac{m}{2}\left(\frac{p_\delta}{m} + \dot{u}_0\right)^2 - \int_u f(u)\,\mathrm{d}u\right) , \tag{3.54}$$

which reflects the non-parameterised or implicit form of the planar system's response parameters u_1, u_2. Hence, (3.54) is an explicit expressions for the solution trajectories of the field $\mathbf{F}$ in (3.4). Fundamental function analysis suggest the first derivative of Eq.(3.54) at $u = u_{\mathsf{arb}}$ must vanish

$$\frac{\mathrm{d}\dot{u}(t)}{\mathrm{d}u}\bigg|_{u_{\mathsf{arb}}} := 0 = -\frac{1}{2}\sqrt{\frac{2}{m}}\, f\,(u_{\mathsf{arb}})\, {}_\delta G_{\mathsf{arb}}^{-\frac{1}{2}} , \tag{3.55a}$$

with

$$ {}_{\delta}G_{\mathsf{arb}} = \int_{u} f(u)\,\mathrm{d}u\Big|_{u_0} + \frac{m}{2}\left(\frac{p_\delta}{m} + \dot{u}_0\right)^2 - \int_{u} f(u)\,\mathrm{d}u\Big|_{u_{\mathsf{arb}}} = C_1 - \int_{u} f(u)\,\mathrm{d}u\Big|_{u_{\mathsf{arb}}} , \quad (3.55b) $$

which is only the case for all solutions of $u(t)$ satisfying

$$ f\left(u_{\mathsf{arb}}\right) = 0\,. \quad (3.56) $$

Hence, $u_{\mathsf{arb}} = 0$, provided $f(u)$ is a causal function,[39] and extreme values of velocity are given as

$$ \dot{u}_{\mathsf{Ex}} = \pm\sqrt{\frac{2}{m}}\,C_1^{\frac{1}{2}} = \pm\sqrt{\frac{2}{m}}\left(\int_0^{u_0} f(u)\,\mathrm{d}u + \frac{m}{2}\left(\frac{p_\delta}{m} + \dot{u}_0\right)^2\right)^{\frac{1}{2}} . \quad (3.57) $$

If (3.57) represents global extreme solutions its second derivative at u_{arb} must not be equal zero

$$ \frac{\mathrm{d}^2\dot{u}(t)}{\mathrm{d}u^2}\Big|_{u_{\mathsf{arb}}} = \frac{1}{4}\sqrt{\frac{2}{m}}\left[2\frac{\mathrm{d}}{\mathrm{d}u}f(u)\Big|_{u_{\mathsf{arb}}}\,{}_{\delta}G_{\mathsf{arb}}^{-\frac{1}{2}} - f\left(u_{\mathsf{arb}}\right){}_{\delta}G_{\mathsf{arb}}^{-\frac{3}{2}}\right] \neq 0 \quad (3.58) $$

which holds true for both linear and nonlinear restoring forces $f(u)$. It is easy to see that (3.56) corresponds to the equilibrium point solution of (3.4) and can equally be obtained from the gradient of the Hamiltonian function $V(\mathbf{u})$ in Eq.(3.27) by setting the force magnitude $p_0 = 0$. Finally, maximum values of acceleration $\ddot{u}_{\mathsf{Ex}} = \{\ddot{u}_{\mathsf{min}},\, \ddot{u}_{\mathsf{max}}\}$ are obtained directly by modifying Eq.(3.48) to yield

$$ \ddot{u}_{\mathsf{Ex}} = -\frac{f(u)}{m}\,, \quad (3.59) $$

where u is the corresponding value of the displacement when the acceleration takes its extreme value. It is important to point out that for classes of nonlinear restoring functions $f(u)$ with at least one extreme solution other than $u_{\mathsf{min}},\, u_{\mathsf{max}} \in u_{\mathsf{Ex}}$, as shown in Fig. 3.1, maximum acceleration values $\ddot{u}_{\mathsf{Ex}}$ occur at $u_{\mathsf{a}} \ni u_{\mathsf{Ex}}$ with $u_{\mathsf{min}} < u_{\mathsf{a}} < u_{\mathsf{max}}$, which satisfy the relations

$$ \frac{\mathrm{d}}{\mathrm{d}u}f(u)\Big|_{u_{\mathsf{a}}} = 0 \qquad \text{and} \qquad \frac{\mathrm{d}^2}{\mathrm{d}u^2}f(u)\Big|_{u_{\mathsf{a}}} \neq 0\,. \quad (3.60) $$

Separation of variables in (3.51a) and subsequent integration between the interval

$$ u_{\mathsf{Ex}} = \{u_{\mathsf{min}},\, u_{\mathsf{max}}\} = \{u\left(t_{\mathsf{min}}\right),\, u\left(t_{\mathsf{max}}\right)\}\,, \quad (3.61) $$

where $\{t_{\mathsf{min}},\, t_{\mathsf{max}}\} = t_{\mathsf{Ex}}$ are the time points of extreme displacement, yields a general expression

[39] Modelling of rheological (hysteresis) behaviour using the widely spread methods of serial or parallel arranged structural stiffness and damping elements can lead to non-causal restoring force functions where zero displacement accounts for system internal forces and vice versa.

for the nonlinear oscillation period of (3.48)

$$T_\delta = \sqrt{2m} \int_{u_{\min}}^{u_{\max}} \frac{\mathrm{d}u}{\sqrt{-\int\limits_u f(u)\,\mathrm{d}u + C_1}}\,, \tag{3.62}$$

where limits of integration $u_{\min}$, $u_{\max}$ are obtained from (3.52) and the index δ refers to the type of the applied forcing function.

3.3.2 Step excitation

An idealised step excitation is modelled using a Heaviside function for the right-hand side of (3.3), defined as [271]

$$H(t-t_0) = \begin{cases} 1 & \text{if} \quad t \geq t_0 \\ 0 & \text{if} \quad t < t_0\,. \end{cases} \tag{3.63}$$

Thus, setting $t_0 = 0$ and $p_0 = p_0 H(t)$, Eq.(3.3) becomes

$$m\ddot{u}(t) + f(u) = p_0\,, \tag{3.64}$$

and integration with respect to $u(t)$ expresses the SDOF system's total energy in analogy to Eq.(3.21a)

$$\frac{m}{2}\dot{u}^2(t) + \int_u f(u)\,\mathrm{d}u - C_2 = p_0\,u(t) \tag{3.65a}$$

with the constant

$$C_2 = \frac{m}{2}\,\dot{u}_0^2 + \int_u f(u)\,\mathrm{d}u\Big|_{u=u_0} - p_0\,u_0\,. \tag{3.65b}$$

Values of extreme displacement are obtained from (3.65a) by setting $\dot{u}(t) = 0$

$$\int_u f(u)\,\mathrm{d}u\Big|_{u=u_{\mathsf{Ex}}} - p_0\,u_{\mathsf{Ex}} = C_2\,. \tag{3.66}$$

Following the same approach which leads to Eq.(3.54), the velocity is given as a function of the displacement

$$\dot{u}^2(t) = \frac{2}{m}\left(p_0 u(t) - \int_u f(u)\,\mathrm{d}u + C_2\right)\,. \tag{3.67}$$

First

$$\frac{\mathrm{d}\dot{u}(t)}{\mathrm{d}u}\bigg|_{u_{\mathsf{arb}}} := 0 = \frac{1}{\sqrt{2m}}\Big(p_0 - f\left(u_{\mathsf{arb}}\right)\Big)\;{}_{\mathrm{H}}G_{\mathsf{arb}}^{-\frac{1}{2}} \tag{3.68a}$$

and second derivative with respect to u

$$\left.\frac{\mathrm{d}^2\dot{u}(t)}{\mathrm{d}u^2}\right|_{u_{\mathsf{arb}}} \neq 0 \neq \frac{1}{\sqrt{2m}}\left(-\frac{\mathrm{d}}{\mathrm{d}u}f(u)\Big|_{u_{\mathsf{arb}}}\,{}_{\mathrm{H}}G_{\mathsf{arb}}^{-\frac{1}{2}} - \frac{1}{2}\Big(p_0 - f\left(u_{\mathsf{arb}}\right)\Big)^2\,{}_{\mathrm{H}}G_{\mathsf{arb}}^{-\frac{3}{2}}\right) \tag{3.68b}$$

where

$${}_{\mathrm{H}}G_{\mathsf{arb}} = p_0 u(t) - \int_u f(u)\,\mathrm{d}u\Big|_{u=u_{\mathsf{arb}}} + C_2 \tag{3.69}$$

are only satisfied if

$$f\left(u_{\mathsf{arb}}\right) = p_0\,, \tag{3.70}$$

which resembles the displacement of Eq.(3.64) if p_0 where a static loading. Hence, the step excited SDOF oscillates around its static equilibrium displacement $u_{\mathsf{arb}} \equiv u_{\mathsf{eq}}$ due to the magnitude p_0 of the Heaviside function (3.63). This again is equivalent to the fixed-point solution of the first-order system given in (3.16). Extreme values of velocity occur at $u = u_{\mathsf{eq}}$. Thus, together with (3.67)

$$\dot{u}_{\mathsf{Ex}} = \pm\sqrt{\frac{2}{m}}\left(p_0 u_{\mathsf{eq}} - \int_0^{u_{\mathsf{eq}}} f(u)\,\mathrm{d}u + C_2\right)^{\frac{1}{2}}\,. \tag{3.71}$$

Minimum and maximum acceleration $\ddot{u}_{\mathsf{Ex}} = \{\ddot{u}_{\mathsf{min}},\, \ddot{u}_{\mathsf{max}}\}$ are directly obtained from Eq.(3.64)

$$\ddot{u}_{\mathsf{Ex}} = \frac{1}{m}\big(p_0 - f(u_{\mathsf{a}})\big) \tag{3.72}$$

with $\ddot{u}_{\mathsf{max}}$ if $p_0 \geq 0$, $f(u) \leq 0$ and $\ddot{u}_{\mathsf{min}}$ if $p_0 \leq 0$, $f(u) \geq 0$. For restoring forces having values $u_{\mathsf{a}} \neq u_{\mathsf{Ex}}$ but $u_{\mathsf{min}} < u_{\mathsf{a}} < u_{\mathsf{max}}$ as previously shown in Fig. 3.1, the peak acceleration is given by equation (3.60).

Similarly to section 3.3.1 the nonlinear oscillation period is obtained from a subsequent integration of the system's energy equation, Eq.(3.65a),

$$T_{\mathrm{H}} = \sqrt{2m}\int_{u_{\mathsf{min}}}^{u_{\mathsf{max}}} \frac{\mathrm{d}u}{\sqrt{-\int_u f(u)\,\mathrm{d}u + p_0 u(t) + C_2}}\,, \tag{3.73}$$

with u_{min}, u_{max} from (3.66) and the index H referring to the excitation force function defined in (3.63). The nonlinear frequency corresponding to the periods found in equations (3.62) and (3.73) is given as the inverse of the period

$$f_{\mathsf{NL}} = \frac{1}{T}\,, \tag{3.74}$$

where T stands either for T_δ or T_{H} and is identical to the well-known definition for linear systems.

3.4 Examples of nonlinear restoring forces

By selecting two typical nonlinear restoring forces, namely $f_1(u)$ and $f_2(u)$, the results derived in the previous section 3.3 will be used to obtain analytical expressions of extreme values for displacement, velocity and acceleration as well as oscillation frequencies for impulse (including free vibration) and step excited systems. High-order embedded Runge-Kutta adaptive integration algorithms are used for numerical comparison and verification of the analytical solutions.

3.4.1 $f_1(u) = k_\beta \operatorname{sgn}(u) |u|^b$

An asymmetrical,[40] one-term polynomial-type restoring force with a constant coefficient k_β

$$f_1(u) = k_\beta \operatorname{sgn}(u) |u|^b , \qquad b,\, k_\beta,\, u \in \mathbb{R}, \qquad b \geq 0,\ k_\beta \neq 0 \tag{3.75}$$

is shown in Fig. 3.2(a) for various values of the nonlinear exponent b. The first integral of equation (3.75) with respect to the unknown displacement $u(t)$ yields

$$\int_u f_1(u)\, \mathrm{d}u = \frac{k_\beta}{b+1} |u|^{b+1} , \tag{3.76}$$

which is easily proven by the inverse operation

$$\frac{\partial}{\partial u} \int_u f_1(u)\, \mathrm{d}u = k_\beta |u|^b \frac{\partial |u|}{\partial u} = k_\beta \operatorname{sgn}(u) |u|^b . \tag{3.77}$$

In order to obtain unique and conclusive results of extreme response values and oscillation period, a stability analysis of the autonomous system in equation (3.3), as outlined in section 3.2 of this chapter, is of fundamental importance. Although this can be accomplished in a variety of ways after existence and uniqueness of solutions of (3.3) have been proven, it is commonly suggested to start with obtaining the equilibrium points of the nonlinear first-order system as given in Eq.(3.15), which is followed by an investigation of the local phase flow of (3.4) around these stationary points. Basic steps of this so-called linearised analysis have been described in section 3.2.2. The methods developed for such a local evaluation of equilibrium points are most widely applicable to a vast range of nonlinear systems. Unfortunately, there are numerous cases where linearisation of (3.4) leads to ambiguous results, and, as will be seen below, no decisive conclusions for the behaviour of the nonlinear system can be drawn from the analysis of Eq.(3.17a) and thus making a global nonlinear analysis necessary.

Although a nonlinear stability investigation can be used in a much larger domain of the flow F compared to linear analysis, sometimes they are applicable to the entire phase space, their distinctive disadvantage lies within the fact of the limited range of feasible system configurations over which they can be employed. Ultimately, in some rare circumstances when linear and nonlinear

[40] With respect to the ordinate (y-axis) in a cartesian coordinate system.

approaches both fail, this leads to cumbersome trial-and-error examination, i.e. numerical integration, of complex and hardly manageable differential systems as a last resort of stability evaluation. However, given the special case of conservative Hamiltonian systems as assumed in this chapter, precise theorems exist allowing to formulate clear statements about the systems behaviour in the entire phase space domain of interest.

3.4.1.1 Linearisation

Using Eq.(3.15) the second-order equation is rewritten as a system of coupled first-order differential equations with $f(u) \equiv f_1(u_1)$

$$\begin{Bmatrix} \dot{u}_1 \\ \dot{u}_2 \end{Bmatrix} = \begin{Bmatrix} u_2 \\ \widehat{p}_0 - \omega_n^2 \operatorname{sgn}(u_1) |u_1|^b \end{Bmatrix}, \qquad \text{where} \quad \mathbf{u} = \begin{Bmatrix} u_1 \\ u_2 \end{Bmatrix} \in \mathbb{R}^2, \tag{3.78}$$

is the vector of initial conditions according to (3.3b), $\widehat{p}_0 = p_0/m$ are the mass-normalised force magnitude, and the term

$$\omega_n^2 = \frac{k_\beta}{m} \equiv 4\pi^2 f_n^2 \tag{3.79}$$

is the natural frequency in rad/s and f_n the natural frequency in Hz of the linear reference system. The vector of control parameters comprises of $\widehat{p}_0$, ω_n^2, $b \in \mathbf{z}$. Therefore, the vector field is a map in the phase plane such that $\mathbf{F} : \mathbb{R}^2 \times \mathbb{R}^3 \to \mathbb{R}^2$. The stationary points of (3.78) are obtained according to (3.16) yielding for an impulse load on the system in (3.78)

$$\mathbf{u}_{\mathrm{Eq},1} = \begin{Bmatrix} 0 \\ 0 \end{Bmatrix} \qquad \text{for} \quad p_0 = p_\delta, \tag{3.80a}$$

and in case of step excitation

$$\mathbf{u}_{\mathrm{Eq},2/3} = \begin{Bmatrix} \operatorname{sgn}(u_1) \left[\frac{p_0}{k_\beta \operatorname{sgn}(u_1)} \right]^{\frac{1}{b}} \\ 0 \end{Bmatrix} \qquad \text{for} \quad p_0 \neq 0, \tag{3.80b}$$

with the two solutions $\operatorname{sgn}(u_1) > 0 \to \mathbf{u}_{\mathrm{Eq},2}$ and $\operatorname{sgn}(u_1) < 0 \to \mathbf{u}_{\mathrm{Eq},3}$ since $\operatorname{sgn}(u_1) = 1$ if $p_0 > 0$ and $\operatorname{sgn}(u_1) = -1$ if $p_0 < 0$. Thus, the system's new equilibrium points due to step loading are entirely defined by the magnitude of the applied force, whereas $\mathbf{u}_{\mathrm{Eq},1}$ remains equal zero regardless of the value for p_δ. It is easily verified that all three solutions in Eq.(3.80) are identical to u_{arb} from (3.56) and (3.70), respectively.

The vector field in (3.78) is $\mathcal{C}^1$-continuous in its scalar components and therefore, according to Peano's theorem from section 3.2.1, solutions $\mathbf{u}(t)$ in the sense of equation (3.7) do exist for exponents $b \in \mathbb{R}_+$. This can be understood as the cause for restricting b to the domain defined in (3.75). Application of Bendixson's criterion from (3.10) with

$$\nabla \cdot \mathbf{F}(\mathbf{u}, \mathbf{z}) = 0 \tag{3.81}$$

suggests that possible periodic orbits for (3.78) may exist. With the first derivative of the restoring force $f_1(u_1)$ derived as

$$\frac{\mathrm{d}}{\mathrm{d}u_1} f_1(u_1) = k_\beta \left(\frac{\mathrm{d}}{\mathrm{d}u_1} \operatorname{sgn}(u_1) \, |u_1|^b + \operatorname{sgn}(u_1) \, \frac{\mathrm{d}}{\mathrm{d}u_1} \, |u_1|^b \right) = b \, k_\beta \, |u_1|^{b-1} \,, \tag{3.82}$$

the Jacobian matrix product from Eq.(3.17b) is given by

$$\mathbf{JF} = \begin{bmatrix} 0 & 1 \\ -b\,\omega_\mathrm{n}^2 \, |u_1|^{b-1} & 0 \end{bmatrix} \tag{3.83a}$$

together with two eigenvalues according to Eq.(3.17c)

$$\lambda_{1/2} = \pm \sqrt{-b\,\omega_\mathrm{n}^2 \, |u_1|^{b-1}} \tag{3.83b}$$

and eigenvectors

$$\mathbf{x_1} = \begin{Bmatrix} 1 \\ \lambda_1 \end{Bmatrix} \,, \qquad \mathbf{x_2} = \begin{Bmatrix} 1 \\ \lambda_2 \end{Bmatrix} \,. \tag{3.83c}$$

Linearisation around the first stationary point $\mathbf{u}_{\mathrm{Eq},1}$ from (3.80a) shows that this is a degenerate equilibrium point with zero eigenvalues

$$\lambda_1 = \lambda_2 = 0 \,, \tag{3.84}$$

and eigenvectors according to (3.18), which implicates that the entire phase plane would be fixed and trajectories run parallel to the u_1-axis [241]. Thus, in case of $\mathbf{u}_{\mathrm{Eq},1}$ the stability classification for the nonlinear system remains unclear.

A different situation arises for the other two equilibrium points $\mathbf{u}_{\mathrm{Eq},2/3}$ given in Eq.(3.80b). In order to ensure existence of the nonlinear force f_1 in (3.75) for all possible values of displacement, e.g. $-\infty < u_1 < \infty$, the exponent b is defined to be positive real-valued. Furthermore, making the sensible presumptions of a positive mass m leaves only for the stiffness coefficient k_β the unrestricted $\mathbb{R}^1$ space. For $k_\beta < 0$ both eigenvalues in (3.83b) become $\lambda_{1/2} \in \mathbb{R}^1$ and of opposite sign, thus $\mathbf{u}_{\mathrm{Eq},2/3}$ are hyperbolic-class equilibrium points, or more precise, saddles. The corresponding eigenvectors are given by (3.83c) and define an unstable ($\mathbf{x_1}$) and stable ($\mathbf{x_2}$) linear subspace. This renders the linearised system (3.17a) unstable at both fixed points in forward and reversed (negative) time.[41] According to the stable manifold theorem from above, the stable and unstable (or vice versa) manifolds of the nonlinear system (3.4) are tangent to the eigenvector subspace of the linear system, and thus, together with the structure-preserving mapping of Hartman-Grobman, see section 3.2.2, both stationary points $\mathbf{u}_{\mathrm{Eq},2/3}$ of the nonlinear system are unstable if $k_\beta < 0$.

On the other hand, setting $k_\beta > 0$ but leaving the values of the parameter vector $\mathbf{z}$ from (3.4)

[41] In case of an unstable solution for a nonlinear system it is important to exactly define the space *and* time domain of the instability. The same is true, however, in case of a stable solution.

constant leads to two complex conjugate eigenvalues

$$\lambda_2 = \lambda_1^* , \qquad \lambda_1, \lambda_2 \in \mathbb{C} \tag{3.85}$$

and complex eigensubspaces spanned by the two vectors from (3.83c). Therefore, the linearised system possess centres at the equilibrium points $\mathbf{u}_{\mathrm{Eq},2/3}$ of the nonlinear system. Utilizing the theorem of Shoshitaishvili together with the fact that fixed-point linear approximations having eigenvalues with zero real part are structurally unstable, as mentioned above, the stability of the nonlinear system at $\mathbf{u}_{\mathrm{Eq},2/3}$ remains unknown when using the method of linearisation.

The problem of partly zero eigenvalues (one zero, one negative real) is discussed in Hale *et al* [242] for a uncoupled first-order system with a similar right-hand side polynomial term as in (3.78), although much less general since the exponent b is restricted to $b \geq 1$ and $b \in \mathbb{N}$. The problem of the originally coupled systems is solved by introducing an augmented scalar function via Taylor approximation (locally stable equilibrium) such that the system becomes uncoupled and stability is proven by ensuring stability of one scalar differential equation of the uncoupled system of equations. Unfortunately, this procedure assumes a certain structure of the coupled nonlinear differential system and application of the method to (3.78) gives for the auxiliary function $\mathcal{C}^0$-continuity. Hence, no clear statement about local stability is possible.

Intuition suggests that for zero stiffness in equation (3.15) the SDOF system has no oscillation. Mathematically speaking, for the marginal value of $k_\beta \equiv 0$ the equilibrium from (3.80a) becomes

$$\mathbf{u}_{\mathrm{Eq},1} = \begin{Bmatrix} u_{1,\mathrm{cr}}^* \\ 0 \end{Bmatrix} , \qquad u_{1,\mathrm{cr}}^* \in \mathbb{R} \tag{3.86}$$

where $-\infty < u_{1,\mathrm{cr}}^* < \infty$ corresponds to every single point on the u_1-axis of the phase space diagram. Hence, every value of displacement $u(t)$ is a fixed point as long as $u_2 \equiv 0$. As an immediate result, for any initial condition u_0 the SDOF remains fixed at $\mathbf{u}_{\mathrm{Eq},1}$ with $u_{1,\mathrm{cr}}^* = u_0$ since this is already an equilibrium point. A very similar, but nontrivial case of non-oscillatory system behaviour with $k_\beta > 0$ and $p_0 \neq 0$ due to force balancing in the differential equation which will be discussed below. As in here, the main criteria is a vanishing potential energy function, which is indeed the case for (3.21a) if $k_\beta \equiv 0$. Therefore, with the kinetic energy not equal to zero, no equilibrium solutions exist. The SDOF performs a linear translation with constant speed u_0, also referred to as rigid body mode [227]. In the case of $k_\beta \equiv 0$ and $p_0 \neq 0$, the second differential equation in (3.78) becomes equal to $m\,\dot{u}_2 = p_0$, which, assuming $m = \mathrm{const}$, gives a constant acceleration of magnitude p_0/m. Repeated integration with respect to time leads to a linear function for the velocity $u_2(t)$ and a quadratic function ($\mathcal{C}^2$-continuous) in time t for the displacement $u_1(t)$. Hence, $u(t)$ grows without bounds as $t \to \infty$ and equilibrium solutions for the system in (3.78) lie at infinity as can be seen from Eq.(3.80b) by setting $k_\beta \equiv 0$.

3.4.1.2 Nonlinear analysis

Since a nonlinear analysis for all three fixed-point solutions, $\mathbf{u}_{\mathrm{Eq},i}$ with $i = 1, 2, 3$ becomes due to results of the previous section inevitable, the energy function (3.21) of the system together with (3.76) is written as

$$V_{f_1}(\mathbf{u}) = \frac{1}{2}\,u_2^2 + \frac{\omega_{\mathrm{n}}^2}{b+1}\,|u_1|^{b+1} - \widehat{p}_0\,u_1\,, \tag{3.87a}$$

and

$$V_{f_1,0}(\mathbf{u}_0) = \frac{1}{2}\,u_{02}^2 + \frac{\omega_{\mathrm{n}}^2}{b+1}\,|u_{01}|^{b+1} - \widehat{p}_0\,u_{01}\,, \tag{3.87b}$$

as energy due to the initial conditions according to Eq.(3.21b). It is easy to prove that (3.87a) satisfies (3.19). Thus, $V_{f_1}(\mathbf{u})$ is the Hamiltonian of the nonlinear system in (3.78). It can therefore be used in the nonlinear stability analysis as Lyapunov function with the orbital derivative as defined in (3.22) equal to zero

$$\mathcal{D}_{\mathrm{F}} V_{f_1}(\mathbf{u}) = 0\,, \tag{3.88}$$

which has been predicted for general Hamiltonian systems in Eq.(3.26). First, the stationary point $\mathbf{u}_{\mathrm{Eq},1} = \{0,\ 0\}^{\mathrm{T}}$ from (3.80a) of the oscillator in (3.15) due to impulse excitation[42] with $p_0 \equiv 0$ is considered. It is easily verified that Eq.(3.28) is not satisfied for the degenerate critical point $\mathbf{u}_{\mathrm{Eq},1}$ and usage of Morse's theorem is inappropriate. Therefore, applying Lyapunov's second theorem from section 3.2.3 to equation (3.87a) leads to $(i) V_{f_1}(\mathbf{u}_{\mathrm{Eq},1}) = 0$, $(ii) V_{f_1}(\mathbf{u}) > 0$ everywhere except at $\mathbf{u} = \mathbf{u}_{\mathrm{Eq},1}$, and $(iii) \mathcal{D}_{\mathrm{F}} V_{f_1}(\mathbf{u}) = 0$ everywhere, see (3.88). Thus, (3.15) is stable in the domain, but not asymptotically stable at $\mathbf{u}_{\mathrm{Eq},1}$. Global stability is easily ensured using (3.25) above leading to the limit expression

$$\lim_{\|\mathbf{u}\| \to \infty} V_{f_1}(\mathbf{u}) = \infty\,, \tag{3.89}$$

since $V_{f_1}(\mathbf{u})$ is radially unbounded for a monotonously growing vector norm $\|\mathbf{u}\|$. Application of the less restrictive LaSalle theorem, in order to prove asymptotic stability, gives for the positive definite, $C^2\,(\Omega_c)$ continuous function in (3.87a) indeed a compact domain where

$$\Omega_c = \left\{\mathbf{u} \in \mathbb{R}^2 \middle| V_{f_1}(\mathbf{u}) \leq C\right\} \tag{3.90}$$

with $C \in \mathbb{R}$, $C \leq \infty$. But the fact of equation (3.88) being valid in a domain D such that[43] $\Omega_c \subset D$, leads to

$$\Omega_c \equiv \Omega_0\,, \tag{3.91}$$

[42] As agreed above, this includes free vibration of the system likewise.

[43] In fact, if $V_{f_1}(\mathbf{u})$ is radially unbounded as given in (3.89), equation (3.88) holds for the entire phase space $\mathbb{R}^2$.

hence, there are largest invariant sets other than, but including, the origin in Ω_0. This becomes immediately apparent considering that if Eq.(3.88) holds, the Lyapunov function (3.87a) must be constant along the trajectories of any solution $\mathbf{u}(t)$ of the system (3.78), as explained above. Therefore, the solution curves in the phase plane are given by

$$0 = \frac{1}{2}u_2^2 + \frac{\omega_n^2}{b+1}|u_1|^{b+1} - V_{f_1,0}(\mathbf{u}_0) \ , \tag{3.92}$$

describing periodic orbits around the globally stable, but not asymptotic stable fixed point $\mathbf{u}_{\mathrm{Eq},1}$ from (3.80a). It is not difficult to verify that the particular case above does not only hold for non-degenerate stationary points but for Hamilton systems in general. This essentially proves that nontrivial periodic solutions of autonomous systems cannot be asymptotic stable in the sense of Lyapunov.

Given the case of constant right-hand side in the differential system in (3.78), equation (3.80b) shows that $\mathbf{u}_{\mathrm{Eq},2} \equiv \mathbf{u}_{\mathrm{Eq},3}$ if p_0 is changed into $-p_0$, thus both fixed points are symmetric with respect to the u_2 axis and is sufficient to examine the stability of either of them. In here $\mathbf{u}_{\mathrm{Eq},2}$ is chosen. The non-degenerate critical point satisfies (3.28a) and is together with (3.30b) categorised as the centre of the nonlinear system. Performing a coordinate transformation as described in section 3.2.2 shifts $\mathbf{u}_{\mathrm{Eq},2}$ into the origin of the phase space. Contrary to the stability analysis of $\mathbf{u}_{\mathrm{Eq},1}$ above, the conditions for Lyapunov's second theorem are not met this time, including the proof of non-asymptotic stability, due to the fact that $V_{f_1}(\mathbf{u})$ as given in (3.87) is not positive definite everywhere except at $\mathbf{u}_{\mathrm{Eq}} \equiv 0$ as requested by item *(ii)* in theorem 2. However, using LaSalle instead does not require $V_{f_1}(\mathbf{u})$ to be positive definite and together with (3.92) global stability of the two critical points $\mathbf{u}_{\mathrm{Eq},2/3}$ is ensured. In fact, the trajectories as solutions of (3.78) are given by an algebraic curve of order $b+1$ similar to (3.92) but with an additional term accounting for the step load magnitude p_0, thus

$$0 = \frac{1}{2}u_2^2 + \frac{\omega_n^2}{b+1}|u_1|^{b+1} - \widehat{p}_0\, u_1 - V_{f_1,0}(\mathbf{u}_0) \ . \tag{3.93}$$

Since Bendixson's criterion from (3.10) with its application in (3.81) to the system (3.83) does not rule out periodic orbits *a priori* , it is sensible to apply Poincaré-Bendixson in order to conclusively establish the existence of periodic orbits. All three equilibrium points in (3.80) are equally dealt with by assuming the fixed point which belongs to each $\mathbf{u}_{\mathrm{Eq},i}$, see section 3.2.1 above, coincides with the origin.[44)] A compact invariant domain R as required by theorem 1 is defined by the annular region

$$R = \left\{\mathbf{u} \in \mathbb{R}^2 \middle| C_{r1} \le V_{f_1}(\mathbf{u}) \le C_{r2}\right\} \ , \qquad \text{with} \qquad C_{r1} < C_{r2}, \quad C_{r1},\, C_{r2} \in \mathbb{R} \tag{3.94}$$

constructed from the intersection of two simple closed curves around the equilibrium point $\mathbf{u}_{\mathrm{Eq},i}$ but with $\mathbf{u}_{\mathrm{Eq},i} \ni R$, hence R is closed, bounded and thus compact and contains ordinary points

[44)] This assumption has been used previously and is mathematically justified by a simple coordinate transformation.

only. The outer boundary of R is given by $V_{f_1}(\mathbf{u}) = C_{r2}$ and the inner by $V_{f_1}(\mathbf{u}) = C_{r1}$. It has been shown above that the orbital derivative from (3.22) is the projection of the $\mathcal{C}^1$ function $V_{f_1}(\mathbf{u})$ onto the solution of (3.4) or, in other words, onto the flow $\mathbf{F}$ of the phase plane. Therefore, if $\mathcal{D}_{\mathbf{F}} V_{f_1}(\mathbf{u}) < 0$ on any boundary C_r of $V_{f_1}(\mathbf{u})$, the flow points inwards, and, if $\mathcal{D}_{\mathbf{F}} V_{f_1}(\mathbf{u}) > 0$ it points out of the simply enclosed region. From fundamental relations of differential geometry and topology it is obvious that a periodic orbit can only exist within R, if $\mathbf{F}$ points outwards on the boundary C_{r1} and inwards on C_{r2}. Or, as in the case of Hamiltonian systems, the orbital derivative is equal zero everywhere and hence, the flow is tangent to both curves $V_{f_1}(\mathbf{u}) = C_{r1}$ and $V_{f_1}(\mathbf{u}) = C_{r2}$ for $R \in \mathbb{R}$ and any solution $\mathbf{u}(t)$ can neither leave nor approach $\mathbf{u}_{\mathrm{Eq},i}$ as $t \to \infty$. Therefore, at least one periodic orbit must exist in the annular compact region defined in (3.94).

It is interesting to note that the application of Poincaré-Bendixson to first-integral systems reveals one of the major shortcomings of the theorem itself. As shown above, each solution $\mathbf{u}(t)$ of (3.83) describes a trajectory in the three-dimensional function space of (3.87a) which corresponds to a so-called level set of constant energy, either (3.92) or (3.93), and hence to a constant C_r. Since there are infinite values for $C_r \in \mathbb{R}$ contained in the closed interval $[C_{r1};\, C_{r2}]$ there is an infinite number of periodic orbits contained in the compact region R. However, Poincaré-Bendixson can only establish the existence of at least one of these orbits, but not whether it is unique or not; see section 3.2.1 above.

In section 3.2.4 of this chapter various methods of stability analysis for periodic solutions have been discussed, foremost of all Poincaré mapping and the theorem of stable and unstable manifolds of periodic orbits. The apparent advantage of both methods is often attributed to their nature of being explicit schemes for the evaluation of oscillating systems [241]. However, explicit in this case implies that the exact analytical solution of the orbit, or a close approximation, must be known in order to uniquely satisfy stability criteria associated with each method. Analytical solutions for systems of differential equations can be obtained in a variety of ways. The most obvious, although only applicable to a marginally small number of simple or well-posed problems, is the search for one non-trivial exact solution $\mathbf{u}(t)$ of the flow $\mathbf{F}$, which only needs to hold in the phase space domain of interest $D \subset \mathbb{R}^n$ and not in the entire feasible solution space $\mathbb{R}^n$. Approximate analytical solutions are attained using much celebrated perturbation techniques and averaging methods for which a large body of literature exists. Some examples of classical texts can be found in [31, 127, 272, 273].

Instead of stable manifold theorems, a much simpler but equally effective approach in the case of Hamiltonian systems can be derived by combining the results of the Poincaré-Bendixson criterion with the definition of Lyapunov stability for periodic solutions given in section 3.2.4 above. By defining an invariant set R according to (3.94) and letting C_{r1} approach C_r from below and C_{r2} approach C_r from above such that

$$\lim_{C_{r1} \to C_r} \left(\inf_{\substack{\mathbf{v} \in C_r \\ \mathbf{w} \in C_{r1}}} \|\mathbf{v} - \mathbf{w}\| \right) = 0\,, \quad \text{and} \quad \lim_{C_{r2} \to C_r} \left(\inf_{\substack{\mathbf{v} \in C_r \\ \mathbf{w} \in C_{r2}}} \|\mathbf{v} - \mathbf{w}\| \right) = 0\,, \tag{3.95}$$

where $C_{r1}, C_{r2} > 0$ and $C_{r1}, C_{r2} \in \mathbb{R}$ defines a new invariant set R_c as

$$R_c = \left\{ \mathbf{u} \in \mathbb{R}^2 \middle| V_{f_1}(\mathbf{u}) \equiv C_r \right\}, \qquad \text{with} \qquad C_r \in \mathbb{R}, \tag{3.96}$$

which is a subset of R, i.e. $R_c \subset R$, and therefore compact and stable. Furthermore, together with definition 1 from section 3.2.4, R_c is equivalent to the periodic orbit Γ_c defined in Eq.(3.32), which originates from the solution[45] $\mathbf{u}(t)$ of the associated $\mathcal{C}^2$-continuously differentiable function

$$V_{f_1}(\mathbf{u}) \equiv C_r \tag{3.97}$$

given in (3.87). Thus, every solution $\mathbf{u}(t)$ of (3.78) satisfying (3.97) is in combination with definition 2 from section 3.2.4 orbitally stable.

3.4.1.3 Uniqueness

Derivation of the results above clearly establishes existence and stability of equilibrium points and periodic orbits, both associated with periodic solutions of the differential system in (3.78). However, one fundamental question remains: Is at least one solution of (3.78) satisfying dependency on initial conditions according to (3.7) unique in its existence? Theory presented in section 3.2.1 suggest usage of the Lipschitz criterion in (3.13) to establish uniqueness of solutions. Continuity of $\mathbf{F}$ and its first derivative

$$\|\mathbf{JF}\| = b\,\omega_n^2\,|u_1|^{b-1} \tag{3.98}$$

as given in (3.83a) is ensured in the entire phase space $\mathbb{R}^2$ since $\mathbf{JF}(\mathbf{u})$ does exist for all $\mathbf{u} \in \mathbb{R}^2$, but because (3.98) is not uniformly bounded in $\mathbb{R}^2$,

$$\lim_{\mathbf{u}\to\pm\infty} \|\mathbf{JF}\| = \pm\infty \qquad \forall\, \mathbf{u} \in \mathbb{R}^2, \tag{3.99}$$

it follows that (3.83) is locally[46] but not globally Lipschitz continuous as long as $b \geq 1$. Nevertheless, in conjunction with (3.98) a constant can always be found for any compact domain $D_l \subset \mathbb{R}^2$ such that

$$D_l = \left\{ \mathbf{u} \in \mathbb{R}^2 \middle| \, \|\mathbf{JF}\| \leq l \right\} \tag{3.100}$$

and therefore (3.78) is Lipschitz in D_l. Note that D_l is not limited in size in the phase plane, which is essential for global stability in (3.89) above. Contrary, for $0 < b < 1$ equation (3.98) becomes unbounded at $\mathbf{u} \equiv \mathbf{u}_l = 0$, irrespective of the limit approach direction,

$$\lim_{\mathbf{u}\to-0} \|\mathbf{JF}\| = -\infty, \qquad \text{and} \qquad \lim_{\mathbf{u}\to+0} \|\mathbf{JF}\| = +\infty, \tag{3.101}$$

[45] It should be clear from the topological results presented in sections 3.2.2 to 3.2.4 that there is exactly one periodic orbit for the solutions of (3.78) confined in the set as defined in (3.96).

[46] For any compact subset $S_l \subset \mathbb{R}^2$ of the phase space there exists a constant l such that (3.13) is satisfied. Therefore, (3.83) is locally Lipschitz.

and (3.78) is not locally Lipschitz in a neighborhood of $\mathbf{u} = 0$.

The problem of discontinuous and non-Lipschitz right hand sides as in equation (3.4) has long been known in dynamics, but was rigorously approached mathematically for the first time in [66] by Filippov. Even then it took two more decades to reconsider Filippov's work and make first attempts to expand it. At present, various different methods for proving existence and stability of such not well-behaving differential systems have been established and are currently under critical discussion. It is beyond the scope of this work to give a concise and almost complete overview of these new results since most of them unfortunately do not contain generalised statements for uniqueness, which is the essential problem of the system in (3.78). However, some of the approaches more suitable for the degenerate critical point of (3.78) are summarised under the expression of terminal dynamics system and have been briefly acknowledged in chapter 2. A remarkable and highly influential result has been presented by Bhat and Bernstein in [59], where the authors examine a classical gradient system with a transcendental energy function and show that the action integral has several extremal solutions and hence, Hamilton's principle [258] cannot uniquely determine the system's phase space trajectory even in the absence of random disturbances or noise.[47] This immediately implies that the existence of a Hamiltonian for the conservative system such as (3.78) does not necessarily ensure the important property of unique solutions.

Single or scalar non-Lipschitzian first-order differential equations in the form of Eq.(3.75) with $k_\beta \equiv 1$ and a constant value for the exponent b have been examined in [60, 274–277] for example. Most of the first-order examples originate either from fluid mechanics or circuit systems theory with a strong emphasis on process stabilisation for the latter. Application of results for one-dimensional first-order equations to the system in (3.78) is not feasible by basic theorems [61] since periodic solutions cannot occur in $\mathbb{R}^1$. Unfortunately the literature on second and higher order systems is sparse. In [278, 279] Jiang uses a flow generating equation similar to (3.78), although with $p \equiv 0$, to trace the trajectory of a bouncing particle. Despite being discontinuous the system is still Lipschitz. Re-examining Hartman's proposition [68] briefly mentioned in section 2.3 of the previous chapter, Robinson [280] introduced a method for phase spaces other than planar, i.e. $\mathbb{R}^n$ with n greater than 2, which establishes existence of the solution, but no uniqueness. In [64] Bernis and Kwong analysed a third-order differential equation which is allowed to be discontinuous and, more important, does not satisfy the Lipschitz condition of (3.12). Unfortunately, the theorems presented are only valid for either positive or negative applied loading and nonzero initial conditions. The authors Rios and Wolenski [281] established a theorem for strong invariance, an expression used in the same context as the term invariant manifold above, for one-sided autonomous Lipschitz systems where the vector field is separable into a single zone satisfying (3.12) and a finite number of zones around it which do not. However, for a general attempt to solve (3.78), where trajectories of the solution $\mathbf{u}(t)$ enter Lipschitz and non-Lipschitz zones with each cycle performed in the phase space, such an approach is unacceptable.

In order to clarify and illustrate the problem of non-uniqueness together with the implica-

[47] In comparison to [51, 53], where noise is an essential requirement for non-determinacy of the chaotic system.

tion it has for the analysis of the nonlinear flow $\mathbf{F}$, a simplified form of (3.78) as given in [279] considers the case

$$\dot{\mathbf{u}} = \left\{ \begin{array}{c} u_2 \\ -k_\beta \, |u_1|^b \, \frac{1}{t} \end{array} \right\} \qquad \text{with} \qquad b = \frac{1}{2}, \qquad k_\beta = 12 \, . \tag{3.102}$$

It is easily seen that the above equation has at least two solutions. The problem can be significantly generalised since (3.102) is a special case of the non-autonomous second-order equation

$$\ddot{u} = - \left(b^2 - b\right) |u|^{\frac{1}{b}} \, t^{b-3} \tag{3.103}$$

with $b \equiv 2$ and $k_\beta = 6 \left(b^2 - b\right)$. If one assumes $t > 0$, equation (3.103) possess the two solutions $u_{S_1} \equiv 0$ (trivial solution) and $u(t)_{S_2} = -t^b$, the latter one becoming $u(t)_{S_2} = -t^2$ for Eq.(3.102). Additionally, by relaxing the previous assumption, a third solution $u_{S_3}(t) = 0$ for $t \leq 0$ can be found satisfying both (3.102) and (3.103) if the initial conditions at $t = 0$ are equal to zero

$$u_1(0) = u_2(0) = 0 \, , \qquad \text{or} \qquad u(0) = \dot{u}(0) = 0 \, , \tag{3.104}$$

respectively. In connection with standard results for ordinary differential equations, see theorem 13 in [282] for example, such non-uniqueness implies the existence of an infinite number of solutions for the vector field in (3.78), all satisfying the initial conditions in (3.104).

As noted above, Bernis and Kwong [64], although not explicitly performed in the paper, used Picard iteration [238] in connection with the contraction mapping theorem, which is also the standard procedure for Lipschitz-continuous problems [241], to prove unique solutions for the non-autonomous third-order equation $\dddot{x}(t) = -t^\alpha \, x^\beta(t)$. Values for β are allowed to be negative as long as $\beta > -(\alpha + 1)/3$, hence the problem is clearly non-Lipschitz. Due to the simply structured right-hand side of the system successive integration can be performed with relative ease.

As a consequence of the lack of suitable general theorems for establishing uniqueness of solutions for (3.78) if $0 < b < 1$, it can be seen as beneficiary to adopt a similar approach as [64] above using Picard's successive iteration method. This is justified for a number of reasons. First, the method will establish whether a solution other than the trivial ones exist for different conditions of the nonlinear flow such as zero initial values and/or zero excitation. Secondly, although a closed form solution might not be obtainable, a series representation of $\mathbf{u}(t)$ can give valuable information on the structure of an analytical solution. And thirdly, any approximation derived using the method asymptotically approaches a feasible, existent solution of the nonlinear problem [257]. This is true for both trivial and nontrivial solutions alike, as will be seen in what follows.

Picard's method is based on the fact that every solution of (3.4) has to satisfy (3.7). Hence, an approximate solution for the nonlinear flow $\mathbf{F}$ can be generated by repeated application of (3.7) leading to a series representation

$$\tilde{\mathbf{u}}_{j+1}(t) = \mathbf{u}_0 + \int_0^t \mathbf{F}\Big(\tilde{\mathbf{u}}_j \, (\xi)\Big) \, \mathrm{d}\xi \, , \qquad \text{with} \quad \tilde{\mathbf{u}}_0(t) \equiv \mathbf{u}_0 \, , \qquad j = 0, 1, 2, \, \ldots \, . \tag{3.105}$$

Eventually, $\tilde{\mathbf{u}}(t)$ approaches the exact solution of the flow (3.4) as $j \to \infty$. As pointed out earlier, in case of a non-Lipschitzian $\mathbf{F}$, several solutions for the nonlinear problem can exist depending on the initial values, and hence, there is no guarantee that (3.105) converges towards a nontrivial solution of $\mathbf{F}$ in all cases. The simple textbook example $\dot{x} = 2\sqrt{x}$ with $x(t=0) = x_0 = 0$ and the two solutions $x_{S_1} \equiv 0$ and $x(t) = 0$ for $t < 0$, and $x(t) = t^2$ for $t \geq 0$ clearly illustrates this. Application of Picard's formula leads to $x_j(t) \equiv 0$ for all consecutive $j \in \mathbb{N}$.

However, usage of (3.105) for the first-order differential system in (3.78) gives as first approximation for $j = 0$

$$\tilde{\mathbf{u}}_1(t) = \mathbf{u_0} + \begin{Bmatrix} v_0\, t \\ A_1\, t \end{Bmatrix}, \qquad \text{with} \qquad \mathbf{u_0} = \begin{Bmatrix} u_0 \\ v_0 \end{Bmatrix}, \tag{3.106}$$

and $A_1 = \widehat{p}_0 - \omega_{\mathrm{n}}^2 \operatorname{sgn}(u_0)\, |u_0|^b$. All vectors of the approximate solution $\tilde{\mathbf{u}}_j(t)$ have the same structure as in (3.78), thus $\tilde{\mathbf{u}}_j(t) = \{\widetilde{u}_j,\, \widetilde{v}_j\}^{\mathrm{T}}$. Setting $j = 1$ and inserting (3.106) into (3.105) leads to the second approximation

$$\tilde{\mathbf{u}}_2(t) = \mathbf{u_0} + \begin{Bmatrix} v_0\, t + \frac{1}{2}\, A_1\, t^2 \\ \widehat{p}_0\, t - \omega_{\mathrm{n}}^2\, A_2(t) \end{Bmatrix}, \tag{3.107a}$$

where

$$A_2(t) = \int_0^t (u_0 + v_0 \xi)^b \, \mathrm{d}\xi = \frac{(u_0 + v_0\, t)^{b+1} - u_0^{b+1}}{v\,(b+1)}. \tag{3.107b}$$

A subsequent integration with $j = 3$ becomes impossible in closed form with both the signum and absolute value function in place in (3.78). Hence, assuming that u_2 from (3.107a) should be positive, it is required that

$$u_0,\, v_0,\, \widehat{p}_0 \geq 0\,, \qquad \text{and} \qquad A_1 \geq 0\,. \tag{3.108a}$$

This is no loss of generality but implies for the step magnitude to be

$$\widehat{p}_0 \geq \omega_{\mathrm{n}}^2 u_0^b\,, \tag{3.108b}$$

a constraint which is easily satisfied. It follows that

$$\tilde{\mathbf{u}}_3(t) = \mathbf{u_0} + \begin{Bmatrix} \left(v_0 + \frac{1}{2}\widehat{p}_0\, t\right) t - \omega_{\mathrm{n}}^2\, A_3(t) \\ \widehat{p}_0\, t - \omega_{\mathrm{n}}^2 \left(u_0 + \frac{1}{2}\, v_0\, t + \frac{1}{6}\, A_1\, t^2\right) t \end{Bmatrix} \tag{3.109a}$$

with the time varying function

$$A_3(t) = \int_0^t A_2\,(\xi)\, \mathrm{d}\xi = \frac{t}{v_0(b+1)} \Big((u_0 + v_0\, t)^{b+1} - u_0^{b+1} \Big)\,. \tag{3.109b}$$

A second assumption becomes necessary in order to be able to proceed with analytical integration. Taking into account (3.108a) and setting $\tilde{u}_3(t)$ from (3.109b) to be either positive or negative immediately leads to the following two cases

$$\begin{aligned} &(i) && \omega_n^2 A_3(t) > u_0 + v_0\, t + \frac{1}{2}\widehat{p}_0\, t^2 && \rightarrow && \operatorname{sgn}(\tilde{u}_3(t)) = -1 \\ &(ii) && \omega_n^2 A_3(t) < u_0 + v_0\, t + \frac{1}{2}\widehat{p}_0\, t^2 && \rightarrow && \operatorname{sgn}(\tilde{u}_3(t)) = 1\,. \end{aligned} \tag{3.110}$$

Since it is always possible to adjust all parameters in (3.110) in such a way that either of the two cases is true, the approach remains universal by choosing (ii) for example. Hence, repeated application of (3.105) together with (3.109a) gives

$$\tilde{\mathbf{u}}_4(t) = \mathbf{u_0} + \left\{ \begin{array}{c} \left(v_0 + \frac{1}{2}\widehat{p}_0\, t\right) t - \frac{\omega_n^2}{2}\, t^2 \left(u_0 + \frac{1}{3} v_0\, t + \frac{1}{12} A_1\, t^2\right) \\ \widehat{p}_0\, t - \omega_n^2\, A_4(t) \end{array} \right\} \tag{3.111a}$$

where

$$A_4(t) = \int_0^t \left(u_0 + v_0 \xi + \frac{1}{2} p_0 \xi^2 - \omega_n^2 A_3\,(\xi)\right)^b \mathrm{d}\xi\,. \tag{3.111b}$$

Unfortunately, it is the above function for $A_4(t)$ which makes it virtually impossible to obtain a closed-form explicit expression for $\tilde{\mathbf{u}}_4(t)$. Nevertheless, with suitable further assumptions

$$\begin{aligned} &(i) && \tilde{u}_4(t) < 0 && \rightarrow && p_0\, t < A_{C,4} && \forall\, t\,, && t_p \le t < \infty\,, \\ &(ii) && \tilde{u}_4(t) > 0 && \rightarrow && p_0\, t > A_{C,4} && \forall\, t\,, && 0 \le t < t_p\,, \end{aligned} \tag{3.112a}$$

where

$$A_{C,4} = \omega_n^2\, t \left(u_0 + \frac{1}{3} v_0\, t + \frac{1}{12} A_1\, t^2\right) - 2\, v_0 \tag{3.112b}$$

and t_p such that the equation $p_0 = A_{C,4}$ is satisfied, Picard's scheme can be continued until $\tilde{\mathbf{u}}_j(t)$ with $j \gg 3$ reaches any desired accuracy. All integrals encountered along this way have to be solved numerically. Without explicitly performing this rather simple task it should be clear from the derived results above, the differential first-order system in (3.78) possess at least one *nontrivial* solution for $u_0 \neq 0$, $v_0 \neq 0$ and $p_0 \neq 0$.

It still has to be ruled out that (3.78) does not exhibit signs of terminal behaviour discussed in chapter 2 when passing through the degenerate point $(0, 0)$. A simple examination of the phase space trajectories of (3.78), which can be explicitly plotted using either (3.54) or (3.67), reveals that the origin is only part of a periodic orbit if $u_0 = v_0 = 0$ and $\widehat{p}_0 \neq 0$. Thus, a nontrivial solution can be obtained applying these conditions to (3.105) resulting in

$$\tilde{\mathbf{u}}_1(t) = \left\{ \begin{array}{c} 0 \\ \widehat{p}_0\, t \end{array} \right\}, \qquad \tilde{\mathbf{u}}_2(t) = \left\{ \begin{array}{c} \frac{1}{2} t \\ 1 \end{array} \right\} \widehat{p}_0\, t\,, \qquad \tilde{\mathbf{u}}_3(t) = \left\{ \begin{array}{c} \frac{1}{2} t \\ 1 - \frac{\omega_n^2}{2\widehat{p}_0^2} \frac{t^{2b}}{2b+1} \end{array} \right\} \widehat{p}_0\, t \tag{3.113a}$$

and

$$\tilde{\mathbf{u}}_4(t) = \left\{ \begin{array}{c} \frac{1}{2}t - B_1\, t^{2b+1} \\ 1 - \frac{\omega_n^2}{6\,\widehat{p}_0}\, t^2 \end{array} \right\} \widehat{p}_0\, t\,, \quad \text{with} \qquad B_1 = \frac{\omega_n^2}{2\,\widehat{p}_0^2}\,\frac{1}{(2b+1)(2b+2)}\,. \tag{3.113b}$$

Once again, without questioning the general character of this approach, the first assumption for approximating the displacement in case of zero initial conditions is derived for $\widetilde{u}_4$ to be smaller zero. This implies that all subsequent equations including (3.113b) are only applicable for times

$$t \geq \left[\frac{1}{2\,B_1}\right]^{\frac{1}{2b+1}}\,, \tag{3.114}$$

which is a negligible small time frame for the periodic system under investigation. For example, if $\omega_n \approx \widehat{p}_0$ and $b = 0.5$, Eq.(3.114) gives $t \geq 2.45$s. It is easy to see that the opposite sign in (3.114) leads to results for the time range $0 \leq t \leq t_{B_1}$ where t_{B_1} is the time as obtained from equation (3.114). The next step produces with $\widetilde{u}_4 < 0$, thus $\operatorname{sgn}(\widetilde{u}_4)\,|\widetilde{u}_4| = -\widetilde{u}_4$,

$$\tilde{\mathbf{u}}_5(t) = \left\{ \begin{array}{c} \left(\frac{1}{2}\,p_0 - \frac{\omega_n^2}{24}\,t^2\right) t^2 \\ p_0\, t + \omega_n^2\, B_2(t) \end{array} \right\}\,, \quad \text{where} \quad B_2(t) = \int_0^t \left[\widehat{p}_0\,\xi\left(B_1 \xi^{2b+1} - \frac{1}{2}\,\xi\right)\right]^b \mathrm{d}\xi \tag{3.115a}$$

leads to

$$B_2(t) = \frac{t^{2b+1}}{2b+1}\left[(2B_3(t) - p_0)^b \left(2 - \frac{4B_3(t)}{p_0}\right)^{-b} {}_2\mathsf{F}_1\left(1 + \frac{1}{2b}, -b, 2 + \frac{1}{2b}, \frac{2}{p_0}\,B_3(t)\right)\right],$$

and

$$B_3(t) = B_1\, p_0\, t^{2b}\,. \tag{3.115b}$$

The expression ${}_2\mathsf{F}_1(...)$ stands for the Gaussian hypergeometric function [109], see appendix B.1. It should be noted that further analytical integration is possible, although omitted here, provided that the necessary assumptions are made which simplify both the signum and absolute value function in (3.78).

The above derivation clearly shows that a nontrivial solution for $\mathbf{u}(t)$ exists even in the case of zero initial conditions. Furthermore, if both initial conditions and excitation force are zero no solution other than the trivial one can be obtained, since it follows from (3.113) that $\tilde{\mathbf{u}}_j(t) \equiv 0$ with $j = 1, 2, \ldots, \infty$. This result is of fundamental nature for the system (3.78) since it can be seen as a newly derived prove of applicability of Okamura's uniqueness theorem [67] for the nonlinear flow in (3.78) if $p \equiv 0$. In brief, the theorem states that given a continuous flow $\mathbf{F}(\mathbf{u})$ defined in a domain $D \subset \mathbb{R}^2$ with $(t_0, \mathbf{u}_0) = (0, 0)$ and $\mathbf{F}\big(\mathbf{u}_0(t_0)\big) \equiv 0$, and supposing the Lyapunov function in equation (3.87a) exists and is *(i)* locally Lipschitz with respect to $\mathbf{u}$ at the origin, satisfies *(ii)* $V(\mathbf{u}_0) \equiv 0$, *(iii)* $V(\mathbf{u}) > 0$ if $|\mathbf{u}| \neq 0$, and *(iv)* the orbital derivative from (3.22) gives

$\mathcal{D}_{\mathrm{F}}V(\mathbf{u}) \leq 0$ within the interior of D, then the IVP in (3.4) with $(t_0, \mathbf{u}_0) = (0,0)$ has only the trivial solution $\mathbf{u}(t) \equiv 0$. It easy to verify that (3.78) complies with all of the above conditions and therefore justifies the findings obtained from application of Picard's method.

This leads to the conclusion, equivalently derived from Picard's method and Okamura's theorem above, that (3.4), although being non-Lipschitz, has only a trivial solution if $\mathbf{u}_0 = p_0 = 0$. Therefore, if $\mathbf{u}_0 \neq 0$ or $p_0 \neq 0$ or a combination of both, then $\tilde{\mathbf{u}}_{j+1}(t)$ as obtained from (3.105) converges for $j \to \infty$ to a nontrivial solution of the system (3.78).

It has become clear now that both trivial and nontrivial solutions exist and under what circumstances they occur. What remains still unanswered is the question if the nontrivial solutions are unique. A suitable approach to this specific aspect of the non-Lipschitz problem can be found in [63], arising from stability considerations for nonlinear electrical power systems [283]. The standard notation of equilibrium points of the nonlinear flow as given in (3.16) has been questioned on several occasions [284, 285]. Motivated by the fact that all time derivatives should be zero at an equilibrium point of (3.4), Köksal [284] introduces the condition

$$\mathbf{F}^{(j)}(\mathbf{u}_{\mathrm{Eq},i}) = 0\,, \qquad i = 1,2\,; \quad j = 1,2,\ldots,\infty \tag{3.116a}$$

where

$$\mathbf{F}^{(j)}(\mathbf{u}) = \mathbf{J}\mathbf{F}^{(j-1)}(\mathbf{u}) \cdot \mathbf{F}(\mathbf{u})\,, \tag{3.116b}$$

which every stationary point $\mathbf{u}_{\mathrm{Eq},i}$ must satisfy. With $\mathbf{F}^{(1)} = \mathbf{F}$, the above formulation clearly includes the classical notation of (3.16) as a special case. Although the paper [284] is in parts erroneous, some mathematical statements are imprecise and the first theorem can be proved invalid, the entire approach remains untouched. Venkatasubramaniam *et al* [63] formalised the conceptual idea of [284] and placed it on a more rigorous mathematical basis. Furthermore, the authors established definitions for the existence and uniqueness of first-order, locally non-Lipschitz differential equations. They also introduced, independently of Zak [50, 60] and others [49, 51, 59], the concept of terminal behaviour, although called 'impasse behaviour', where the impasse point of order $j = \infty$, obtained by successive utilization of (3.116), stands as a barrier for the continued predictability of the oscillatory system's trajectories. In other words, if the system passes through such a point, all past knowledge about its velocity as a vector quantity[48] is lost [55].

With $\mathbf{F}^{(1)} = \left\{\mathrm{F}_1^{(1)}, \mathrm{F}_2^{(1)}\right\}^{\mathrm{T}}$ from (3.116) being identical to $\mathbf{F}$ in (3.78),

$$\mathbf{F}^{(1)}(\mathbf{u}, \mathbf{z}) \equiv \mathbf{F}(\mathbf{u}, \mathbf{z})\,, \tag{3.117}$$

the second-order state space vector derivative according to [284] is together with (3.82) derived as

$$\mathbf{F}^{(2)} = \mathbf{J}\mathbf{F}^{(1)} \cdot \mathbf{F}^{(1)} = \begin{Bmatrix} \mathrm{F}_1^{(2)} \\ \mathrm{F}_2^{(2)} \end{Bmatrix} = \begin{Bmatrix} \mathrm{F}_2^{(1)} \\ -u_2 b \omega_{\mathrm{n}}^2 |u_1|^{b-1} \end{Bmatrix}. \tag{3.118}$$

[48] It is well known that a vector contains two items of information, direction and absolute value.

Further, by using the basic definition $|x| = x\ \mathrm{sgn}(x)$ in [186] for $x \neq 0$ and the chain rule of differential calculus [58], the expression

$$\begin{aligned}\frac{\partial}{\partial u_1}|u_1|^{b-1} &= \frac{\partial}{\partial u_1}\big(u_1\,\mathrm{sgn}(u_1)\big)^{b-1}\\ &= (b-1)\,|u_1|^{b-2}\,\frac{\partial}{\partial u_1}\big(u_1\,\mathrm{sgn}(u_1)\big)\\ &= (b-1)\,\mathrm{sgn}(u_1)\,|u_1|^{b-2}\\ &= A_2(u_1)\end{aligned} \tag{3.119}$$

is obtained, leading to

$$\mathbf{F}^{(3)} = \left\{\begin{array}{c} \mathrm{F}_2^{(2)} \\ -b\,\omega_\mathrm{n}^2\,\left(u_2^2\,A_2(u_1) + |u_1|^{b-1}\,\mathrm{F}_2^{(1)}\right)\end{array}\right\}. \tag{3.120}$$

By setting $j \equiv 4$ in (3.116) the method is more involved yielding for the elements of the Jacobian

$$\mathbf{JF}^{(3)} = \begin{bmatrix} \frac{\partial \mathrm{F}_1^{(3)}}{\partial u_1} & \frac{\partial \mathrm{F}_1^{(3)}}{\partial u_2} \\ \frac{\partial \mathrm{F}_2^{(3)}}{\partial u_1} & \frac{\partial \mathrm{F}_2^{(3)}}{\partial u_2}\end{bmatrix}, \tag{3.121a}$$

with

$$\begin{aligned}\frac{\partial}{\partial u_1}\mathrm{F}_1^{(3)} &= \frac{\partial}{\partial u_1}\mathrm{F}_2^{(2)} = -u_2\,b\,\omega_\mathrm{n}^2\,\frac{\partial}{\partial u_1}|u_1|^{b-1} = -u_2\,b\,\omega_\mathrm{n}^2\,A_2(u_1)\ ,\\ \frac{\partial}{\partial u_2}\mathrm{F}_1^{(3)} &= \frac{\partial}{\partial u_2}\mathrm{F}_2^{(2)} = -b\,\omega_\mathrm{n}^2\,|u_1|^{b-1}\ ,\end{aligned} \tag{3.121b}$$

and

$$\begin{aligned}\frac{\partial}{\partial u_1}\mathrm{F}_2^{(3)} = -u_2\,b\,\omega_\mathrm{n}^2(b-1)\frac{\partial}{\partial u_1}\mathrm{sgn}(u_1)\,|u_1|^{b-2} - b\,\omega_\mathrm{n}^2\frac{\partial}{\partial u_1}\Big(\omega_\mathrm{n}^2\,\mathrm{sgn}(u_1)\,|u_1|^{2b-1}\\ - p_0\,|u_1|^{b-1}\Big)\end{aligned} \tag{3.121c}$$

where, using both product and chain rule [58],

$$\begin{aligned}\frac{\partial}{\partial u_1}\mathrm{sgn}(u_1)\,|u_1|^{b-2} &= \mathrm{sgn}(u_1)\,\frac{\partial}{\partial u_1}|u_1|^{b-2}\\ &= (b-2)\,|u_1|^{b-3}\\ &= A_3(u_1)\ ,\end{aligned} \tag{3.121d}$$

$$\begin{aligned}\frac{\partial}{\partial u_1}\operatorname{sgn}(u_1)\,|u_1|^{2b-1} &= (2b-1)\operatorname{sgn}(u_1)\,|u_1|^{2b-2}\,\frac{\partial}{\partial u_1}\big(\operatorname{sgn}(u_1)\;u_1\big)\\ &= (2b-1)\,|u_1|^{2b-2}\\ &= B_2(u_1)\;,\end{aligned} \tag{3.121e}$$

and $B_1(u_1) = \operatorname{sgn}(u_1)\,|u_1|^{2b-1}$ leads to

$$\frac{\partial}{\partial u_1}\mathrm{F}_2^{(3)} = -u_2^2\,b\,\omega_\mathrm{n}^2\,(b-1)\;A_3(u_1) - b\,\omega_\mathrm{n}^2\Big(\omega_\mathrm{n}^2\,B_2(u_1) - p_0\,A_2(u_1)\Big) \tag{3.121f}$$

as well as

$$\frac{\partial}{\partial u_2}\mathrm{F}_2^{(3)} = -2\,u_2\,b\,\omega_\mathrm{n}^2\,A_2(u_1)\;. \tag{3.121g}$$

Substitution of (3.121) into (3.121c), which together with (3.121b) and (3.121g) is inserted back into (3.121a) leads after multiplication with $\mathbf{F}$ from (3.78), as defined in (3.116), to

$$\mathbf{F}^{(4)} = b\,\omega_\mathrm{n}^2\begin{Bmatrix} -u_2^2\,A_2(u_1) - p_0\,|u_1|^{b-1} + \omega_\mathrm{n}^2\,B_1(u_1) \\ -u_2^3\,(b-1)\,A_3(u_1) - u_2\left(\omega_\mathrm{n}^2\,B_2(u_1) + p_0\,A_2(u_1) - 2\omega_\mathrm{n}^2\,C_2(u_1)\right)\end{Bmatrix} \tag{3.122}$$

with $C_2(u_1) = (b-1)\,|u_1|^{2b-2}$. The authors in [286] provide a uniqueness theorem which takes advantage of the fact that even if the flow of a system such as (3.78) does not satisfy the Lipschitz condition at a critical point $\mathbf{u}_{\mathrm{cr}} = \{u_{1,\mathrm{cr}}, u_{2,\mathrm{cr}}\}^{\mathrm{T}}$ as given in (3.101) where $\mathbf{u}_{\mathrm{cr}} \equiv \mathbf{u}_l$, it is still differentiable at $\mathbf{u}_{\mathrm{cr}}$. By deriving the state space derivatives as shown in Eqs.(3.118), (3.120) and (3.122), "better-behaving" higher-order functions are obtained which might be eligible to fulfill equation (3.12). The fundamental difference to existing theorems lies in the fact that only the j-th order solution of (3.116) needs to satisfy the Lipschitz condition in order to guarantee a unique solution $\mathbf{u}(t)$ of the flow $\mathbf{F}^{(1)} \equiv \mathbf{F}$ of (3.117). This is a remarkable result and has been demonstrated to work well for quite a wide range of first-order scalar and vector differential systems [63, 283, 286]. Unfortunately, in the case of (3.78) the problem is more complex. Obviously, application of condition (3.13) to equation (3.118), which gives

$$\left\|\mathbf{J}\mathbf{F}^{(2)}\right\| = b^2\,\omega_\mathrm{n}^4\,|u_1|^{2b-2}\;, \tag{3.123}$$

is not bounded if $\mathbf{u} \to \mathbf{u}_l \equiv 0$, and hence $\mathbf{F}^{(2)}$ is not Lipschitzian either. The same applies to $\left\|\mathbf{J}\mathbf{F}^{(3)}\right\|$, which is obtained using (3.121a) to (3.121g). In fact, it is easily verified, none of the $\mathbf{F}^{(j)}$ with $j = 1, 2, \ldots, \infty$ above satisfies either equation (3.12) or (3.13) from section 3.2.1. It is now proposed in this work to use Peano's theorem[49] [67] instead of the Lipschitz conditions to prove uniqueness of order j solutions in (3.116). Before the theorem can be stated, the following definition is needed:

Definition 3. *Two vectors* $\mathbf{u}, \bar{\mathbf{u}} \in \mathbb{R}^n$ *with* $\mathbf{u} = \{u_1, \ldots, u_n\}^{\mathrm{T}}$ *and* $\bar{\mathbf{u}} = \{\bar{u}_1, \bar{u}_2, \ldots, \bar{u}_n\}^{\mathrm{T}}$

[49] This should not be confused with Peano's existence theorem which simply requires continuity of the vector field, see section 3.2.1 of this chapter.

are defined to be $\mathbf{u} \leq \bar{\mathbf{u}}$, *if and only if,* $u_i \leq \bar{u}_i$ *for* $1 \leq i \leq n$. *The flow*

$$\mathbf{F}(t, \mathbf{u}) = \left\{ F_1(t, \mathbf{u}), \ldots, F_n(t, \mathbf{u}) \right\}^{\mathrm{T}} \tag{3.124}$$

is defined non-decreasing in t *if* $\mathbf{F}(t_1, \mathbf{u}) \leq \mathbf{F}(t_2, \mathbf{u})$ *whenever* $(t_1, \mathbf{u})$ *and* $(t_2, \mathbf{u})$ *are elements of the domain*

$$D_+ = \left\{ t, a \in \mathbb{R} : t_0 \leq t \leq t_0 + a\,;\ \mathbf{u} \in \mathbb{R}^n : \|\mathbf{u} - \mathbf{u}_0\| \leq b \right\}, \tag{3.125}$$

and $t_1 \leq t_2$. *The flow in* (3.124) *is defined to be non-decreasing in* $\mathbf{u}$ *if* $\mathbf{F}(t, \mathbf{u}) \leq \mathbf{F}(t, \bar{\mathbf{u}})$ *whenever* $(t_1, \mathbf{u})$ *and* $(t_1, \bar{\mathbf{u}}) \in D_+$ *and* $\mathbf{u} \leq \bar{\mathbf{u}}$. *Moreover,* $\mathbf{F}(t, \mathbf{u})$ *is quasi-nondecreasing in* $\mathbf{u}$ *if for each* $i = 1, 2, \ldots, n$ *the scalar components of the flow in equation* (3.124) *are* $F_i(t, \mathbf{u}) \leq F_i(t, \bar{\mathbf{u}})$ *whenever* $\mathbf{u} \leq \bar{\mathbf{u}}$ *and* $u_i = \bar{u}_i$. *If* $\mathbf{F}(t, \mathbf{u})$ *is neither non-decreasing nor quasi-non-decreasing in* $\mathbf{u}$, *then it is non-increasing in* $\mathbf{u}$. *Results for* t *are analogous.*

With this definition of an increasing or decreasing vector field in mind, the theorem can now be given as follows.

Theorem 4 (Peano's Uniqueness Theorem). *Let* $\mathbf{F}(t, \mathbf{u})$ *be continuous in the closed set* D_+, *non-increasing in* $\mathbf{u}$ *for each fixed* t *in the interval* $[t_0,\ t_0 + a]$, *and for all* $(t, \mathbf{u})$, $(t, \bar{\mathbf{u}})$ *in* D_+ *the flow* $\mathbf{F}$ *satisfies*

$$\left(\mathbf{F}(t, \mathbf{u}) - \mathbf{F}(t, \bar{\mathbf{u}}) \right) \cdot (\mathbf{u} - \bar{\mathbf{u}}) \leq 0\,, \tag{3.126}$$

then the initial value problem (3.4) *has at most one* n*-dimensional solution in* $[t_0,\ t_0 + a]$.

It is easy to see that $\mathbf{F}$ of (3.78) is defined for all $\mathbf{u} \in \mathbb{R}^2$ even if $b < 1$ and becomes only singular if $b < 0$. This continuity of the system in (3.78) throughout the domain D_+ ensures that $\dot{u}_1 = u_2$ together with $\dot{u}_2 = \widehat{p}_0 - \omega_{\mathrm{n}}^2 \operatorname{sgn}(u_1) |u_1|^b$ is a non-increasing flow field in $\mathbf{u} = \{u_1,\ u_2\}^{\mathrm{T}}$ for all $t \in [0, \infty)$. Application of (3.126) to the autonomous flow $\mathbf{F}^{(2)}$ from (3.118) yields at the critical point $\mathbf{u} \equiv \mathbf{u}_l = 0$ given in (3.101)

$$\mathbf{F}^{(2)}(\bar{\mathbf{u}}) \cdot \bar{\mathbf{u}} = -\omega_{\mathrm{n}}^2 \begin{Bmatrix} |\bar{u}_1|^{b+1} \\ u_2^2\, b\, |\bar{u}_1|^{b-1} \end{Bmatrix}. \tag{3.127}$$

Taking into account that the velocity varies with the square root of the displacement, see Eq.(3.67), hence $u_2(t) \propto \sqrt{u_1(t)}$, the expression $u_2^2\, b\, |\bar{u}_1|^{b-1}$ in (3.127) is simplified to $b\, |u_1|^b$. This clearly shows $\mathbf{F}^{(2)}$ satisfies Peano's condition in (3.126) for all $\bar{\mathbf{u}} \in \mathbb{R}^n$. Letting the trajectory of the solution $\bar{\mathbf{u}}(t)$ approach the critical point $\mathbf{u}_l = 0$

$$\lim_{\bar{\mathbf{u}} \to \pm \mathbf{0}} \begin{Bmatrix} |\bar{u}_1|^{b+1} \\ |\bar{u}_1|^{b} \end{Bmatrix} = \mathbf{0}\,, \tag{3.128}$$

proves uniqueness of the second-order solution of the flow $\mathbf{F}(\mathbf{u})$ from (3.78) at $\mathbf{u}_l$. This is identical to the approach of Venkatasubramanian *et al* in [286], but the authors there require the higher-order

solutions to satisfy the more stringent Lipschitz criterion of (3.12) and (3.13), respectively. However, here the same conclusions are reached using Peano's condition for j-th order flows failing to satisfy Lipschitz. Thus, since the order two solution $\mathbf{F}^{(2)}$ is also an order one solution, the fact that equation (3.127) has a unique solution for the point $\mathbf{u} \equiv 0$, establishes uniqueness of solution for the original flow because $\mathbf{F} \equiv \mathbf{F}^{(1)}$ according to (3.116). Finally, this provides uniqueness of both, trivial and nontrivial solutions $\mathbf{u}(t)$ starting at zero initial values $\mathbf{u}(t_0) = \mathbf{u}_0 = 0$ of the first-order differential system in (3.78). In fact, it is a simple exercise to show that Peano's condition not only holds for (3.116) if $j = 2$, but equation (3.126) remains valid for all $j \in \mathbb{N}$ and hence, $\mathbf{F}(\mathbf{u}_0) = 0$ is a strong solution of order ∞ in the sense of [286].

Up to now, the above findings regarding existence and uniqueness of the non-Lipschitzian vector field in Eq.(3.78) only take into account the flow $\mathbf{F}$ and its solution(s) $\mathbf{u}(t)$. If one assumes for the results derived in this chapter that the system stays free of the effects of non-conservative, non-smooth and non-autonomous restoring and applied forces, it is advantageous to consider the Lyapunov function of (3.78) not only for stability analysis as performed above, but also for the derivation of uniqueness statements for trajectories of the flow in (3.78). This approach relies mainly on one theorem and should therefore be seen as an alternative way of ruling out multiple solutions of nonlinear first-order differential systems, which have a scalar function of the type given in (3.87) but otherwise fail to satisfy the local Lipschitz conditions at certain critical points $\mathbf{u}_{\mathrm{cr}} = \{u_{1,\mathrm{cr}}, u_{2,\mathrm{cr}}\}^{\mathrm{T}}$ such as $\mathbf{u}_{\mathrm{cr}} = \mathbf{u}_l = 0$. The theorem used in here is the lesser known Brauer-Sternberger Uniqueness Theorem given in this case as a Perron-type formulation[50] and can be found in [67] for example. A slightly modified version more suitable for the problem under consideration is given here.

Theorem 5 (Brauer-Sternberger's Uniqueness Theorem). *Let there be a function $h(t, y)$ which is continuous in an interval ${}_aI_+ = \{t \in \mathbb{R} : t_0 < t \leq t_0 + a\}$ for $y \geq 0$, and for every $t_1 \in {}_aI_+$ assume that $y(t) \equiv 0$ is the only differentiable function within the interval ${}_1I_+ = \{t \in \mathbb{R} : t_0 < t < t_1\}$ and continuous in ${}_2I_+ = \{t \in \mathbb{R} : t_0 \leq t \leq t_1\}$ for which*

$$\frac{\partial}{\partial t} y_+(t_0) = \lim_{t \to +t_0} \frac{y(t) - y(t_0)}{t - t_0} \tag{3.129}$$

exists and both of the following two conditions

$$(i) \quad \frac{\partial}{\partial t} y(t) = h(t, y(t)) \ \forall t \in {}_1I_+, \qquad \text{and} \qquad (ii) \quad y(t_0) = \frac{\partial}{\partial t} y_+(t_0) = 0 \tag{3.130}$$

hold. Furthermore, assume the field $\mathbf{F}(t, \mathbf{u})$ of Eq.(3.4) is continuous in D_+ from definition 3; and there exists a Lyapunov function $L(t, \mathbf{u} - \bar{\mathbf{u}})$ defined and continuously differentiable in

[50] Perron's uniqueness theorem [249, 287] is a generalisation of the uniform Lipschitz condition given in (3.12) for first-order scalar equations.

$D_0 = \{ (t, \Delta\mathbf{u}) : (t, \mathbf{u}) \in D_+ , \ (t, \bar{\mathbf{u}}) \in D_+ \}$ *with* $\Delta\mathbf{u} = \mathbf{u} - \bar{\mathbf{u}}$ *such that*

$$\textit{(iii)} \quad L(t,0) \equiv 0 , \qquad \textit{and} \qquad \textit{(iv)} \quad L(t,\Delta\mathbf{u}) > 0 \quad \textit{if} \quad \|\Delta\mathbf{u}\| \neq 0 , \tag{3.131}$$

and for all $(t, \Delta\mathbf{u}) \in D_0$ *with* $t \neq t_0$ *the orbital derivative from Eq.*(3.22) *yields*

$$\mathcal{D}_{\mathbf{F}} L(t,\Delta\mathbf{u}) = \frac{\partial}{\partial t} L(t,\Delta\mathbf{u}) + \frac{\partial}{\partial \mathbf{u}} L(t,\Delta\mathbf{u}) \cdot \big(\mathbf{F}(t,\mathbf{u}) - \mathbf{F}(t,\bar{\mathbf{u}}) \big) \leq h\big(t, L(t,\Delta\mathbf{u})\big) . \tag{3.132}$$

Then the initial value problem in (3.4) *has at most one solution in* ${}_2I_+$.

It should be noted that the function $h\big(t, L(t,\Delta\mathbf{u})\big)$ can be arbitrarily chosen as long as it satisfies both (3.129) and (3.130). With $\Delta\mathbf{u} \equiv 0$ in the above theorem it is easily verified that the Hamiltonian equation (3.87a) of the system in (3.78) complies with *(iii)* because $V_{f_1}(\mathbf{0}) = 0$ for zero initial values which is the case under consideration here. By setting $\mathbf{u} \equiv \mathbf{u}_l = 0$ condition *(iv)* gives

$$V_{f_1}(-\bar{\mathbf{u}}) = \frac{1}{2}(-\bar{u}_2)^2 + \frac{\omega_n^2}{b+1} |-\bar{u}_1|^{b+1} + p_0 \bar{u}_1 \quad > 0 \qquad \text{for} \qquad \|\bar{\mathbf{u}}\| \neq 0 , \tag{3.133}$$

which is true for all $\bar{\mathbf{u}} \in \mathbb{R}^2$ since according to equation (3.155) below, if

$$\mathbf{u}_0 \equiv 0 , \ p_0 > 0 \qquad \text{then} \qquad u_1 \geq 0 \ \forall \ t \qquad \text{where} \qquad t \in {}_aI_+ . \tag{3.134}$$

Otherwise, if $p_0 < 0$ then $u_1 \leq 0 \ \forall t \in {}_aI_+$. Application of (3.132) leads for $\mathbf{u} \equiv \mathbf{u}_l$ to

$$\mathcal{D}_{\mathbf{F}} V_{f_1}(-\bar{\mathbf{u}}) \cdot \big(\mathbf{F}(\mathbf{0}) - \mathbf{F}(\bar{\mathbf{u}}) \big) = \begin{Bmatrix} \omega_n^2 \operatorname{sgn}(-\bar{u}_1) |-\bar{u}_1|^b - p_0 \\ -\bar{u}_2 \end{Bmatrix} \cdot \begin{Bmatrix} -\bar{u}_2 \\ \omega_n^2 \operatorname{sgn}(\bar{u}_1) |\bar{u}_1|^b \end{Bmatrix} ,$$

which can be simplified, assuming without loss of generality $\bar{u}_1 \geq 0 \ \forall \ t \in {}_aI_+$ if $p_0 > 0$, to

$$\begin{aligned} &= \bar{u}_2 \left(\omega_n^2 \bar{u}_1^b + p_0 \right) - \omega_n^2 \bar{u}_1^b \\ &= \bar{u}_2 \, p_0 . \end{aligned} \tag{3.135}$$

In order for $h\big(t, L(t,\Delta\mathbf{u})\big)$ from (3.132) to conform with *(i)* in theorem 5 the following condition must be satisfied

$$\frac{\partial}{\partial t} V_{f_1}(\Delta\mathbf{u}) = h\big(t, V_{f_1}(\Delta\mathbf{u})\big) = \Delta u_2 \frac{\partial}{\partial t} \Delta u_2 + \left(\omega_n^2 \operatorname{sgn}(\Delta u_1) |\Delta u_1|^b - p_0 \right) \frac{\partial}{\partial t} \Delta u_1 \tag{3.136}$$

where $\Delta\mathbf{u} = \{\Delta u_1, \Delta u_2\}^{\mathrm{T}} = \{u_1 - \bar{u}_1, u_2 - \bar{u}_2\}^{\mathrm{T}}$ and $\partial\Delta\mathbf{u}/\partial t = \big\{\partial\Delta u_1/\partial t, \partial\Delta u_2/\partial t\big\}^{\mathrm{T}}$. With $\mathbf{u}$ being the critical point at the origin of the coordinate system, this simplifies in conjunction with (3.134) to

$$\frac{\partial}{\partial t} V_{f_1}(\Delta\mathbf{u}) \bigg|_{\mathbf{u}=0} = \bar{u}_2 \frac{\mathrm{d}}{\mathrm{d}t} \bar{u}_2 + \bar{u}_2 \left(\omega_n^2 \bar{u}_1^b + p_0 \right) , \tag{3.137a}$$

or, together with the equation of motion (3.3) and $\mathrm{d}\bar{u}_2 / \mathrm{d}t \equiv \dot{\bar{u}}_2 = \widehat{p_0} - \omega_{\mathrm{n}}^2\, \bar{u}_1^b$ to

$$\begin{aligned} &= 2\, p_0\, \bar{u}_2 \\ &\equiv h\big(V_{f_1}(-\bar{\mathbf{u}})\big)\,. \end{aligned} \tag{3.137b}$$

It should be noted since (3.136) is continuous and differentiable, hence smooth within$_2 I_+$, the limit approaching t_0 from the right in (3.129) exists. With $\bar{\mathbf{u}}\,(t_0 = 0) = 0$ and therefore

$$\frac{\partial}{\partial t}\, V_{f_1}(t = 0) = 0 \tag{3.138}$$

in Eq.(3.137a), condition *(ii)* in theorem 5 holds and thus, together with (3.137) equation (3.130) is satisfied. Furthermore, since *(iii)* and *(iv)* in (3.131) have been proven in (3.133) above, both functions $V_{f_1}(\Delta\mathbf{u})$ and $h\big(V_{f_1}(\Delta\mathbf{u})\big)$ are feasible in terms of the Brauer-Sternberger's theorem. Finally, this allows for condition (3.132) to be written in conjunction with both, (3.135) and (3.137), as

$$\mathcal{D}_{\mathbf{F}} V_{f_1}(-\bar{\mathbf{u}}) \cdot \big(\mathbf{F}\,(\mathbf{0}) - \mathbf{F}\,(\bar{\mathbf{u}})\big) \leq h\big(V_{f_1}(\Delta\mathbf{u})\big)$$

leading to the simple inequality

$$1 \leq 2\,, \tag{3.139}$$

which holds for all $\mathbf{u} \in D_+$ according to (3.125) with $n = 2$ in the case of system (3.78), despite assuming $p_0 > 0$ in (3.134). For opposite signs, e.g. $p_0 < 0$, the proof is identical.

As a last comment in this section on proving uniqueness for the solution (3.7) of the nonlinear vector field in (3.78), one can comprehend how inappropriate the sole application of Lipschitz's condition (3.12) for the specific system in (3.83) is by a simply considering the following. It has been shown in (3.115a) using Picard's method that for zero initial conditions $\mathbf{u}_0 = 0$ the nontrivial solution is only obtained if $p_0 \neq 0$. In other words, whether closed orbit solution for (3.83) do exist is simply determined by adding a constant to the differential terms in the system of nonlinear equations. However, this constant vanishes entirely when using the condition as given in (3.13). Hence, the sole difference between oscillation and no oscillation remains hidden from the classical but too stringent Lipschitz criterion.

This finally concludes the proof of uniqueness for solutions with zero initial values of the non-Lipschitzian system in (3.78), which has been achieved in two rather different approaches. Using a recently suggested method by Köksal [284] for deriving higher-order equilibria, it was possible to show that even if the j-th critical point does not fulfill the Lipschitz requirement as suggested in [286], the trajectory passing through it has a unique solution if the nonlinear flow satisfies Peano's theorem. The second approach, being completely independent of the first, takes advantage of the existence of a Lyapunov function for the system under consideration, which, together with

the Brauer-Sternberger uniqueness theorem, can be utilised to establish unique solutions, if the systems fails to be Lipschitz-continuous at specific critical points along the trajectories of the nonlinear flow passing through these singularities.

3.4.1.4 Extreme response values

Impulse excitation. Maximum values of displacement in case of an impulse excited or freely vibrating system are obtained from Eq.(3.51b) together with (3.76) and the simplified notation $u = u_1$ and $\dot{u} = u_2$

$$C_1 = \frac{m}{2}\left(\frac{p_\delta}{m} + \dot{u}_0\right)^2 + \frac{k_\beta}{b+1}\,|u_0|^{b+1} \tag{3.140}$$

which leads for Eq.(3.52) to

$$u_{\mathsf{Ex}} = \operatorname{sgn}(u_{\mathsf{Ex}})\left[\frac{b+1}{k_\beta}\,C_1\right]^{\frac{1}{b+1}} \tag{3.141a}$$

so that $u_{\mathsf{Ex}} = \{u_{\mathsf{min}},\, u_{\mathsf{max}}\}$ where $u_{\mathsf{min}} \leq 0$ and $u_{\mathsf{max}} \geq 0$. Hence, Eq.(3.141a) determines either u_{min} or u_{max}. Because the system oscillates around the equilibrium point $u_{\mathsf{eq}} = 0$, see (3.56), the complementary quantity is obtained from the relation

$$u_{\mathsf{min}} = -u_{\mathsf{max}}\,. \tag{3.141b}$$

Due to the restriction of feasible values for both, stiffness coefficient $k_\beta > 0$ and stiffness exponent $b \geq 0$, see above, it follows for the constant C_1 in (3.140)

$$C_1 > 0 \qquad \forall \quad u_0,\, \dot{u}_0\,, p_0 \in \mathbb{R} \tag{3.142}$$

and Eq.(3.141a) will always yield real-valued solutions. Substitution of (3.140) into (3.57) gives extreme values for velocity. Since $f_1(u)$ becomes maximum at both boundaries u_{Ex}, i.e. there are no other minima/maxima for $f_1(u)$ within the interval $u_{\mathsf{min}} \leq u(t) \leq u_{\mathsf{max}}$, equation (3.75) substituted into (3.59) yields the expression for peak acceleration values

$$\ddot{u}_{\mathsf{Ex}} = -\frac{k_\beta}{m}\operatorname{sgn}(u_{\mathsf{Ex}})\,|u_{\mathsf{Ex}}|^b\,, \tag{3.143}$$

since $f_1(u)$ is strictly monotonic for all $b \in \mathbb{R}$. The oscillation period of the system in (3.78) is obtained by applying (3.62)

$${}_{\mathrm{f}_1}T_\delta = \sqrt{2m}\int_{u_{\mathsf{min}}}^{u_{\mathsf{max}}}\left(-\frac{k_\beta}{b+1}\,|u|^{b+1} + C_1\right)^{-\frac{1}{2}}\,\mathrm{d}u \tag{3.144a}$$

and must be rewritten as a sum of two integration intervals covering $(u_{\mathsf{min}};\, 0)$ and $(0;\, u_{\mathsf{max}})$, respectively, due to the singularity of the first derivative of the absolute value function $|u|$ at $u = 0$. The first term of this sum is shifted into the positive real-valued domain $\mathbb{R}_+$ for the independent

variable by substituting $u(t) = -u(t)$, thus

$$-\int_{|u_{\min}|}^{0} (\ldots)^{-\frac{1}{2}}\, \mathrm{d}u = \int_{0}^{|u_{\min}|} (\ldots)^{-\frac{1}{2}}\, \mathrm{d}u\,, \tag{3.144b}$$

and Eq.(3.144a), together with (3.141b) can be expressed as

$${}_{\mathrm{f}_1}T_\delta = \frac{2}{\omega_{\mathrm{n}}}\sqrt{2(b+1)}\int_{0}^{u_{\max}} \frac{\mathrm{d}u}{\sqrt{-u^{b+1}+C_{1,\mathrm{f}_1}}}\,, \qquad u_{\max} \geq 0 \tag{3.144c}$$

where

$$\omega_{\mathrm{n}}^2 = \frac{k_\beta}{m}\,, \qquad \text{and} \qquad C_{1,\mathrm{f}_1} = \frac{b+1}{k_\beta}\,C_1\,. \tag{3.144d}$$

This allows for the definition of an oscillation frequency f_{n} for an equivalent linear reference system with $b \equiv 1$ and identical mass and stiffness coefficient parameters defined as

$$f_{\mathrm{n}} = \frac{\omega_{\mathrm{n}}}{2\pi}\,. \tag{3.144e}$$

Equation (3.144c) can either be solved using available textbooks such as Byrd *et al* [288], or algebraic manipulation software [289]. The first alternative is used below for the step excited system where algebraic software cannot obtain a closed-form solution, whereas the latter method gives in the actual case

$${}_{\mathrm{f}_1}T_\delta = \frac{2\,u_{\max}}{\omega_{\mathrm{n}}}\sqrt{\frac{2(b+1)}{C_{1,\mathrm{f}_1}}}\;{}_2\mathsf{F}_1\left(\frac{1}{2};\,\frac{1}{1+b};\,1+\frac{1}{1+b};\,\frac{u_{\max}^{b+1}}{C_{1,\mathrm{f}_1}}\right) \tag{3.144f}$$

with ${}_2\mathsf{F}_1(\ldots)$ as hypergeometric function [109]. Comparing Eq.(3.144f) to (3.141a) in conjunction with (3.144d) and bearing in mind $u_{\max} \geq 0$, gives

$$\frac{u_{\max}^{b+1}}{C_{1,\mathrm{f}_1}} = 1\,. \tag{3.145}$$

Hence, (3.144f) can be simplified to [290]

$${}_{\mathrm{f}_1}T_\delta = \frac{2\,u_{\max}}{\omega_{\mathrm{n}}}\sqrt{\frac{2(b+1)}{C_{1,\mathrm{f}_1}}}\,\sqrt{\pi}\,\frac{\Gamma\left(1+\frac{1}{1+b}\right)}{\Gamma\left(\frac{1}{2}+\frac{1}{1+b}\right)}\,. \tag{3.146}$$

It should be emphasised that all of the above derived expressions are valid for b, k_β, $u \in \mathbb{R}$ with the only constraint from (3.75), $b \geq 0$ and $k_\beta \geq 0$, due to stability and existence reasons as explained earlier in this section. Furthermore, by setting $b = 1$, Eq.(3.146) gives together with (3.141a) and the special values of the Gamma function, namely $\Gamma\left(3/2\right) = \sqrt{\pi}/2$, and $\Gamma\left(1\right) = 1$,

the well-known relation for the linear system

$$ {}_{\mathrm{f}_1}T_\delta = \frac{1}{f_\mathrm{n}} . \tag{3.147} $$

Returning to Eq.(3.144c) and introducing a special case by setting $b = 2$ in (3.144c) leads to the possible predictions of multiple oscillation frequencies if the response of the SDOF system with $f_1(u)$ is approximated in terms of trigonometric functions. It is obvious that the polynomial discriminant D_s

$$ D_s = \left(-\frac{C_{1,\mathrm{f}_1}}{2} \right)^2 , \tag{3.148a} $$

of the cubic equation

$$ -u^3 + C_{1,\mathrm{f}_1} = 0 \tag{3.148b} $$

is always greater zero and hence, Eq.(3.148b) has one real and two conjugate complex solutions [58]

$$ \chi_1 = \sqrt[3]{C_{1,\mathrm{f}_1}} = u_\mathsf{max} , \qquad \overline{\chi_2} = \frac{1}{2}\left(-1 - \mathrm{i}\sqrt{3}\right) u_\mathsf{max} , \qquad \chi_3 = \overline{\chi_2}^* . \tag{3.149} $$

This allows for the elliptic integral

$$ {}_{\mathrm{f}_1}T_\delta = \frac{2}{\omega_\mathrm{n}}\sqrt{6} \int_0^{u_\mathsf{max}} \frac{\mathrm{d}u}{\sqrt{-u^3 + C_{1,\mathrm{f}_1}}} , \qquad u_\mathsf{max} > 0 , \tag{3.150} $$

to be rewritten in Legendre's canonical form according to equation (B.11) and solved for using case $\langle 243.00 \rangle$ in [288]

$$ {}_{\mathrm{f}_1}T_\delta = \frac{2}{\omega_\mathrm{n}}\sqrt{6}\,\eta\,\mathsf{F}(\psi, \kappa) , \tag{3.151a} $$

where $\mathsf{F}(\psi, \kappa)$ is the incomplete elliptic integral of the first kind with argument ψ and modulus κ, see appendix B, which are given as

$$ \eta^2 = \frac{1}{u_\mathsf{max}\sqrt{3}} , \qquad \kappa^2 = \frac{1}{4}\left(2 + \sqrt{3}\right) , \qquad \text{and} \qquad \cos(\psi) = 2 - \sqrt{3} . \tag{3.151b} $$

It is easy to see that (3.151b) has multiple solutions

$$ \psi_{\left(j - \frac{2}{k}\right)} = (j-1)\,\pi + (-1)^k\,\psi_0 , \qquad j = 1, 3, 5, \ldots, n , \quad k = 1, 2 \tag{3.151c} $$

as shown in table 3.1 with the fundamental one being

$$ \psi_0 = \arccos\left(2 - \sqrt{3}\right) . \tag{3.151d} $$

Table 3.1 – Restoring force $f_1(u) = k_\beta \operatorname{sgn}(u_1) |u_1|^b$ - Impulse excitation: Multiple solutions for oscillation period integral in equations (3.150).

j	k	$\psi_{(j-\frac{2}{k})}$
1	1	$\psi_{-1} = -\psi_0$
	2	$\psi_0 = \psi_0$
3	1	$\psi_1 = 2\pi - \psi_0$
	2	$\psi_2 = 2\pi + \psi_0$
5	1	$\psi_3 = 4\pi - \psi_0$
	2	$\psi_4 = 4\pi + \psi_0$
⋮	⋮	⋮

It is important to note that all $\psi_{(j-\frac{2}{k})}$ in (3.151c) are projections of ψ_0 into the fundamental solution domain $0 \leq \psi \leq \pi$ of the inverse cosine function in (3.151d). Therefore, the $(0, \pi)$-interval normalised j-th argument is given as

$$\widehat{\psi}_{(j-\frac{2}{k})} = \frac{\psi_{(j-\frac{2}{k})}}{n-1}, \qquad j = 1, 3, 5, \ldots, n, \tag{3.151e}$$

and together with the identity from [291]

$$\mathsf{F}(m\,\pi \pm \phi, \kappa) = 2\,m\mathsf{K}(\kappa) \pm \mathsf{F}(\phi, \kappa) \tag{3.151f}$$

equation (3.151a) can be rewritten as

$${}_{\mathrm{f}_1}T_\delta = \frac{1}{(2j-1)} \frac{\sqrt{6}}{\omega_\mathrm{n}} \eta_\mathsf{E} \left(2\mathsf{K}(\kappa) - \mathsf{F}(\psi_0, \kappa)\right) \qquad j = 1, 2, \ldots, n \tag{3.152}$$

giving odd multiples of the fundamental oscillation frequency $f_{\mathsf{NL}} = 1/{}_{\mathrm{f}_1}T_\delta$ from Eq.(3.151a). Results similar to Eqs.(3.151a) and (3.152) are obtained if $b \equiv 3$. Unfortunately, for $b > 3$, $b \in \mathbb{N}$, the application of elliptic integrals is restricted to a limited number of special cases and their usage is constrained in the same way as for (3.151a) and (3.152) to natural numbers for b only. Various reduction methods for these so-called hyperelliptic integrals to ordinary elliptic integrals with a polynomial of order not higher than four under the root of (3.150) can be found in [288,291,292].

Step excitation. If the nonlinear SDOF system is excited by a p_0-scaled step load according to Eq.(3.63), peak displacement values are derived from (3.66)

$$|u_{\mathsf{Ex}}|^{b+1} - \frac{p_0}{k_\beta}(b+1)\,u_{\mathsf{Ex}} - C_{2,\mathrm{f}_1} = 0, \tag{3.153a}$$

where

$$u_{\mathsf{Ex}},\, p_0,\, k_\beta,\, b,\, C_{2,\mathrm{f}_1} \in \mathbb{R}\,, \qquad \text{and} \qquad k_\beta\,, b > 0\,, \tag{3.153b}$$

together with

$$C_{2,\mathrm{f}_1} = \frac{b+1}{k_\beta}\, C_2 \qquad \text{and} \qquad C_2 = \frac{m}{2}\,\dot{u}_0^2 + \frac{k_\beta}{b+1}\,|u_0|^{b+1} - p_0\, u_0 \tag{3.153c}$$

from equation (3.65b). Using the definition for the absolute value $|u_{\mathsf{Ex}}| = u_{\mathsf{Ex}} \big/ \operatorname{sgn}(u_{\mathsf{Ex}})$ but bearing in mind $-\infty < u_{\mathsf{Ex}} < \infty$, and substituting $u_{\mathsf{Ex}} = \pm u_{\mathsf{p}}$, Eq.(3.153a) can be transformed into

$$u_{\mathsf{p}}^{b+1} \mp A_{\mathsf{p}}\, u_{\mathsf{p}} - C_{2,\mathrm{f}_1} = 0\,, \qquad A_{\mathsf{p}} = p_0\, \frac{(b+1)}{k_\beta}\,, \tag{3.154}$$

giving effectively two equations with the constraint of $u_{\mathsf{p}} \geq 0$. All negative solutions for u_{p} from (3.154) are discharged. The maximum positive displacement amplitude $u_{\mathsf{max}} > 0$ is obtained with "–" for the second term and the maximum negative amplitude $u_{\mathsf{min}} < 0$ with the "+" sign for A_{p}. From all real solutions of (3.154) the maximum positive is selected in both cases of $\mp A_{\mathsf{p}}$ and extreme values are given by $u_{\mathsf{max}} = u_{\mathsf{p}}$ and $u_{\mathsf{min}} = -u_{\mathsf{p}}$, respectively. If no positive solution can be obtained from (3.154) for one of the two options of A_{p}, than $u_{\mathsf{Ex}} = \{u_{\mathsf{min}},\, u_{\mathsf{max}}\}$ is confined to the range of either solely negative or positive values only.

Unfortunately, equation (3.154) can only be solved entirely analytically for a limited number of special cases. If the full admissible range of the exponent b in (3.75) is required, one such case is given if all initial conditions (3.3b) are equal zero. Hence, with $C_{2,\mathrm{f}_1} = 0$ the solutions for (3.154) become

$$u_{\mathsf{p},1} = 0 \qquad \text{and} \qquad u_{\mathsf{p},2} = \operatorname{sgn}(p_0)\,|A_{\mathsf{p}}|^{\frac{1}{b}} = \begin{cases} u_{\mathsf{max}} = u_{\mathsf{p},2},\; u_{\mathsf{min}} = u_{\mathsf{p},1} & \text{if } p_0 > 0 \\ u_{\mathsf{min}} = u_{\mathsf{p},2},\; u_{\mathsf{max}} = u_{\mathsf{p},1} & \text{if } p_0 < 0 \end{cases}. \tag{3.155}$$

Another case of explicit analytical results for (3.153a) is given if $b \leq 3$, $b \in \mathbb{N}$ and $C_{2,\mathrm{f}_1} \neq 0$. Equation (3.154) then becomes a nonlinear third or fourth order expression solvable by algorithms presented in [58, 160]. However, in order to take advantage of the full range of feasible parameter values in (3.153a), equation (3.154) must be solved numerically [159, 289].

From (3.71) follows for extreme values of velocity

$$\dot{u}_{\mathsf{Ex}} = \pm\sqrt{\frac{2}{m}}\left(p_0 u_{\mathsf{eq}} - \frac{k_\beta}{b+1}\,|u_{\mathsf{eq}}|^{b+1} + C_2\right)^{\frac{1}{2}} \tag{3.156a}$$

where the new equilibrium point u_{eq} is obtained by means of (3.70)

$$u_{\mathsf{eq}} = \operatorname{sgn}(u_{\mathsf{eq}})\left[\frac{p_0}{k_\beta\, \operatorname{sgn}(u_{\mathsf{eq}})}\right]^{\frac{1}{b}} \tag{3.156b}$$

and $\mathrm{sgn}(u_{\mathsf{eq}})$ must be chosen such that the term in brackets in (3.156b) is positive. It is obvious that (3.156b) coincides with the new equilibrium point of the system obtained in (3.80) above. Since the restoring force takes absolute maximum values $|f_1(u)|$ at $u_{\mathsf{Ex}} = \{u_{\mathsf{min}},\, u_{\mathsf{max}}\}$, see Fig. 3.2, peak values of acceleration are given by (3.72)

$$\ddot{u}_{\mathsf{Ex}} = \frac{1}{m}\left(p_0 - k_\beta\,\mathrm{sgn}(u_{\mathsf{Ex}})\,|u_{\mathsf{Ex}}|^b\right)\,. \tag{3.157}$$

Inserting Eq.(3.76) into (3.73) yields an equation for the oscillation period

$${}_{\mathrm{f_1}}T_{\mathrm{H}} = \frac{1}{\omega_{\mathrm{n}}}\sqrt{2(b+1)}\int\limits_{u_{\mathsf{min}}}^{u_{\mathsf{max}}} \frac{\mathrm{d}u}{\sqrt{-\,|u|^{b+1} + \frac{b+1}{k_\beta}\,p_0\,u + C_{2,\mathrm{f_1}}}}\,. \tag{3.158}$$

The entire domain of feasible values for u_{Ex} is divided into positive and negative halves similar to Eq.(3.154), and, assuming the most general case with $u_{\mathsf{min}} < 0$, $u_{\mathsf{max}} > 0$, the integral in equation (3.158) is rewritten as a sum

$$\int\limits_0^{|u_{\mathsf{min}}|} \frac{\mathrm{d}u}{\sqrt{-u^{b+1} - \frac{b+1}{k_\beta}\,p_0\,u + C_{2,\mathrm{f_1}}}} + \int\limits_0^{u_{\mathsf{max}}} \frac{\mathrm{d}u}{\sqrt{-u^{b+1} + \frac{b+1}{k_\beta}\,p_0\,u + C_{2,\mathrm{f_1}}}}\,, \qquad u \geq 0\,, \tag{3.159}$$

which incorporates the cases of $u_{\mathsf{min}} < u_{\mathsf{max}} < 0$, and $0 > u_{\mathsf{min}} > u_{\mathsf{max}}$ by adjusting the integration limits accordingly. It is impossible to solve (3.158) analytically in its most general form as given in Eq.(3.159) with $b > 0$, $b \in \mathbb{R}$. Therefore, the following three special cases have been selected which yield closed-form expressions for the oscillation period of the nonlinear SDOF system in (3.78).

(i) *Zero initial conditions and $b \in \mathbb{R}$:* With $u_0 = \dot{u}_0 = 0$ from Eq.(3.3) the integration constant $C_{2,\mathrm{f_1}}$ in (3.158) is zero. Without loss of generality it can be assumed Eq.(3.155) yields

$$u_{\mathsf{Ex}} = \{0;\, u_{\mathsf{max}}\} \tag{3.160a}$$

with $u_{\mathsf{max}} \geq 0$, and $p_0 > 0$ as necessary condition. Hence, the first integral in (3.159) becomes zero and ${}_{\mathrm{f_1}}T_{\mathrm{H}}$ in (3.158) is obtained from

$${}_{\mathrm{f_1}}T_{\mathrm{H}} = A_{\mathrm{f_1}}\int\limits_0^{u_{\mathsf{max}}} \frac{\mathrm{d}u}{\sqrt{u\left(-u^b + \frac{b+1}{k_\beta}\,p_0\right)}}\,, \qquad A_{\mathrm{f_1}} = \frac{2}{\omega_{\mathrm{n}}}\sqrt{2(b+1)}\,, \tag{3.160b}$$

which, after further algebraic manipulation, partial integration [289, 292] and substitution of $u_{\mathsf{max}} = u_{\mathsf{p},2}$ from (3.155), leads to

$${}_{\mathrm{f_1}}T_{\mathrm{H}} = 2\sqrt{\pi}\,A_{\mathrm{f_1}}\left(\frac{p_0}{k_\beta}(b+1)\right)^{\frac{1}{2}\left(\frac{1}{b}-1\right)} \frac{\Gamma\left(\frac{1}{2b}+1\right)}{\Gamma\left(\frac{1+b}{2b}\right)}\,. \tag{3.160c}$$

For the complementary case of $u_{\mathsf{Ex}} = \{u_{\mathsf{min}};\, 0\}$ and $u_{\mathsf{min}} \leq 0$, the necessary condition of

$p_0 < 0$ changes the sign of the second term under the square root of the first integral in (3.159) into "+", and hence, with the second integral vanishing, Eq.(3.159) takes the same form as (3.160b) but with $|u_{\min}|$ as upper limit. Thus, Eq.(3.160c) is also the solution in this case, but it must read

$$-\frac{p_0}{k_\beta}(b+1)\,, \qquad \text{or} \qquad \frac{|p_0|}{k_\beta}(b+1) \qquad \text{since} \qquad p_0 < 0 \tag{3.161}$$

for the expression in brackets in (3.160c). By setting $b = 1$ in equation (3.160c) the linear case can be obtained as demonstrated in (3.147) above.

(ii) $\underline{b = 2}$: With the nonlinear stiffness exponent equal to 2, the expressions under the square roots in (3.159) are rendered as third-order polynomials and the initial conditions do not necessarily need to be zero in order to obtain closed-form solutions for these ordinary elliptic integrals. With a cubic term in $u(t)$ each of the two polynomials in (3.159) has three solutions. The nature of these two triples

$$\xi = \left\{\xi_i \in \mathbb{R} \cup \mathbb{C} \,\middle|\, i = 1,2,3\right\} \qquad \text{and} \qquad \chi = \left\{\chi_i \in \mathbb{R} \cup \mathbb{C} \,\middle|\, i = 1,2,3\right\} \tag{3.162a}$$

is such that at least each one of them has one real-valued component, which is equal to the upper limit of the respective integral

$$\xi_1 = |u_{\min}|\,, \qquad \text{and} \qquad \chi_1 = u_{\max}\,. \tag{3.162b}$$

The other two solutions are either real or complex depending on the nature of the polynomial discriminant D_s

$$D_s = \left(\frac{b+1}{k_\beta}p_0\right)^3 + \left(\frac{C_{2,\mathrm{f}_1}}{2}\right)^2\,, \qquad b,\, k_\beta,\, p_0,\, C_{2,\mathrm{f}_1} \in \mathbb{R}\,, \quad b,\, k_\beta > 0\,, \tag{3.163}$$

see [58], and hence, on the sign and magnitude of the step force p_0. This makes it necessary to consider both cases in [288], namely $\langle 243.00 \rangle$ as above for $D_s > 0$, e.g. one real and two conjugate complex solutions; and case $\langle 236.00 \rangle$ for $D_s < 0$ with three real solutions of either of the polynomials in (3.159) such that

$$\xi_1 > 0 \geq \xi_2 > \xi_3\,, \qquad \text{or} \qquad \chi_1 > 0 \geq \chi_2 > \chi_3\,, \tag{3.164}$$

obeying Vieta's lemma in equation (A.8), together with Eq.(3.162b) for ξ_1 and χ_1, respectively. Results for $D_s > 0$ are already given in equation (3.151) above. Although the expression under the square root in (3.150) does not contain the linear term in u with the factor $(b+1)p_0/k_\beta$, see (3.158), Legendre's canonical forms in case of one real and two complex conjugate solutions according to B.2 are similar for both integrands in (3.159) and (3.150).

Contrary, if $D_s < 0$ the integral (3.159) yields

$$\int_0^{\alpha_{\mathrm{f}_1}} \frac{\mathrm{d}u}{\sqrt{-u^3 - \frac{3}{k_\beta}\, p_0\, u + C_{2,\mathrm{f}_1}}} = \eta_\xi \mathsf{F}_\xi\left(\psi, \kappa\right) \tag{3.165a}$$

with

$$\eta_\xi = \frac{2}{\sqrt{\xi_1 - \xi_3}}, \qquad \kappa^2 = \frac{\xi_1 - \xi_2}{\xi_1 - \xi_3}, \qquad \sin^2\psi = \frac{\xi_1}{\xi_1 - \xi_2}. \tag{3.165b}$$

if $\alpha_{\mathrm{f}_1} \equiv \xi_1 = |u_{\mathsf{min}}|$ is the upper integration limit. The same result is obtained for the second integral of the sum in (3.159) with $\chi_1 = u_{\mathsf{max}}$ as upper limit if $D_s < 0$. Finally, independent of whether $\xi_i, \chi_i\,, i = 1, 2, 3$ are all real or partially real and complex, the total oscillation period is obtained as sum of the two parts in (3.159)

$${}_{\mathrm{f}_1}T_{\mathrm{H}} = A_{\mathrm{f}_1}\Big(\eta_\xi \mathsf{F}_\xi\left(\psi, \kappa\right) + \eta_\chi \mathsf{F}_\chi\left(\psi, \kappa\right)\Big). \tag{3.166}$$

(iii) $\underline{b = 3:}$ For quartic polynomials in Eq.(3.159) the approach for determining ${}_{\mathrm{f}_1}T_{\mathrm{H}}$ is identical to the above. Each polynomial has now four roots ξ_i and χ_i with $i = 1, \ldots, 4$ leads again to two meaningful combinations, i.e. two real, two conjugate complex or four real solutions, depending on the sign of the discriminant D_s of the reduced-order cubic resolvent polynomial given in table A.2 of appendix A. With the set of parameters considered at the moment, equation (A.6) must be written as

$$y^3 + 4\, C_{2,\mathrm{f}_1}\, y - \left(\frac{b+1}{k_\beta}\, p_0\right)^2 = 0 \tag{3.167a}$$

with

$$D_s = \left(\frac{4}{3}\, C_{2,\mathrm{f}_1}\right)^3 + \left(\frac{b+1}{k_\beta}\, p_0\right)^4. \tag{3.167b}$$

according to (A.1d). Provided all parameters involved in (3.167a) stay within their previously defined domains of definition as given, for example, in (3.163), it has been shown in [270] together with the explicit solution for a third-order polynomial from [160], that (3.167a) never possess three real-valued solutions of which one is positive and two are negative. This would ultimately result in two pairs of complex conjugated solutions [58] for the primary quartic equation under the square roots in (3.159), and hence, no real-valued upper integration limits, neither u_{min} nor u_{max} would exist. This clearly shows how the physically impossible case is ruled out mathematically by accurate definition of the feasible domains for all participating parameters. Depending upon the nature of the solutions of Eq.(3.167a), either case $\langle 257.00 \rangle$ for real-valued roots; or case $\langle 259.00 \rangle$ for partially real-valued and conjugate complex roots of (3.159) must be chosen in Byrd *et al* [288]. Subsequently, the oscillation period of the SDOF with stiffness exponent $b = 4$ traversing between $u_{\mathsf{Ex}} = \{u_{\mathsf{min}};\, u_{\mathsf{max}}\}$ is given by

summation of both parts of the interval, leaving exactly the same result as in Eq.(3.166).

It is worth mentioning that for the case $0 < u_{\min} < u_{\max}$ the first integral in (3.159) becomes zero and ${}_{f_1}T_H$ is obtained solely from the second integral evaluated at the limits $(u_{\min};\, u_{\max})$. Similarly, for $u_{\min} < u_{\max} < 0$, equation (3.166) consists of $A_{f_1}\eta_\xi F_\xi(\psi,\kappa)$ only, with the first term in (3.159) computed at lower and upper limits $(|u_{\max}|\,;\,|u_{\min}|)$, respectively, and the second integral in (3.159) equal to zero. These results are direct consequences from the non-negative domain of solutions defined for Eq.(3.154) above.

As explained earlier, the usage of tabulated function for solving (3.158) is restricted to natural numbers for the nonlinear exponent $b \in \mathbb{N}$. Due to the extra term $u(t)$ in Eq.(3.158) compared to (3.144a), reduction of hyperelliptic integrals with $(b > 3)$ to cases with at most quartic polynomials under the square root becomes more complicated and reduces application of analytical function tables even further to selected, special cases. For example, if $b \leq 6$ equation $\langle 579.00 \rangle$ in [288] can be used, whereas for $4 \leq b \leq 12$ case $\langle 113 - C \rangle$ in [292] is applicable.

3.4.1.5 Shock spectra

Impulse excitation. By choosing an appropriate set of random parameters for the stiffness coefficient k_β, the excitation magnitude p_δ, as well the initial conditions u_0, $\dot{u}_0$ and mass m, the above derived formulas can be examined visually. Figure 3.3 shows for an impulse excited system the maximum displacement $u_{\max}$ normalised to the linear static displacement $u_{\text{stat,lin}}$

$$u_{\text{norm}} = \frac{u_{\max}}{u_{\text{stat,lin}}}, \qquad \text{where} \qquad u_{\text{stat,lin}} = \frac{p_\delta}{k_\beta}, \tag{3.168}$$

a type of scaling which is commonly used in shock spectra diagrams for linear systems, see [226, 293] for example. Similarly, Fig. 3.4 displays the nonlinear oscillation frequency f_{NL} according to Eq.(3.74), normalised to the frequency f_n of an equivalent linear system with $b = 1$

$$f_{\text{norm}} = \frac{f_{\text{NL}}}{f_n}. \tag{3.169}$$

Both figures feature identical system parameters with f_n as independent variable. From first inspection the linear and nonlinear displacement response in figure 3.3 seem not to be very different at all. However, whereas for small f_n, hence small stiffness coefficients k_β, response for the entire range of different u_0 is equal, the four lines separate as f_n takes on higher values. Furthermore, increasing nonlinearity from Fig. 3.3 (b) to (d) gives less distinguishable system responses due to different initial displacement u_0. This can lead to the false conclusion that, as b grows, all nonlinear responses become almost identical. This is clearly not the case as the normalised frequency in figure 3.4 indicates. As expected, for the linear system in 3.4(a), the ratio from Eq.(3.169) is equal to 1, irrespective of the change of stiffness k_β. That this is not true for nonlinear systems addressed in this work and has been discussed above. The way the nonlinear frequency changes does not only depend on the initial energy of the system, and hence on the initial conditions, it depends considerably on the system's nonlinear stiffness coefficient k_β as well, and therefore on

f_n as the only free variable. Whereas for each $b = \mathtt{const}$ in Fig. 3.4(b) to (d) the nonlinear frequency seems to be independent of u_0 for small values of the restoring force parameter k_β, the initial displacement gains more influence as k_β increases. In fact, f_NL is directly dominated by the initial displacement, since for $u_0 < 1$ the ratio defined in Eq.(3.169) decreases and f_NL becomes considerably smaller than its linear counterpart f_n. Contrary, for $u_0 \geq 1$, f_NL approaches f_n and the ratio f_norm becomes nearly one with increasing k_β.

In summary, with the selected range of parameters for both figures 3.3 and 3.4, the system gives comparable results in the linear and nonlinear case in terms of maximum response amplitude u_max for the lower end of the stiffness coefficient k_β as pictured in Fig. 3.3. However, the nonlinear oscillation frequency differs considerably for systems with $b > 1$ from the linear case shown in Fig. 3.4(a). Moreover, the total nonlinear system response, i.e. amplitude and frequency, becomes incomparable for the upper end of the k_β-range and is significantly different from behaviour exhibited by the linear reference system in graph (a) of both figures.

Shock spectra similar to those obtained for linear systems in [226, 293] can be plotted using the analytical results derived above and setting the conditions u_0, $\dot{u}_0$ in Eq.(3.3b) equal to zeros, i.e. the system is at rest when the impulse is applied, thus $u(0) = 0$, $\dot{u}(0) = p_\delta/m$. In this special case the extreme displacement in Eq.(3.141a) can be normalised by the mass m in the nonlinear system leaving a new $\overline{u}_\mathsf{Ex,m}$ as function of p_δ, b and k_β only,

$$u_\mathsf{Ex} = \mathrm{sgn}(u_\mathsf{Ex})\,\frac{1}{\overline{m}_\delta}\left[\frac{b+1}{(2\pi f_\mathrm{n})^2}\,\frac{p_\delta^2}{2}\right]^{\frac{1}{b+1}} = \mathrm{sgn}(u_\mathsf{Ex})\,\frac{\overline{u}_\mathsf{Ex,m}}{\overline{m}_\delta}\,, \tag{3.170a}$$

with the mass scaling factor due to impulse excitation

$$\overline{m}_\delta = \frac{1}{\left(\frac{1}{m}\right)^{\frac{2}{b+1}}} = m^{\frac{2}{b+1}}\,, \tag{3.170b}$$

and $\overline{u}_\mathsf{Ex,m} = \overline{m}_\delta\,\{u_\mathsf{min};\, u_\mathsf{max}\}$. Equation (3.170a) can be generalised further by scaling it to the linear static displacement from (3.168)

$$u_\mathsf{Ex} = \mathrm{sgn}(u_\mathsf{Ex})\,\frac{m}{\overline{m}_\delta}\,u_\mathsf{stat,lin}\,\overline{u}_\mathsf{Ex,m,s} \tag{3.170c}$$

together with

$$\overline{u}_\mathsf{Ex,m,s} = \frac{(2\pi\, f_\mathrm{n})^2}{p_0}\,\overline{u}_\mathsf{Ex,m}\,. \tag{3.170d}$$

Simplifying the mass ratio in (3.170c) with the conditions for stable oscillations from Eq.(3.75)

$$\overline{m}_{\delta,\mathrm{f_1}} = \frac{m}{\overline{m}_\delta} = m^{\frac{b}{b+1}} \tag{3.170e}$$

allows one to rewrite the extreme displacement in its final normalised form as

$$u_{\mathsf{Ex}} = \operatorname{sgn}(u_{\mathsf{Ex}})\ \overline{m}_{\delta,\mathrm{f_1}}\, u_{\mathsf{stat,lin}}\, \overline{u}_{\mathsf{Ex,m,s}}\,. \tag{3.171}$$

The dimensionless displacement $\overline{u}_{\mathsf{Ex,m,s}}$, which is effectively the minimum/maximum dynamic magnitude given in (3.141a) normalised to the SDOF's mass m and the static displacement of the equivalent linear system from (3.168), is plotted for various degrees of nonlinearity in the shock spectra in figure 3.5. With given system parameters of m, p_0, k_β and b, the equivalent linear frequency

$$f_{\mathrm{n}} = \frac{1}{2\pi}\sqrt{\frac{k_\beta}{m}} \tag{3.172}$$

can be calculated. By following the appropriate straight line of p_0 in Fig. 3.5, $\overline{u}_{\mathsf{Ex,m,s}}$ is retrieved and using Eq.(3.171) together with (3.170e) and (3.168), the extreme (minimum/maximum) displacement u_{Ex} is obtained.

In a similar manner the nonlinear oscillation period from Eq.(3.146) can than be expressed in a mass and linear equivalent frequency normalised version as

$${}_{\mathrm{f_1}}T_\delta = \frac{m}{\overline{m}_\delta}\,\frac{4\sqrt{\pi}}{p_0^2}\,\overline{u}_{\mathsf{Ex,m}}\,\frac{\Gamma\left(1+\frac{1}{1+b}\right)}{\Gamma\left(\frac{1}{2}+\frac{1}{1+b}\right)}\,\frac{f_{\mathrm{n}}}{f_{\mathrm{n}}} = \overline{m}_{\delta,\mathrm{f_1}}\,\frac{{}_{\mathrm{f_1}}\overline{T}_{\delta,\mathrm{m}}}{f_{\mathrm{n}}}\,, \tag{3.173}$$

with $\overline{u}_{\mathsf{Ex,m}}$ from Eq.(3.170a) and the mass ratio $m/\overline{m}_\delta$ according to (3.170e). For any given k_β and m the value for f_{n} is given by (3.172) and ${}_{\mathrm{f_1}}\overline{T}_{\delta,\mathrm{m}}$ is obtained from the inverse of the ratio $f_{\mathsf{NL}}/f_{\mathrm{n}}$ in the normalised oscillation frequencies given in figure 3.6, thus

$${}_{\mathrm{f_1}}\overline{T}_{\delta,\mathrm{m}} = \frac{f_{\mathrm{n}}}{f_{\mathsf{NL}}}\,. \tag{3.174}$$

Step excitation. Similar expressions are derived for step excitation. With $C_{2,\mathrm{f_1}} = 0$ from equation (3.153c) the mass-normalised maximum displacement $\overline{u}_{\mathsf{Ex,m}}$ relates to u_{Ex} via Eq.(3.154)

$$u_{\mathsf{max}} = \left(\frac{1}{m}\right)^{\frac{1}{b}}\,\overline{A}_{\mathsf{p}}^{\frac{1}{b}} \tag{3.175a}$$

and gives together with

$$\overline{m}_{\mathrm{H,f_1}} = \frac{m}{\overline{m}_{\mathrm{H}}} = m\left(\frac{1}{m}\right)^{\frac{1}{b}} = m^{\frac{b-1}{b}} \qquad \text{and} \qquad \overline{A}_{\mathsf{p,norm}}^{\frac{1}{b}} = \overline{A}_{\mathsf{p}}^{\frac{1}{b}}\,\frac{(2\pi f_{\mathrm{n}})^2}{p_0} \tag{3.175b}$$

for the maximum displacement

$$u_{\mathsf{max}} = \overline{m}_{\mathrm{H,f_1}}\, u_{\mathsf{stat,lin}}\, \overline{A}_{\mathsf{p,norm}}^{\frac{1}{b}}\,. \tag{3.176}$$

The dimensionless values for $\overline{A}_{\mathrm{p,norm}}^{\frac{1}{b}}$ are plotted as shock spectra in Fig. 3.7 for various values of b and different step load magnitudes p_0. The equivalent linear static displacement $u_{\mathsf{stat,lin}}$ is similarly defined as in (3.168),

$$u_{\mathsf{stat,lin}} = \frac{p_0}{k_\beta}\,. \tag{3.177}$$

From (3.160c) follows for the oscillation period

$${}_{\mathrm{f_1}}T_{\mathrm{H}} = 2\ {}_{\mathrm{T}}\overline{m}_{\mathrm{H,f_1}} \times \frac{{}_{\mathrm{f_1}}\overline{T}_{\mathrm{H,m}}}{f_{\mathrm{n}}} \tag{3.178}$$

where the mass normalising factor ${}_{\mathrm{T}}\overline{m}_{\mathrm{H,f_1}}$ is denoted as

$${}_{\mathrm{T}}\overline{m}_{\mathrm{H,f_1}} = \left(\frac{1}{m}\right)^{\frac{1}{2}\left(\frac{1}{b}-1\right)} \tag{3.179a}$$

and the dimensionless, normalised nonlinear period

$${}_{\mathrm{f_1}}\overline{T}_{\mathrm{H,m}} = \frac{f_{\mathrm{n}}}{f_{\mathsf{NL}}} \tag{3.179b}$$

is obtained from the results plotted in figure 3.8. By choosing the SDOF system parameters randomly as $m = 5.15\mathsf{kg}$, $k_\beta = 2.03314 \times 10^6\mathsf{N/m^3}$, $p = 10\mathsf{N}$ and $b = 3$, for example, table 3.2 compares the maximum displacement u_{max} and both oscillation periods ${}_{\mathrm{f_1}}T_\delta$ and ${}_{\mathrm{f_1}}T_{\mathrm{H}}$ for impulse and step excitation of the system in (3.78). All values obtained from the closed-form solutions, equations (3.141a), (3.146), (3.155) and (3.160c) were verified by numerical integration procedures [1,157,294]. Results obtained using the slightly less accurate method of graphically derived values from all four shock spectra given in Figs. 3.5 to 3.8 compare very well to values derived from direct evaluation of the more complex analytical formulas given in this chapter. Although application of the spectra is limited to the range of system parameters for which they are plotted, it is straightforward to extend all of the straight lines in each of the logarithmic-scaled plots of the four figures in order to account for the desired domain of displacement and frequency values.

3.4.2 $f_2(u) = k_\alpha u + k_\beta u^3$

The second nonlinear restoring force under consideration here is the well-known Duffing-type geometrical nonlinearity

$$f_2(u) = k_\alpha\, u(t) + k_\beta\, u^3(t) \qquad \text{with} \qquad k_\alpha,\, k_\beta,\, u(t),\, t \in \mathbb{R} \tag{3.180}$$

with k_α, k_β being constant stiffness coefficients. Since its first appearance in [4], Eq.(3.180) has been extensively studied as part of various differential systems [8, 18, 82, 83, 229, 295]. A brief overview of these findings has been examined in chapter 2. Key results of existence, uniqueness and stability analysis will be presented in a similar layout as in section 3.4.1 above, followed by novel analytical expressions for extreme values of response together with newly derived shock

Table 3.2 – Comparison of SDOF system response results for closed form solution and shock spectra in case of impulse and step excitation. System defining values: mass $m = 5.15\text{kg}$, nonlinear stiffness coefficient $k_\beta = 2.03314 \times 10^6\text{N/m}^3$, load magnitude $p = 10\text{N}$ and nonlinearity exponent $b = 3$. Linear static displacement $u_{\text{stat,lin}} = 4.9185 \times 10^{-6}\text{m}$. Equivalent linear oscillation frequency $f_\text{n} = 100\text{Hz}$.

Impulse						
$\overline{m}_{\delta,\text{f}_1}$	$\overline{u}_{\text{Ex,m,s}}$	${}_{\text{f}_1}\overline{T}_{\delta,\text{m}}$	$u_{\max}$	$u_{\max}$	${}_{\text{f}_1}T_\delta$	${}_{\text{f}_1}T_\delta$
Eq.(3.170e)	Fig. 3.5(c)	Fig. 3.6(c)	Eq.(3.171)	Eq.(3.141a)	Eq.(3.173)	Eq.(3.146)
2.2694	190	0.4	0.0661m	0.0662m	0.5673s	0.5646s
Step						
$\overline{m}_{\text{H,f}_1}$	$\overline{A}^{\frac{1}{b}}_{\text{p,norm}}$	${}_{\text{f}_1}\overline{T}_{\text{H,m}}$	$u_{\max}$	$u_{\max}$	${}_{\text{f}_1}T_\text{H}$	${}_{\text{f}_1}T_\text{H}$
Eq.(3.175b)	Fig. 3.7(c)	Fig. 3.8(c)	Eq.(3.176)	Eq.(3.155)	Eq.(3.178)	Eq.(3.160c)
2.9822	1850	0.043	0.0270m	0.0271m	0.8032s	0.8101s

spectra for simple yet accurate response prediction of the SDOF system.

3.4.2.1 Linearisation

Using the previously introduced common substitution $u_1 = u$ and $u_2 = \dot{u}$ the second-order differential equation in (3.3) is transformed into the first-order system

$$\begin{Bmatrix} \dot{u}_1 \\ \dot{u}_2 \end{Bmatrix} = \begin{Bmatrix} u_2 \\ \widehat{p}_0 - \omega_\alpha^2\, u_1 - \omega_\beta^2\, u_1^3 \end{Bmatrix} \tag{3.181}$$

where $\omega_\alpha^2 = k_\alpha/m$, $\omega_\beta^2 = k_\beta/m$ and $\widehat{p_0} = p_0/m$. The natural frequency of a linear reference system is introduced similar to (3.79) as f_n and relates to (3.181)

$$4\,\pi^2 f_\text{n}^2 = \omega_\alpha^2 = \frac{k_\alpha}{m}, \qquad \text{thus,} \qquad f_\text{n} = \frac{1}{2\,\pi}\sqrt{\frac{k_\alpha}{m}}. \tag{3.182}$$

Setting $\mathbf{F}(\mathbf{u}) = 0$ and $p_0 \equiv 0$ it is well known [249] the system in (3.181) has three solutions which can be given in closed form using the second equation in (3.181)

$$0 = u_1\left(u_1^2 + \frac{1}{k_\gamma}\right) \qquad \text{where} \qquad k_\gamma = \frac{k_\beta}{k_\alpha}, \tag{3.183a}$$

hence,

$$\mathbf{u}_{\text{Eq},1} = \begin{Bmatrix} 0 \\ 0 \end{Bmatrix}, \qquad \text{and} \qquad \mathbf{u}_{\text{Eq},2/3} = \begin{Bmatrix} \pm\sqrt{-\frac{1}{k_\gamma}} \\ 0 \end{Bmatrix}. \tag{3.183b}$$

It is easy to see that in case of $k_\alpha,\ k_\beta > 0$ in (3.180), commonly referred to as stiffening spring force, $\mathbf{u}_{\mathrm{Eq},2/3}$ are complex and therefore no valid stationary points. Contrary, softening and snap-through restoring forces with $k_\alpha > 0,\ k_\beta < 0$ and $k_\alpha < 0,\ k_\beta > 0$, respectively, and thus $k_\gamma < 0$, allow for three equilibrium points of the oscillator. As defined in section 3.3.1 of the current chapter the above case with $p_0 \equiv 0$ corresponds to both free vibration and impulse excitation where the Dirac impulse is incorporated into the systems via the initial velocity.

For step excitation, i.e. $p_0 \neq 0$, the equilibrium points of oscillation must be obtained from

$$0 = u_1^3 + \frac{1}{k_\gamma}\, u_1 - \frac{p_0}{k_\beta}\,, \tag{3.184a}$$

with the solution discriminant D_s according to (A.1d)

$$D_s = \left(\frac{1}{3\,k_\gamma}\right)^3 + \left(-\frac{p_0}{2\,k_\beta}\right)^2 \tag{3.184b}$$

and three cases for D_s as given in table A.1. It is apparent from (3.184b) that the sign of the step load magnitude p_0 has no influence on the sign of D_s, and hence the nature of equilibrium points. This simply reflects the fact that all system responses are symmetrical with respect to the direction of action of p_0. If $k_\gamma > 0$ there will always be one real solution only, explicitly obtainable using (A.2), hence

$$\mathbf{u}_{\mathrm{Eq},1} = \begin{Bmatrix} w_1 + v_1 \\ 0 \end{Bmatrix}, \qquad \text{with} \qquad w_1 = \left(\frac{p_0}{2\,k_\beta} + \sqrt{D_s}\right)^{\frac{1}{3}}, \quad v_1 = -\frac{1}{3k_\gamma\, w_1}\,, \tag{3.185}$$

and two solutions with $\mathbf{u}_{\mathrm{Eq},2/3} \in \mathbb{C}$. In case of softening or snap-through springs, i.e. $k_\gamma < 0$, up to three real-valued solutions of (3.184a) are possible and can be obtained using (A.3) given in appendix A. The linearised version of system (3.181) is derived from (3.17b)

$$\mathbf{JF} = \begin{bmatrix} 0 & 1 \\ -\omega_\alpha^2 - 3\,\omega_\beta^2\, u_1 & 0 \end{bmatrix} \tag{3.186a}$$

leading to eigenvalues such that (3.17d) is satisfied

$$\lambda_{1/2} = \pm\sqrt{-\omega_\alpha^2 - 3\,\omega_\beta^2\, u_1^2}\,, \tag{3.186b}$$

and eigenvectors according to (3.17f)

$$\mathbf{x}_1 = \begin{Bmatrix} 1 \\ \lambda_1 \end{Bmatrix}, \qquad \mathbf{x}_1 = \begin{Bmatrix} 1 \\ \lambda_2 \end{Bmatrix}. \tag{3.186c}$$

It becomes apparent that for $k_\alpha, k_\beta > 0$ only centres can exist for the linearised system since $\lambda_1, \lambda_2 \in \mathbb{C}$ for all $u_1 \equiv u_{\mathrm{eq}} \in \mathbb{R}$ and therefore all $\mathbf{u}_{\mathrm{Eq},i}$ in (3.183b) and (3.185) are classified as

Table 3.3 – Equilibrium points of (3.181) according to Eqs.(3.183) and (3.184) with appropriate eigenvalues of the linearised system (3.186b).

	hardening $k_\alpha,\, k_\beta > 0$	**softening** $k_\alpha > 0,\, k_\beta < 0$	**snap-trough** $k_\alpha < 0,\, k_\beta > 0$
$p_0 \equiv 0$	$\mathbf{u}_{\mathrm{Eq},1} = \{0,0\}^{\mathrm{T}} \longrightarrow \lambda_{1/2} = \pm\sqrt{-\omega_\alpha^2}$		
	centre	*centre*	*saddle*
	no other equilibrium	$\mathbf{u}_{\mathrm{Eq},2/3} = \left\{\pm\sqrt{\frac{1}{-k_\gamma}}, 0\right\}^{\mathrm{T}} \longrightarrow \lambda_{1/2} = \pm\sqrt{2\,\omega_\alpha^2}$	
		saddle	*centre*
$p_0 \neq 0$	$0 = u_1^3 + \frac{1}{k_\gamma}\,u_1 - \frac{p_0}{k_\beta}\,, \quad \mathbf{u}_{\mathrm{Eq},i} = \{u_{\mathrm{eq},i}, 0\} \neq 0\,, \quad i = 1,2,3. \quad (*)$		
	1 real: $\mathbf{u}_{\mathrm{Eq},1} > 0$	1 real if: $\left(\frac{1}{3\,\lvert k_\gamma\rvert}\right)^3 \leq \left(\frac{p_0}{2\,k_\beta}\right)^2$; 3 real if otherwise	
	$\lambda_{1,2} \in \mathbb{C}$ $\rightarrow$ *centre*	$\lambda_{1,2} \in \mathbb{C}$ if: $3\left\lvert\omega_\beta^2\right\rvert\, u_{\mathrm{eq},i}^2 < \omega_\alpha^2$ $\rightarrow$ *centre* $\lambda_{1,2} \in \mathbb{R}$ if otherwise $\rightarrow$ *saddle*	$\lambda_{1,2} \in \mathbb{C}$ if: $\lvert\omega_\alpha^2\rvert < 3\,\omega_\beta^2\, u_{\mathrm{eq},i}^2$ $\rightarrow$ *centre* $\lambda_{1,2} \in \mathbb{R}$ if otherwise $\rightarrow$ *saddle*

non-hyperbolic equilibrium points. For $k_\gamma < 0$ and $p_0 \equiv 0$ all three stationary points in (3.183) can be centres as well as saddle equilibria. A complete summary of all possible cases is given in table 3.3. It is worth noting that identical conclusions can be reached using Morse theory for Hamiltonian systems as given in section 3.2.4. The majority of the above derived results regarding stability of the linearised system are well-known and are scattered across numerous publications. However, to the authors knowledge, closer examination of constant right-hand-side excitation for the system in (3.181) has only been considered sparsely. The need for a coherent and precise approach as basis for the derivations to come in this section justifies the presentation of some of the known results of the Duffing system given above.

3.4.2.2 Nonlinear analysis and uniqueness

Due to the incomplete picture of the true stability nature of (3.181) received by analysing the linear system in the previous section, a global approach is required. It is easy to verify that the energy function

$$V_{f_2}(\mathbf{u}) = \frac{1}{2}\,u_2^2 + \frac{1}{2}\,\omega_\alpha^2\,u_1^2 + \frac{1}{4}\,\omega_\beta^2\,u_1^4 - \widehat{p}_0\,u_1 \tag{3.187}$$

resembles the Hamiltonian of (3.181) by using the definition in (3.19). Thus, (3.187) can be employed as Lyapunov function satisfying all conditions of theorem 2. Energy input due to initial values $\mathbf{u}_0$ is equal to

$$V_{f_2,0}(\mathbf{u}_0) = V_{f_2}(\mathbf{u} \equiv \mathbf{u}_0)\,. \tag{3.188}$$

The proof for existence and uniqueness of (3.181) are easily obtained using Lipschitz's condition in (3.13) since together with (3.186a) a constant and finite l can always be found. With Eq.(3.22) for the orbital derivative being equal to zero, the level sets of solution trajectories for (3.181) are constant as expected for conservative systems.

Stability and derivation of explicit solution of the freely vibrating oscillator have been the subject of numerous publications, see [16–18] for examples. However, in the case of a non-zero right-hand side of (3.3) the qualitative significant changes have received considerably less attention in the literature and will therefore be derived and examined below using the theoretical framework presented in sections 3.2.1 to 3.2.4. For the sake of consistency and due to the fact that no coherent description of all possible states of the freely vibrating system could be found in literature, key results are revisited in the light of derivations introduced in this chapter and briefly summarised in what follows.

For $p_0 \equiv 0$, i.e. no applied forcing, Figure 3.9 shows the system's energy equation (3.187) incorporating all four possible combinations of the parameter pair (k_α, k_β). The hardening-type stiffness in (a) is a classical case of a Lyapunov function satisfying all conditions *(i)-(iii)* in theorem 2. With (3.187) being unbounded as $\|\mathbf{u}\| \to \infty$, see (3.89) for comparison, $\mathbf{u}_{\mathrm{Eq},1}$ from table 3.3 is globally stable. Contrary for graph (b) which shows the softening-type spring. The non-degenerate equilibrium remains only stable if the total initial energy is smaller than

$$V_{f_2,0}(\mathbf{u}_0) < V_{f_2,\mathrm{cr}}(\mathbf{u}_{\mathrm{cr}}) = \frac{1}{2}\omega_\alpha^2 u_{1,\mathrm{cr}}^2 + \frac{1}{4}\omega_\beta^2 u_{1,\mathrm{cr}}^4 , \tag{3.189}$$

where $\mathbf{u}_{\mathrm{cr}} \equiv \mathbf{u}_{\mathrm{Eq},2/3}$ from table 3.3. Hence, global stability is not ensured since

$$\lim_{\|\mathbf{u}\|\to\infty} V_{f_1}(\mathbf{u}) = -\infty \tag{3.190}$$

and the largest set of stable trajectories is given as

$$\Omega_c = \left\{\mathbf{u} \in \mathbb{R}^2 \middle| V_{f_2}(\mathbf{u}) \leq V_{f_2,\mathrm{cr}}(\mathbf{u}_{\mathrm{cr}})\right\} \tag{3.191}$$

which is equivalent to a condition for all points of the flow in the phase space expressed by a fourth-order algebraic equation

$$0 \leq |V_{f_2}(\mathbf{u})| - V_{f_2,\mathrm{cr}}(\mathbf{u}_{\mathrm{cr}}) , \tag{3.192}$$

bearing in mind that $p_0 \equiv 0$ in V_{f_2} from (3.187). It is easy to see in Fig. 3.9 although (b) and (c) share the same extreme points along the u_1-axis, the snap-through spring features global stability independent of parameter values or initial energy levels. However, for $V_{f_2,0}(\mathbf{u}_0) > 0$ a saddle-node bifurcation takes place in system (c), where along with the stable equilibrium $\mathbf{u}_{\mathrm{Eq},2}$ from table 3.3 a second centre $\mathbf{u}_{\mathrm{Eq},3}$ appears in the negative half-plane of the phase space and the trajectories of the system start passing through the unstable saddle $\mathbf{u}_{\mathrm{Eq},1} = \{0,0\}^{\mathrm{T}}$ instead of being tangent to it as in the case of a single centre. With (3.187) violating condition *(ii)* in theorem 2, LaSalle's approach must be used again, since it is possible to find a *positive* constant C for any point $\mathbf{u} \in \mathbb{R}$

of the phase space such that

$$\Omega_c = \left\{ \mathbf{u} \in \mathbb{R}^2 | V_{f_2}(\mathbf{u}) \leq C \right\} \tag{3.193}$$

is a compact positively invariant set. With $V_{f_2}(\mathbf{u})$ being unbounded, i.e. the limit in Eq.(3.190) above gives $+\infty$, the snap-through system is globally stable. It is worth noting that for any initial conditions $\mathbf{u}_0 \equiv \mathbf{u}_{\mathrm{Eq},2/3}$ no oscillation can occur since the system has already acquired a minimum-energy position.

Finally, graph (d) in 3.9 clearly shows that when both k_α and $k_\beta < 0$ there is no feasible combination for a stable system (3.181).

In case of $p_0 \neq 0$ all energy functions in Fig. 3.9 change to distorted, non-symmetrical 2D surfaces shown in figure 3.10. Although there is some similarity between both graphs in (a) of Figs. 3.9 and 3.10, the new equilibrium point has moved to the right[51)] if $p_0 > 0$ and must be obtained as solely real-valued solution of (3.184). As seen before in Fig. 3.9(a), the hardening spring system also appears to be globally stable if subjected to step excitation. However, due to the fact that (3.187) fails to comply with *(ii)* in theorem 2, LaSalle's principle in theorem 3 must be employed for the proof. Graph (b) underlines the fact that for $k_\alpha, k_\beta < 0$ the system remains unstable despite an additionally introduced positive right-hand side.

The parameter pair $(k_\alpha > 0, k_\beta < 0)$ produces two scenarios shown in (c) and (d) of figure 3.10. For the first, no equilibrium point can be established since the applied step load is greater than the critical loading

$$p_0 > p_{0,\mathrm{cr}}\,, \tag{3.194}$$

which will be given for the case of zero initial values in section 3.4.2.3 below. It is important to note that for analytical or numerical calculation of all three equilibrium points of the softening oscillator the roots of equation $(*)$ in table 3.3 can be used. However, for plotting the graph of zero solutions for the original system in (3.181) the more precise variant

$$\mathrm{sgn}(k_\beta)\; u^3 + \frac{\mathrm{sgn}(k_\alpha)}{|k_\gamma|}\, u - \frac{p_0}{|k_\beta|} \equiv \frac{m}{|k_\beta|}\left(\omega_\beta^2\, u^3 + \omega_\alpha^2\, u - \widehat{p}_0\right) \tag{3.195}$$

must be employed from which immediately follows that even if $p_0 > p_{0,\mathrm{cr}}$, hence in numerical integration method the system appears to be unstable, equation $(*)$ still possesses three real roots. This underlines the fact that the critical step load magnitude for the softening stiffness cannot be established with the derivations above and further analysis as presented in the following section 3.4.2.3 is required. Finally, equation (3.195) also shows that the case of a single zero solution only occurs if $D_s = 0$ but if $p_0 >$ the magnitude $|p_0|$ is already greater than $p_{0,\mathrm{cr}}$ and stability is lost.

[51)] It is easy to verify that in case of a negative force magnitude $p_0 < 0$ some or all newly emerging stationary points of the nonlinear system would move into the opposite direction. However, depending upon the value of all initial conditions u_0, $\dot{u}_0$ and their contribution towards the oscillators total energy $V_{f_2,0}(\mathbf{u}_0)$ these new equilibrium points can lie in the negative half-plane of the phase space, hence $\mathbf{u}_{\mathrm{Eq},i} < 0$ for some or all i.

Only if $D_s < 0$ are there three real solutions of which two are positive according to Vieta's lemma in (A.8), say $\mathbf{u}_{\mathrm{Eq},1} < 0 < \mathbf{u}_{\mathrm{Eq},2} < \mathbf{u}_{\mathrm{Eq},3}$ and the system *can* have one non-degenerate equilibrium point at $\mathbf{u}_{\mathrm{Eq},2}$ with an energy function as shown in Fig. 3.10(d). Although it is clear to see that $\mathbf{u}_{\mathrm{Eq},2}$ must be smaller than the maximum displacement u_{max} obtained from (3.197a), stability of this solely feasible solution will be established after introducing further results in 3.4.2.3.

The last case considered here for stability analysis with $p_0 \neq 0$ in (3.181) is shown in both graphs (e) and (f) of Fig. 3.10 which depict the energy function for the step excited snap-through system. From plotting (3.184a) with respect to u_1 it becomes immediately clear that there exists for $p_0 > 0$ ($p_0 < 0$) always one positive (negative) root only which ensures stability of the system regardless of values for initial condition or applied loading. Unfortunately, no statement can be made at this point whether the system trajectories can be classified as a homoclinic or heteroclinic orbits, which is the essential difference between (e) and (f) of figure 3.10. This is left to section 3.4.2.3 below.

Although in general no definite stability conclusions can be drawn for marginally stable stationary points of the linearised system, see [230, 241], it should be noted that all results given above by the nonlinear analysis are in agreement with implications presented in table 3.3 from the previous section.

3.4.2.3 Extreme response values

Impulse excitation. For free vibration and impulse excited systems the equation of motion is rewritten according to (3.51a) with the constant C_1 from (3.51b) containing all initial energy and the simplified notation $u = u_1$, $\dot{u} = u_2$

$$C_1 = \frac{m}{4}\Big(2\,(\widehat{p_\delta} + \dot{u}_0)^2 + 2\,\omega_\alpha^2\,u_0^2 + \omega_\beta^2\,u_0^4\Big) \tag{3.196}$$

where $\widehat{p_\delta} = p_\delta/m$ is the mass-normalised impulse magnitude. Extreme values of displacement $u_{\mathsf{Ex}} = \{u_{\mathsf{min}}, u_{\mathsf{max}}\}$ are obtained using equation (3.52), thus

$$u^4 + \frac{2}{k_\gamma}\,u^2 - \frac{4}{k_\beta}\,C_1 = 0\,, \tag{3.197a}$$

which can be reduced to a second-order algebraic form by employing the substitution $z \equiv u^2$ and an explicit solution is obtained via standard procedures [186]

$$z_{1/2} = -\frac{1}{k_\gamma} \pm \sqrt{\frac{1}{k_\gamma^2} + \frac{4}{k_\beta}\,C_1}\,. \tag{3.197b}$$

Due to $u = \pm\sqrt{z}$ the substitution must be $z \geq 0$ which rules out z_2 in (3.197b) for the hardening-type stiffness. Therefore, if $k_\alpha, k_\beta > 0$

$$u_{\mathsf{Ex}} = \pm\sqrt{-\frac{1}{k_\gamma} + \sqrt{\frac{1}{k_\gamma^2} + \frac{4}{k_\beta}\,C_1}}\,, \qquad \text{with} \qquad C_1 \geq 0\,, \tag{3.198}$$

and no oscillation for zero initial values. Contrary, for $k_\alpha > 0, k_\beta < 0$

$$u_{\mathsf{Ex}} = \pm\sqrt{\frac{1}{|k_\gamma|} - \sqrt{\frac{1}{k_\gamma^2} - \frac{4}{|k_\beta|}\,C_1}}\,, \tag{3.199a}$$

which immediately enables one to derive the criteria for stable oscillation of the softening-type stiffness system from the inner square root expression of (3.199a)

$$C_1 < \frac{|k_\beta|}{4\,k_\gamma^2}\,, \tag{3.199b}$$

ensuring that $z_{1/2} \in \mathbb{R}$ and $u_{\mathsf{Ex}} = \{0, 0\}$ if $C_1 \equiv 0$. Since the constant C_1 is a measure for the initial energy of the system, Eq.(3.199b) is equal to the condition in (3.189). The relationship between both allows one to obtain the statement that no stable softening stiffness type system is possible if $C_1 < 0$, which is easily understood by examining Fig. 3.9(b). At the energy function minimum in the vicinity of the origin all energy must be positive. It is only if the system leaves beyond the maximum stable orbit, which coincides with $\mathbf{u}_{\mathrm{Eq},2/3}$ from above at points $u_2(t) = 0$, that $V_{f_2}(\mathbf{u})$ takes negative values. Since the oscillator is autonomous, hence $V_{f_2}(t,\ \mathbf{u}) \equiv V_{f_2,0}(\mathbf{u}_0)\ \forall\ t$, a negative C_1 means instability for (3.181) in case of $k_\alpha > 0, k_\beta < 0$.

Plotting the graph for the energy function (3.187) with snap-trough type stiffness parameters $k_\alpha < 0, k_\beta > 0$ it is easy to show that Eq.(3.199b) gives exactly the difference of energy levels between the sinks at $\mathbf{u}_{\mathrm{Eq},2,3} = \left\{\pm\sqrt{1/|k_\gamma|}, 0\right\}^{\mathrm{T}}$ and the unstable saddle at $\mathbf{u}_{\mathrm{Eq},1} = \{0, 0\}^{\mathrm{T}}$. Noting that the square root in (3.197b) is always positive in this case since the maximum negative value for C_1 is obtained from

$$\frac{\mathrm{d}}{\mathrm{d}u_0}\,C_1 = -\,|k_\alpha|\,u_0 + k_\beta\,u_0^3 \equiv 0 \qquad \text{thus} \qquad u_0 = \pm\sqrt{\frac{1}{|k_\gamma|}}\,, \tag{3.200a}$$

which reinserted into (3.196) gives

$$C_{1,\mathsf{max}} = -\,\frac{k_\alpha^2}{4\,k_\beta} = -\,\frac{k_\beta}{4\,k_\gamma^2}\,, \tag{3.200b}$$

the extreme displacement for positive initial values in (3.15) can be derived from (3.197b) considering the appropriate signs

$$u_{\mathsf{Ex}} = \sqrt{\frac{1}{|k_\gamma|} \pm \sqrt{\frac{1}{k_\gamma^2} + \frac{4}{k_\beta}\,C_1}}\,, \tag{3.200c}$$

as long as the outer square root is greater than zero, hence, as long as

$$\frac{4}{k_\beta}\,C_1 < 0\,. \tag{3.200d}$$

This is exactly the energy limit which keeps the trajectory level sets inside of one of the energy

sinks in Fig. 3.9. For the special setup of $C_1 \equiv C_{1,\max}$ the system switches instantaneously into the stable equilibrium $\mathbf{u}_{\mathrm{Eq},2} = \left\{\sqrt{1/|k_\gamma|}, 0\right\}^{\mathrm{T}}$ and no oscillation takes place. Contrary, for $C_1 \equiv 0$ the minus sign in (3.200c) must be retained and the equation gives $u_{\mathsf{Ex}} = \{0, 0\}$, i.e. the systems stays at its marginally stable saddle equilibrium. Finally, the case of

$$\frac{4}{k_\beta} C_1 > 0 \tag{3.201a}$$

allows for oscillation in both half-spaces of the phase plane, positive and negative. Periodic orbits occur with the origin as saddle and $\mathbf{u}_{\mathrm{Eq},2/3}$ from (3.183b) as stable centres. The extreme displacement is then given as

$$u_{\mathsf{Ex}} = \pm \sqrt{\frac{1}{|k_\gamma|} + \sqrt{\frac{1}{k_\gamma^2} + \frac{4}{k_\beta} C_1}} \,. \tag{3.201b}$$

According to (3.54) the velocity of the system can be expressed as a function of the displacement in an algebraic equation describing the trajectory of oscillation for a given energy level C_1

$$\dot{u}^2(u) = \frac{2}{m} C_1 - \omega_\alpha^2 u^2 - \frac{1}{2} \omega_\beta^2 u^4 \,. \tag{3.202}$$

Maximum values $\dot{u}_{\mathsf{Ex}}$ of Eq.(3.202) are given at the respective stationary points $\mathbf{u}_{\mathrm{Eq},i}$ as listed in table 3.3, which leads for hardening/softening stiffness with $\mathbf{u}_{\mathrm{Eq},1} = \{0, 0\}^{\mathrm{T}}$ to

$$\dot{u}_{\mathsf{Ex}} = \pm \sqrt{\frac{2}{m} C_1} \tag{3.203}$$

where according to (3.198) $C_1 \geq 0 \;\forall\; u_0$ despite $k_\beta < 0$. As mentioned above, the phase space trajectories of the snap-through system if (3.201a) is fulfilled represent periodic orbits travelling between more than one stable equilibrium point and maximum velocity values are either given in (3.203) or obtained from (3.202) by setting $u \equiv u_{\mathsf{eq}}$ leading to

$$\dot{u}_{\mathsf{Ex}} = \pm \frac{\sqrt{4\, C_1\, k_\beta + |k_\alpha|^2}}{m\, \omega_\beta \sqrt{2}} \tag{3.204}$$

whichever yields the larger value. Contrary, if the initial energy level C_1 is negative, i.e. $C_1 < 0$, equation (3.204) must be used because (3.203) would give complex, and hence unfeasible values.

The acceleration function is obtained by simply rearranging the equation of motion in (3.48), thus

$$\ddot{u}(t) = -\omega_\alpha^2 u(t) - \omega_\beta^2 u^3(t) \,. \tag{3.205}$$

It is easy to see that (3.205) has only for hardening-type systems with $\omega_\alpha^2, \omega_\beta^2 > 0$ one solution for the extreme acceleration $\ddot{u}_{\mathsf{Ex}} = \{\ddot{u}_{\mathsf{min}}, \ddot{u}_{\mathsf{max}}\}$, namely at $u_{\mathsf{min}}, u_{\mathsf{max}}$, respectively. For softening $\omega_\alpha^2 >, \omega_\beta^2 < 0$ and snap-through $\omega_\alpha^2 < 0, \omega_\beta^2 > 0$ restoring forces it is necessary to obtain u_{a}

following the approach in (3.60)

$$\frac{\mathrm{d}}{\mathrm{d}u} f_2(u)\Big|_{u_a} = \omega_\alpha^2 + 3\,\omega_\beta^2 u_a^2\,, \qquad \text{hence} \qquad u_a = \pm\sqrt{\frac{1}{3\,k_\gamma}}\,, \tag{3.206}$$

and clearly $\mathrm{d}^2 f_2(u)/\,\mathrm{d}u^2 = 6\,\omega_\beta^2 u_a \neq 0$ if $u_a \neq 0$, thus $f_2\,(u_a)$ is an extreme solution. Depending on the values for both parameters ω_β^2 and ω_β^2 the minimum and maximum acceleration are obtained by substituting either $u_{\min}, u_{\max}$ or u_a back into (3.205). It becomes apparent from (3.205) that despite equal values for mass and stiffness coefficients all three systems have significantly different peak accelerations.

Using (3.62) gives the oscillation period

$${}_{f_2}T_\delta = 2\sqrt{2}\int\limits_{u_{Ex}} \frac{\mathrm{d}u}{\sqrt{-\omega_\beta^2\,u^4 - 2\,\omega_\alpha^2\,u^2 + 4\,C_1}}\,, \tag{3.207a}$$

which has to be normalised with respect to the first term under the square root similar to (3.197a) in order to apply standardised cases of integration from Byrd *et al* [288]

$${}_{f_2}T_\delta = \frac{2\sqrt{2}}{|\omega_\beta|}\int\limits_{u_{Ex}} \frac{\mathrm{d}u}{\sqrt{-\operatorname{sgn}\!\left(\omega_\beta^2\right)\,u^4 - \frac{2}{k_\gamma}\,u^2 + \frac{4}{\left|\omega_\beta^2\right|}\,C_1}} \tag{3.207b}$$

with the integration limits $u_{Ex} = \{u_{\min}, u_{\max}\}$ as obtained in (3.198), (3.199a) and (3.200c) or (3.201b) above. It is important to note that the expression under the square root in (3.207) is identical to (3.197a), hence from basic calculus it follows, if the system has a real-valued set of extreme displacement $u_{Ex} = \{u_{\min}, u_{\max}\}$, which is the solution of (3.197a), then the integral in (3.207) has no singularity within the integration limits.[52)]

In case of $\omega_\beta^2 = \left|\omega_\beta^2\right|$, i.e. for hardening and snap-through systems, the expression under the square root above can be rewritten in Legendre's canonical form, see appendix B.2, if (3.197a) has four real-valued roots,

$$(\chi_1 - u)\,(u - \chi_2)\,(u - \chi_3)\,(u - \chi_4) \qquad\qquad \chi_i \in \mathbb{R}\,, \quad i = 1, \ldots, 4 \tag{3.208a}$$

together with the ordering condition

$$\chi_1 > \chi_2 > \chi_3 > \chi_4\,. \tag{3.208b}$$

Assuming $\chi_4 < 0 < \chi_1$ with $\chi_1 \equiv u_{\max}$ and $\chi_4 \equiv u_{\min}$ the integration in (3.207) must be split

[52)] For the type of application considered in here it is sufficient for the integrand in (3.207) to have at least two real-valued solutions which are associated with a physical meaning, the extreme displacement. However, this is no necessary condition. By plotting (3.197a) it can easily be seen, equation (3.207) gives real values for the oscillation period even in the case of all four roots of the integrand being complex.

into

$$\frac{{}_{f_2}T_\delta}{2\sqrt{2}}\,|\omega_\beta| = \int_{u_{min}}^{0} \ldots \,\mathrm{d}u + \int_{0}^{u_{max}} \ldots \,\mathrm{d}u \tag{3.209}$$

where an exact solution for the first term is obtained using case $\langle 252.00 \rangle$ in [288] with the following constant values

$$\eta = \frac{2}{\sqrt{(\chi_1 - \chi_3)\,(\chi_2 - \chi_3)}}, \qquad \kappa = \sqrt{\frac{(\chi_1 - \chi_2)\,(\chi_3 - \chi_4)}{(\chi_1 - \chi_3)\,(\chi_2 - \chi_4)}} \tag{3.210a}$$

and

$$\sin^2\psi_1 = \frac{-\chi_4\,(\chi_1 - \chi_3)}{\chi_1\,(\chi_3 - \chi_4)}\,. \tag{3.210b}$$

The second term in (3.209) is solved for according to $\langle 257.00 \rangle$ in [288]. Both constants η and κ are equal to (3.210a), but (3.210b) becomes

$$\sin^2\psi_2 = \frac{\chi_1\,(\chi_2 - \chi_4)}{-\chi_4\,(\chi_1 - \chi_2)}\,. \tag{3.210c}$$

The complete closed-form solution for the integral expression in (3.209) is then given by

$${}_{f_2}T_\delta = \frac{2\sqrt{2}}{|\omega_\beta|}\,\eta\Big[\mathsf{F}(\psi_1,\kappa) + \mathsf{F}(\psi_2,\kappa)\Big]\,, \tag{3.210d}$$

with $\mathsf{F}(\psi_i,\kappa)$ according to [109,290] and appendix B. In the special case of positive initial values for the snap-trough system, the extreme displacement u_{Ex} lies entirely within the positive half of the phase plane, $0 < u_{min} < u_{max}$, and (3.207) can be written as a single-term expression

$$\frac{{}_{f_2}T_\delta}{2\sqrt{2}}\,|\omega_\beta| = \int_{u_{min}}^{u_{max}} \ldots \,\mathrm{d}u = \int_{\chi_2}^{\chi_1} \ldots \,\mathrm{d}u\,. \tag{3.211a}$$

Applying again $\langle 257.00 \rangle$ [288] but with the lower limit equal to χ_2 gives

$${}_{f_2}T_\delta = \frac{2\sqrt{2}}{|\omega_\beta|}\,\eta\mathsf{F}(\psi,\kappa)\,, \tag{3.211b}$$

with η and κ from (3.210a), but

$$\sin^2\psi = 1\,, \tag{3.211c}$$

hence, due to $\mathsf{K}(\kappa) = \mathsf{F}\big(\frac{\pi}{2},\kappa\big)$, see [290], Eq.(3.211b) simplifies to

$${}_{f_2}T_\delta = \frac{2\sqrt{2}}{|\omega_\beta|}\,\eta\mathsf{K}(\kappa)\,. \tag{3.211d}$$

With the inverse function arcsin of (3.211c) being restricted to the domain of definition [160]

$$-\frac{\pi}{2} \leq \psi \leq \frac{\pi}{2}\,, \tag{3.211e}$$

for the argument ψ, it is easy to see that (3.211c) has multiple solutions at

$$\psi_j = \frac{1}{(2j-1)}\,\frac{\pi}{2} \qquad\qquad j = 1, 2, 3, \ldots, n\,. \tag{3.211f}$$

Using the previously introduced relationship in Eq.(3.151f) gives for (3.211b) in conjunction with (3.211f) multiple oscillation frequencies

$$f_{\mathrm{NL},j} = \frac{1}{{}_{\mathrm{f}_2}T_{\delta,j}}\,, \qquad \text{where} \qquad {}_{\mathrm{f}_2}T_{\delta,j} = \frac{2\sqrt{2}}{(2j-1)}\,\frac{\eta}{|\omega_\beta|}\,\mathsf{K}(\kappa)\;. \tag{3.211g}$$

In case of the softening type stiffness $\omega_\beta^2 = -\left|\omega_\beta^2\right|$ analytical solutions of the period in equation (3.207) are obtained in a similar manner as above. According to appendix B.2 the Legendre form of the polynomial under the square root if there are four real-valued roots present now gives

$$(u-\chi_1)\,(u-\chi_2)\,(u-\chi_3)\,(u-\chi_4) \qquad\qquad \chi_i \in \mathbb{R}\,, \quad i = 1, \ldots, 4 \tag{3.212}$$

and still enabling one to use $\langle 257.00 \rangle$ in [288] to yield either (3.210d) or (3.211d) together with the constants in (3.210a), (3.210c) and (3.211c). Furthermore, with the approach introduced in (3.211e) and (3.211f), similar results for multiple oscillation frequencies of the nonlinear system are obtained [270].

Step excitation. If the system in (3.181) has a non-zero right-hand side $p_0 \neq 0$ the integration constant containing all energy at $t = t_0$ is given in (3.65b)

$$C_2 = \frac{m}{4}\left(2\,\dot{u}_0^2 + 2\,\omega_\alpha^2\,u_0^2 + \omega_\beta^2\,u_0^4 - 4\,p_0\,u\right) \tag{3.213}$$

and extreme values of displacement must be obtained from

$$u^4 + \frac{2}{k_\gamma}\,u^2 - \frac{4\,p_0}{k_\beta}\,u - \frac{4}{k_\beta}\,C_2 = 0\,. \tag{3.214}$$

Employing a commonly used method from [58] briefly described in appendix A.2, this algebraic equation can be solved analytically. According to table A.2, if equation (A.1c), i.e. the reduced form of the cubic resolvent term Eq.(A.6), has three real roots of which two are negative, then the fourth-order equation (3.214) has only complex roots and therefore no physically meaningful solution. By rewriting (3.214) in the form of (A.6)

$$y^3 + 2\,P\,y^2 + \left(P^2 - 4\,R\right)y - Q^2 = 0\,, \qquad \text{with} \quad P = \frac{2}{k_\gamma^2},\; Q = -\frac{4\,p_0}{k_\beta},\; R = -\frac{4}{k_\beta}\,C_2, \tag{3.215a}$$

the reduced third-order equation (A.1c) is obtained as

$$z^3 + S\,z + T = 0\,, \qquad \text{where} \qquad S = -\frac{P^2}{3} - 4\,R\,, \quad \text{and} \quad T = P\left(\frac{8}{3}\,R - \frac{2}{27}\,P^2\right) - Q^2\,. \tag{3.215b}$$

In conjunction with Eq.(A.1d) where $D_s = (S/2)^3 + (T/2)^2$ and the requirement $D_s \geq 0$ according to table A.1, hence $(S/2)^3 \leq (T/2)^2$ if $S/2 < 0$, the following condition is derived

$$-\frac{1024}{9\,(k_\gamma\,k_\beta)^2}\,C_2^2 - \frac{4}{729\,k_\beta^6}\Big[C_2\left(1152\,k_\alpha^4\,k_\beta - 2916\,k_\beta^5 + 15552\,k_\alpha\,k_\beta^2\,p_0\right) - 16\,k_\alpha^6 - 243\,k_\alpha^2\,k_\beta^4 - 432\,k_\alpha^3\,k_\beta\,p_0 - 2916\,k_\beta^2\,p_0^2\Big] \leq 0\,. \tag{3.215c}$$

Although (3.215c) holds for all three types of (3.180), hardening, softening and snap-through systems, instability occurs only for the second one with $k_\alpha > 0, k_\beta < 0$ as has been demonstrated above. Hence, a true advantage for ruling out non-feasible systems is only given in that case and (3.215c) can be rewritten by substituting $k_\beta \equiv -\,|k_\beta|$. In the majority of practical situations, stiffness parameters are given as a property of the oscillator. Equation (3.215c) can then be used to limit the initial energy input C_2 or the applied step force magnitude p_0. Or, in the case C_2 and p_0 are given, the equation obtains parameters for stiffness coefficients $k_\alpha > 0, k_\beta < 0$ in order to yield a stable system. However, it should be noted that (3.215c) is necessary *and* sufficient since it prevents (3.215b) from having three non-multiple real-valued solutions, of which according to Vieta's lemma (A.8) two are negative and one is positive. This implies, that if (3.215b) has a single real-valued root this must be positive, subjected to $p > 0$, which is the fundamental assumption for the derivation of four complex roots of (3.214) above.

With the system in (3.181) at rest for $t \equiv t_0$ the initial energy (3.213) equates to $C_2 = 0$ and (3.214) can be rewritten as third-order equation with one root equal to zero, i.e. $u_{\min} = 0$, if $p_0 > 0$ is assumed

$$u^3 + \frac{2}{k_\gamma}\,u - \frac{4}{k_\beta}\,p_0 = 0\,. \tag{3.216}$$

It is easy to see this is similar to equation (3.184a) which derives stationary points of system (3.181). Hence, with (3.184b) there is a $D_s > 0$ for all p_0 if $k_\alpha, k_\beta > 0$ and (3.216) has exactly one real solution $u_{\max}$, which must be positive due to Vieta's lemma [58], and two complex conjugate $\overline{u}$, $\overline{u}^*$ such that $u_{\max} \cdot \overline{u} \cdot \overline{u}^* = 4p_0/k_\beta$. Values for $u_{\max}$ are obtained similar to (3.185) using the scheme in A.1.

A different situation arises for softening-type restoring forces $k_\alpha > 0, k_\beta < 0$ since now three real solutions are possible if $D_s < 0$ where

$$D_s = \left(\frac{2}{3\,k_\gamma}\right)^3 + \left(2\,\frac{p_0}{k_\beta}\right)^2\,. \tag{3.217a}$$

is derived according to (A.1d). Similar to (3.195) above, the precise nature of solutions is revealed

using

$$\operatorname{sgn}(k_\beta)\, u^3 + \frac{\operatorname{sgn}(k_\alpha)}{|k_\gamma|}\, u - \frac{p_0}{|k_\beta|} \tag{3.217b}$$

from (3.195) instead of (3.216) although for calculating all three roots of the problem both equations are valid with (3.216) being easier to analyse analytically. Setting (3.217b) equal to zero gives together with $p_0 \equiv 0$ exactly three real-valued solutions, see (3.199a) above. As $p_0 > 0$ increases, the two roots in the positive half-plane eventually merge to a single one. At this point, the applied force is equal to the critical force $p_{0,\mathrm{cr}}$ from (3.194). Increasing the force magnitude further leaves the system with one remaining real, negative-valued root and two newly emerging complex conjugate roots, which render the oscillator unstable. With equation (3.217b) having a maximum on the positive u-axis at

$$-3\,u^2 + \frac{2}{|k_\gamma|} = 0 \qquad \longrightarrow \qquad u_{\mathrm{Max}} = \sqrt{\frac{2}{3\,|k_\gamma|}}\,, \tag{3.217c}$$

the function value of (3.217b) at this point u_{Max} is equal to $p_{0,\mathrm{cr}}$. Hence, rearranging equation (3.217b) where $\operatorname{sgn}(k_\beta) = -1$ gives an explicit expression for the critical force magnitude of the softening-stiffness oscillator

$$p_{0,\mathrm{cr}} = \frac{1}{3}\sqrt{\frac{2}{3}}\,\frac{|k_\beta|}{|k_\gamma|^{\frac{3}{2}}}\,, \tag{3.218}$$

for zero initial values, thus $C_2 = 0$. If $p_0 > p_{0,\mathrm{cr}}$ as in (3.194) the system is unstable. It is easily verified that the condition of a multiple real-valued root on the positive u-axis requires $D_s \equiv 0$ in (3.217a), see [58], hence $\left(2/(3\,|k_\gamma|)\right)^3 = \left(2p_0/k_\beta\right)^2$, and solving for p_0 yields (3.218). However, the disadvantage of this approach is that an explicit expression for u_{Max} remains hidden.

The last case to consider here in terms of extreme displacement values for the system in (3.181) with $p_0 \neq 0$ is the snap-through stiffness type. As has been shown in the previous section 3.4.2.2, for the pair $k_\alpha < 0, k_\beta > 0$ the nonlinear system is globally stable. For $C_2 \equiv 0$ the energy function (3.187) has four roots $u_{\mathrm{r},i}$ with $i = 1, ..., 4$ and $u_{\mathrm{r},1} = 0$, of which three coincide with solutions of (3.216), e.g. $u_{\mathrm{r},i}$, $i = 1, ..., 3$, bearing in mind (3.216) has been simplified due to $u_{\mathrm{r},1} = 0$. It is easy to show that for any combination of parameters $k_\alpha < 0, k_\beta > 0$, $p_0 > 0$ two roots of (3.187) are negative, one remains zero ($u_{\mathrm{r},1}$), and one is always positive, say $u_{\mathrm{r},4}$ for example, which gives the maximum displacement of the system and is likewise obtainable from Eq.(3.216). It is important to note that this only holds as long as $D_s < 0$ in (3.217a), hence

$$p_0 < \frac{1}{3}\sqrt{\frac{2}{3}}\,\frac{|k_\beta|}{|k_\gamma|^{\frac{3}{2}}}\,. \tag{3.219}$$

which is similar to (3.218) for the softening system.[53] Only then the energy function (3.187) of

[53] Plotting the function in (3.217b) for the two cases $k_\alpha > 0, k_\beta < 0$ and $k_\alpha < 0, k_\beta > 0$ shows that both are mirror images of each other with u-axis as mirror axis.

the snap-through system has *one* local maximum $V_{f_2}(u_{\mathrm{Max}}, 0) > 0$ at $u_{\mathrm{Max}} < 0$ obtained as root from (3.184a), and *two* local minima at $u_{\mathrm{Min},1} < u_{\mathrm{Max}} < 0$ and $0 < u_{\mathrm{Min},2}$, respectively, which are also solutions of equation (3.184a). The function values $V_{f_2}(u_{\mathrm{Min,i}}, 0)$ of both minima are smaller than zero with one being a global negative extremum. Since the solution u_{max} of the extreme displacement $u_{\mathsf{Ex}} = \{0, u_{\mathsf{max}}\}$ is obtained as the maximum positive root of (3.216), the energy level set of (3.187), at which the orbital motion takes place, is equal to zero. With a local maximum $V_{f_2}(u_{\mathrm{Max}}, 0) > 0$ it is therefore easily understood that only by adding a constant value to (3.187) this zero energy level of oscillation can be increased. Such a constant is given by C_2 defined in Eq.(3.213). However, the derived results in this paragraph are only valid if $C_2 \equiv 0$ and therefore, for zero initial conditions, the step excited system in (3.181) *cannot* reach a heteroclinic orbit as shown in Fig. 3.10(f), regardless the values and combinations of all involved parameters k_α, k_β and p_0.

Expressing the velocity as a function of the displacement according to (3.67) yields in connection with the restoring force (3.180)

$$\dot{u}^2 = 2\,\widehat{p}_0\,u - \omega_\alpha^2\,u^2 - \frac{\omega_\beta^2}{2}\,u^4 + 2\,\widehat{C}_2\,, \tag{3.220}$$

where $\widehat{C}_2 = C_2/m$ is the mass-normalised initial energy from (3.213). Extreme values of $\dot{u}(t)$ occur when the trajectory passes through points in the phase plane which are in line with stable equilibrium points. Hence, together with (3.71) $\dot{u}_{\mathsf{Ex}} = \{\dot{u}_{\mathsf{min}}, \dot{u}_{\mathsf{max}}\}$ are given at $u \equiv u_{\mathsf{eq}}$ similar to (3.204)

$$\dot{u}_{\mathsf{Ex}} = \pm\sqrt{2\,\widehat{p}_0\,u_{\mathsf{eq}} - \omega_\alpha^2\,u_{\mathsf{eq}}^2 - \frac{1}{2}\,\omega_\beta^2\,u_{\mathsf{eq}}^4 + 2\,\widehat{C}_2}\,. \tag{3.221}$$

The extreme acceleration of the system is obtained from (3.72)

$$\ddot{u}_{\mathsf{Ex}} = \widehat{p}_0 - \omega_\alpha^2\,u_{\mathsf{a}} - \omega_\beta^2\,u_{\mathsf{a}}^3 \tag{3.222}$$

where for the hardening-type stiffness oscillator $u_{\mathsf{a}} \equiv u_{\mathsf{Ex}}$. For softening and snap-through restoring force systems u_{a} must be obtained from (3.60), which equates in the special case of $f_2(u)$ to (3.206). Thus, depending on the actual values of $\widehat{p}_0$, ω_α^2 and ω_β^2 minimum and maximum acceleration are obtained using either u_{min}, u_{max} or $\pm u_{\mathsf{a}}$.

Finally, the period of oscillation can be given together with (3.73)

$${}_{\mathrm{f}_2}T_{\mathrm{H}} = 2\sqrt{2}\int_{u_{\mathsf{Ex}}} \frac{\mathrm{d}u}{\sqrt{-\omega_\beta^2\,u^4 - 2\,\omega_\alpha^2\,u^2 + 4\,\widehat{p}_0\,u + 4\,\widehat{C}_2}} \tag{3.223}$$

where $u_{\mathsf{Ex}} = \{u_{\mathsf{min}}, u_{\mathsf{max}}\}$ is gained from (3.216). The solution of the integral is very similar to various cases examined above such as (3.151), (3.158) and (3.207). The sign change of ω_β^2 for either hardening or softening systems is handled the same way as in equation (3.212).

In its most general version (3.223) will have two real-valued and two complex conjugate

roots $\chi_1, \chi_2 \in \mathbb{R}$, $\chi_3, \chi_4 \in \mathbb{C}$ and limits of integrations given as $\chi_2 = u_{\min} \leq 0 \leq \chi_1 = u_{\max}$. Rewriting the expression under the square root according to (B.15) enables one to use $\langle 259.00 \rangle$ in [288], thus

$$ {}_{f_2}T_H = \frac{2\sqrt{2}}{|\omega_\beta|}\,\eta\,\mathsf{F}(\psi,\kappa) \tag{3.224a} $$

where

$$ \eta = \frac{1}{\sqrt{S_1 S_2}}\,, \quad S_1^2 = (\chi_1 - \chi_b)^2 + \chi_a^2\,, \quad S_2^2 = (\chi_2 - \chi_b)^2 + \chi_a^2\,, $$
$$ \chi_a^2 = -\frac{(\chi_3 - \chi_4)^2}{4}\,, \quad \chi_b^2 = \frac{\chi_3 + \chi_4}{2}\,, \quad \kappa^2 = \frac{(\chi_1 - \chi_2)^2 - (S_1 - S_2)^2}{4\,S_1 S_2} \tag{3.224b} $$

and $\cos\psi = -1$. Due to the definition of ψ in [288] interchanging the integration limits of (3.223) leads to $\cos\psi = 1$. Therefore, with the case given above the final solution for the argument is

$$ \cos^2\psi = 1\,. \tag{3.224c} $$

Similar to (3.211), this results in multiple solutions for ψ otherwise strictly defined in $0 \leq \psi_0 \leq \pi$ only. In an extended domain $k\,\pi$ with $k = 1, 2, \ldots, n$ the argument can take on discrete values $\psi_{(k-1)} = k\,\pi$, all of which must be normalised to the domain of ψ_0 in order to be feasible. Therefore,

$$ \psi_{(k-1)} = \frac{k}{j}\,\pi\,, \qquad \text{with} \quad k = 1, 2, \ldots, j \quad \text{and} \quad j = 1, 2, \ldots, n\,. \tag{3.224d} $$

It is easy to see that for every new j in (3.224d) there is only one new solution if $k = 1$. All other values for $\psi_{(k-1)}$ are equivalent to the preceding step with $j - 1$. This allows for a simplification of (3.224d) to

$$ \psi_j = \frac{\pi}{j}\,, \tag{3.224e} $$

and together with (3.151f) multiple solutions for ${}_{f_2}T_H$ are obtained as

$$ {}_{f_2}T_H = \frac{4\sqrt{2}}{j\,|\omega_\beta|}\,\eta\,\mathsf{K}(\kappa)\,, \qquad j = 1, 2, \ldots, n\,. \tag{3.224f} $$

With the inverse of (3.224f) the oscillation frequency $f_{NL,j}$ is derived as defined in (3.74).

3.4.2.4 Shock spectra

For free vibration or impulse excitation, equations (3.198), (3.199a), (3.200c) and (3.201b) give explicit values of the extreme displacement u_{Ex} for all three possible combinations of the stiffness coefficients k_α, k_β of the nonlinear system in (3.181). Similar to the example in section 3.4.1.5 these results can be used to establish plots of u_{Ex} normalised to the extreme displacement of an equivalent linear system with identical values for all parameters but $k_\beta = 0$, the so-called shock

spectra. However, normalisation with respect to the nonlinear system's mass m is difficult and it is therefore suggested to base these spectra on initial values of energy G_1 as derived in (3.196) rather than the commonly used initial condition of displacement and velocity. Given the fact that G_1 can effectively be split into three components due to displacement, velocity and impulse force,[54] respectively. This has the distinct advantage of being able to separately link the influence of all three of them on to the total extreme displacement of the system.

Similar rules apply to Eq.(3.207) for the nonlinear oscillation period ${}_{f_2}T_\delta$. With the last expression under the square root of (3.207b) representing a stiffness coefficient k_β and mass normalised energy term

$$\widehat{C}_{1,\beta} = \frac{C_1}{\left|\omega_\beta^2\right|} \tag{3.225}$$

the period can together with $\omega_\beta^2 = k_\beta / m$ be rewritten as

$${}_{f_2}T_\delta = m\,\widehat{{}_{f_2}T_\delta}\,, \tag{3.226}$$

where $\widehat{{}_{f_2}T_\delta}$ is solely a function of the stiffness coefficient ratio $k_\gamma = k_\beta / k_\alpha$ and $\widehat{C}_{1,\beta}$. Both methods for displacement and period normalisation allow for the set up of shock spectra similar to figures 3.5 and 3.6 from section 3.4.1.5 above.

For the step loading excited oscillator the situation is slightly different. The fact that (3.214) for the most general case of $C_2 \neq 0$, $p_0 \neq 0$ cannot be solved analytically does not necessarily mean a shock spectra is unobtainable. Deriving u_{Ex} numerically and normalising it with respect to the nonlinear system's mass m and the static displacement of the linear equivalent oscillator $u_{stat,lin} = p_0 / k_\alpha$ yields diagrams analogous to figure 3.7, although less universally applicable since mass-normalisation is confined to specific values for m. The majority of linear response spectra for transient excitation modes are generally given with zero initial conditions for the system under consideration [89, 226, 296] mainly due to two simple facts. First, it is not always possible to yield closed-form solutions if complicated excitation function are considered. Secondly, and most important, the principle of linear superposition is valid enabling one to consider maximum response values and initial conditions separately. Therefore, $C_2 \equiv 0$ in (3.214) leads directly to (3.216), an analytical solution for u_{Ex} independent of the nonlinear oscillator's mass m can be derived and thus, linear static displacement normalised spectra similar to Fig. 3.7 are easily obtained. Correspondingly, with $\widehat{C}_2 \equiv 0$ in (3.223), the nonlinear oscillation period ${}_{f_2}T_H$ due to step excitation can be reformulated in the same manner as (3.226) above giving similar graphs of normalised oscillation frequency as in figure 3.8 obtained for the system in section 3.4.1.

[54] This part is equal to zero in case of free vibration.

3.5 Summary

In this chapter several new results were derived, which, to the author's knowledge, have been published for the first time. In section 3.2.4 the known fact has been used that for non-hyperbolic unstable equilibrium points the linearised eigenspace is identical to the asymptotes of the hyperbola in the phase plane, in order to prove the principle is also valid for stable equilibrium points. Retaining terms of up to order two from the same Taylor approximation, one can show that for the stable fixed point the eigenvectors of the linearised system are identical to the slope of diameters of the invariant integral manifold ellipse, irrespective whether the fixed point is degenerate or not.

The known framework of general expressions for extreme response values and the nonlinear oscillation period for SDOF systems has been considerably extended in section 3.3.1. This allowed the derivation of new analytical solutions for nonlinear conservative systems having either $f_1 = k_\beta \operatorname{sgn}(u) |u|^b$ or $f_2 = k_\alpha u + k_\beta u^3$ as a restoring force. Although explicit expressions were not obtained in all cases, these new results present a significant improvement compared to currently available solutions in the literature, mainly due to the following two reasons. Firstly, a much wider range of nonlinear systems can be included and cases with nonzero initial conditions and *simultaneously* constant right-hand-side forcing function can be treated, whereas previously only one *or* the other was incorporated at any given time. Secondly, it has been explicitly shown that multi-harmonic trial solutions used for various approximate analytical methods such as the method of harmonic balance or various KBM schemes are justified since, depending on the type of excitation, odd or even multiples of a fundamental nonlinear oscillation frequency are naturally contained in the exact solution of the system if analysed using special functions.

Furthermore, utilising two rather different approaches, it has been proved for the strongly nonlinear force f_1 that unique solutions do exist even in the case of values smaller than 1 for the nonlinearity exponent b, where the system in conjunction with zero initial values fails to satisfy the Lipschitz condition. Picard's iteration method clearly indicated that only for the case of zero initial conditions *and* zero forcing no other solution than the trivial one exist, but for any other combination of either nonzero initial values or nonzero forcing magnitude the oscillator exhibits only nontrivial solutions. However, it required the analytical approximate solution using Picard's scheme together with an extension of the multiple-equilibrium method from [284, 286] to prove that already the less stringent Peano uniqueness theorem instead of the more conservative Lipschitz condition as originally suggested in [286] is necessary *and* sufficient for uniqueness of the nontrivial solution of the f_1-type stiffness system. The second method, for reasons of reliability, entirely independent of the first, involved both the nonlinear flow of the system and its Lyapunov function. The lesser known Brauer-Sternberger theorem was somewhat modified to ensure the modulation function $h\big(t, L(t, \Delta\mathbf{u})\big)$ for the nonlinear system's Lyapunov function exists. By obtaining an inequality expression valid for the entire domain of definition of the Lyapunov function in the phase space, uniqueness of both trivial and nontrivial solution were assured.

Results of extreme value solutions have been utilised to establish normalised shock spectra for both of the nonlinear systems under study. However, due to the single-term nature of f_1 mass

normalisation is easier to perform and published shock spectra are therefore far more versatile. Mass normalisation for f_2 is not always possible and explicitly plotted spectra for the nonlinear system are omitted. However, in both cases these spectra should only be utilised for approximate calculations or pre-design stage studies. They are derived from analytical results given in sections 3.4.1 and 3.4.2, respectively, which are far more exact than any of the graphs in figures 3.5 to 3.8.

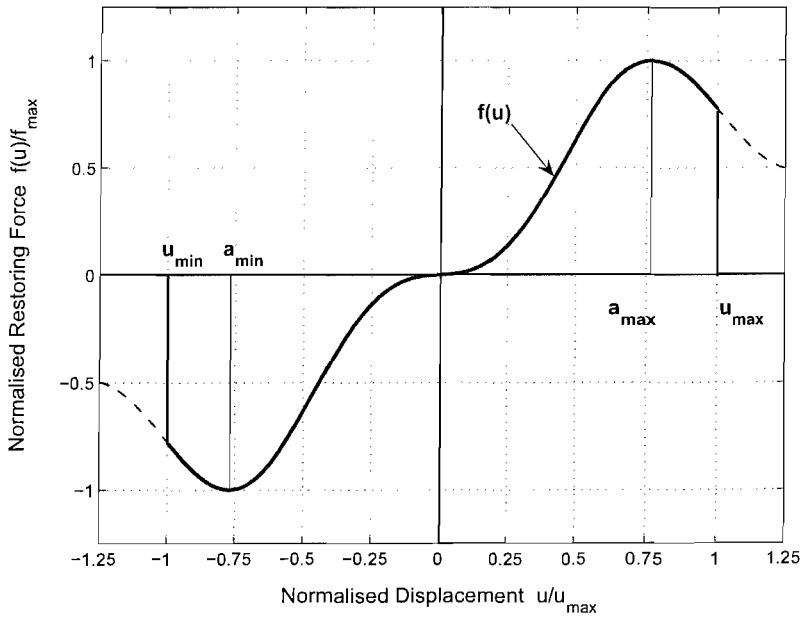

Figure 3.1 – Nonlinear restoring force with extrema other than $u_{\mathrm{Ex}} = \{u_{\mathrm{min}};\, u_{\mathrm{max}}\}$. The labels a_{min} and a_{max} mark the displacement at which the minimum/maximum acceleration occurs.

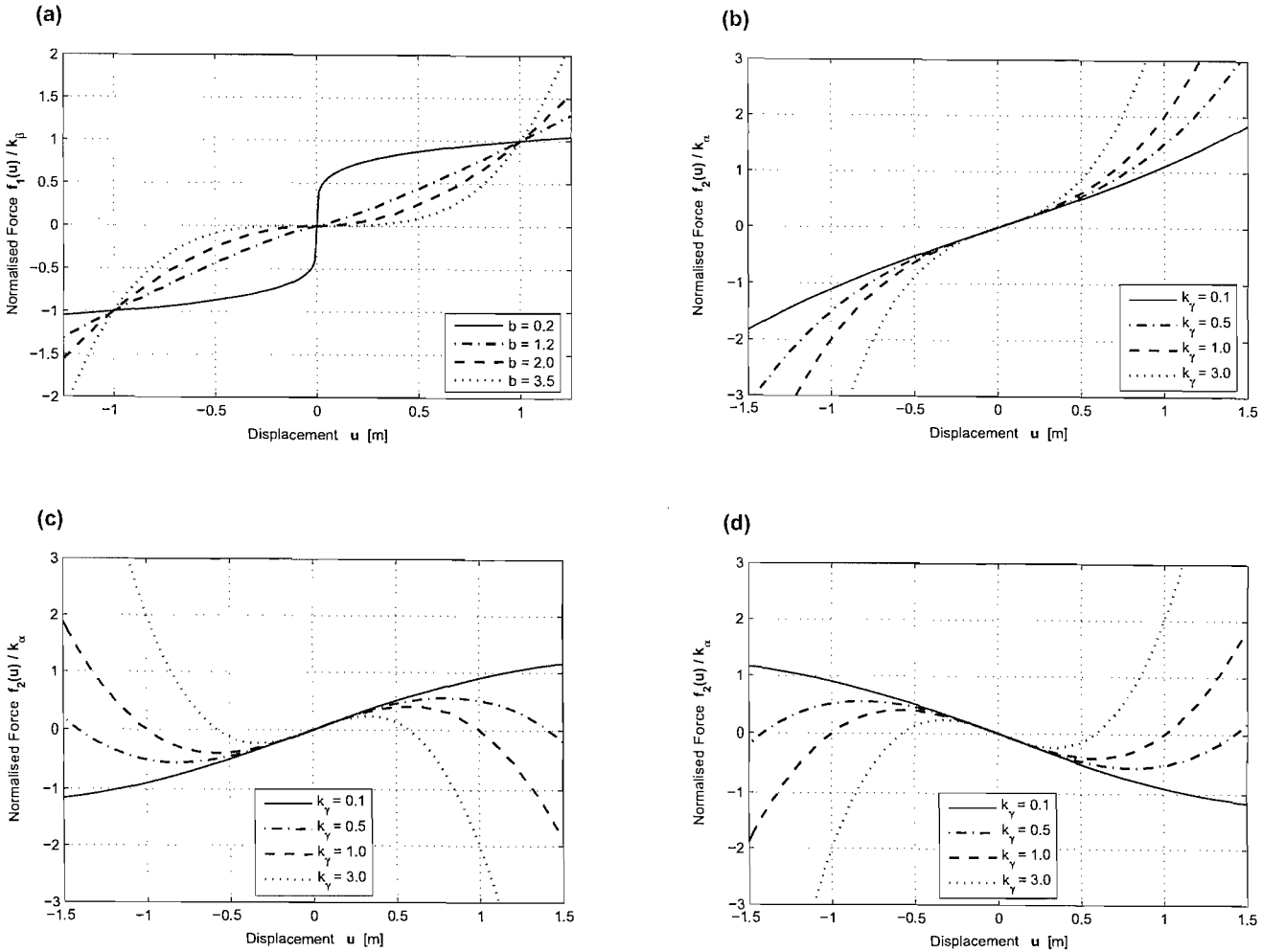

Figure 3.2 – Normalised nonlinear restoring force characteristics for both nonlinear forces $f_1(u)$ and $f_2(u)$: **(a)** $f_1(u) = k_\beta \operatorname{sgn}(u)\,|u|^b$ for different values of b, **(b)** stiffening-type $f_2(u) = k_\alpha u + k_\beta u^3$, **(c)** softening-type $f_2(u) = k_\alpha u - k_\beta u^3$, **(d)** snap-through $f_2(u) = -k_\alpha u + k_\beta u^3$.

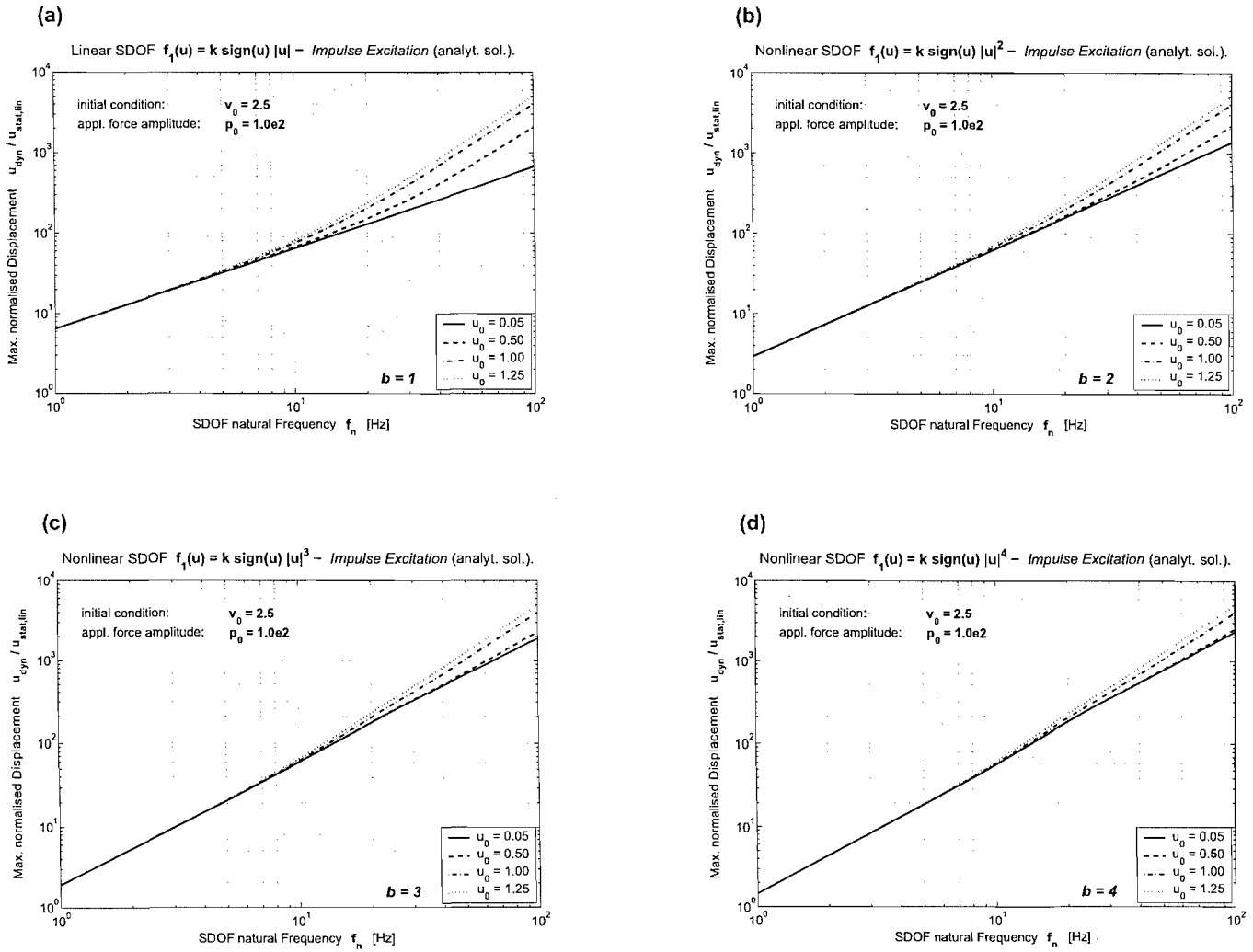

Figure 3.3 – Nonlinear restoring force $f_1(u)$ - *impulse excitation*: Maximum normalised displacement $u_{\text{norm}} = u_{\text{dyn}}/u_{\text{stat,lin}}$ for different values of b versus linear equivalent frequency f_{n}. Initial conditions: $u_0 = 0.05,\ 0.5,\ 1,\ 1.25\text{m}$, $v_0 = \dot{u}_0 = 2.5\text{m/s}$. Impulse magnitude $p_0 = 100\text{N}$. Parameters: $\omega_{\text{n}} = 2\pi f_{\text{n}}$ rad/s, mass $m = 1\text{kg}$, stiffness coefficient $k_\beta = k = m\omega_{\text{n}}^2\ \text{N/m}^{\text{b}}$.

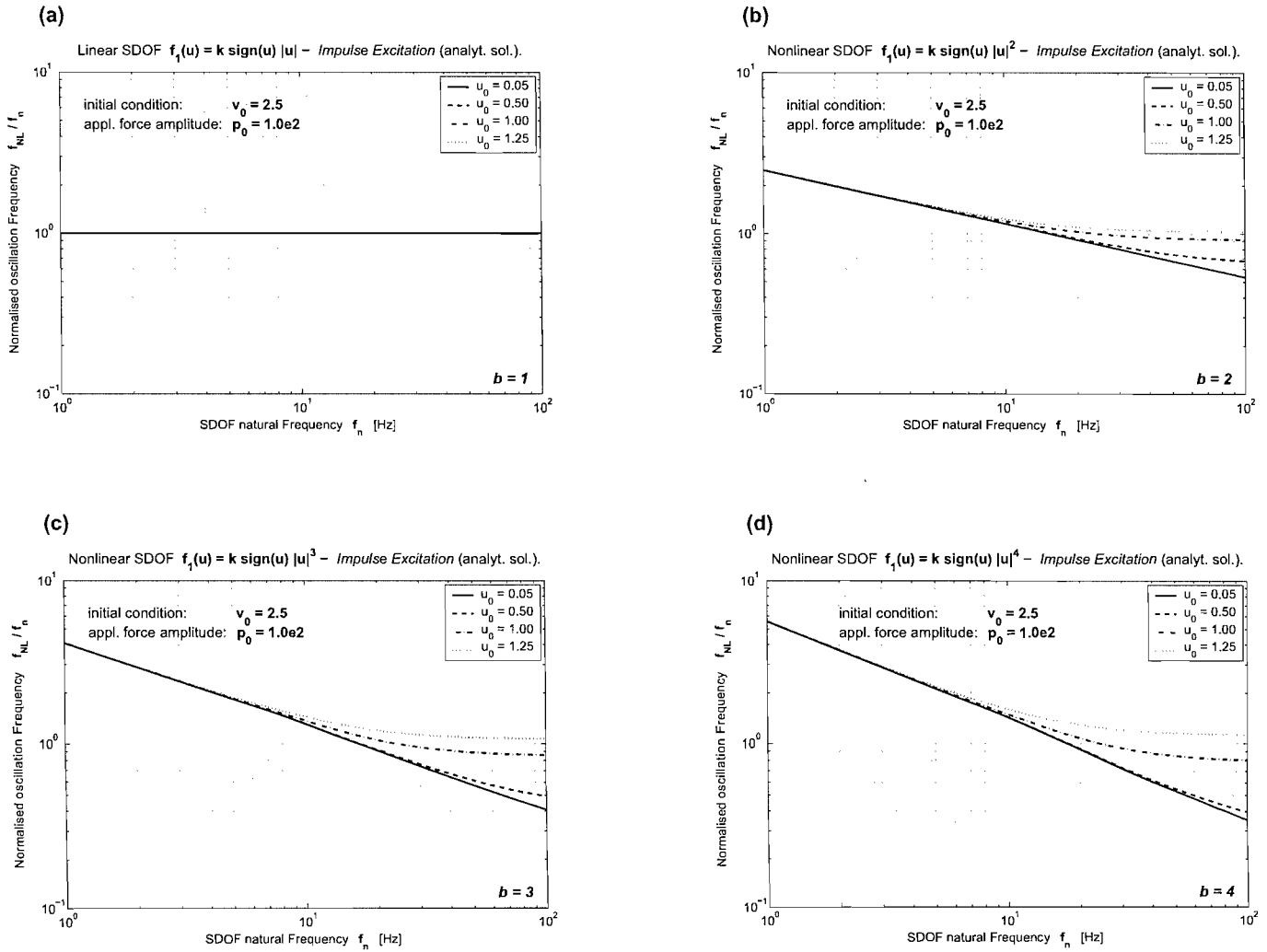

Figure 3.4 – Nonlinear restoring force $f_1(u)$ - *impulse excitation*: Normalised oscillation frequency $f_{\text{norm}} = f_{\text{NL}}/f_{\text{n}}$ for different values of b versus linear equivalent frequency f_{n}. Initial conditions: $u_0 = 0.05,\ 0.5,\ 1,\ 1.25\text{m}$, $v_0 = \dot{u}_0 = 2.5\text{m/s}$. Impulse magnitude $p_0 = 100\text{N}$. Parameters: $\omega_{\text{n}} = 2\pi f_{\text{n}}\ \text{rad/s}$, mass $m = 1\text{kg}$, stiffness coefficient $k_\beta = k = m\,\omega_{\text{n}}^2\ \text{N/m}^{\text{b}}$.

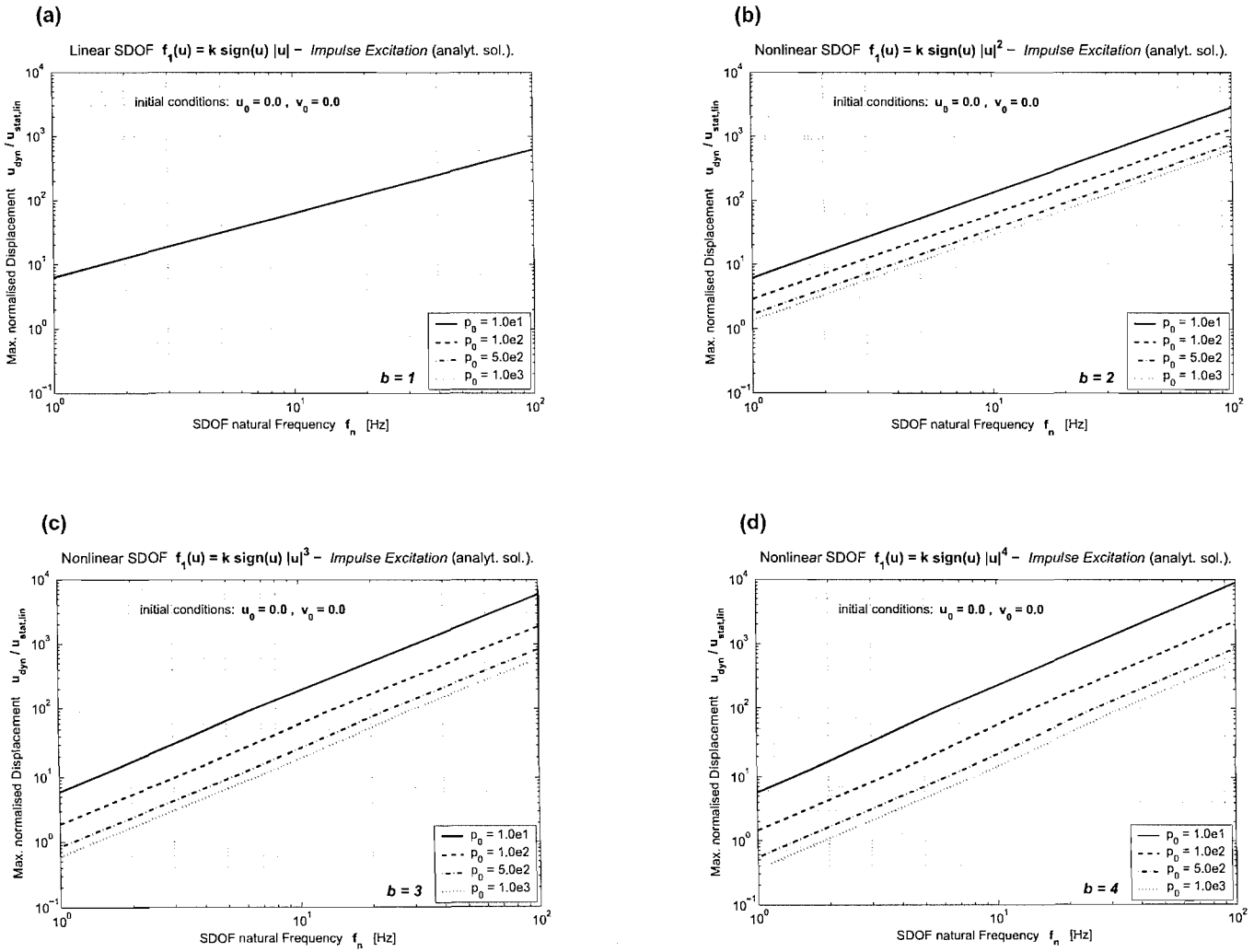

Figure 3.5 – Nonlinear restoring force $f_1(u)$ - *impulse excitation*: Shock spectra for maximum normalised displacement $\overline{u}_{\mathrm{Ex,m,s}} \equiv u_{\mathrm{dyn}} \big/ u_{\mathrm{stat,lin}}$. The dynamic displacement given as $u_{\mathrm{dyn}} = \overline{m}_{\delta,\mathrm{f}_1} u_{\mathrm{max}}$ is mass-normalised. System conditions: $u_0 = v_0 = \dot{u}_0 = 0$ (before the impulse is applied). Impulse magnitude $p_0 = 10$, 100, 500, 1000 N.

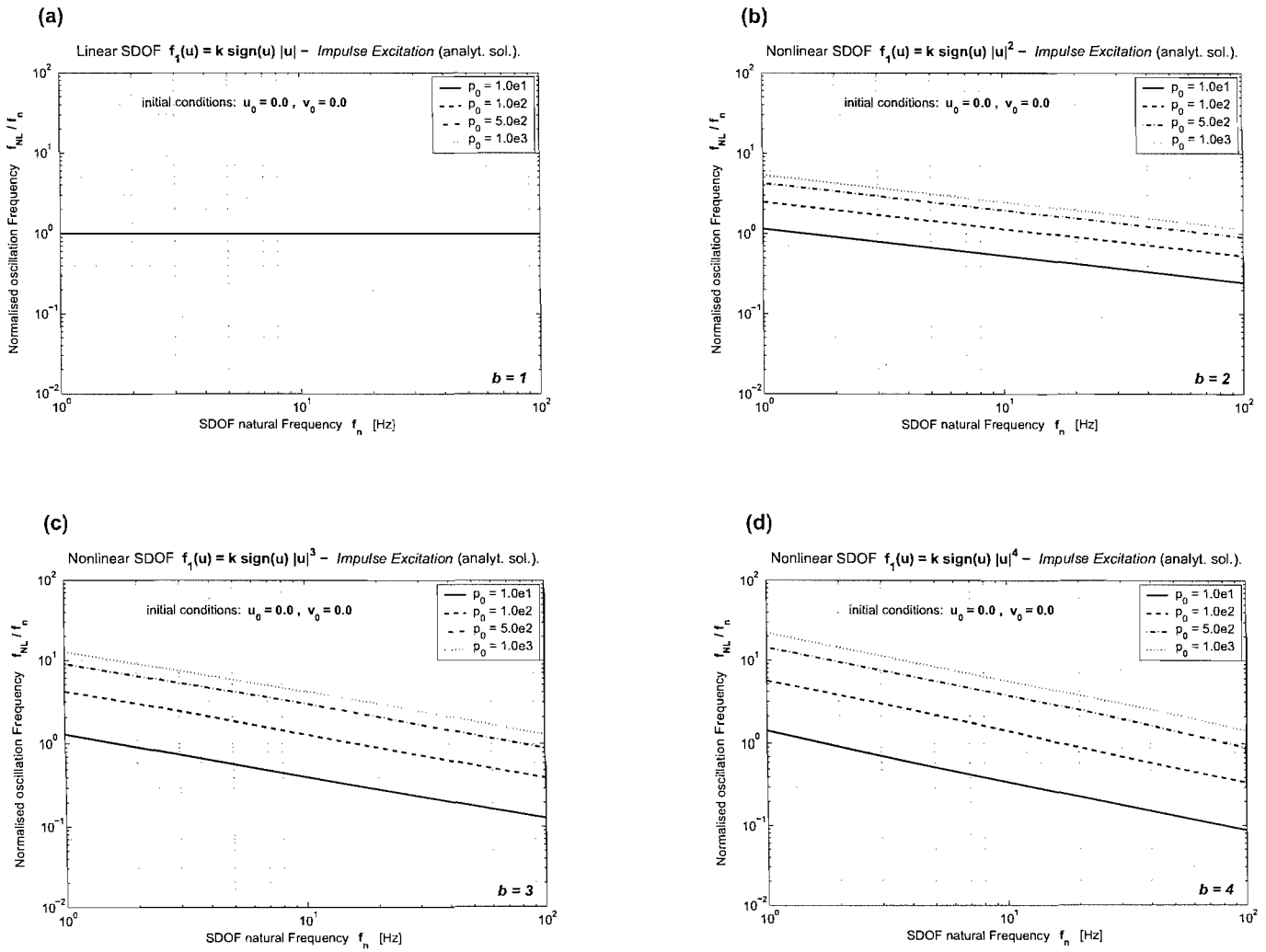

Figure 3.6 – Nonlinear restoring force $f_1(u)$ - *impulse excitation*: Normalised oscillation frequency $1 \Big/ {}_{f_1}\overline{T}_{\delta,m} \equiv f_{NL} \Big/ f_n$. The nonlinear frequency f_{NL} is mass-normalised. System conditions: $u_0 = v_0 = \dot{u}_0 = 0$ (before the impulse is applied). Impulse magnitude $p_0 = 10,\ 100,\ 500,\ 1000$ N.

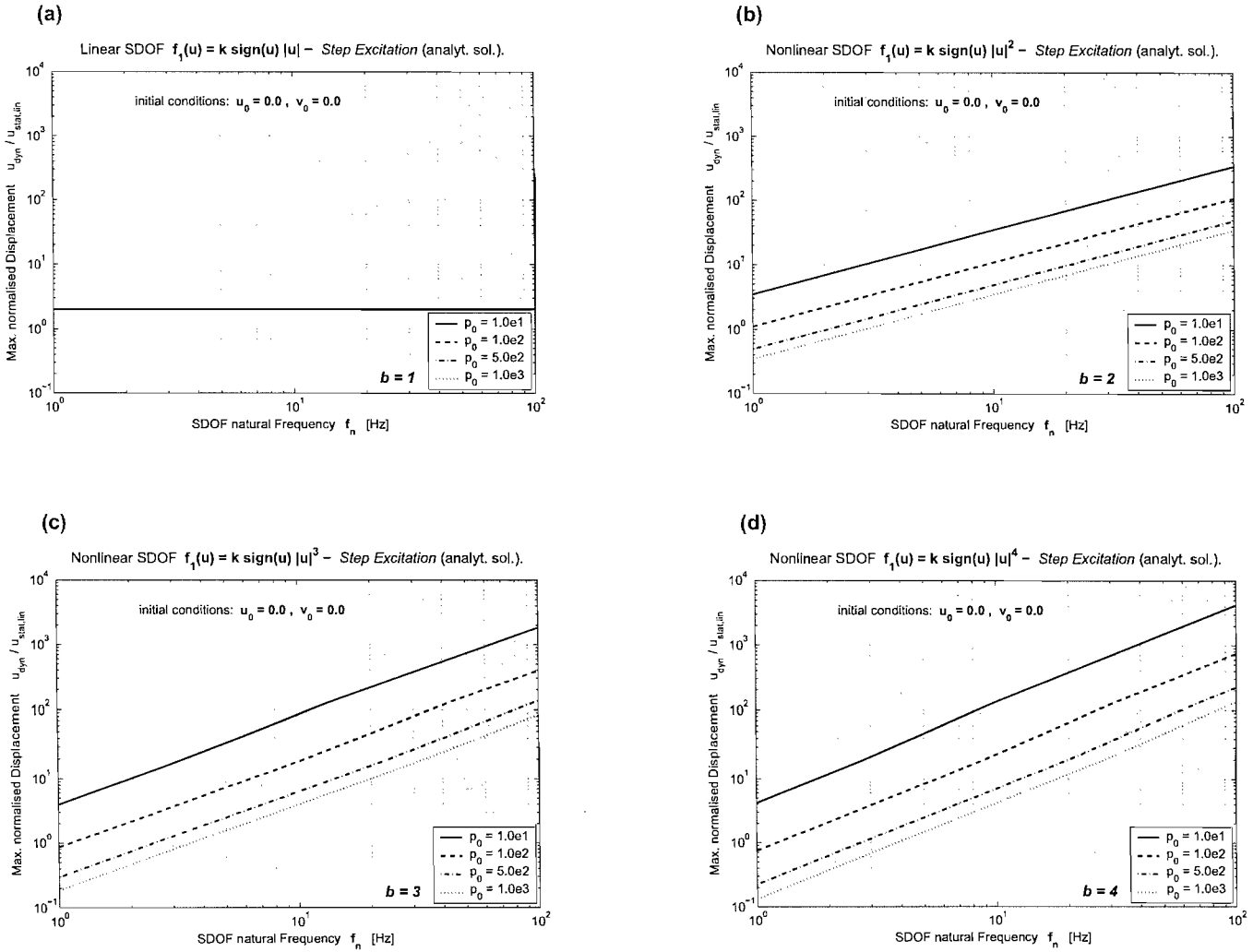

Figure 3.7 – Nonlinear restoring force $f_1(u)$ - *step excitation*: Shock spectra for maximum normalised displacement $\overline{A}^{\frac{1}{b}}_{\mathrm{p,norm}} \equiv u_{\mathrm{dyn}} \big/ u_{\mathrm{stat,lin}}$. The dynamic displacement given as $u_{\mathrm{dyn}} = \overline{m}_{\mathrm{H},\mathrm{f}_1} u_{\mathrm{max}}$ is mass-normalised. Initial conditions: $u_0 = 0\mathrm{m}$, $v_0 = \dot{u}_0 = 0\mathrm{m/s}$. Step magnitude $p_0 = 10,\ 100,\ 500,\ 1000\mathrm{N}$.

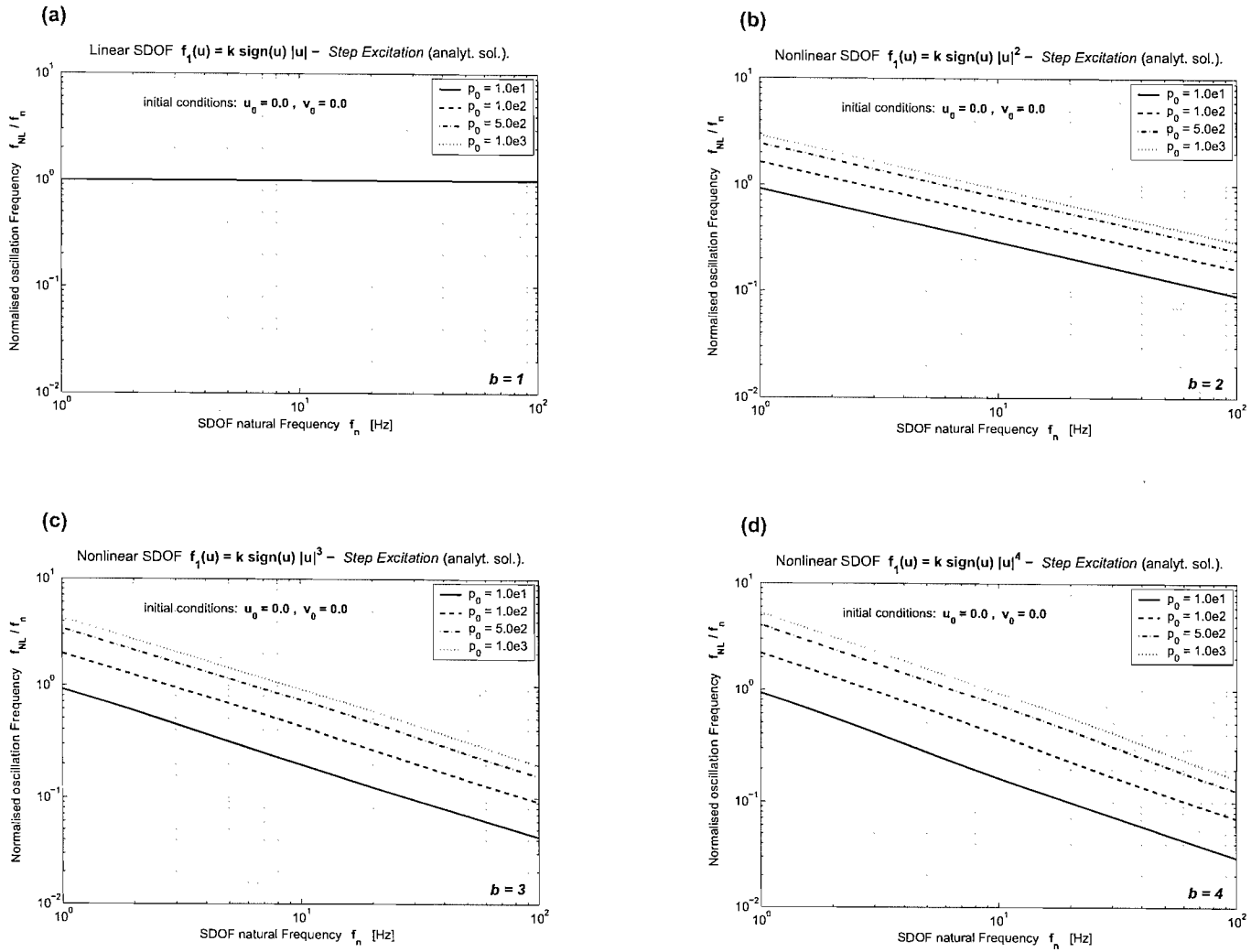

Figure 3.8 – Nonlinear restoring force $f_1(u)$ - *step excitation*: Normalised oscillation frequency $1\Big/{}_{f_1}\overline{T}_{H,m} \equiv f_{NL}\Big/f_n$. The nonlinear frequency f_{NL} is mass-normalised. Initial conditions: $u_0 = 0\text{m}$, $v_0 = \dot{u}_0 = 0\text{m/s}$. Step magnitude $p_0 = 10,\ 100,\ 500,\ 1000\text{N}$.

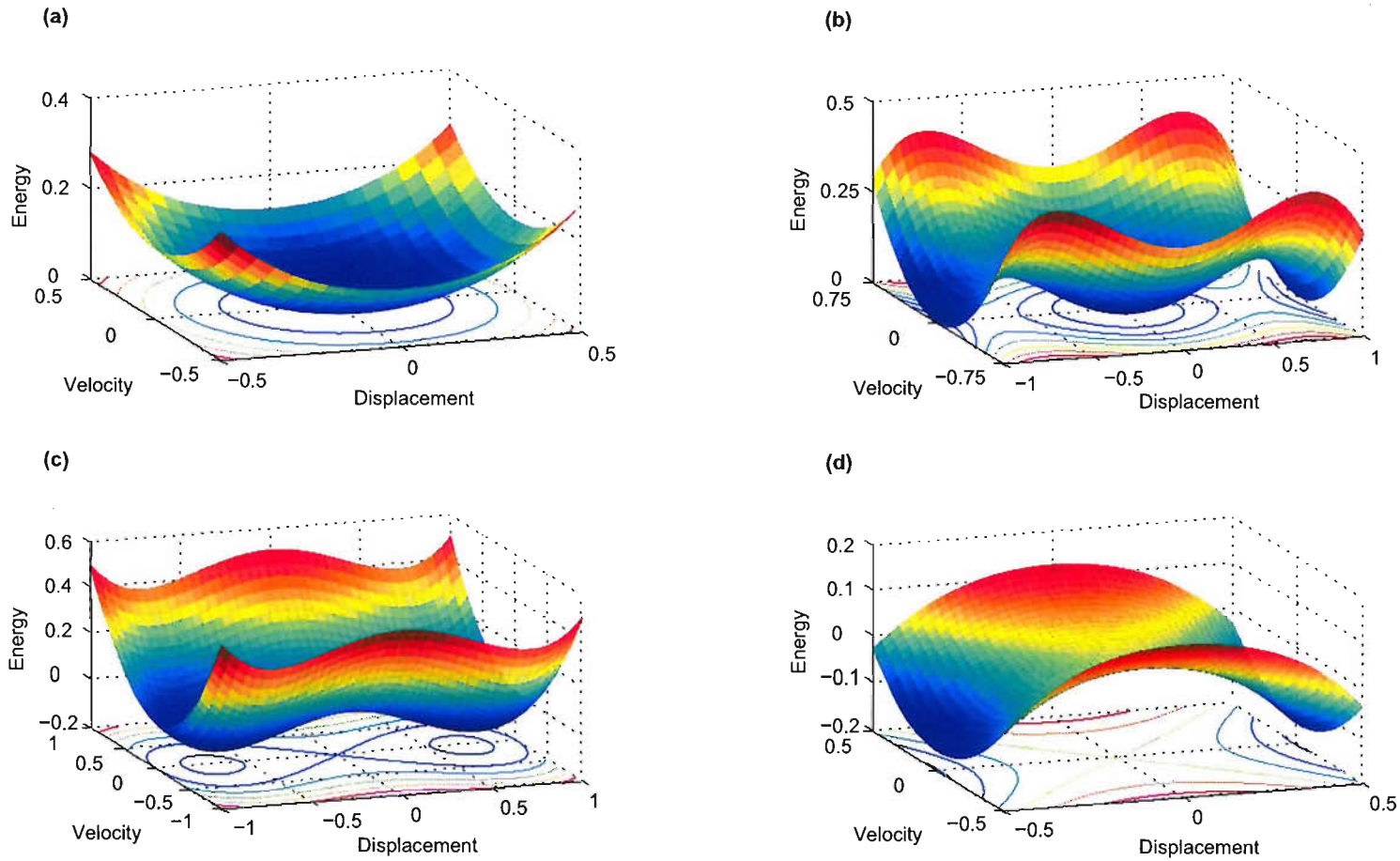

Figure 3.9 – Nonlinear restoring force $f_2(u)$ - *free vibration/impulse excitation*: Energy levels for different parameter ranges. **(a)** hardening, $k_\alpha, k_\beta > 0$, **(b)** softening, $k_\alpha > 0, k_\beta < 0$, **(c)** snap-through, $k_\alpha < 0, k_\beta > 0$, **(d)** unstable, $k_\alpha < 0, k_\beta < 0$.

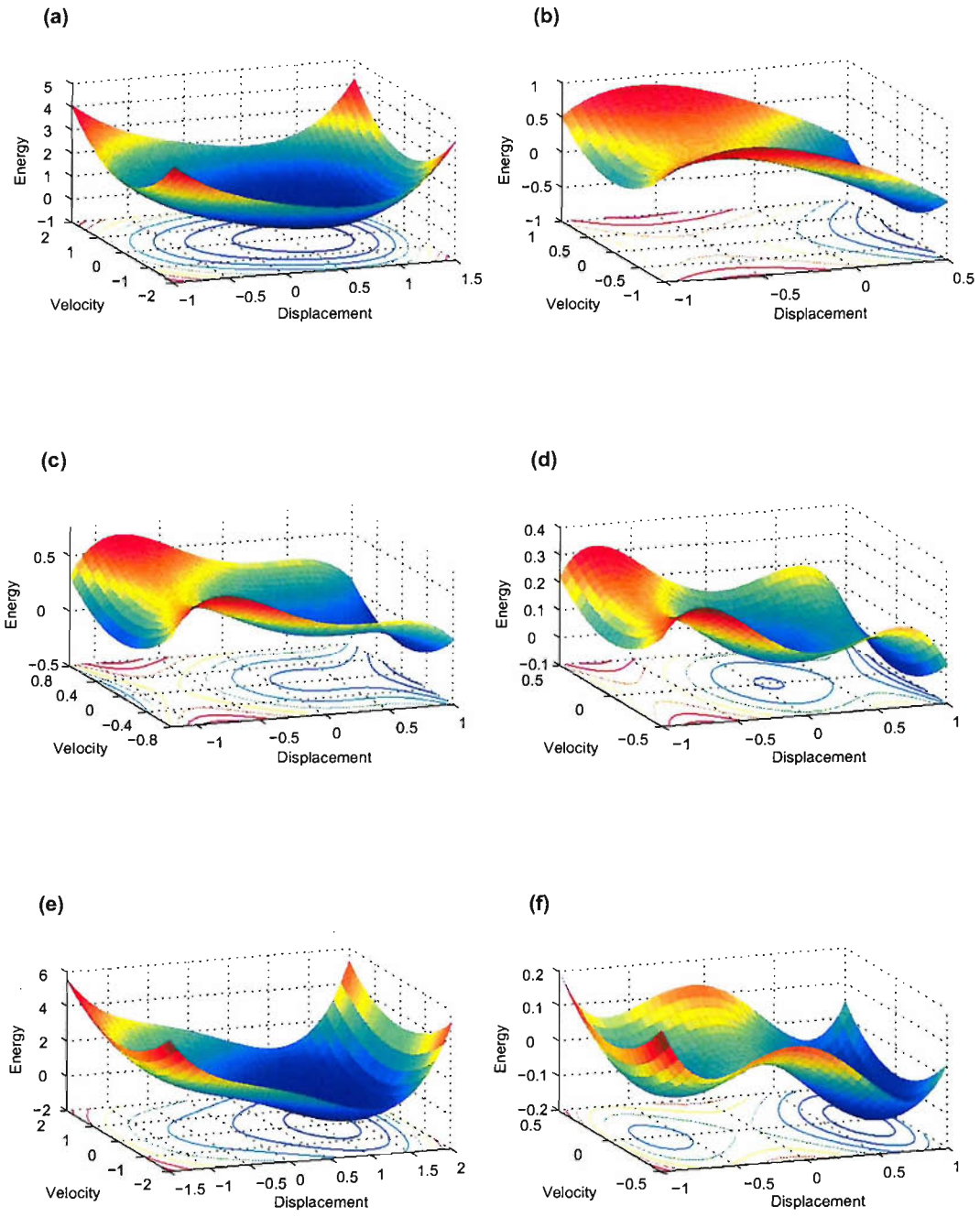

Figure 3.10 – Nonlinear restoring force $f_2(u)$ - *step excitation*: Energy levels for different stiffness parameter ranges. **(a)** hardening, $k_\alpha, k_\beta > 0$, **(b)** unstable, $k_\alpha, k_\beta < 0$, **(c)** softening, $k_\alpha > 0, k_\beta < 0$, and $p_0 > p_{0,\mathrm{cr}}$, **(d)** softening, $k_\alpha > 0, k_\beta < 0$, and $p_0 < p_{0,\mathrm{cr}}$, **(e)** snap-through, $k_\alpha < 0, k_\beta > 0$, and $p_0 > p_{0,\mathrm{cr}}$, **(f)** snap-through, $k_\alpha < 0, k_\beta > 0$, and $p_0 < p_{0,\mathrm{cr}}$.

CHAPTER 4

NONLINEAR AUTONOMOUS SDOF SYSTEMS TIME DOMAIN SOLUTIONS

4.1 Introduction

The previous chapter established, apart from explicit stability conditions, closed-form analytical expressions for obtaining the extreme response values of two autonomous nonlinear SDOF systems. Applying these novel results, approximate analytical time domain solutions for the two oscillators under study will be derived in this chapter.

Essentially, two different approaches will be presented. The first method relies on employing a suitable one-term trial solution with an appropriate number of free parameters which are obtained from algebraic equations involving known extreme response values of the nonlinear system similar to the collocation method.[1)] The second approach, involving multiple-term approximation, consists of two independent procedures. First, applying the well-established basic concept of variational methods a nonlinear least-square scheme is developed using the aforementioned single-term collocation solution as a fundamental approximation, around which higher-order trial functions are generated. Secondly, the previously introduced Picard iteration method utilised in section 3.4.1.3 to prove uniqueness of solutions for the $f_1(u)$ restoring force system, is successfully transformed into a simple analytical approximation algorithm ultimately converging towards the exact solution. Both single and multi-term solutions account for step-excited SDOF systems. Under special circumstances the system is allowed to possess nonzero initial conditions for displacement and velocity.[2)]

[1)] In a strict mathematical sense the collocation method is a projection method for solving integral and differential equations in which the approximate solution is determined from the condition that the equation be satisfied at certain given points. A precise definition is given in [58, 297].

[2)] A second-order non-massless dynamical system with an external nonzero (or constant) excitation force and zero

The chapter is outlined as follows. Before deriving any approximation, section 4.2 presents exact solutions for the freely vibrating Duffing[3] system in (3.181). Although the solutions for *either* zero initial velocity *or* zero initial displacement are well-known, especially the former, it is shown in sections 4.2.1 and 4.2.2 that all three instances of the oscillator, namely hardening, softening and snap-through type systems can be described mathematically using only one single Jacobian elliptic function regardless of the signs and values of k_α and k_β. This makes it possible to find a new solution for the Duffing system, with general non-zero initial values incorporating a phase delay as shown in section 4.2.3. The results of 4.2.1 and 4.2.2, including all linear second-order homogeneous differential systems, can now be obtained as special cases of this new solution.

Section 4.3 introduces single-term analytical approximations for both systems having either $f_1(u) = k_\beta \operatorname{sgn}(u)\,|u|^b$ or $f_2(u) = k_\alpha\, u + k_\beta\, u^3$ as the restoring force. Influenced by the sign of k_α and k_β, numerous trial functions $\tilde{u}(t)$ are proposed in 4.3.1 modelling the exact but unknown displacement function $u(t)$ due to $f_2(u)$ with various degrees of accuracy. These solutions are strongly dependent upon the method used for obtaining the free parameters in $\tilde{u}(t)$. Two independent numerical measures are defined, namely the average e_{av} and total e_{tot} error, which make it unnecessary to obtain a purely numerical solution of the governing differential system through direct integration in order to assess the quality of the approximation when any of the new trial functions is used. Section 4.3.2 examines a newly developed procedure of approximating the oscillator's acceleration $\ddot{u}(t)$, rather than its displacement function $u(t)$, born out of the fact that no suitable trial function was found for $u(t)$. Although this does not lead to a closed-form expression for $u(t)$, it is of considerable importance in interpolation of experimentally obtained acceleration data. However, it also makes it necessary to define a new set of error measures denoted as average $e_{\mathrm{av,a}}$ and total $e_{\mathrm{tot,a}}$ acceleration errors for systems where the velocity and displacement are only obtainable by numerical integration of an analytical approximation function.[4]

The error introduced into the differential system, by using an approximation instead of the exact solution, can be significantly reduced if the single-term trial function is replaced by a series of functions. Starting with a variational approach based on the Galerkin method the procedure is outlined in section 4.4. Subsequent modification, which allow for employing the appropriate single-term solution from section 4.3 as a fundamental approximation, makes this new method require far less terms in the approximation series to notably minimise e_{av} and e_{tot} than conventional variational approaches.

Successfully utilising an integral solution method in the form of the previously introduced Picard iteration scheme, a second, and from the variational approach independent, multiple-term approximation procedure is established in 4.4.2 for both nonlinear systems with $f_1(u)$ or $f_2(u)$. Due to the special circumstances of the step excitation, such as single-signed displacement response combined with zero initial conditions, highly accurate analytical solutions can be obtained for $f_1(u)$ type systems if the nonlinearity exponent b belongs to the set of non-zero, non-negative

initial conditions always has nonzero initial acceleration.

[3] The nonlinear restoring force containing the complete third-order polynomial with the displacement as independent variable, e.g. $f_{\mathrm{compl}}(u) = a\,u + b\,u^2 + c\,u^3$, is generally not referred to as Duffing equation.

[4] This should not be confused with direct numerical integration of the governing differential system.

integer numbers. For the Duffing type system, with restoring force $f_2(u)$, the integral equations are even easier to solve. This allows for the derivation of closed-form expressions for the step-excited system having non-zero initial values of displacement and velocity.

4.2 Exact analytical solutions

The first-order Duffing system from section 3.4.2 of the previous chapter can be rewritten as an equivalent second-order equation

$$\ddot{u} + \omega_\alpha^2\, u + \omega_\beta^2\, u^3 = \widehat{p}_0 \tag{4.1a}$$

with the general initial conditions

$$u(t \equiv 0) = u_0\,, \qquad \dot{u}(t \equiv 0) = \dot{u}_0 \equiv v_0\,, \tag{4.1b}$$

and the constant values $\omega_\alpha^2 = k_\alpha/m$, $\omega_\beta^2 = k_\beta/m$, and $\widehat{p}_0 = p_0/m$.

4.2.1 *Zero initial velocity*

An exact analytical solution for the freely vibrating, hardening-type oscillator, i.e. $\widehat{p}_0 \equiv 0$ and $k_\alpha, k_\beta > 0$, subjected to

$$u_0 \neq 0\,, \qquad \text{and} \qquad v_0 = 0\,, \tag{4.2a}$$

was given by Davis [233] assuming a solution in terms of Jacobian elliptic functions[5] [109,288]

$$u(t) = A\,\mathrm{cn}(\omega_\mathrm{J}\, t, \kappa) = A\,\mathrm{cn} \tag{4.2b}$$

where both, the nonlinear oscillation frequency ω_J and the modulus κ are obtained by substituting (4.2b) into (4.1) and equating coefficients of cn and cn^3 equal to zero [295],

$$\omega_\mathrm{J} = \sqrt{\omega_\alpha^2 + \omega_\beta^2\, A^2}\,, \qquad \kappa = \sqrt{\frac{\omega_\beta^2\, A^2}{2\,\omega_\mathrm{J}^2}}\,. \tag{4.2c}$$

Since the system in (4.1) is conservative, all energy input at $t \equiv 0$ due to u_0 remains unchanged and the oscillation amplitude is obtained as $A = u_0$.

Together with the periodicity of the Jacobian cosine function given in [288] as $4\,\mathsf{K}(\kappa)$ the nonlinear oscillation frequency ω_J in rad/s relates to the period T_NL derived in the previous chapter as [298]

$$\omega_\mathrm{J} = \frac{4\mathsf{K}(\kappa)}{T_\mathsf{NL}}\,, \tag{4.3}$$

[5] See also appendix B.3 for more details.

where $\mathsf{K}(\kappa)$ is the complete elliptic integral of the first kind [288], see B.3. In the linear case of system (4.1), i.e. $k_\beta \equiv 0$, Eq.(4.2c) gives for the modulus $\kappa = 0$, thus $\mathsf{K}(0) = \pi/2$, which leads together with $f_{\mathsf{NL}} = 1/T_{\mathsf{NL}}$ for Eq.(4.3) to the well known result for the linear oscillator [228]

$$\omega_{\mathrm{J}} = 2\,\pi\,f_{\mathrm{n}}\,, \qquad \text{and} \qquad u(t) = A\cos\left(\omega_{\mathrm{J}}\,t\right)\,, \tag{4.4}$$

since $\mathrm{cn}(\omega_{\mathrm{J}}\,t, 0) = \cos\left(\omega_{\mathrm{J}}\,t\right)$.

If the softening-type stiffness force in (4.1) with $k_\alpha > 0, k_\beta < 0$ is subjected to identical conditions (4.2), Chen and Cheung [295] suggested a Jacobian sine solution of the form

$$u(t) = A\,\mathrm{sn}(\omega_{\mathrm{J}}\,t, \kappa)\,.$$

Clearly, this solution violates the initial conditions in (4.2a) and is therefore invalid. Contrary to the authors approach it can be shown that the solution of Davis in (4.2b) also holds for the softening Duffing system and the conditions imposed on the solution in [295] are not necessary. Hence, substitution of (4.2b) into (4.1a) yields both oscillation frequency and modulus as given in (4.2c). With $k_\beta = -\,|k_\beta|$ this can be written as

$$\omega_{\mathrm{J}} = \sqrt{\omega_\alpha^2 - \left|\omega_\beta^2\right|\,u_0^2}\,, \qquad \text{and} \qquad \kappa_{\mathrm{c}} = \sqrt{\frac{-\left|\omega_\beta^2\right|\,u_0^2}{2\,\omega_{\mathrm{J}}^2}} = \mathrm{i}\kappa \qquad \kappa_{\mathrm{c}} \in \mathbb{C}\,. \tag{4.5}$$

From equation (3.199a) it follows that the maximum displacement for a stable softening system is

$$u_{\mathsf{Ex}} = \pm\sqrt{\frac{k_\alpha}{|k_\beta|}}\,. \tag{4.6}$$

With $p_0 \equiv 0$ in (4.1) all energy input into the system originates from $u_0 \neq 0$. Hence, for a stable system it is required that $u_0 < u_{\mathsf{Ex}}$. In the limit case of u_0 approaching u_{Ex} from below, both oscillation frequency and elliptic modulus in (4.5) result in

$$\lim_{u_0 \to u_{\mathsf{Ex}}} \omega_{\mathrm{J}} = 0\,, \qquad \lim_{\omega_{\mathrm{J}} \to 0} \kappa_{\mathrm{c}} = \mathrm{i}\,\infty \qquad \text{with} \qquad \mathsf{K}(\mathrm{i}\,\infty) = 0\,, \tag{4.7a}$$

with the oscillation period in (4.3) approaching infinity

$$T_{\mathsf{NL}} = \lim_{\nu \to \omega_\alpha^2} \frac{4\mathsf{K}\left(\sqrt{\frac{-\omega_\alpha^2}{2(\omega_\alpha^2 - \nu)}}\right)}{\sqrt{\omega_\alpha^2 - \nu}} = \infty\,, \qquad \text{where} \qquad 0 \leq \nu \leq \omega_\alpha^2\,, \tag{4.7b}$$

and thus, no oscillation can take place in the now unstable system. It should be noted that ν approaches ω_α^2 from the smaller values since (4.7b) represents a single-sided limit due to a stable-unstable domain transition. Clearly, with equation (4.5) the modulus κ_{c} for the softening system is purely imaginary. Although in general κ_{c} can take any real or complex value, for application to engineering problems its range is usually restricted to $0 \leq \kappa \leq 1$. This is not a necessary condition to be imposed on the solution parameters in (4.3) as suggested by Chen and Cheung [295].

Equation (4.2b) perfectly satisfies the ODE in (4.1) with the initial conditions in (4.2a), despite a complex valued modulus where $\kappa > 0$. However, it is possible to express the complete elliptic integral $\mathsf{K}(\mathrm{i}\kappa)$ with $0 < \kappa < \infty$ in terms of a real-valued modulus using (B.23) in appendix B.3. Therefore, equation (4.3) which denotes the relationship of ω_J with the analytically obtained oscillation period T_{NL} from the previous chapter becomes

$$\omega_\mathrm{J} = \frac{4\,\kappa_1'\mathsf{K}(\kappa_1)}{T_{\mathsf{NL}}}\,. \tag{4.8}$$

In order to use the real-valued modulus κ_1 for the solution of (4.1a) the Jacobian cosine is rewritten referring to $\langle 160.01 \rangle$ in [288] and hence, Eq.(4.2b) transforms into

$$u(t) = A\,\mathrm{cd}\left(\sqrt{1+\kappa^2}\,\omega_\mathrm{J}\,t, \kappa_1\right)\,. \tag{4.9}$$

Finally, the snap-through system with $k_\alpha < 0, k_\beta > 0$ and initial conditions from (4.2a) is considered. The energy function of the two-well potential given in Fig. 3.9(c) clearly indicates the existence of two qualitatively different solutions. Rewriting equation (3.200d), where the system's initial energy is defined in (3.196), leads to the inequality

$$u_0 < \sqrt{\frac{2}{|k_\gamma|}}\,. \tag{4.10}$$

If (4.10) is satisfied the system trajectories are closed periodic orbits around one of the two equilibrium points $\mathbf{u}_{\mathrm{Eq},2,3} = \left\{\pm\sqrt{1/|k_\gamma|}, 0\right\}^\mathrm{T}$ given in (3.183b), depending on whether the initial displacement u_0 is positive or negative. It is therefore sensible to assume a solution similar to [295]

$$u(t) = A\,\mathrm{dn}(\omega_\mathrm{J}\,t, \kappa) \tag{4.11a}$$

where, after substituting (4.11a) into (4.1a) and equating all terms equal to zero, nonlinear oscillation frequency and modulus are obtained as

$$\omega_\mathrm{J} = \sqrt{\frac{1}{2}\omega_\beta^2\,u_0^2}\,, \qquad \kappa = \sqrt{2 - \frac{|\omega_\alpha^2|}{\omega_\mathrm{J}^2}}\,. \tag{4.11b}$$

From $u(t \equiv 0) = A$ it follows $A = u_0$. Clearly, for the limiting case of (4.10). i.e. $u_0 \equiv \sqrt{2/|k_\gamma|}$, the nonlinear frequency and modulus in (4.11b) become $\omega_\mathrm{J} = |\omega_\alpha|$, $\kappa = 1$, respectively, which results for (4.11a) in $u(t) = A\,\mathrm{sech}\,(|\omega_\alpha|\,t)$. A plot of the hyperbolic secant function sech reveals that no oscillation takes place and the system reaches the unstable saddle at $\mathbf{u}_{\mathrm{Eq},1} = \{0,0\}^\mathrm{T}$ in infinite time. The same result can be obtained from section 3.4.2.3, where ${}_{\mathrm{f}_2}T_\delta$ converges to infinity as u_0 approaches $\sqrt{2/|k_\gamma|}$ from the smaller values. If the initial displacement is chosen such that $u_0 \equiv u_{\mathsf{eq}} = \sqrt{1/|k_\gamma|}$, thus it corresponds to one of the systems's equilibrium points $\mathbf{u}_{\mathrm{Eq},2} = \{u_{\mathsf{eq}}, 0\}^\mathrm{T}$ from (3.183b), it was shown in the previous chapter that no oscillation takes place. Indeed, with $u_0 \equiv u_{\mathsf{eq}}$ equation (4.11b) gives for the modulus $\kappa = 0$ and (4.11a) simplifies

to $u(t) = u_0$, hence the system stays at rest. Therefore, if

$$\frac{1}{\sqrt{|k_\gamma|}} < u_0 < \sqrt{\frac{2}{|k_\gamma|}} \qquad \text{it follows that} \qquad 0 < \kappa < 1 \,. \tag{4.12}$$

For $u_0 < 1/\sqrt{k_\gamma}$ the modulus in (4.11b) becomes imaginary and (B.23) can be used to yield the real-valued modulus κ_1. However, this requires (4.11a) to be changed into

$$u(t) = u_0 \,\mathrm{nd}\Big(\sqrt{1+\kappa^2}\,\omega_\mathrm{J}\, t, \kappa_1\Big) \,, \tag{4.13}$$

with the function nd given in appendix B.3. It is worth mentioning that (4.11a) produces the desired solution even if $\kappa \in \mathbb{C}$ but explicit numerical calculation of the Jacobian elliptic function might not be possible with the majority of available algorithms.[6)]

If equation (4.10) for the snap-through system is not satisfied any longer, i.e. $v_0 > \sqrt{2/|k_\gamma|}$, the system's motion describes a closed orbit trajectory in the phase space. By examining Fig. 3.9(c) in chapter 3 one might follow the approach of Chen and Cheung [295] and introduce a Jacobian cosine solution similar to (4.2b) with adjusted parameters according to (4.2c), thus $\omega_\alpha^2 = -|\omega_\alpha^2|$. However, the versatility of Jacobian elliptic functions makes such an approach obsolete. It has been shown in (4.12) above that for $u_0 = \sqrt{2/|k_\gamma|}$ the modulus κ is equal to one. Hence, for $u_0 > \sqrt{2/|k_\gamma|}$ it follows that $\kappa > 1$ and the original solution in (4.11a) with the Jacobian delta function dn transforms into [290]

$$u(t) = u_0 \,\mathrm{cn}(\kappa\,\omega_\mathrm{J}\, t, \kappa_2) \,, \qquad \text{where} \qquad \kappa_2 = \frac{1}{\kappa} \,. \tag{4.14}$$

This is equal to the solution derived by the authors in [295] but has been obtained here by an original algebraic manipulation without employing a new trial function. This simple but elegant transformation is owed to the inherit features of Jacobian elliptic functions.

To summarise, the homogenised ($\widehat{p}_0 \equiv 0$) snap-through system in equation (4.1a) subjected to the initial values in (4.2a) can entirely be described by the single solution given in (4.11a) valid for all values of the modulus $0 \leq \kappa$ and $\kappa \in \mathbb{R}, \mathbb{C}$. Furthermore, the nonlinear frequency equation (4.3) holds for all three system configurations, e.g. stiffening, softening and snap-through springs.

4.2.2 *Zero initial displacement*

It was shown in section 3.3.1 that a classical Dirac-impulse excitation can be applied to the system in (4.1a) via initial conditions, even for the case of strongly nonlinear restoring forces. It can therefore be regarded as important to find solutions for (4.1a) with $\widehat{p}_0 \equiv 0$ subjected to

$$u_0 \equiv 0 \,, \qquad \text{and} \qquad v_0 \neq 0 \,. \tag{4.15}$$

[6)] The problem is discussed in more detail in appendix B.3.

Surprisingly, this problem has so far not received much attention in the literature. Approximate solutions have been given in [105, 107, 139] and closed-from results for coupled systems with complex-valued stiffness are derived in [150, 153]. Unfortunately, none of the solutions are applicable to the above problem of a general Duffing system with its three different types of restoring force.

In searching for a feasible trial function which satisfies the differential equation subjected to the initial values (4.15), the following solution is proposed

$$u(t) = B\ \mathrm{sn}(\omega_{\mathrm{J}}\, t, \kappa) = B\ \mathrm{sn}\,, \tag{4.16a}$$

where sn is the Jacobian sine function. Differentiation with respect to t leads to velocity and acceleration, respectively,

$$\dot{u}(t) = B\,\omega_{\mathrm{J}}\ \mathrm{cn}\,\mathrm{dn}\,, \qquad \ddot{u}(t) = -B\,\omega_{\mathrm{J}}^2\ \mathrm{sn}\left(\kappa^2\,\mathrm{cn}^2 + \mathrm{dn}^2\right)\,. \tag{4.16b}$$

Substitution of both equations (4.16a) and (4.16b) into (4.1a), bearing in mind $\widehat{p}_0 \equiv 0$ and making use of the relations [109]

$$\kappa^2\,\mathrm{sn}^2 + \mathrm{dn}^2 = 1\,, \qquad \mathrm{sn}^2 + \mathrm{cn}^2 = 1\,, \tag{4.17}$$

leads to

$$B\left[\omega_\alpha^2 - \omega_{\mathrm{J}}^2\left(1+\kappa^2\right)\right]\mathrm{sn} + B\left[2\,\omega_{\mathrm{J}}^2\,\kappa^2 + B^2\,\omega_\beta^2\right]\mathrm{sn}^3 = 0\,. \tag{4.18}$$

As shown before, setting the coefficients of sn and sn^3 equal to zero gives the non-trivial solutions for both nonlinear oscillation frequency ω_{J} and modulus κ similar to (4.2c)

$$\omega_{\mathrm{J}} = \sqrt{\omega_\alpha^2 + \frac{B^2}{2}\,\omega_\beta^2}\,, \qquad \kappa = \sqrt{-\,B^2\,\frac{\omega_\beta^2}{2\,\omega_{\mathrm{J}}^2}}\,. \tag{4.19}$$

The constant B depends on the initial velocity condition v_0, according to (4.16b) as $B = v_0/\omega_{\mathrm{J}}$, which gives for ω_{J} a quartic solution reducible to the quadratic form

$$z^2 - \omega_\alpha^2\, z - \omega_\beta^2\,\frac{v_0^2}{2} = 0\,, \qquad \text{using} \qquad z = \omega_{\mathrm{J}}^2\,, \qquad z > 0,\ z \in \mathbb{R}\,. \tag{4.20}$$

For $\left|-\omega_\alpha^2\right|^2/4 \geq \left|\omega_\beta^2\right|\ v_0^2/2$ equation (4.20) has always at least one real solution, thus

$$v_0^2 < \frac{\left|\omega_\alpha^2\right|}{2\ \left|k_\gamma\right|} \tag{4.21}$$

is a stability requirement for the softening system $k_\alpha > 0, k_\beta < 0$, which can also be derived using the energy based approach in (3.199b) with C_1 from (3.196). It is worth pointing out that both equations (4.21) and (3.199b) neither apply to hardening nor to snap-through systems. The

explicit solution to (4.20) is easily obtained from a standard reference [186] as

$$z_{1/2} = \frac{\omega_\alpha^2}{2} \pm \sqrt{\left(\frac{-\omega_\alpha^2}{2}\right)^2 + \omega_\beta^2 \frac{v_0^2}{2}} \quad . \tag{4.22}$$

Discharging z_2 due to the conditions in (4.20) gives for the oscillation period

$$\omega_\mathrm{J} = \sqrt{\frac{\omega_\alpha^2}{2} + \sqrt{\frac{(\omega_\alpha^2)^2}{4} + \omega_\beta^2 \frac{v_0^2}{2}}} \, , \tag{4.23a}$$

and the modulus from (4.19) can be rewritten as

$$\kappa = \sqrt{-\frac{\omega_\beta^2 v_0^2}{2\,\omega_\mathrm{J}^4}} \, . \tag{4.23b}$$

Both ω_J and κ are linked to the results from chapter 3 via (4.3) and Eq.(4.23) apply to all three system parameter configurations, namely $k_\alpha, k_\beta > 0$, $k_\alpha > 0, k_\beta < 0$ and $k_\alpha < 0, k_\beta > 0$ with condition (4.21) for the softening system. However, given the fact that κ is complex for hardening and snap-through systems since $\omega_\beta^2 > 0$, solution (4.16a) can be transformed into

$$u(t) = \frac{v_0}{\omega_\mathrm{J}} \kappa_1' \, \mathrm{sd}\Big(\sqrt{1+\kappa^2}\,\omega_\mathrm{J}\, t, \kappa_1\Big) \tag{4.24}$$

using [288] with κ_1 and κ_1' according to (B.23). The initial conditions given in (4.15), which, as mentioned before, also imply Dirac-impulse excitation, have a rather surprising consequence for the snap-through system. Since C_1 in (3.196) is always greater or equal zero, condition (3.200d) fails and the oscillator responds for all initial and system parameter values with trajectories along the heteroclinic orbit, i.e. around both equilibrium points $\mathbf{u}_{\mathrm{Eq},2/3}$ in (3.183b). Thus, extreme displacement for snap-through systems due to impulse excitation can never be single-sign valued even in the case of small force magnitudes.

4.2.3 General initial conditions

Comparison of the preceding results suggest that, similar to linear oscillating systems, the solution for general nonzero initial conditions can be obtained by an oscillatory elliptic function with a phase offset φ to compensate for the time delay between the initial displacement and velocity contribution to the overall displacement amplitude A. Hence, a feasible trial function for the solution of (4.1a) subjected to the initial conditions $u_0 \neq 0, v_0 \neq 0$ is assumed as

$$u(t) = A \, \mathrm{cn}(\omega_\mathrm{J}\, t - \varphi, \kappa) = A \, \mathrm{cn} \tag{4.25a}$$

and the time derivatives

$$\dot{u} = -\omega_\mathrm{J} A \, \mathrm{dn} \, \mathrm{sn} \, , \qquad \text{and} \qquad \ddot{u} = \omega_\mathrm{J}^2 A\Big(\big(2\kappa^2 - 1\big) \, \mathrm{cn} - 2\kappa^2 \, \mathrm{cn}^3\Big) \, . \tag{4.25b}$$

Substitution of (4.25) into (4.1a) with $\widehat{p}_0 \equiv 0$ and equating all coefficients of cn and cn^3 equal to zero leads for all three cases, i.e. hardening, softening and snap-through stiffness forces, to identical expressions for the oscillation period and modulus as given in (4.2c), leaving only the amplitude A and the phase φ as remaining unknowns. Bearing in mind that for distinctive times

$$t_{\mathsf{min/max}} = n\,\frac{\mathsf{K}(\kappa)}{\omega_{\mathrm{J}}} \qquad \text{with} \qquad n = 1, 2, 3, \ldots \tag{4.26}$$

equation (4.25a) must yield $\pm u_{\mathsf{max}}$ but the elliptic cosine function is bounded for all parameters such that

$$-1 \;\leq\; \mathrm{cn}(\omega_{\mathrm{J}}\, t - \varphi, \kappa) \;\leq\; 1 \qquad \forall \quad \omega_{\mathrm{J}}, t, \varphi, \kappa\,, \tag{4.27}$$

immediately suggests $A \equiv u_{\mathsf{max}}$. However, the exact proof can be given by rewriting equation (4.25a) with $t \equiv 0$,

$$u_0 = A\,\mathrm{cn}(-\varphi, \kappa)\;, \qquad v_0 = -\omega_{\mathrm{J}} A\,\mathrm{dn}(-\varphi, \kappa)\,\mathrm{sn}(-\varphi, \kappa)\;. \tag{4.28a}$$

Using the identities from (4.17) the initial velocity can be expressed as

$$v_0^2 = \frac{A^4\, k_\beta}{2\,\kappa^2\, m}\left\{1 - \kappa^2\left[1 - \mathrm{cn}^2(-\varphi, \kappa)\right]\right\}\left\{1 - \mathrm{cn}^2(-\varphi, \kappa)\right\}\;, \tag{4.28b}$$

where the elliptic function cn is substituted by u_0/A from (4.28a) and (4.28b)

$$\frac{1}{2\,\kappa^2} = \frac{1}{A^2}\left(\frac{1}{k_\gamma} + A^2\right)\;. \tag{4.28c}$$

Finally, together with the result for the modulus from (4.2c) this leads to a quartic equation for the oscillation amplitude

$$A^4 + \frac{2}{k_\gamma}\,A^2 - \frac{4}{k_\beta}\,C_1 = 0\,, \tag{4.28d}$$

with C_1 from (3.196) in chapter 3. Comparison of (4.28d) with equation (3.197a) clearly shows that $A \equiv u_{\mathsf{max}}$ as suggested. Setting $\mathrm{cn}(-\varphi, \kappa) = \mathrm{cn}(\varphi, \kappa)$ the phase φ is obtained from (4.28a)

$$\varphi = \mathrm{arccn}\left(\frac{u_0}{A}, \kappa\right) \tag{4.29}$$

where arccn is the inverse Jacobian elliptic cosine function [288].

For the special case of $u_0 = 0$, $v_0 \neq 0$ from the previous section, (4.29) becomes $\varphi = \mathsf{K}(\kappa)$ and (4.25a) simplifies to [288]

$$u(t) = A\,\mathrm{cn}(\omega_{\mathrm{J}}\, t - \mathsf{K}(\kappa)\,, \kappa) = A\,\mathrm{sn}(\omega_{\mathrm{J}}\, t, \kappa) = A\,\mathrm{sn}\,, \tag{4.30}$$

which is identical to (4.16a). Similar, the initial conditions $u_0 \neq 0$, $v_0 = 0$ imply that $u_{\mathsf{max}} = u_0$

and (4.29) gives $\varphi = \operatorname{arccn}(1, \kappa)$, which can be rewritten using the identity [288]

$$\operatorname{arccn}(y, \kappa) = \operatorname{arcsn}\left(\sqrt{1 - y^2}, \kappa\right) , \tag{4.31}$$

hence, $\varphi = \operatorname{arcsn}(0, \kappa) = \mathsf{F}(\arcsin(0), \kappa) = 0$ and (4.25a) results in $u(t) = A\,\mathrm{cn}(\omega_{\mathrm{J}}\, t, \kappa)$, which is equivalent to Eq.(4.2b) in section 4.2.1. By setting $k_\beta \equiv 0$ in (4.1a) it is clear that equation (4.25a) also accounts for the linear system. With $\omega_{\mathrm{J}} = \omega_\alpha$ and $\kappa = 0$ from (4.2c) the solution above simplifies to

$$u(t) = A_{\mathrm{lin}} \cos\left(\omega_\alpha\, t - \varphi\right) \tag{4.32a}$$

where

$$A_{\mathrm{lin}} = \sqrt{u_0^2 + \frac{v_0^2}{\omega_\alpha^2}} , \qquad \text{and} \qquad \varphi = \arctan\left(\frac{v_0}{u_0\, \omega_\alpha}\right) \tag{4.32b}$$

correspond to the well-know constants of the linear system [228].

4.3 Single-term analytical approximations

Although it is desirable to obtain closed-form solutions for the autonomous system under study, when given in its most general configuration of nonzero initial conditions and constant excitation magnitude $\widehat{p}_0 \neq 0$, there are significant mathematical difficulties to be overcome. When searching for such exact solutions various single-term trial functions were examined, with the aim of determining their unknown coefficients so that the governing differential equation of the nonlinear system is satisfied for all time within the interval $t \in [t_0, t_0 + T_{\mathsf{NL}}]$. For oscillatory systems as (4.1) this leads to nonlinear algebraic transcendental equations and makes it difficult therefore to find explicit solutions. This is especially so if some of the parameters to be determined are only implicitly available, as is the case for the modulus κ in the Jacobian elliptic function. However, it will be shown in what follows that a number of these newly derived trial solutions do approximate the system's nonlinear response behaviour very well despite not satisfying the equation of motion entirely.

The advantage of employing such empirically chosen functions clearly lies in the fact that the process of deriving the analytical approximation does not need any functional analysis framework, other than a simple collocation procedure. Unlike the case of general perturbation methods such as Linstedt-Poincaré or various averaging techniques (KBM), which largely draw their mathematical justification either from series expansion theory or the theory of parameter variation, single-term approximations introduced here merely present a 'natural' approach towards the problem.

4.3.1 $f_2(u) = k_\alpha u + k_\beta u^3$

The phase plane analysis in the previous chapter shows that the step-excited Duffing systems oscillates around the new equilibrium $\mathbf{u}_{\mathrm{Eq},2/3}$ depending on the sign of $\widehat{p}_0$. Hence, for the governing

equation in (4.1a) subjected to zero initial conditions

$$u_0 \equiv 0\,, \qquad \text{and} \qquad v_0 \equiv 0 \tag{4.33a}$$

a trial solution of the type

$$u(t) = A\ \mathrm{dn}(\omega_{\mathrm{J}}\, t - \varphi, \kappa) - B = A\ \mathrm{dn} - B \tag{4.33b}$$

is proposed. The term dn refers to the Jacobian delta function, see appendix B.3, and A, B are unknown constants to be determined together with the oscillation frequency ω_{J}, the phase φ and the elliptic modulus κ. The time derivative of (4.33b) yields

$$\dot{u}(t) = -A\,\omega_{\mathrm{J}}\kappa^2\,\mathrm{cn}\,\mathrm{sn}\,, \qquad \text{and} \qquad \ddot{u}(t) = A\,\omega_{\mathrm{J}}^2\kappa^2\,\mathrm{dn}\left(\mathrm{sn}^2 - \mathrm{cn}^2\right)\,, \tag{4.33c}$$

then substituting into (4.1a) and using the identities in (4.17) gives

$$\left(\omega_\beta^2\,A^2 - 2\,\omega_{\mathrm{J}}^2\right) A\,\mathrm{dn}^3 - 3\,\omega_\beta^2 A^2 B\,\mathrm{dn}^2 + \left(\omega_\alpha^2 - \omega_{\mathrm{J}}^2\left(2-\kappa^2\right) + 3\,\omega_\beta^2\,B^2\right) A\,\mathrm{dn} - \omega_\alpha^2\,B - \omega_\beta^2\,B^3 = \widehat{p}_0\,. \tag{4.34}$$

It is clear to see that utilising the previous method of equating all factors of the elliptic function in (4.34) separately to zero does not lead to the desired solution. Therefore, (4.33b) must be regarded as an approximation, not as an exact solution of the problem in (4.1a). The quality of the approximation can be significantly influenced by the way all unknown constants in (4.33b) are obtained. Two different approaches will be proposed in what follows. The first is rather simple and results are good, but problems arise for certain ranges of parameters, especially in case of low nonlinear stiffness ratios $k_\gamma = k_\beta/k_\alpha$ and small loading magnitudes p_0. Obtaining all constants of (4.33b) using the second method is more involved but the results presented are much less in error and there is no limitation on the range of the parameters involved.

Method 1. Comparison of (4.34) with (4.1a) at some time t when $\mathrm{dn} = 0$, due to quasi-static loading[7] for example, shows that

$$B \equiv u_{\mathsf{eq}} \tag{4.35}$$

with u_{eq} as the new oscillation equilibrium from (3.185). Given the condition of zero initial velocity, i.e. $\dot{u}\,(t=0) = \dot{u}_0 = 0$, equation (4.33c) becomes in the non-trivial case of A, ω_{J}, $\kappa \neq 0$

[7] The results derived in this chapter are only valid for steady-state system response. For conservative, externally excited systems this is equal to the response observed at a finite time point when the transient influence of cross-modulation between oscillator and applied force can be neglected. In the most general case, such as quasi-static loading processes, this time point lies at infinity. It is therefore a fundamental requirement for a valid steady-state response solution to comply with these time-domain "boundary" conditions of the system. Furthermore, the Jacobian delta function only reaches zero for $\kappa > 1$. Indeed, using [288] $\mathrm{dn}(\omega_{\mathrm{J}}\, t, \kappa) = \mathrm{cn}(\kappa\omega_{\mathrm{J}}\, t, \kappa_1)$ where $\kappa > 1$ and $\kappa_1 = 1/\kappa$, it follows that $\mathrm{cn}(\omega_{\mathrm{J}}\, t, 1) \equiv \mathrm{sech}\,(\omega_{\mathrm{J}}\, t)$, which becomes equal to zero for $\omega_{\mathrm{J}}\, t \to \infty$, and thus no oscillation takes places.

equivalent to

$$\mathrm{cn}(-\varphi,\kappa)\,\mathrm{sn}(-\varphi,\kappa)=0\,, \tag{4.36a}$$

where φ is satisfying either

$$\varphi=\begin{cases}\varphi_c=j_c\mathsf{K}(\kappa) & j_c=1,3,5,\ldots \;\rightarrow\; \mathrm{cn}=0\,, \quad \text{or}\\ \varphi_s=j_s\mathsf{K}(\kappa) & j_s=0,2,4,\ldots \;\rightarrow\; \mathrm{sn}=0\,.\end{cases} \tag{4.36b}$$

It it easy to see that for $\varphi=\varphi_s$ together with (4.33b) the relation between the two constants A and B would yield

$$A=-B\,, \tag{4.36c}$$

which produces an unfeasible solution, since the maximum oscillation amplitude of (4.33b) remains smaller than predicted in [270], i.e. $|u_{\mathsf{eq}}|<u_{\mathsf{max}}$. Therefore,

$$\varphi=\varphi_c=\mathsf{K}(\kappa)\;, \tag{4.37a}$$

and the constant A equates to

$$A=u_{\mathsf{max}}+u_{\mathsf{eq}}\,, \tag{4.37b}$$

giving for the time-varying displacement $u(t)$ at values of $\omega_{\mathrm{J}}\,t=2j\mathsf{K}(\kappa)$ for the argument of equation (4.33b) with $j=1,3,5,\ldots$ a maximum oscillation amplitude of u_{max} which is identical to results in [270]. The modulus κ is obtained from the initial condition for the displacement $u_0=0$ from (4.33b), leading together with $\mathrm{dn}(-\mathsf{K}(\kappa)\,,\kappa)=\sqrt{1-\kappa^2}$, see [109] for example, to

$$0=A\sqrt{1-\kappa^2}-B\;, \qquad \text{and thus} \qquad \kappa=\sqrt{1-\left(\frac{u_{\mathsf{eq}}}{u_{\mathsf{max}}+u_{\mathsf{eq}}}\right)^2}\,. \tag{4.37c}$$

The nonlinear oscillation frequency ω_{J} can be derived from the approximated governing equation (4.34) by setting $t\equiv 2j\,\mathsf{K}(\kappa)\,/\omega_{\mathrm{J}}$ with $j=0,1,2,\ldots$, thus

$$\mathrm{dn}(2j\,\mathsf{K}(\kappa)-\mathsf{K}(\kappa)\,,\kappa)=\sqrt{1-\kappa^2} \tag{4.38a}$$

and

$$\omega_{\mathrm{J}}=\sqrt{\frac{Q_1}{Q_2}} \tag{4.38b}$$

as a closed-form explicit expression, where

$$Q_1 = \widehat{p}_0 + \omega_\alpha^2 B + \omega_\beta^2 B^3 - \omega_\beta^2 A^3 q_1^3 + 3\,\omega_\beta^2 A^2 B\, q_1 - \left(\omega_\alpha^2 A + 3\,\omega_\beta^2 A\, B^2\right)\sqrt{q_1}$$
$$Q_2 = A\Big(\left(2-\kappa^2\right)\sqrt{q_1} - 2\,q_1^3\Big) \tag{4.38c}$$

with $q_1 = \left(1-\kappa^2\right)$. Alternatively, ω_J is related to the nonlinear oscillation period from the previous chapter as

$$\omega_\mathrm{J} = \frac{2\,\mathsf{K}(\kappa)}{T_\mathsf{NL}}\ . \tag{4.39}$$

This establishes all constants introduced with the trial solution (4.33b). The difference between (4.39) and (4.3) by a factor 2 originates from the double-periodicity of the delta function dn compared to either Jacobian sine sn or cosine cn functions.

The main problem for the only modest approximation, when using the suggested method, lies with the poor modelling performance of higher order derivatives of the displacement, especially acceleration. Substitution of $t \equiv T_\mathsf{NL}/2 = \mathsf{K}(\kappa)\,/\omega_\mathrm{J}$ into (4.33c) should yield the maximum acceleration $\ddot{u}_\mathsf{max}$ according to (3.222). However, (4.33c) above gives instead

$$\ddot{\widehat{u}}_\mathsf{max} = -\,A\,\omega_\mathrm{J}^2\left(1-\frac{B}{A}\right) = -\,u_\mathsf{max}\,\omega_\mathrm{J}^2 \tag{4.40a}$$

where ω_J^2 must hold for the initial acceleration condition $\ddot{u}(t\equiv 0) = \ddot{u}_0 = \widehat{p}_0$ obtained from the equation of motion (4.1), thus

$$\ddot{\widehat{u}}_0 = A\,\kappa^2\omega_\mathrm{J}^2\sqrt{1-\kappa^2} \tag{4.40b}$$

Supposing (4.33b) identically satisfies (4.1a), thus (4.33c) is the exact acceleration solution for the system, $\ddot{\widehat{u}}_0$ would be equal to $\widehat{p}_0$. Despite this not being the case, and therefore $\ddot{\widehat{u}}_0 \neq \widehat{p}_0$ and $\ddot{\widehat{u}}_\mathsf{max} \neq \ddot{u}_\mathsf{max}$, equation (4.40) can be rearranged to yield

$$\ddot{\widehat{u}}_\mathsf{max} = -\,\ddot{\widehat{u}}_0\left(\frac{u_\mathsf{max}}{u_\mathsf{eq}}+1\right)\ . \tag{4.40c}$$

It is important to notice that u_max can at most be twice as large as u_eq, since both are obtained from nearly identical equations, (3.216) and (3.184a), respectively, hence

$$\begin{aligned} k_\beta\,u^3 + 2\,k_\alpha\,u - 4\,p_0\,u = 0 \quad &\rightarrow \quad u_\mathsf{max}\,, \\ k_\beta\,u^3 + k_\alpha\,u - p_0\,u = 0 \quad &\rightarrow \quad u_\mathsf{eq}\,, \end{aligned} \tag{4.40d}$$

and the maximum displacement becomes $u_\mathsf{max} = 2\,u_\mathsf{eq}$ if $k_\beta \equiv 0$, which is the well-known result for a step-excited linear system [299]. If $k_\beta \neq 0$ the maximum displacement will be in the range

$$u_\mathsf{eq} \leq u_\mathsf{max} < 2\,u_\mathsf{eq}\,, \tag{4.40e}$$

and therefore, from (4.40c) it follows

$$2\,\ddot{\widehat{u}}_0 \leq \ddot{\widehat{u}}_{\max} < 3\,\ddot{\widehat{u}}_0\,, \tag{4.40f}$$

which is only feasible for selected parameter ranges. It is for these ranges where approximation (4.33b) yields the least errors if used in conjunction with method 1. The fact that (4.40f) is not uniquely satisfied for any combination of $\omega_\alpha^2, \omega_\beta^2$ and $\widehat{p}_0$ is easily verified by solving the nonlinear system numerically using direct integration. However, the method given above is applicable to all three types of Duffing systems without restrictions.

Method 2. The rather poor representation of higher-order derivatives of the displacement function using the previous method results in unacceptably large errors for considerable parameter ranges, as will be seen in a subsequent error analysis in the next section. The main objective of the second method is therefore to adjust all free variables of the trial solution (4.33) in such a way that initial or minimum/maximum conditions of velocity and acceleration approximation are equally satisfied.

Instead of obtaining the constant B by comparison of the governing equation (4.1) with the approximation in (4.34), both constants A and B are derived using initial and maximum value considerations of the expected solution. However, the phase φ must satisfy the same conditions as given in (4.36b). Thus, considering $\dot{u}(t \equiv 0)$ in (4.33c) it follows that $\varphi = \mathsf{K}(\kappa)$ analogous to the previous result. At $t = T_{\mathsf{NL}}/2$, where $T_{\mathsf{NL}} = 2\,\mathsf{K}(\kappa)\,/\omega_{\mathrm{J}}$ according to (4.39) holds, the approximation in (4.33b) must yield the maximum displacement $u_{\max}$ from section 3.4.2.3, hence

$$u_{\max} = A - B\,. \tag{4.41a}$$

With the initial condition $u_0 \equiv 0$ and the identity for the Jacobian delta function in cases of odd multiples of the argument $\mathsf{K}(\kappa)$ from (4.37c), equation (4.33b) gives

$$0 = A\,\mathrm{dn}(-\mathsf{K}(\kappa)\,,\kappa) - B = A\sqrt{1-\kappa^2} - B\,. \tag{4.41b}$$

Both equations lead to

$$A = -\,\frac{u_{\max}}{\sqrt{1-\kappa^2}-1} \tag{4.41c}$$

where the modulus κ is still unknown. With the initial acceleration $\ddot{u}(t \equiv 0) = \ddot{u}_0 \equiv \widehat{p}_0$ readily available from the equation of motion (4.1a) if subjected to the assumed initial conditions in (4.33a), the second time-derivative of the approximation (4.33c) must satisfy

$$\ddot{u}_0 = A\omega_{\mathrm{J}}^2\kappa^2\sqrt{1-\kappa^2}\,. \tag{4.42}$$

It should be noted that all conditions of the second method derived so far are valid for all three Duffing-type oscillators. Now, for adjusting the approximation in (4.33b) to maximum acceleration values the following two cases must be distinguished simply due to the condition of (3.206) which

originates from (3.60). For hardening-type stiffness terms, the first case considered here, extreme displacement values u_{Ex} always coincide with extreme values for the restoring force in the system as can be seen in figure 3.2. Thus, extreme displacement and extreme acceleration are given at multiples of half of the nonlinear oscillation period and (4.33c) is rewritten

$$\ddot{u}_{\mathsf{max}} = \ddot{u}\left(t \equiv T_{\mathsf{NL}}/2\right) = -A\omega_{\mathsf{J}}^2\kappa^2 \qquad \text{where} \qquad \frac{T_{\mathsf{NL}}}{2} = \frac{\mathsf{K}(\kappa)}{\omega_{\mathsf{J}}} \tag{4.43a}$$

according to (4.39), giving together with (4.41c) an implicit equation for the modulus κ

$$0 = \frac{-4\,u_{\mathsf{max}}}{\sqrt{1-\kappa^2}-1}\left(\frac{\mathsf{K}(\kappa)}{T_{\mathsf{NL}}}\,\kappa\right)^2 + \ddot{u}_{\mathsf{max}}\,, \tag{4.43b}$$

which can be solved for κ numerically using commonly available root finding algorithms [159, 289,294]. This allows for calculating all unknown terms A, B and ω_{J} in (4.33) by using (4.41c), (4.41a) and (4.39), respectively.

In the second case of a softening system $\omega_\alpha^2 > 0, \omega_\beta^2 < 0$ and snap-through $\omega_\alpha^2 < 0, \omega_\beta^2 > 0$ the restoring force maximum displacement and extreme acceleration do not necessarily coincide, depending on the specific parameter values for ω_α^2, ω_β^2 and $\widehat{p}_0$. In general, maximum acceleration occurs at u_{a} derived in (3.60), which simplifies for the Duffing oscillator to (3.206). Using the displacement function (4.33b) this is written as

$$u_{\mathsf{a}} \equiv u\left(t = t_{\mathsf{a}}\right) = A\,\mathrm{dn}(\omega_{\mathsf{J}}\,t_{\mathsf{a}} - \mathsf{K}(\kappa)\,,\kappa) - B\,, \tag{4.44a}$$

and can be transformed into

$$t_{\mathsf{a}} = \frac{1}{\omega_{\mathsf{J}}}\left[\mathrm{arcdn}\left(\frac{u_{\mathsf{max}}+B}{A},\kappa\right) + \mathsf{K}(\kappa)\right], \tag{4.44b}$$

where arcdn is the inverse Jacobian delta function, see appendix B.3, in order to obtain t_{a} after making use of (4.39), (4.41c), (4.41a) and (4.42) for calculating ω_{J}, A, B and κ, respectively. Equation (4.44b) is then used for (4.33c) leading to the approximation for $\ddot{u}_{\mathsf{max}}$

$$\ddot{u}_{\mathsf{max}} = A\,\omega_{\mathsf{J}}^2\kappa^2\,\mathrm{dn}(\omega_{\mathsf{J}}\,t_{\mathsf{a}} - \mathsf{K}(\kappa)\,,\kappa)\left[\mathrm{sn}^2(\omega_{\mathsf{J}}\,t_{\mathsf{a}} - \mathsf{K}(\kappa)\,,\kappa) - \mathrm{cn}^2(\omega_{\mathsf{J}}\,t_{\mathsf{a}} - \mathsf{K}(\kappa)\,,\kappa)\right], \tag{4.44c}$$

which represents at the same time an implicit equation for the modulus κ in order to let (4.33c) yield $\ddot{u}_{\mathsf{max}}$ at $t = t_{\mathsf{a}}$ rather than $\ddot{u}_0$ at $t = 0$. Note that apart from κ all constants in (4.44c) are known from (4.41c), (4.39) and (4.44b), respectively. In the special case of $u_{\mathsf{a}} = u_{\mathsf{Ex}}$, hence $t_{\mathsf{a}} \equiv T_{\mathsf{NL}}/2$, (4.44b) above is redundant and the modulus κ is either obtained by equating (4.33c) using $\ddot{u}_0$ and therefore employing (4.42), or to the maximum acceleration $\ddot{u}_{\mathsf{max}}$ by solving (4.43b), whichever minimises the approximation error which will be introduced below.

A final note on establishing all constants for the hardening type system must be made. It might seem unnecessary to use (4.39) for deriving the nonlinear oscillation frequency ω_{J} since the same

can be achieved by employing the condition for the initial acceleration value $\ddot{u}_0 \equiv \widehat{p}_0$ after the modulus κ has been obtained from (4.43b). However, due to the fact that equation (4.33b) is only an approximation of an unknown exact solution for (4.1a) the choice of all free parameters in the trial function heavily influences the approximation error and its distribution over one oscillation period. In the case of determining ω_J by using the *exact* result for the oscillation period T_{NL} obtained in the previous chapter this error is minimized.

4.3.1.1 Error estimation

Due to the fact that the approximations for displacement, velocity and acceleration in equation (4.33) do not completely satisfy the governing differential equation (4.1a) for all $t \in [0, \infty]$, a small error will remain. Fortunately, by simple analysis it has been shown [270] that this error stays bounded for all parameters in (4.1a). If the trial function in (4.33) would be the exact solution of the problem, the following must hold for all time t

$$R(t,u) = \widehat{m}\,\ddot{u}(t) + \widehat{k_\alpha}\,u(t) + \widehat{k_\beta}\,u^3(t) - 1 = 0 \qquad \forall \quad t\,, \tag{4.45}$$

where $\widehat{m} = m/p$, $\widehat{k_\alpha} = k_\alpha/p$, $\widehat{k_\beta} = k_\beta/p$ represent normalisation with respect to the excitation force magnitude p. However, since (4.33b) does not render (4.1a) equal to zero, substitution of (4.33) into (4.45) leaves a time-dependent residual function $R(t,u) \neq 0$. The stability analysis in the previous chapter showed that the step-excited Duffing system oscillates between $[0, \pm u_{max}]$, where the sign of the maximum displacement depends on the sign of p_0. Thus, for a constant force the displacement response is always *single-signed*, either positive or negative for all t. This allows for at least two possible definitions for an error measure of the residue $R(t,u) \neq 0$ due to the approximating function (4.33b).

First, the *mean or averaged error* e_{av} is defined by integrating $R(t,u)$ over one period of oscillation

$$e_{av} = \frac{1}{T}\int_t R(t,u)\,\mathrm{d}t = \frac{1}{T}\left(\widehat{m}\,\dot{u}(t)\Big|_0^T + \widehat{k_\alpha}\int_0^T u(t)\,\mathrm{d}t + \widehat{k_\beta}\int_0^T u^3(t)\,\mathrm{d}t - T \right). \tag{4.46}$$

and normalised by the nonlinear oscillation period $T \equiv T_{NL}$. Bearing in mind that the velocity of the system is periodic within the interval $[-\dot{u}_{max}, \dot{u}_{max}]$ it is easy to see that the term involving $\dot{u}(t)$ on the right-hand side of (4.46) will vanish completely and hence, the average error is solely given in terms of displacement. This makes (4.46) a very suitable indicator for evaluating the quality of approximation for the displacement of the system (4.1a) without having to know first and higher-order derivatives. However, it must be noted that e_{av} leads to useful results only if

$$u(t) \geq 0 \qquad \text{or} \qquad u(t) \leq 0\,, \qquad \text{thus} \qquad \operatorname{sgn}(u(t)) = \texttt{const} \qquad \forall\, t\,. \tag{4.47}$$

A second way of evaluating the overall approximation quality of equation (4.1) can be defined as

the *mean total error* given by

$$e_{\mathsf{tot}} = \frac{1}{T}\int_0^T \sqrt{[R(t,u)]^2}\,\mathrm{d}t = \frac{1}{T}\int_0^T |R(t,u)|\,\mathrm{d}t\,, \qquad T \equiv T_{\mathsf{NL}}\,, \tag{4.48}$$

and takes into account all three dynamic quantities, namely displacement, velocity and acceleration by transforming negative values into positive (square) and re-scaling them to the original force level (square-root). Hence, (4.48) is a much tighter error measurement than (4.46) since no averaging-out of positive and negative values for the velocity takes place. Equation (4.48) is valid for all values of $u(t)$, $\dot{u}(t)$ and $\ddot{u}(t)$, i.e. none of the system's response functions needs to satisfy a condition similar to (4.47). However, no information is given by e_{tot} on how the error is distributed between all three quantities within the approximate system. It becomes immediately clear that the main advantage of both definitions lies in the fact that no direct numerical integration solution of the nonlinear governing differential equation needs to be established in order to evaluate the quality of approximation for functions such as (4.33). It is therefore possible to assess any of the trial functions employed with respect to its suitability for modelling (4.1), subjected to the initial conditions in (4.33a), by two easily obtainable numerical values.

Together with (4.33) the individual terms of the right-hand side in (4.46) can be rewritten as

$$u(t)\Big|_0^T = -A\kappa^2\omega_{\mathsf{J}}\,\mathrm{sn}\,\mathrm{cn}\,, \tag{4.49a}$$

$$\int_0^T u(t)\,\mathrm{d}t = \frac{A}{\omega_{\mathsf{J}}}\left(\mathrm{am} - \mathrm{am}_{\mathsf{K}}\right) - BT\,, \tag{4.49b}$$

$$\begin{aligned}\int_0^T u^3(t)\,\mathrm{d}t = \frac{1}{2\omega_{\mathsf{J}}\sqrt{1-\kappa^2\,\mathrm{sn}^2}}\Big[\Big\{&A^3\kappa^2\,\mathrm{sn}\,\mathrm{cn} + 6\,A^2B\,\mathsf{E}\left(\mathrm{am}_{\mathsf{K}},\kappa\right) - 2\,B^3T\,\omega_{\mathsf{J}} \\ &+ \left(6\,AB^2 - A^3\left(\kappa^2-2\right)\right)\mathrm{am} + \left(A^3\left(\kappa^2-2\right) - 6\,AB^2\right)\mathrm{am}_{\mathsf{K}}\Big\} \\ &\sqrt{1-\kappa^2\,\mathrm{sn}^2} - 6\,A^2B\,\mathsf{E}\left(\mathrm{am},\kappa\right)\mathrm{dn}\Big]\,,\end{aligned} \tag{4.49c}$$

where $\mathsf{E}\left(\ldots,\kappa\right)$ is the elliptic integral of the second kind and sn, cn, am are the Jacobian sine, cosine and amplitude functions, respectively, with the following arguments

$$\mathrm{sn} = \mathrm{sn}\left(T\omega_{\mathsf{J}} - \mathsf{K}(\kappa)\,,\kappa\right)\,, \qquad \mathrm{cn} = \mathrm{cn}\left(T\omega_{\mathsf{J}} - \mathsf{K}(\kappa)\,,\kappa\right)\,, \tag{4.49d}$$

$$\mathrm{am} = \mathrm{am}\left(T\omega_{\mathsf{J}} - \mathsf{K}(\kappa)\,,\kappa\right)\,, \qquad \mathrm{am}_{\mathsf{K}} = \mathrm{am}\left(-\mathsf{K}(\kappa)\,,\kappa\right)\,. \tag{4.49e}$$

Together with the nonlinear oscillation frequency ω_{J} given in (4.39) where $T_{\mathsf{NL}} \equiv T$ and the modulus obtained either from equation (4.37c), (4.42), or (4.43b), the elliptic sine and cosine in (4.49d) simplify to

$$\mathrm{sn} = \mathrm{sn}\left(3\mathsf{K}(\kappa)\,,\kappa\right) = -1\,, \qquad \text{and} \qquad \mathrm{cn} = \mathrm{cn}\left(3\mathsf{K}(\kappa)\,,\kappa\right) = 0\,. \tag{4.49f}$$

Using the fact that the amplitude function $\mathrm{am}(\ldots,\kappa)$ is defined as the inverse of the elliptic integral of the first kind [291]

$$\mathsf{F}(\phi,\kappa) = \int_0^{\phi} \frac{\mathrm{d}\theta}{\sqrt{1-\kappa^2\sin^2\theta}} \qquad \longleftrightarrow \qquad \mathrm{am}(\mathsf{F}(\sin\phi,\kappa)\,,\kappa) = \phi \tag{4.49g}$$

together with the definition of the sn and cn functions [288]

$$\mathrm{sn}(z,\kappa) = \sin\left(\mathrm{am}(z,\kappa)\right)\,, \qquad \mathrm{cn}(z,\kappa) = \cos\left(\mathrm{am}(z,\kappa)\right)\,, \tag{4.49h}$$

gives for (4.49e) the special values of

$$\mathrm{am}(3\mathsf{K}(\kappa)\,,\kappa) = \frac{3\pi}{2}\,, \qquad \mathrm{am}(-\mathsf{K}(\kappa)\,,\kappa) = -\frac{\pi}{2}\,. \tag{4.49i}$$

This simplifies equations (4.49a) to (4.49c) considerably yielding

$$\dot{u}(t)\Big|_0^T = 0\,, \tag{4.50a}$$

$$\int_0^T u(t)\,\mathrm{d}t = T\left(\frac{A\,\pi}{2\mathsf{K}(\kappa)} - B\right)\,, \tag{4.50b}$$

$$\int_0^T u^3(t)\,\mathrm{d}t = \frac{-T}{4\mathsf{K}(\kappa)}\left(4\mathsf{K}(\kappa)\,B^3 + 12\,A^2\mathsf{E}(\kappa)\,B + A\,\pi\left(A^2\left(\kappa^2-2\right) - 6\,B^2\right)\right)\,. \tag{4.50c}$$

The average error e_{av} of the approximation during one cycle of oscillation is now given by substituting all terms of (4.50) back into (4.46). Unfortunately, for the more complex equation (4.48) of the total error e_{tot} no closed-form expression can be found if the approximation function in (4.33b) is used. Thus, (4.48) must be solved numerically.

Results - hardening-type system. Results of the above analysis using the single-term approximation from (4.33) for a hardening-type spring are shown in Figs. 4.1 to 4.4. Both, average and total error are given in percent depending on the step excitation magnitude $\hat{p}$ and the nonlinear stiffness ratio k_γ. Four different linear stiffness coefficients $k_\alpha = m\,(2\pi f_n)^2$ were selected with $f_n = 0.5\,\mathsf{Hz}$, $5\,\mathsf{Hz}$, $50\,\mathsf{Hz}$, and $500\,\mathsf{Hz}$, respectively, and a constant mass of $m = 0.3\,\mathsf{kg}$. Average and total error in both figures 4.1 and 4.2 have been obtained using the simpler parameter approximation method 1 for the trial solution (4.33) whereas Figs. 4.3 and 4.4 were derived by employing the more accurate second method.

For the first method the average error e_{av} in Fig. 4.1 as a sole indicator of the displacement approximation quality over one oscillation period yields for only very few combinations of $\hat{p}$ and k_γ values of more than 5 %. An even smaller region in 4.1(a) shows average errors of up to 20 %, which is clearly caused by small loading magnitudes in conjunction with low nonlinear stiffness ratios for equivalent linear frequencies of $f_n = 0.5\,\mathsf{Hz}$ and $f_n = 5\,\mathsf{Hz}$, see both graphs in (a) and (b). Beyond ranges of $0 < p \leq 20\,\mathsf{N}$ and $0 \leq k_\gamma \leq 15$ in Fig. 4.1(a) the average error decreases

rapidly below 2 % in a strong monotonic fashion approaching zero for large loading levels and highly nonlinear stiffness ratios. Similarly for Fig. 4.1(b) with an equivalent linear frequency of $f_n = 5$ Hz. For higher values of f_n, Fig. 4.1(c) and (d), e_{av} is more equally spread over the entire range of $p_0 - k_\gamma$ values and converges more slowly towards zero, but never exceeding in both cases the relatively small values of 0.55 % and 0.055 %, respectively, even in 'problematic' regions where $p_0 \approx 0$, $k_\gamma \approx 0$.[8)] Virtually identical behaviour is observed for the total error of the hardening-type spring in Fig. 4.2. Due to the definition of e_{tot} in equation (4.48) levels are generally higher than for e_{av}, since averaging-out of positive and negative values for the velocity does not occur. The four plots in Fig. 4.2 give an estimate of how well all three dynamic quantities of the system, e.g. displacement, velocity and acceleration are approximated by the trial solution in (4.33) using method 1 to obtain all unknown parameters. High total error levels of up to 20% are limited to narrow pockets of small loading magnitudes and stiffness ratios similar to the results for the average error e_{av} in Fig. 4.1. Comparison of figure 4.1 with 4.3 and figure 4.2 with 4.4, respectively, clearly shows the higher overall accuracy of approximation when obtaining the trial function (4.33b) parameters using method 2. For both e_{av} and e_{tot} values in Fig. 4.3 and 4.4 are only fractions of those obtained by employing the first method shown in Fig. 4.1 and 4.2.

Despite the fact that the trial function in (4.33) is valid for all three types of Duffing restoring forces as defined in (3.180), approximation of softening and snap-through type oscillators yields unacceptable large error levels for both e_{av} and e_{tot} compared to the results of Figs. 4.1 to 4.4, especially for low to moderate nonlinear stiffness ratios $0 < k_\gamma \leq 30$ and small excitation magnitudes in case of equivalent linear frequency systems with $f_n = 0.5$ Hz and 5 Hz. For higher f_n this behaviour is less pronounced and both error measures e_{av} and e_{tot} reach similar levels as presented above, especially for large values of k_γ and p_0.

4.3.1.2 Softening restoring force

Method 1 - Far from instability regions. Significant improvement to the shortcoming of the trial function in (4.33b) for small values of load magnitude p_0 and nonlinear stiffness ratio k_γ in case of softening-type systems ($k_\alpha > 0, k_\beta < 0$) can be made by introducing a second approximation of the form

$$u(t) = A\Big[1 - \frac{1}{2}\left(\mathrm{cn}^2(\omega_J\, t, \kappa) + \mathrm{sn}^2(\omega_J\, t - \varphi, \kappa)\right)\Big] = A\Big[1 - \frac{1}{2}\left(\mathrm{cn}^2 + \mathrm{sn}_\varphi^2\right)\Big] \tag{4.51a}$$

with the time derivatives

$$\dot{u}(t) = A\omega_J\left(\mathrm{sn}\,\mathrm{cn}\,\mathrm{dn} - \mathrm{sn}_\varphi\,\mathrm{cn}_\varphi\,\mathrm{dn}_\varphi\right) \tag{4.51b}$$

$$\ddot{u}(t) = A\omega_J^2\Big(\left(\mathrm{dn}^2 - \kappa^2\,\mathrm{sn}^2\right)\mathrm{cn}^2 - \mathrm{cn}_\varphi^2\,\mathrm{dn}_\varphi^2 - \mathrm{sn}^2\,\mathrm{dn}^2 + \left(\kappa^2\,\mathrm{cn}_\varphi^2 + \mathrm{dn}_\varphi^2\right)\mathrm{sn}_\varphi^2\Big) \tag{4.51c}$$

[8)] It should be noted that there is no linear relationship between values selected for f_n and the resulting error e_{av}. The fact that the maximum values for the average error relate to each other by the same factor of 10 as the linear equivalent frequencies has been achieved by selecting appropriate ranges of both independent quantities p_0 and k_γ.

and abbreviations are as follows

$$\mathrm{pq} = \mathrm{pq}\,(\omega_\mathrm{J}\, t, \kappa)\ , \qquad \mathrm{pq}_\varphi = \mathrm{pq}\,(\omega_\mathrm{J}\, t - \varphi, \kappa)\ , \tag{4.52}$$

and pq stands for any of the Jacobian elliptic functions in (4.51), see also appendix B.3. Applying the above approximation is especially advantageous for softening-spring type Duffing oscillators, since their load level is restricted due to stability criterions presented in the previous chapter and combinations of moderate to high nonlinearity ($k_\gamma > 10$) but small magnitudes p_0, for which (4.33) is not very efficient, are more likely to occur in practice. However, (4.51) holds also perfectly true for hardening-type springs, especially in cases where results obtained with (4.33) lead to unacceptably high values for e_{av} or e_{tot}.

The elliptic sine function $\mathrm{sn}(0,\kappa) = 0$ together with both the zero initial displacement and velocity $u_0 \equiv 0$ and $\dot{u}_0 \equiv 0$, respectively, makes it possible to obtain two solutions for the phase lag φ from equation (4.51b)

$$0 = \mathrm{sn}_\varphi\, \mathrm{cn}_\varphi\, \mathrm{dn}_\varphi\ , \tag{4.53}$$

which are identical to (4.36b). Hence, $\varphi = \mathsf{K}(\kappa)$ and the trial function in (4.51) can together with (B.24) be simplified to

$$u(t) = A\Big[1 - \frac{1}{2}\left(\mathrm{cn}^2 + \mathrm{cd}^2\right)\Big] \tag{4.54a}$$

$$\dot{u}(t) = \frac{A\,\omega_\mathrm{J}}{\mathrm{dn}^3}\left(\mathrm{dn}^4 - \kappa^2 + 1\right)\,\mathrm{sn}\,\mathrm{cn} \tag{4.54b}$$

$$\ddot{u}(t) = \frac{A\,\omega_\mathrm{J}^2}{\mathrm{dn}^4}\Big[\left(1 - \kappa^2 + \mathrm{dn}^4\right)\mathrm{cn}^2\,\mathrm{dn}^2 - \Big\{\left(1 - \kappa^2 + \mathrm{dn}^4\right)\mathrm{dn}^2 + \left(3\kappa^2 - 3 + \mathrm{dn}^4\right)\kappa^2\,\mathrm{cn}^2\Big\}\,\mathrm{sn}^2\Big]\ . \tag{4.54c}$$

With

$$\Big[1 - \frac{1}{2}\left(\mathrm{cn}^2 + \mathrm{cd}^2\right)\Big] = 1 \qquad \text{at times} \qquad t \equiv \frac{T_{\mathsf{NL}}}{2} = \frac{j\,\mathsf{K}(\kappa)}{\omega_\mathrm{J}}\ , \qquad j = 1,3,5,\ldots \tag{4.55a}$$

the constant A is determined from (4.54a)

$$A = u_{\mathsf{max}}\ . \tag{4.55b}$$

As mentioned before, the point of maximum acceleration for the softening stiffness system does not in general coincide with u_{max} at $t = T_{\mathsf{NL}}/2$. Analogous to (4.44) the time where $\ddot{u}_{\mathsf{max}}$ occurs is designated t_a and (4.54a) is written as

$$u_\mathsf{a} = A\Big[1 - \frac{1}{2}\left(\mathrm{cn}^2(\omega_\mathrm{J}\, t_\mathsf{a}, \kappa) + \mathrm{cd}^2(\omega_\mathrm{J}\, t_\mathsf{a}, \kappa)\right)\Big]\ , \tag{4.56a}$$

thus

$$0 = 2\left(1 - \frac{u_{\mathsf{a}}}{A}\right) - \mathrm{cn}^2(\omega_{\mathrm{J}}\, t_{\mathsf{a}}, \kappa) - \mathrm{cd}^2(\omega_{\mathrm{J}}\, t_{\mathsf{a}}, \kappa) \tag{4.56b}$$

is an implicit equation for obtaining t_{a} numerically. The modulus κ for (4.56b) is obtained by setting $t \equiv 0$ in (4.54c). Together with $\ddot{u}_0 = \widehat{p}_0$ as the initial value for the acceleration leads to

$$0 = A\left(\frac{2\,\mathsf{K}(\kappa)}{T_{\mathsf{NL}}}\right)^2 \left(\kappa^2 - 2\right) + \widehat{p}_0\,, \tag{4.56c}$$

yielding κ through numerical root-finding. Finally, inserting t_{a} into the acceleration approximation (4.54c) having $\ddot{u}\,(t_{\mathsf{a}}) = \ddot{u}_{\mathsf{max}}$ gives

$$0 = \frac{A\,\omega_{\mathrm{J}}^2}{\mathrm{dn}^4}\left\{\left[\mathrm{dn}^6 - \kappa^2 - \kappa^2\left(\mathrm{dn}^4 + \kappa^2 - 1\right)\mathrm{sn}^2 + 1\right]\mathrm{cn}^2 - \left[\mathrm{dn}^6 + \left(\kappa^2 - 1\right)^2\right]\mathrm{sn}^2\right\} - \ddot{u}_{\mathsf{max}} \tag{4.56d}$$

as a new equation for the modulus κ, where the acceleration trial function (4.54c) is now adjusted to the maximum acceleration value $\ddot{u}_{\mathsf{max}}$ instead of the initial value $\ddot{u}_0 = \widehat{p}_0$ in order to minimise approximation errors. It must be mentioned that for low ratios of $\widehat{p}_0/\ddot{u}_{\mathsf{max}}$, i.e. the maximum acceleration from (3.206) is substantially higher than the initial, steps in equation (4.56b) and (4.56d) must be repeatedly applied in order to yield acceptable error levels. Thus, with the new modulus from (4.56d) a more accurate displacement approximation is obtained, hence a more accurate t_{a} can be calculated from (4.56a) giving in turn a new κ from (4.56d). Obviously, this iterative procedure converges to the exact approximation value defined by the smallest possible error introduced into (4.1) due to the trial function in (4.54)

For the special case of $t_{\mathsf{a}} = T_{\mathsf{NL}}/2$, i.e. extreme acceleration values do coincide with values of extreme displacement at half period, steps (4.56a) to (4.56c) above can be ignored and the modulus κ is directly obtained from (4.54c), which simplifies for $\omega_{\mathrm{J}}\, t = \mathsf{K}(\kappa)$ to

$$\ddot{u}_{\mathsf{max}} = A\,\omega_{\mathrm{J}}^2\left(\kappa^2 - 2\right)\,, \tag{4.57a}$$

thus, giving the implicit equation

$$0 = \left(\frac{2\,\mathsf{K}(\kappa)}{T_{\mathsf{NL}}}\right)^2 \left(\kappa^2 - 2\right) - \frac{\ddot{u}_{\mathsf{max}}}{u_{\mathsf{max}}} \tag{4.57b}$$

from which κ is obtained using previously introduced numerical methods [159, 289].

Substitution of (4.54) into (4.1) and integration over one period leads to

$$\dot{u}(t)\Big|_0^T = 0\,, \tag{4.58a}$$

$$\int_0^T u(t)\,\mathrm{d}t = -\frac{A}{2\kappa^2\omega_\mathrm{J}}\Big[\mathsf{E}(\mathrm{am}(-\mathsf{K}(\kappa)\,,\kappa)) - \mathsf{E}(\mathrm{am}(3\mathsf{K}(\kappa)\,,\kappa)) + \mathsf{E}(\mathrm{am}(4\mathsf{K}(\kappa)\,,\kappa)) - 4\kappa^2\mathsf{K}(\kappa)\Big]\,. \quad (4.58b)$$

Together with the definition for the nonlinear oscillation frequency ω_J in (4.39), the identities in (4.49i) and the relation $\mathrm{am}\,(4\mathsf{K}(\kappa)\,,\kappa) = 2\,\pi$ from [288], the integral of the displacement function in (4.58b) can be reduced to

$$\int_0^T u(t)\,\mathrm{d}t = \frac{1}{2}\,A\,T_\mathsf{NL}\,. \quad (4.58c)$$

Unfortunately, a closed-from solution for the third integral in (4.46) involving $u^3(t)$ cannot be established if the trial function (4.54) is employed and its value must be determined numerically. The average error introduced by the approximation into the system can now be obtained from rewriting (4.46) as

$$e_\mathsf{av} = \frac{1}{T}\left(\frac{1}{2}\,\omega_\alpha^2 A\,T_\mathsf{NL} + \omega_\beta^2 A^3 \int_0^T \Big[1 - \frac{1}{2}\left(\mathrm{cn}^2 + \mathrm{cd}^2\right)\Big]^3\,\mathrm{d}t - T\right)\,, \quad (4.59)$$

with $T \equiv T_\mathsf{NL}$. Finally, the total error e_tot is obtained by substitution of (4.54) into definition (4.48) and subsequent numerical integration.

Using the trial function in (4.51) for a softening-type Duffing stiffness both approximation error measures e_av and e_tot are given in percent in Figs. 4.5 and 4.6. Due to stability restrictions only specific combinations of step force magnitudes p_0 and stiffness ratios k_γ are feasible. Selection of non-feasible parameter values immediately leads to an unstable system. Similar to the results for hardening-type oscillators presented above, the approximation errors for the entire range of selected values for p_0 and k_γ decrease significantly with larger values for the linear stiffness coefficient k_α, which is obtained by setting $k_\alpha = (2\pi f_\mathrm{n})^2\,m$ and successively increasing f_n from 0.5 Hz to 500 Hz using the factor of 10 for graphs (a)-(d) of both figures. However, contrary to Figs. 4.1 and 4.2 larger values for e_av and e_tot occur now for moderate values of p_0 and k_γ, which in the case of softening systems coincide with regions close to unstable solutions.

A very similar outcome has been observed when applying (4.33) to hardening-type oscillators, thus improving solutions for method 1 pictured in figure 4.1 and 4.2 significantly, but omitted here for the sake of clarity. Nonetheless, it follows from these results and the results for the softening system presented above that the purpose of introducing (4.51) for modelling specific areas where the approximation in (4.33) failed to give acceptable results has been achieved. For combinations of small loading and low to moderate stiffness ratios both errors e_av and e_tot stay significantly below values obtained with the trial function (4.33), due to differences in the shape of the two approximation solutions (4.33) and (4.54) respectively. However, results obtained from (4.54) for the hardening-type system fail to reach similarly low error levels realised with the sec-

ond method of the previous section shown in Fig. 4.3 and 4.4.

Method 1 - Close to instability regions. It becomes apparent from both figures Figs. 4.5 and 4.6 that results for the softening oscillator having parameters which render the system close to instability are far from satisfactory. This is especially striking if compared to the acceptable results for the hardening system in Figs. 4.3 and 4.4. Remedies for the softening system, such as to adopt the trial function (4.33b) when p_0 and k_γ are far from highly erroneous regions, i.e. from parameter ranges just before the systems becomes unstable, do work but lack the required efficiency.

A closer look at the causes leading to unacceptable values for e_{av} and e_{tot} suggest a fundamental qualitative shape change in the system's response functions for displacement, velocity and acceleration if stiffness and load parameters originate from the yellow and red coloured regions of Figs. 4.5 and 4.6. These areas have a feature in common, namely that extreme values for displacement and acceleration do not occur at the same time $t = T_{\mathsf{NL}}/2$. Thus, due to the limited ability of the displacement trial function (4.54a) to model the shape of the exact solution accurately enough, calculation of t_{a} to the required precision fails despite the capability of the iterative procedure in (4.56). The only successful route lies in establishing a new trial function. Fortunately, the above approximation in (4.54) proves very versatile and a change of power for the Jacobian cosine delivers a substantially less error-laden response approximation, which is *only* effective for the softening system sufficiently close to instability. Whether this criterion is fulfilled for the oscillator in (4.1) is easily *a priori* verified using (3.219) derived in the previous chapter. The term 'sufficiently close' stands for an estimated relative difference margin of up to 10 % for both k_γ and p_0 as obtained from (3.219).

The modified trial function is given as

$$u(t) = A\Big[1 - \frac{1}{2}\left(\mathrm{cn}^4 + \mathrm{cd}^2\right)\Big] \tag{4.60a}$$

$$\dot{u}(t) = \frac{A\,\omega_{\mathsf{J}}}{\mathrm{dn}^3}\left(2\,\mathrm{dn}^4\,\mathrm{cn}^2 - \kappa^2 + 1\right)\,\mathrm{sn}\,\mathrm{cn} \tag{4.60b}$$

$$\begin{aligned}\ddot{u}(t) = A\,\omega_{\mathsf{J}}^2\Big\{&2\left(\mathrm{dn}^2 - \kappa^2\,\mathrm{sn}^2\right)\mathrm{cn}^4 - 6\,\mathrm{dn}^2\,\mathrm{sn}^2\,\mathrm{cn}^2 \\ &- \frac{1}{\mathrm{dn}^4}\Big[\left(\kappa^2 - 1\right)\mathrm{cn}^2 + \left(\kappa^2\,\mathrm{cn}^2 + \kappa^2 - 1\right)\mathrm{sn}^2\Big]\Big\}\end{aligned} \tag{4.60c}$$

with $A \equiv u_{\mathsf{max}}$, t_{a}, u_{a} and κ analogous to equation (4.55) and the iteration scheme in (4.56), respectively. Results for the above solution have not been plotted here explicitly, but it can be stated that both average and total error are well below the levels shown in Figs. 4.5 and 4.6 for the narrow 10 %-band close to unfeasible combinations of p_0 and k_γ.

Method 2 - Generalised solution. Both approximation (4.54) and (4.60) produce reasonable results if all involved parameter are not only within their required limits, but well away from any overlapping areas where either (4.54) or (4.60) could be used. Since it is impossible to give a clear definition of such a boundary in terms of p_0 and k_γ values for these two regions other than by calculating the approximation errors e_{av} and e_{tot} using both formulas simultaneously, it

is desirable to have a single solution for the softening system which can be applied to all feasible combinations of load magnitude and stiffness ratio. Such a general solution is presented in the following paragraph.

In order to prevent above mentioned approximation errors arising from explicitly calculating the time t_a, only the terms $u\,(t = T_{NL}/2) = u_{max}$, $\ddot{u}(t \equiv 0) = \ddot{u}_0$ and $\ddot{u}\,(T_{NL}/2) = \ddot{u}_{max}$ are considered. Thus, with three known constants the same number of unknown parameters can be included in a feasible trial function obeying the initial conditions in (4.33a), which effectively are boundary conditions since $u\,(t_0) = u_0 = u\,(t_0 + T_{NL})$ and $\dot{u}\,(t_0) = \dot{u}_0 = \dot{u}\,(t_0 + T_{NL})$.

The newly proposed approximation is given as

$$u(t) = A\,(1 - \mathrm{dn}^{\nu}(\omega_J\, t, \kappa)) = A\,(1 - \mathrm{dn}^{\nu}) \qquad \nu \in \mathbb{R} \tag{4.61a}$$

where A, ν, ω_J and κ are unknown constants to be determined. Together with its time derivatives

$$\dot{u}(t) = A\,\nu\,\kappa^2\omega_J\,\mathrm{sn}\,\mathrm{cn}\,\mathrm{dn}^{\nu-1} \tag{4.61b}$$

$$\ddot{u}(t) = A\,\nu\,\kappa^2\omega_J^2\,\mathrm{dn}^{\nu-2}\Big[\mathrm{cn}^2\,\mathrm{dn}^2 - \left((\nu-1)\,\kappa^2\,\mathrm{cn}^2 + \mathrm{dn}^2\right)\mathrm{sn}^2\Big] \tag{4.61c}$$

the test function (4.61a) can be inserted back into the governing equation (4.1) yielding

$$\begin{aligned} &A\,\nu\,\omega_J^2\left(\nu + \kappa^2\,(1-\nu) - 1\right)\mathrm{dn}^{\nu-2} + A\left(\nu^2\omega_J^2\left(\kappa^2 - 2\right) - \omega_\alpha^2 - 3\,\omega_\beta^2 A^2\right)\mathrm{dn}^{\nu} \\ &\quad + 3\,A^3\omega_\beta^2\,\mathrm{dn}^{2\nu} - A^3\omega_\beta^2\,\mathrm{dn}^{3\nu} + A\,\nu\,\omega_J^2\,(\nu+1)\,\mathrm{dn}^{\nu+2} + A\,\omega_\alpha^2 + A^3\omega_\beta^2 = p_0\,. \end{aligned} \tag{4.62}$$

It is not possible to select an appropriate ν such that the system of equations originating from the requirement that all coefficients of the Jacobian delta function dn with its various exponents in (4.62) must be equal to zero for all time t. For example, if $\nu = 1$ Eq.(4.62) results in

$$q_0 + q_1\,\mathrm{dn} + q_2\,\mathrm{dn}^2 + q_3\,\mathrm{dn}^3 = 0 \tag{4.63}$$

where $q_0 = -p_0 + A\,\omega_\alpha^2 + A^3\omega_\beta^2$, $q_1 = A\left(\omega_J^2\left(\kappa^2 - 2\right) - \omega_\alpha^2 - 3\,A^2\omega_\beta^2\right)$, $q_2 = 3\,A^3\omega_\beta^2$ and $q_4 = A\left(2\omega_J^2 - A^2\omega_\beta^2\right)$. It is easily verified that the system $q_j \equiv 0$ with $j = 1, \ldots, 4$, has no solution. Since from (4.62) it follows that this is true for any $\nu \in \mathbb{R}$, the trial function in (4.61) is only an approximation and not the exact solution of (4.1a). Employing the three known expressions for displacement and acceleration, namely $u_{max} = u\,(t = T_{NL}/2)$, $\ddot{u}_0 = \ddot{u}(t = 0)$ and $\ddot{u}_{max} = \ddot{u}\,(t = T_{NL}/2)$ as introduced above, the following algebraic system is obtained

$$u_{max} = A\left(1 - \left(1 - \kappa^2\right)^{\frac{\nu}{2}}\right) \tag{4.64a}$$

$$\ddot{u}_0 = A\,\nu\,\kappa^2\omega_J^2 \tag{4.64b}$$

$$\ddot{u}_{max} = -\,A\,\nu\,\kappa^2\omega_J^2\left(1 - \kappa^2\right)^{\frac{\nu}{2}}\,. \tag{4.64c}$$

Re-arranging (4.64a) and insertion into (4.64c) immediately leads to an expression for the dis-

placement oscillation amplitude

$$A = \frac{u_{\max}}{1 + \frac{\ddot{u}_{\max}}{\ddot{u}_0}} \,. \tag{4.65a}$$

With

$$\nu = \frac{\ddot{u}_0}{A\,\kappa^2 \left(\frac{2\,K(\kappa)}{T_{\mathrm{NL}}}\right)^2} \tag{4.65b}$$

equation (4.64a) becomes an implicit expression for the modulus

$$0 = A\left\{1 - \left(1-\kappa^2\right)^{\frac{\ddot{u}_0}{2A\kappa^2\left[\frac{2\,K(\kappa)}{T_{\mathrm{NL}}}\right]^2}}\right\} - u_{\max} \tag{4.65c}$$

where κ must be obtained iteratively. It is important to note that for vast ranges of feasible parameter combinations f_{n}, k_γ and $\widehat{p}_0$ the modulus in (4.65c) will be complex-valued, i.e. $\kappa \equiv \kappa_{\mathrm{C}} \in \mathbb{C}$ with $\kappa_{\mathrm{C}} = \kappa_{\mathrm{R}} + \mathrm{i}\,\kappa_{\mathrm{I}}$ and $\kappa_{\mathrm{R}}, \kappa_{\mathrm{I}} \in \mathbb{R}$, see appendix B.3. This in turn implies for the nonlinear oscillation frequency $\omega_{\mathrm{J}} \in \mathbb{C}$ since the complete elliptic integral in (4.39) is complex as shown in Fig. B.1. Moreover, with a complex exponent ν due to (4.65b), the displacement response becomes $u(t) \in \mathbb{C}$ for all t. In this general case only $\Re\{u(t)\}$ is selected since $\Im\{u(t)\}$ does not contain any valuable information regarding the system's response behaviour. Only if κ possess a zero real part, i.e. $\kappa_{\mathrm{C}} = \mathrm{i}\,\kappa$, equation (4.61) can be rewritten [109] as

$$u(t) = A\left(1 - \mathrm{nd}\left(\sqrt{1+\kappa^2}\,\omega_{\mathrm{J}}\,t, \kappa_1\right)\right) \qquad \text{with} \qquad \kappa_1 = \frac{\kappa}{\sqrt{1+\kappa^2}}\,, \tag{4.66}$$

and nd as the inverse elliptic delta function, which is real-valued in the entire interval of one cycle $t \in [t_0, t_0 + T_{\mathrm{NL}}]$.

Unfortunately, neither of the measures defined in (4.46) and (4.48) describing the error of the approximation (4.61a) can be given in closed-form. Both have to be calculated using numerical integration procedures and are shown in Fig. 4.7 and 4.8 for the same range of system parameters previously selected for method 1 above. The results clearly underline the improved performance of the trial function (4.61) compared to (4.54) which is shown in Fig. 4.5 and 4.6. With the average and total error of the second method being fractions of the values obtained from method 1, it is clear that the trial function in (4.61) has a significantly higher approximation accuracy then (4.54).

In order to get a better understanding of what certain values of the measures e_{av} and e_{tot} imply for the approximation quality of all three response functions, namely displacement, velocity and acceleration, time histories have been calculated using the previously defined trial functions along with numerical exact solutions from high-order Runge-Kutta algorithms. Figure 4.9 shows results for hardening and softening spring types employing method 1 in both cases with specially selected parameter combinations of p_0 and k_γ such that average and total error are large. With $f_{\mathrm{n}} \equiv 0.5\,\mathrm{Hz}$ method 1 for hardening Duffing oscillators fails for small values of force and stiff-

ness ratio, hence $p_0 = 0.1\,\mathsf{N}$ and $k_\gamma = 3\,\mathsf{m}^2$ were chosen. Resulting error values are $e_{\mathsf{av}} = 15.7\%$ and $e_{\mathsf{tot}} = 24.9\%$. For the softening stiffness system $p_0 = 0.2\,\mathsf{N}$ and $k_\gamma = -16\,\mathsf{m}^2$ were selected presenting a set of parameter close to instability. Results are $e_{\mathsf{av}} = 14.5\%$ and $e_{\mathsf{tot}} = 35.8\%$. It is interesting to note that despite such rather high errors the approximation of $u(t)$ in Fig. 4.9(a) can still be termed satisfactory, compared with various results in literature for equivalent systems [191,203]. However, the plots for velocity and acceleration clearly indicate the shortcomings of the trial functions to accurately model the higher-order derivatives.

Application of method 2 to both hardening and softening Duffing systems produces a maximum average error of 0.0098% shown in Fig. 4.7(a) and a total error of 0.11% pictured in 4.8(a). A comparison with numerical results for such a softening system having $p_0 = 0.2\,\mathsf{N}$ and $k_\gamma = -16\,\mathsf{m}^2$ is displayed in figure 4.10(a) for displacement, velocity and acceleration. The time-varying approximation residue $R(t)$ defined in (4.45) which forms the basis for obtaining e_{av} and e_{tot} is given in Fig. 4.10(b) below. It becomes clear that simple integration of $R(t)$ leads to a net area for the average error significantly smaller than the one which is obtained from integrating $\sqrt{R^2(t)}$ for the total error.

At this point it is necessary to make an important comment on the symbolic-numerical implementation of both approximations in (4.33b) and (4.61). Apart from not being able to handle complex values for the argument $\omega_{\mathsf{J}}\, t$ or the modulus κ of elliptic integrals or Jacobian functions, the limited number of significant digits in the numerical software package MATLAB® makes it impossible to derive previously pictured error levels e_{av}, e_{tot} as small as $10^{-12}\%$ shown in Fig. 4.7 for example.[9] It requires the combined symbolic-numerical high-accuracy calculation environment of MATHEMATICA® or MAPLE®[10] with an adjustable, problem-specific working precision[11] to obtain these results.

4.3.1.3 Snap-through stiffness force

It has previously been suggested [270] to use

$$u(t) = A\ \mathrm{cn}^{\nu}(\omega_{\mathsf{J}}\, t - \varphi, \kappa)\ , \qquad \text{with} \qquad \nu \in \mathbb{R} \tag{4.67a}$$

as a trial function for snap-through-type Duffing systems where $k_\alpha < 0$ and $k_\beta > 0$. The unknown constants A and φ are easily derived using the initial values from (4.33a) as u_{max} and $\mathsf{K}(\kappa)$,

[9] Although the smallest positive floating-point number in MATLAB® is two bits less than 2^{-1024} (one bit is needed for the 2 and the second one for the sign), i.e. $2^{-1022} \approx 2.2251\,\mathsf{E}-308$, it is the limited ability in representing adjacent double-precision values. For MATLAB® this value can be determined using the function `eps(x)` and ranges on a standard 32-bit system (normal PC or PC cluster) between -15 to -16 decimal points of x.

[10] Various test runs clearly showed large differences in the computational time between both programs required for obtaining results of equal precision. On average, MATHEMATICA® was five to seven times faster than MAPLE® and has therefore been chosen for application to the problem.

[11] For the numerical solution of the implicit modulus functions the working precision was set to 30 giving about 25 significant digits. For the integration of both error functions e_{av} and e_{tot} working precision was 25 and therefore about ten significant digits higher then in an equivalent MATLAB® routine.

respectively. Together with the derivatives for velocity and acceleration

$$\dot{u}(t) = -A\,\nu\,\omega_{\mathrm{J}}\,\mathrm{cn}^{\nu-1}\,\mathrm{sn}\,\mathrm{dn} \tag{4.67b}$$

$$\ddot{u}(t) = A\,\nu\,\omega_{\mathrm{J}}^2\,\mathrm{cn}^{\nu-2}\Big[\left(\kappa^2\,\mathrm{sn}^2 - \mathrm{dn}^2\right)\mathrm{cn}^2 + (\nu-1)\,\mathrm{sn}^2\,\mathrm{dn}^2\Big] \tag{4.67c}$$

the following algebraic expressions are given for $t_0 \equiv 0$

$$u\,(t_0) = 0\,, \quad \dot{u}\,(t_0) = 0^{\nu-1} A\,\nu\,\omega_{\mathrm{J}}\sqrt{1-\kappa^2}\,, \quad \ddot{u}\,(t_0) = -0^{\nu-2} A\,\nu\,\omega_{\mathrm{J}}^2\,(\nu-1)\left(\kappa^2-1\right). \tag{4.68a}$$

Similar, if $t_1 \equiv T_{\mathsf{NL}}/2$

$$u\,(t_1) = A\,, \quad \dot{u}\,(t_1) = 0\,, \quad \ddot{u}\,(t_1) = -A\,\nu\,\omega_{\mathrm{J}}^2\,. \tag{4.68b}$$

In order for the trial function (4.67a) to adhere to the initial conditions in (4.33a) the real exponent must be $\nu > 1$ so that $\dot{u}\,(t_0) = \dot{u}_0$. Moreover, to yield a stable solution for $t \in [t_0,\, T_{\mathsf{NL}}]$, the unknown parameter must satisfy $\nu \geq 2$ since $0^{\nu-2} = \infty$ if $\nu < 2$. However, given $\nu \neq 2$ the approximated system will possess zero initial acceleration which contradicts (3.222). This leads to the conclusion that (4.67) with $\nu > 2$ should only be used for snap-through systems with small stiffness, moderate excitation force and large mass values as this will guarantee large ratios of $\ddot{u}_{\mathsf{max}}/\ddot{u}(0)$, i.e. the error introduced by the approximation failing to satisfy the initial acceleration condition (4.68a) is kept to a minimum. Even in the case of $\nu \equiv 2$, results obtained in [270] for low nonlinear stiffness ratios $k_\gamma < -50\,\mathrm{m}^{-2}$ and small loading levels $p_0 < 100\,\mathrm{N}$ show unacceptable error levels of up to 80 % for e_{av} and more than 100 % for e_{tot}. Only for selected parameter ranges of $f_{\mathrm{n}} \equiv 5,\, 50\,\mathrm{Hz}$ and large values for both k_γ and p_0, levels of average and total error approach regions of 1 % and below. This leaves (4.67) as unsuitable for a single-term approximation of snap-through Duffing systems.

Far more accurate results are obtained using equation (4.61) above. All three unknowns A, ν and κ are obtained from the algebraic set (4.64) according to (4.65). Results for average and total error of this approximation, e_{av} and e_{tot}, respectively, are given in Figs. 4.11 and 4.12.

4.3.2 $f_1(u) = k_\beta\,\mathrm{sgn}\,(u)\,|u|^b$

Examining the restoring force characteristic of $f_1(u)$ for various values of b as given in figure 3.2 indicates significant differences in the qualitative response behaviour of the SDOF system depending on whether b belongs to one of the two intervals $b \equiv b_I \in (0,1)$ or $b \equiv b_{II} \in (1,\infty)$, respectively. In the first case, especially for $u(t) > 1$, small changes in applied force magnitudes, assuming zero initial conditions, result in large amplitudes of oscillation. Contrary, the response behaviour is reversed, i.e. large external forces producing only small changes in displacement, if $b \equiv b_{II}$, especially for $u(t) > 1$. It is easy to verify using numerical solution procedures that compared to k_β and m the influence of the parameter b dominates the response characteristics of the displacement, velocity and acceleration, independent of values for p_0. Therefore, unless stated

otherwise, only changes of b are considered in what follows and all obtained results are applicable to the entire range of feasible values for k_β, m and p_0.

4.3.2.1 Acceleration approximation

It proves difficult to find a suitable one-term approximation for systems of the first category with $b \equiv b_I$ making use of Jacobian elliptic functions. Reasonable average and total error levels are possible using the trial function in (4.61) if b stays within the interval $0.8 \leq b < 1$ independent of whether (4.65c) possess multiple real or complex valued roots.[12] However, if $b \ll 1$ equation (4.61) becomes unsuitable as accurate description of the displacement.

It is interesting to note that for such small values of b the acceleration of the nonlinear oscillator can be approximated using the elliptic cosine function

$$\ddot{\tilde{u}}(t) = (\ddot{u}_0 - \ddot{u}_{\max}) \left[1 - \mathrm{cn}^{\nu}(\omega_J\, t - \varphi, \kappa)\right] + \ddot{u}_{\max}\,, \tag{4.69}$$

where ν, ω_J, φ and κ are yet unknown. From initial conditions for the acceleration $\ddot{\tilde{u}}(t \equiv 0) \equiv \ddot{u}_0$ the phase must yield $\varphi = \mathsf{K}(\kappa)$ and according to (B.25) equation (4.69) can be rewritten as

$$\ddot{\tilde{u}}(t) = (\ddot{u}_{\max} - \ddot{u}_0) \left[\sqrt{1-\kappa^2}\,\mathrm{sd}(\omega_J\, t, \kappa)\right]^{\nu} + \ddot{u}_0 = A \left[\sqrt{1-\kappa^2}\,\mathrm{sd}\right]^{\nu} + B\,. \tag{4.70}$$

Clearly, if $t \equiv 0$ Eq.(4.70) results in $\ddot{u}_0$ and for $t \equiv T_{\mathsf{NL}}/2$ it gives $\ddot{u}_{\max}$ thus satisfying the time domain 'boundary' conditions of the half-interval $[t_0, t_0 + T_{\mathsf{NL}}/2]$. All methods previously introduced in this chapter utilise, apart from the acceleration, known values of extreme displacement and velocity to establish the unknown constants given by the trial function. However, finding an analytical solution for velocity and displacement by integrating (4.70) is only possible for integer-valued exponents, i.e. $\nu \in \mathbb{N}$, but numerical trials with various parameter combinations strongly suggest that ν should be real.

Nevertheless, since differentiating (4.70) with respect to time is possible and yields smooth functions,[13] the following approach is suggested. Rather than obtaining ν and κ by comparison of extreme response values with distinctive values of the approximation functions for displacement and velocity, identical orders of derivative of the acceleration in (4.70) and the system's governing differential equation are used instead. Substitution of (3.75) into (3.3) and obeying both initial conditions identical to (4.33a) together with the restriction on the step excitation function $\not{p} > 0$ leads to the simplification

$$\ddot{u}(t) = \widehat{p}_0 - \omega_\beta^2\, u^b(t)\,, \qquad \text{where} \qquad \widehat{p}_0 = \frac{p_0}{m}\,, \omega_\beta^2 = \frac{k_\beta}{m}\,, \quad b > 0\,. \tag{4.71}$$

since $u(t) \geq 0$ for all $t \in [0, T_{\mathsf{NL}}]$. The first derivative of (4.71) with respect to time is readily

[12] Different values for the modulus κ result in a qualitative change of shape of the elliptic function. Hence, for cases of non-unique solutions of the implicit modulus equation it is possible to chose κ such that e_{av} and e_{tot} are global minima.

[13] Continuous and no singularities in the interval under consideration $t \in [0, T_{\mathsf{NL}}]$.

obtained as

$$\frac{\mathrm{d}}{\mathrm{d}t}\,\ddot{u}(t) = \ddot{u}^{(1)} = -\,b\,\omega_\beta^2\,u^{b-1}\dot{u}\,. \tag{4.72a}$$

Subsequently, second, third and fourth derivatives are given as

$$\ddot{u}^{(2)} = -\,b\,\omega_\beta^2\,u^{b-2}\Big[(b-1)\,\dot{u}^2 + u\,\ddot{u}\Big]\,, \tag{4.72b}$$

$$\dddot{u}^{(3)} = -\,b\,\omega_\beta^2\,u^{b-3}\Big[\dddot{u}\,u^2 + (b-1)\,\dot{u}\Big\{(b-2)\,\dot{u}^2 + 3\,u\,\ddot{u}\Big\}\Big]\,, \tag{4.72c}$$

and

$$\begin{aligned}\ddot{u}^{(4)} = b\,\omega_\beta^2\,u^{b-4}\Big[&-u^{(4)}\,u^3 - (b-1)\Big\{(b-3)\,(b-2)\,\dot{u}^4 + 6\,(b-2)\,u\,\dot{u}^2\,\ddot{u} \\ &+ 4u^2\,\dot{u}\,\dddot{u} + 3\,u^2\,\ddot{u}^2\Big\}\Big]\,,\end{aligned} \tag{4.72d}$$

respectively, with $\dddot{u} = \ddot{u}^{(1)}$ and $u^{(4)} = \ddot{u}^{(2)}$. Together with the derivatives of (4.70) given in appendix B.3.3 this leads to four equations which are evaluated at two different time points $t_1 \equiv 0$ and $t_2 \equiv T_{\mathsf{NL}}/2$ ensuring the trial function matches with values for maximum displacement and acceleration. Hence, for $t \equiv t_1$ Eqs.(4.71) and (4.72) result in

$$\lim_{t\to+0}\ddot{u}^{(1)}(t_1) = -\infty \qquad \lim_{t\to+0}\ddot{u}^{(2)}(t_1) = +\infty \tag{4.73a}$$

$$\lim_{t\to+0}\ddot{u}^{(3)}(t_1) = -\infty \qquad \lim_{t\to+0}\ddot{u}^{(4)}(t_1) = +\infty\,. \tag{4.73b}$$

Although both displacement $u(t)$ and velocity $\dot{u}(t)$ approach zero as $t \to +0$, the expression $\dot{u}^{b-i}$ with $i = 1, ..., 4$ and $b < 1$ has a higher rate of convergence, thus approaches zero faster from larger to smaller values of t. Although more difficult to derive, exactly identical results are obtained from the four derivatives in equation (B.28) clearly ensuring that the approximation satisfies the 'boundary conditions' of the time-domain as an essential requisite for error minimisation. At $t \equiv T_{\mathsf{NL}}$ equation (4.72a)-(4.72c) evaluate to

$$\ddot{u}^{(1)}(t_2) = 0\,, \qquad \ddot{u}^{(2)}(t_2) = -\,b\,\omega_\beta^2\,u_{\mathsf{max}}^{b-1}\,\ddot{u}_{\mathsf{max}}\,, \qquad \dddot{u}^{(3)}(t_2) = 0\,, \tag{4.74a}$$

whereas (4.72d) yields

$$\ddot{u}^{(4)}(t_1) = b\,\omega_\beta^2\,u_{\mathsf{max}}^{b-4}\Big[b\,\omega_\beta^2\,u_{\mathsf{max}}^{b+2}\,\ddot{u}_{\mathsf{max}} - 3\,(b-1)\,u_{\mathsf{max}}^2\,\ddot{u}_{\mathsf{max}}^2\Big]\,. \tag{4.74b}$$

Similar results are given for equation (B.28) at t_1

$$\ddot{\tilde{u}}^{(1)} = 0\,, \quad \ddot{\tilde{u}}^{(2)} = -A\,\nu\,\omega_{\mathsf{J}}^2\,, \quad \ddot{\tilde{u}}^{(3)} = 0\,, \quad \ddot{\tilde{u}}^{(4)} = A\,\nu\,\omega_{\mathsf{J}}^4\left(4\kappa^2 + 3\,\nu - 2\right)\,. \tag{4.75}$$

Equating now derivatives of the same order from both (4.74) and (4.75) gives exactly two equations for the two unknown parameters ν and κ, which can be rearranged to yield an implicit expression

for the modulus

$$-G_1\left(\frac{2\mathsf{K}(\kappa)}{T_{\mathsf{NL}}}\right)^2\left[4\,\kappa^2+\frac{3\,G_1}{A\left(\frac{2\mathsf{K}(\kappa)}{T_{\mathsf{NL}}}\right)^2}-2\right]-G_2=0 \tag{4.76a}$$

with

$$G_1=b\,\omega_\beta^2\,u_{\mathsf{max}}^{b-1}\,\ddot{u}_{\mathsf{max}}\,,\quad G_2=b\,\omega_\beta^2\,u_{\mathsf{max}}^{b-4}\left(b\,\omega_\beta^2\,u_{\mathsf{max}}^{b+2}\,\ddot{u}_{\mathsf{max}}-3(b-1)u_{\mathsf{max}}^2\,\ddot{u}_{\mathsf{max}}^2\right), \tag{4.76b}$$

the exponent ν as

$$\nu=\frac{G_1}{A\,\omega_{\mathsf{J}}^2}\,, \tag{4.76c}$$

and the nonlinear oscillation frequency ω_{J} according to (4.39). In general, for small values of ν the modulus obtained from (4.76a) by numerical root-finding is purely imaginary and transforms together with (B.27) into an elliptic sine function

$$\ddot{\tilde{u}}(t)=A\left[\kappa_1'\sqrt{1-\kappa^2}\,\mathrm{sn}\left(\omega_{\mathsf{J}}\,t\sqrt{1+\kappa^2},\kappa_1\right)\right]^\nu+B \tag{4.77}$$

with κ_1 and κ_1' according to (B.23b). Unfortunately, it is not possible to analytically integrate the acceleration approximation (4.70) in order to yield a closed-form solution for velocity and displacement of the nonlinear oscillator in (3.78). However, by ensuring the error introduced into the system due to (4.70) remains at a minimum, time domain results for $\dot{u}(t)$ and $u(t)$ can always be derived using numerical integration similar to the process of analysing experimentally obtained acceleration data.

It is worth mentioning that (4.70) not only holds for $b\in b_I$ but also for values of b significantly larger than one, i.e. $b\in b_{II}$. Errors do not significantly increase for exponent values up to $b\approx 10$. Using the acceleration approximation function in (4.70), both error measures defined in (4.46) and (4.48) would require time history data for velocity and displacement by numerical integration. Although high accuracy is possible by choosing small enough time steps, the approach is prone to introduce further numerical errors which is especially undesirable in connection with such highly sensitive equations as (4.46) and (4.48). It is therefore suggested to adopt two slightly modified versions of e_{av} and e_{tot} defined as *average* and *total acceleration error*

$$e_{\mathsf{av,a}}=\frac{1}{T_{\mathsf{NL}}}\int_{t_0}^{t_0+T_{\mathsf{NL}}}\ddot{u}(t)\,\mathrm{d}t=\dot{u}(t)\Big|_{t_0\equiv 0}^{T_{\mathsf{NL}}}=0\,, \tag{4.78a}$$

$$e_{\mathsf{tot,a}}=\frac{1}{T_{\mathsf{NL}}}\int_{t_0\equiv 0}^{T_{\mathsf{NL}}}|\ddot{u}(t)|\;\mathrm{d}t\neq 0\,, \tag{4.78b}$$

respectively, where for the latter one the finite value of the integral has to be known, from a numerical differential solver algorithm, for example, in order to be able to judge the approximation

Table 4.1 – Modified average and total error $e_{\mathsf{av,a}}$ and $e_{\mathsf{tot,a}}$ as given in equation (4.78) for the acceleration approximation (4.70) in comparison with results from a Runge-Kutta (4,5) embedded pair algorithm analysis. System parameters: $f_{\mathrm{n}} = 5\,\mathrm{Hz}$, $m = 0.3\,\mathrm{kg}$, $\omega_{\mathrm{n}} = 2\pi f_{\mathrm{n}}$, $k_\beta = m\,\omega_{\mathrm{n}}^2$, and $p_0 = 200\,\mathrm{N}$.

b	u_{max} in [m]	T_{NL} in [s]	$e_{\mathsf{av,a}}$	$e_{\mathsf{av,a}}$ (RK)	$e_{\mathsf{tot,a}}$	$e_{\mathsf{tot,a}}$ (RK)
0.05	1.037E−3	2.003E−2	3.69E−2	0.0	5.95E−1	6.30E−1
0.1	5.129E−2	1.008E−1	3.19E−1	0.0	5.89	6.19
0.5	1.027	2.220E−1	8.45E−1	3.27E−15	5.62E+1	5.70E+1
0.95	1.336	2.021E−1	5.47E−1	1.07E−15	8.29E+1	8.29E+1
0.99	1.348	2.004E−1	1.03E−2	1.17E−15	8.45E+1	8.45E+1
1.5	1.418	1.829E−1	1.94E−1	1.01E−16	9.94E+1	9.93E+1
3	1.393	1.600E−1	6.58E−1	1.40E−15	1.18E+2	1.18E+2
10	1.222	1.293E−1	7.02	5.85E−17	1.36E+2	1.37E+2
30	1.107	1.179E−1	8.26	4.41E−12	1.38E+2	1.43E+2

quality. However, with the condition that $e_{\mathsf{av,a}}$ must be equal to zero there is one independent measure given.

Application of (4.78) to (4.70) for various different values of b is given in table 4.1 together with the maximum displacement u_{max}, oscillation period T_{NL} and average and total acceleration errors, $e_{\mathsf{av,a}}$, $e_{\mathsf{tot,a}}$, respectively, from a corresponding numerical integration procedure (Runge-Kutta). Clearly for the interval of $0 < b < 1$, for which equation (4.70) was initially developed, the average error $e_{\mathsf{av,a}}$ stays below one. Although it should be close (or equal) to zero, similar to $e_{\mathsf{av,a}}$ (RK) from the numerical integration, the approximation in case of $e_{\mathsf{av,a}} = 8.45\,\mathrm{E}-1$ originating from $b \equiv 0.5$ is still very accurate, as shown in figure 4.13 for the normalised acceleration $\ddot{u}(t)/\ddot{u}_{\mathsf{max}}$. Moreover, even for $b = 30$ with $e_{\mathsf{av,a}} = 8.26$, a case where the value for the exponent b lies significantly outside the anticipated range, approximation (4.70) follows the exact numerical solution very closely, see Fig. 4.13. The last two columns in Table 4.1 suggest that the total area under both acceleration functions, obtained using either (4.70) or the RK-scheme, are almost equal. Hence, as an additional sign of versatility, the single-term approximation accounts for energy equality with respect to the exact solution.

It is worth noting that the above solution is also applicable if $p < 0$ but all initial values remain zero $u_0 = \dot{u}_0 \equiv 0$. In this case the system (3.78) is simplified analogous to (4.71) yielding

$$\ddot{u}(t) = \omega_\beta^2\, u_+^b(t) - \widehat{p}_{0,+}\,, \qquad \text{where} \qquad \widehat{p}_{0,+} = \frac{|p_0|}{m}\,, \omega_\beta^2 = \frac{k_\beta}{m}\,, \quad b > 0\,, \tag{4.79}$$

and $u_+^b(t) > 0\,\forall\, t$. The actual displacement is obtained from $u(t) = -u_+(t)$, thus $u(t) < 0\,\forall\, t$.

4.3.2.2 Displacement approximation

Cases with practical design relevance show a nonlinearity exponent within the interval $1 < b \leq 10$ is quite common [87]. Thus, with $b \in b_{II}$ the displacement trial function for the nonlinear system in (3.78) is given by (4.61) with the constants according to (4.64) and (4.65). It is interesting to note that a similar approximation

$$u(t) = A\Big[\mathrm{nd}^{\nu}(\omega_{\mathrm{J}}\, t, \kappa) - 1\Big] \qquad \nu \in \mathbb{R}\,, \tag{4.80}$$

involving the inverse Jacobian delta function nd leads to identical results as (4.61). Since now displacement is approximated and closed-form solutions for velocity and acceleration are easily obtainable by differentiation, see (4.61b)-(4.61c), error measures as defined in (4.47) and (4.48) can be employed without the threat of introducing further numerical uncertainties. With the residue $R(t,u)$ as the time-varying function

$$R(t,u) = \widehat{m}\,\ddot{u}(t) + \widehat{k_\beta}\,\mathrm{sgn}(u(t))\,|u(t)|^b - 1 \tag{4.81}$$

and $\widehat{m} = m/p_0$, $\widehat{k_\beta} = k_\beta/p_0$ the average error according to (4.46) is given as

$$e_{\mathsf{av}} = \widehat{k_\beta} \int_{t_0\equiv 0}^{T_{\mathsf{NL}}} \mathrm{sgn}(u)\,|u|^b\,\mathrm{d}t\,, \tag{4.82a}$$

which can be simplified due to $u(t) > 0\,\forall\, t \in [t_0, T_{\mathsf{NL}}]$

$$e_{\mathsf{av}} = A\,\widehat{k_\beta} \int_{t_0\equiv 0}^{T_{\mathsf{NL}}} (1 - \mathrm{dn}^{\nu})^b\,\mathrm{d}t\,. \tag{4.82b}$$

Similarly, e_{tot} is obtained using (4.48) together with $R(t,u)$ from (4.81). Contrary to equation (4.49) in the previous section, it is now impossible to give a closed-form solution of e_{av} in case of the trial function (4.61) since no analytic integral can be found for an arbitrary exponent $\nu \in \mathbb{R}$. Therefore, employing simple numerical integration results for e_{av} and e_{tot} are given in Table 4.2 for various different values of the governing equation exponent b.

Table 4.2 suggest that if b stays within the interval $0.5 \leq b \leq 3$ the average and total error approach levels similar to the ones obtained in section 4.3.1.2 by employing the same trial function (4.61), thus the quality of approximation for the nonlinear oscillator with $f_1(u)$ as restoring force is equal to results shown in figure 4.10 for the softening Duffing system. In case of $b < 0.6$ or $b > 8$, both e_{av} and e_{tot} increase significantly and well beyond acceptable levels. Similar unsatisfactory values are shown in Figs. 4.5, 4.6, which have been obtained with the trial functions in (4.51) and (4.60). Both are partially unappropriate for certain parameter combinations of p_0 and k_γ, and time-history results for high levels of errors are given in figure 4.9. However, a direct comparison of Figs. 4.9 and 4.14 shows that despite the total error as an quality indicator of the overall approximation being four times larger for the $f_1(u)$ system in the marginal case of $b \equiv 8$,

Table 4.2 – Restoring force $f_1(u)$: Average e_{av} and total e_{tot} error from (4.82) for the displacement approximation using the trial function in (4.61). System parameter values: $f_n = 0.5$ Hz, $m = 0.3$ kg, $\omega_n = 2\pi f_n$, $k_\beta = m\,\omega_n^2$, and $p_0 = 0.1$ N.

b	u_{max} in [m]	$\frac{u_{max}}{u_{eq}}$	T_{NL} in [s]	κ	ν	e_{av} in [%]	e_{tot} in [%]
0.6	7.724 E−3	2.189	0.804	−i 5.203	3.063 E−1	7.991 E−1	2.654
0.8	3.019 E−2	2.085	1.436	−i 2.303	1.311	4.941 E−1	1.711
1.2	1.146 E−1	1.929	2.469	0.9343−i 0.4964	−i 3.069 E−1	3.464 E−1	1.298
2.5	4.257 E−1	1.651	4.007	i 2.623	8.878 E−1	3.075 E−1	1.411
4	6.411 E−1	1.495	4.564	i 9.779	6.066 E−1	2.018	1.293 E+1
5	7.267 E−1	0.508	4.729	i 1.931 E+1	5.433 E−1	5.181	3.686 E+1
8	8.617 E−1	1.316	4.931	i 1.138 E+2	4.392 E−1	1.461 E+1	1.359 E+2

e.g. $e_{tot} = 35.8\%$ versus $e_{tot} = 135.9\%$, the trial solution (4.61) follows the exact numerical one very well compared to the clearly unacceptable results in 4.9(b)-(c) for the higher-order derivatives, i.e. velocity and acceleration. This is entirely due to the fact that approximation method 1 for hardening systems, see section 4.3.1, and Eqs.(4.54), and (4.60) for softening systems is largely unsuitable for modelling displacement derivatives given the chosen parameter combination of Fig. 4.9. This inability, of course, was the motivation for including figure 4.9 in the first place. Contrary, with the trial function in (4.61) errors are equally distributed between displacement and its derivatives.

4.4 Multiple-term analytical approximations

Although the single-term trial functions in (4.33b) and (4.61) prove very versatile, i.e. they can be used for various systems with entirely different nonlinear restoring forces and at the same time deliver highly accurate approximations of the exact solution, there are further possibilities to significantly enhance these results. Using equation (4.61) as a basis, the next section 4.4.1 introduces a variational method for defining the unknown exact solution as a weighted sum of basic approximation solutions. By adding one pair of newly derived, modified trial functions from (4.61) the average and total error can be noticeably reduced. However, an entirely different approach leading to equally high-accuracy results is given in section 4.4.2, employing Picard's analytical approximation method introduced in the previous chapter.

4.4.1 Variational methods

Using the method of Galerkin [300] an approximation $\widetilde{u}(t)$ of the exact displacement solution $u(t)$ is assumed

$$u(t) \approx \widetilde{u}(t) = \psi_0(t) + \sum_{i=1}^{N} c_i\,\psi_i(t) \tag{4.83}$$

where $\psi_i(t)$ with $i = 0, 1, 2, ..., N$ are known trial functions and c_i are yet unknown constants, such that the weighted integral

$$\int_T w(t)\, R(t, \widetilde{u}, \ddot{\widetilde{u}})\, \mathrm{d}t = 0\,, \qquad R(t, \widetilde{u}, \ddot{\widetilde{u}}) = \widehat{m}\, \ddot{\widetilde{u}} + \widehat{f}(\widetilde{u}) - 1 \tag{4.84}$$

of the second-order system (3.3) becomes equal to zero in the domain T between the two prescribed boundaries $[t_0, t_0 + T_{\mathsf{NL}}]$. Force-normalised mass and stiffness are given as $\widehat{m} = m/p_0$ and $\widehat{f}(u) = f(u)/p_0$, respectively. All functions $\psi_i(t)$ with $i = 1, 2, ..., N$ have to satisfy the homogeneous boundary conditions in T, whereas $\psi_0(t)$ is required to fulfil specified (or prescribed) conditions at the interval borders t_0 and $t_0 + T_{\mathsf{NL}}$. With the Bubnov-Galerkin method, usually only referred to as Galerkin method,[14] the weighting function $w(t)$ in (4.84) is equal to the set of trial functions $\psi_i(t)$ with $i = 1, 2, ..., N$, leading to N integral equations of the form (4.84) for exactly N unknown weighting coefficients c_i

$$\int_{t_0}^{t_0+T_{\mathsf{NL}}} \psi_i(t) R(t, \widetilde{u}, \ddot{\widetilde{u}})\, \mathrm{d}t = 0 \qquad i = 1, 2, \ldots, N\,. \tag{4.85}$$

where the acceleration approximation function is given as

$$\ddot{\widetilde{u}} = \frac{\mathrm{d}^2\widetilde{u}}{\mathrm{d}t^2} = \ddot{\psi}_0(t) + \sum_{i=1}^{N} c_i\, \ddot{\psi}_i(t)\,. \tag{4.86}$$

Both the quality of approximation and the fact that $\widetilde{u}$ approaches the exact solution $u(t)$ as $N \to \infty$ depend on various different conditions [95–97]

(i) *Continuity:* Each $\psi_i(t)$ with $i = 0, 1, 2, ..., N$ must be n-times differentiable for all time t within the interval $(t_0, t_0 + T_{\mathsf{NL}})$, where n is the order of the governing differential equation.

(ii) *Boundary conditions:* Each $\psi_i(t)$ with $i \geq 1$ must satisfy the homogeneous form of all specified boundary conditions, whereas $\psi_0(t)$ must satisfy all non-homogenous conditions at t_0 and $t_0 + T_{\mathsf{NL}}$ associated with the differential equation.

(iii) *Independency:* All $\psi_i(t)$ must be a set of complete and linearly independent and continuous functions.[15]

Rewriting the sum of trial functions (4.83) in matrix notation

$$\widetilde{u}(t) = \boldsymbol{\psi}\, \mathbf{c} \tag{4.87a}$$

[14] Bubnov-Galerkin is a special case of the more general Petrov-Galerkin method where trial function and weighting function do not necessarily belong to the same function space [301].

[15] The condition is sometimes ill-formulated requiring $\psi_i(t)$ to be an orthogonal function set. This it not necessary at all to ensure that $\widetilde{u}(t)$ converges towards the exact solution. It only guarantees sparse algebraic matrices used for obtaining the unknown coefficients c_i.

where

$$\boldsymbol{\psi} = \boldsymbol{\psi}(t) = \left\{\psi_0(t) \quad \psi_1(t) \quad \dots \quad \psi_N(t)\right\}, \quad \text{and} \quad \mathbf{c} = \left\{1 \quad c_1 \quad c_2 \quad \dots \quad c_N\right\}^{\mathrm{T}} \tag{4.87b}$$

gives together with (4.85) and (4.84) for the general system in (3.3)

$$\int_{t_0}^{t_0+T_{\mathrm{NL}}} \psi_i(t) \left(\widehat{m}\, \ddot{\boldsymbol{\psi}}\, \mathbf{c} + \widehat{f}\,(\boldsymbol{\psi}\, \mathbf{c}) - 1\right) = 0 \qquad i = 0, 1, 2, \dots, N, \tag{4.88}$$

or in a more compact form

$$\boldsymbol{\Psi}_{\mathrm{m}}\, \mathbf{c} + \boldsymbol{\psi}_{\mathrm{k}}(\mathbf{c}) - \boldsymbol{\psi}_{\mathrm{p}} = 0 \tag{4.89a}$$

with $t_0 \equiv 0$ and

$$\boldsymbol{\Psi}_{\mathrm{m}} = \widehat{m} \int_0^{T_{\mathrm{NL}}} \boldsymbol{\psi}^{\mathrm{T}} \ddot{\boldsymbol{\psi}}\, \mathrm{d}t, \qquad \boldsymbol{\psi}_{\mathrm{k}}(\mathbf{c}) = \int_0^{T_{\mathrm{NL}}} \boldsymbol{\psi}^{\mathrm{T}} \widehat{f}\,(\boldsymbol{\psi}\, \mathbf{c})\, \mathrm{d}t, \qquad \boldsymbol{\psi}_{\mathrm{p}} = \int_0^{T_{\mathrm{NL}}} \boldsymbol{\psi}^{\mathrm{T}}\, \mathrm{d}t. \tag{4.89b}$$

For the special case of $u_0 = v_0 \equiv 0$, $p_0 > 0$ the nonlinear SDOF system in (3.78) simplifies to equation (4.71) and the stiffness term in (4.89b) is rewritten as

$$\boldsymbol{\psi}_{\mathrm{k}}(\mathbf{c}) = \widehat{k_\beta} \int_0^{T_{\mathrm{NL}}} \boldsymbol{\psi}^{\mathrm{T}}\, (\boldsymbol{\psi}\, \mathbf{c})^b\, \mathrm{d}t. \tag{4.90}$$

Together with the definition of the displacement approximation in (4.87) it becomes immediately apparent that $\boldsymbol{\psi}_{\mathrm{k}}(\mathbf{c})$ can only be obtained if $b \in \mathbb{N}$, i.e. b is an integer. Otherwise the unknown coefficients c_i are inseparable from the displacement functions $\psi_i(t)$ and the entire integral remains undetermined.

4.4.2 *Picard iteration*

The iteration scheme introduced by Picard [302,303] for first-order ordinary differential equations has been used in section 3.4.1.3 of the previous chapter to prove uniqueness of the solution of the nonlinear oscillator in (3.78). It has been pointed out that the method can be used to establish a series approximation which converges towards the exact solution of the differential system.[16)] Although deriving a closed-form expression from such an integral series is only feasible in a limited number of nonlinear systems [246], it is possible to obtain a simple iterative scheme applicable to the more complex oscillator in (3.78). Ultimately, this leads to intricate, but analytical, approximate solutions. Depending on the number of leading terms contained in the series these expressions asymptotically approach the exact solution.

[16)] Picard iteration is also valid for linear oscillators, see [241] for example.

Table 4.3 – Picard-Iteration $f_1(u)$ restoring force: Indexing mechanism for $\tilde{\mathbf{u}}_{j+1}(t)$ and $B_{j+1}(t)$.

Index	$j = 1, 3, 5, \ldots$, **odd**	$j = 2, 4, 6, \ldots$, **even**
$\tilde{\mathbf{u}}_{j+1}(t) =$	$\left\{ \begin{matrix} \frac{1}{2}\,\widehat{p}_0\,t^2 - \omega_\beta^2\,B_{j+1}(t) \\ \widehat{p}_0\,t - \omega_\beta^2\,B_{j-2}(t) \end{matrix} \right\}$	$\left\{ \begin{matrix} \frac{1}{2}\,\widehat{p}_0\,t^2 - \omega_\beta^2\,B_{j+2}(t) \\ \widehat{p}_0\,t - \omega_\beta^2\,B_{j-1}(t) \end{matrix} \right\}$
$B_{j+1}(t) =$	$\int_0^t B_j(\xi)\,\mathrm{d}\xi$	$\int_0^t \left(\frac{1}{2}\,\widehat{p}_0\,\xi^2 - \omega_\beta^2\,B_j(\xi)\right)^b \mathrm{d}\xi$

4.4.2.1 $f_1(u) = k_\beta\,\mathrm{sgn}\,(u)\,|u|^b$

For the special case of $u_0 = \dot{u}_0 \equiv 0$ and $p_0 > 0$ the $(j+1)$ order approximation to the system in (4.71) using the general term in (3.105) is given as

$$\tilde{\mathbf{u}}_{j+1}(t) = \begin{Bmatrix} u_{j+1}(t) \\ \dot{u}_{j+1}(t) \end{Bmatrix} = \int_0^t \begin{Bmatrix} \dot{u}_j(\xi) \\ \widehat{p}_0 - \omega_\beta^2 u_j^b(\xi) \end{Bmatrix} \mathrm{d}\xi\,, \tag{4.91}$$

thus leading for $j \equiv 0, 1, 2$ to

$$\tilde{\mathbf{u}}_1 = \begin{Bmatrix} 0 \\ \widehat{p}_0\,t \end{Bmatrix}, \qquad \tilde{\mathbf{u}}_2 = \begin{Bmatrix} \frac{1}{2}\,\widehat{p}_0\,t^2 \\ \widehat{p}_0\,t \end{Bmatrix}, \qquad \tilde{\mathbf{u}}_3 = \begin{Bmatrix} \frac{1}{2}\,\widehat{p}_0\,t^2 \\ \widehat{p}_0\,t - \omega_\beta^2\,B_1(t) \end{Bmatrix}, \tag{4.92a}$$

where

$$B_1(t) = \int_0^t \left(\frac{1}{2}\,\widehat{p}_0\,\xi^2\right)^b = \frac{2^{-b}\,\widehat{p}_0^{\,b}\,t^{2b+1}}{2\,b+1}\,. \tag{4.92b}$$

Explicitly writing the approximations for $j \equiv 3, 4, 5$, hence

$$\tilde{\mathbf{u}}_4 = \begin{Bmatrix} \frac{1}{2}\,\widehat{p}_0\,t^2 - \omega_\beta^2\,B_2(t) \\ \widehat{p}_0\,t - \omega_\beta^2\,B_1(t) \end{Bmatrix}, \quad \tilde{\mathbf{u}}_5 = \begin{Bmatrix} \frac{1}{2}\,\widehat{p}_0\,t^2 - \omega_\beta^2\,B_2(t) \\ \widehat{p}_0\,t - \omega_\beta^2\,B_3(t) \end{Bmatrix}, \quad \tilde{\mathbf{u}}_6 = \begin{Bmatrix} \frac{1}{2}\,\widehat{p}_0\,t^2 - \omega_\beta^2\,B_4(t) \\ \widehat{p}_0\,t - \omega_\beta^2\,B_3(t) \end{Bmatrix}, \tag{4.92c}$$

respectively, where

$$B_2(t) = \int_0^t B_1(\xi)\,\mathrm{d}\xi\,, \quad B_3(t) = \int_0^t \left(\frac{1}{2}\,\widehat{p}_0\,\xi^2 - \omega_\beta^2\,B_2(\xi)\right)^b \mathrm{d}\xi\,, \quad B_4(t) = \int_0^t B_3(\xi)\,\mathrm{d}\xi\,, \tag{4.92d}$$

clearly reveals the indexing mechanism behind every $\tilde{\mathbf{u}}_{j+1}(t)$ and $B_{j+1}(t)$ shown in table 4.3. By choosing a sufficiently high number of terms $j = 1, 2, 3, \ldots, N$ with $N \gg 10$ the displacement-

velocity function vector $\tilde{\mathbf{u}}_{j+1}(t)$ can be approximated in the entire interval $t \in [t_0, t_0 + T_{\mathsf{NL}}]$.[17] However, due to symmetry of the time-history solution with respect to $1/2$ of the nonlinear oscillation period T_{NL} it is sufficient to model $\tilde{\mathbf{u}}(t)$ within $t \in [t_0, t_0 + 1/2\,T_{\mathsf{NL}}]$. Thus, accurate results are available with significantly less terms in the series of table 4.3, i.e. $N \leq 10$.

It must be pointed out that closed-form analytical expressions for the integral functions B_j from (4.92d) for arbitrary $b \in \mathbb{R}$ are only available up to $j = 4$. For higher-order approximations the expressions in Table 4.3 become too complicated to be solved analytically despite using powerful manipulation software.[18] Nevertheless, it is always possible to obtain results for $B_j(t)$, $j > 4$ by numerical integration. In choosing the step-size of such a summation appropriately (adaptive stepping), the numerical error introduced by the integration can be significantly minimised [159,294].

For the case of $b \in \mathbb{N}$ and $j > 5$ it is almost impossible to derive results for B_j entirely by hand. However, using MATHEMATICA® or MAPLE® the task can be eased considerably.[19] Table 4.4 gives the total error[20] in percent for the iteration series (4.91) containing eight, ten, twelve and fourteen terms, respectively. Results clearly show that with a larger number of leading series terms the approximation quality is steadily improved reducing e_{tot} with $\tilde{\mathbf{u}}_{14}(t)$ significantly.

It must be taken into account that vast computational effort has to be put into obtaining the integrals according to Table 4.3. However, once analytical expressions for all $B_j(t)$ are derived, only a small amount of resources is required for calculating the state vector $\tilde{\mathbf{u}}_j$ at any desired time point $t \in [t_0, t_0 + T_{\mathsf{NL}}]$ if compared to pure numerical integration of the differential system in (3.78). But, given for example $b \equiv 8$, where figure 4.15 shows the results of a 10-term approximation series with $e_{\mathsf{tot}} = 5.013\,\mathsf{E}-2\,\%$ and compared to the one-term displacement solution in Fig. 4.14, this effort is clearly justified.

Identical results are obtained for values of $b \leq 10$ with $j \equiv 10$ independent of p_0 and k_β. However, for $10 < b \leq 20$ the number of terms in 4.3 must be increased to $j \approx 14$ thus raising computational costs significantly. Beyond $b = 20$ the iteration process becomes difficult to handle due to the number of series terms involved in the approximation, which must increase to 20 and more in order to guarantee total errors smaller than 0.1 %. Even with the help of the above mentioned manipulation software, obtaining all $B_j(t)$ is extremely resource demanding and virtually impossible using a single-PC modelling environment.

[17] Essentially, Picard iteration is an integral-type approximation and can be seen as the counterpart to differential approximations such as Taylor series. Nevertheless, the approximation must be developed around a fixed point, e.g. $\mathbf{u}_0$. Low-order series in both cases assure satisfactory results only in the close vicinity of $\mathbf{u}_0$.

[18] MAPLE® and MATHEMATICA® performed equally well in obtaining the closed-form of $B_4(t)$. However, since its predecessors B_j with $j = 2, 3$ are bounded to various assumptions for the upper limit t such as $t \leq T_{\mathsf{NL}}/2$, it is not always possible to check convergence of the subsequent solution, thus individual results may vary.

[19] Compared to hand calculation this is a matter of minutes. Nevertheless, it must be mentioned that despite being of simple polynomial form, expressions for $B_j(t)$ with $6 \geq j \geq 14$ are several pages long and need up to 465 minutes evaluation time per expression ($b \equiv 6$, $j \equiv 14$) on a Pentium 4 (3.4 GHz) processor PC.

[20] Average e_{av} and total error e_{tot} were almost identical.

Table 4.4 – Picard-Iteration $f_1(u)$ restoring force: Total error e_{tot} in percent for four different numbers of leading terms in the approximation series (4.91). System parameter values: $f_{\text{n}} = 0.5$ Hz, $m = 0.3$ kg, $\omega_{\text{n}} = 2\pi f_{\text{n}}$, $k_\beta = m\,\omega_{\text{n}}^2$, and $p_0 = 0.1$ N.

b	$\tilde{\mathbf{u}}_8(t)$	$\tilde{\mathbf{u}}_{10}(t)$	$\tilde{\mathbf{u}}_{12}(t)$	$\tilde{\mathbf{u}}_{14}(t)$
2	7.792E−1	5.953E−2	3.156E−3	1.997E−4
3	8.338E−1	5.921E−2	2.994E−3	1.523E−4
4	8.452E−1	5.771E−2	2.701E−3	1.216E−4
5	8.211E−1	5.611E−2	2.634E−3	1.101E−4
8	8.034E−1	5.013E−2	1.886E−3	7.885E−5

4.4.2.2 $f_2(u) = k_\alpha u + k_\beta u^3$

In a strictly similar manner Picard (3.105) gives for the $(j+1)$ order approximation for the Duffing oscillator in (3.181) with $u_0 = \dot{u}_0 \equiv 0$ and $p_0 > 0$

$$\tilde{\mathbf{u}}_{j+1}(t) = \begin{Bmatrix} u_{j+1}(t) \\ \dot{u}_{j+1}(t) \end{Bmatrix} = \int_0^t \begin{Bmatrix} \dot{u}_j(\xi) \\ \widehat{p}_0 - \omega_\alpha^2 u_j(\xi) - \omega_\beta^2 u_j^3(\xi) \end{Bmatrix} \mathrm{d}\xi \;, \tag{4.93}$$

thus leading for $j \equiv 0, 1, 2$ to almost identical equations as given in (4.92). However, careful examination of the Duffing system's response shows that the condition $p > 0$ is not necessary. Furthermore, due to the fact that iteration equation (4.93) has integer-valued exponents and is at most of order three, integrals involved are far more likely to be solvable than for (4.92) where $b \in \mathbb{N}$ is unrestricted. It is therefore possible to obtain an analytical approximation for step excitation *and* non-zero initial conditions. Although deriving expressions of such a solutions is a very laborious process and impracticable without appropriate software, usage of the Picard iteration procedure guarantees convergence of the approximation series toward the exact solution if a sufficiently large number of leading terms is included.

With the general expression from (3.105) equation (4.93) for the system in (3.181) subjected to $u_0 \neq 0$, $\dot{u}_0 \neq 0$ is rewritten as

$$\tilde{\mathbf{u}}_{j+1}(t) = \begin{Bmatrix} u_0 \\ \dot{u}_0 \end{Bmatrix} + \int_0^t \begin{Bmatrix} \dot{u}_j(\xi) \\ \widehat{p}_0 - \omega_\alpha^2 u_j(\xi) - \omega_\beta^2 u_j^3(\xi) \end{Bmatrix} \mathrm{d}\xi \;, \tag{4.94}$$

leading for $j \equiv 0, 1$ to

$$\begin{aligned} \tilde{\mathbf{u}}_1(t) &= \mathbf{u}_0 + \begin{Bmatrix} \dot{u}_0\, t \\ t\left(\widehat{p}_0 - \omega_\alpha^2 u_0 - \omega_\beta^2 u_0^3\right) \end{Bmatrix} , \\ \tilde{\mathbf{u}}_2(t) &= \mathbf{u}_0 + \begin{Bmatrix} \dot{u}_0\, t + \frac{\widehat{p}_0}{2}\, t^2 - \omega_\alpha^2\, A_1(t) - \omega_\beta^2\, B_1(t) \\ \widehat{p}_0\, t - \omega_\alpha^2 C_1(t) - \omega_\beta^2 D_1(t) \end{Bmatrix} , \end{aligned} \tag{4.95a}$$

where

$$A_1 = \frac{u_0}{2}\,t^2\,,\; B_1 = \frac{u_0^3}{2}\,t^2\,,\; C_1 = \int_0^t u_0 + \dot{u}_0\,\xi\;\mathrm{d}\xi\,,\; D_1 = \int_0^t (u_0 + \dot{u}_0\,\xi)^3\;\mathrm{d}\xi\,, \tag{4.95b}$$

and thus,

$$C_1 = t\left(u_0 + \frac{1}{2}\,\dot{u}_0\,t^2\right)\,, \quad D_1 = t\left(u_0^3 + t^2\,u_0^2\,\dot{u}_0 + \frac{3}{5}\,t^4\,u_0\,\dot{u}_0^2 + \frac{1}{7}\,t^6\,\dot{u}_0^3\right)\,. \tag{4.95c}$$

For $j \equiv 2, 3$ equation (4.94) can be expressed as

$$\begin{aligned}
\tilde{\mathbf{u}}_3(t) &= \mathbf{u}_0 + \begin{Bmatrix} \dot{u}_0\,t + \frac{1}{2}\,\widehat{p}_0\,t^2 - \omega_\alpha^2\,A_2(t) - \omega_\beta^2\,B_2(t) \\ \left(\widehat{p}_0\,t - \omega_\alpha^2\,C_2(t) - \omega_\beta^2\,D_2(t)\right) \end{Bmatrix}\,, \\
\tilde{\mathbf{u}}_4(t) &= \mathbf{u}_0 + \begin{Bmatrix} \dot{u}_0\,t + \frac{1}{2}\,\widehat{p}_0\,t^2 - \omega_\alpha^2\,A_3(t) - \omega_\beta^2\,B_3(t) \\ \left(\widehat{p}_0\,t - \omega_\alpha^2\,C_3(t) - \omega_\beta^2\,D_3(t)\right) \end{Bmatrix}\,,
\end{aligned} \tag{4.95d}$$

with

$$\begin{aligned}
A_2(t) &= \int_0^t C_1(\xi)\;\mathrm{d}\xi\,, \quad B_2(t) = \int_0^t D_1(\xi)\;\mathrm{d}\xi\,, \quad A_3(t) = \int_0^t C_2(\xi)\;\mathrm{d}\xi\,, \quad \ldots \\
C_2(t) &= \int_0^t u_0 + \dot{u}_0\,\xi + \frac{1}{2}\,\widehat{p}_0\,\xi^2 - \omega_\alpha^2\,A_1(\xi) - \omega_\beta^2\,B_1(\xi)\;\mathrm{d}\xi\,, \\
D_2(t) &= \int_0^t \left(u_0 + \dot{u}_0\,\xi + \frac{1}{2}\,\widehat{p}_0\,\xi^2 - \omega_\alpha^2\,A_1(\xi) - \omega_\beta^2\,B_1(\xi)\right)^3\;\mathrm{d}\xi\,, \quad \ldots
\end{aligned} \tag{4.95e}$$

This clearly reveals the methodology behind the indexing mechanism and the $(j+1)$ solution is given as

$$\tilde{\mathbf{u}}_{j+1}(t) = \mathbf{u}_0 + \begin{Bmatrix} \dot{u}_0\,t + \frac{1}{2}\,\widehat{p}_0\,t^2 - \omega_\alpha^2\,A_j - \omega_\beta^2\,B_j \\ \left(\widehat{p}_0\,t - \omega_\alpha^2\,C_j - \omega_\beta^2\,D_j\right) \end{Bmatrix} \qquad j = 1, 2, 3, \ldots, N \tag{4.96a}$$

together with

$$\begin{aligned}
A_{j+1}(t) &= \int_0^t C_j(\xi)\;\mathrm{d}\xi\,, \qquad B_{j+1}(t) = \int_0^t C_j(\xi)\;\mathrm{d}\xi\,, \\
C_{j+1}(t) &= \int_0^t u_0 + \dot{u}_0\,\xi + \frac{1}{2}\,\widehat{p}_0\,\xi^2 - \omega_\alpha^2\,A_j(\xi) - \omega_\beta^2\,B_j(\xi)\;\mathrm{d}\xi\,, \\
D_{j+1}(t) &= \int_0^t \left(u_0 + \dot{u}_0\,\xi + \frac{1}{2}\,\widehat{p}_0\,\xi^2 - \omega_\alpha^2\,A_j(\xi) - \omega_\beta^2\,B_j(\xi)\right)^3\;\mathrm{d}\xi\,.
\end{aligned} \tag{4.96b}$$

Results of total error e_{tot} for a hardening stiffness-type Duffing system are given in table 4.5. Despite being easier to solve than the equations in table 4.3, the iteration procedure (4.96) re-

Table 4.5 – Picard-Iteration for Duffing system - hardening spring $k_\alpha > 0, k_\beta > 0$: Total error e_{tot} in percent for four different numbers of leading terms in the approximation series (4.96). Initial conditions: $u_0 \equiv 0.35$ m and $\dot{u}_0 \equiv 1.25$m/s. System parameters: $f_\text{n} = 0.5$ Hz, $m = 0.3$ kg, $\omega_\text{n} = 2\pi f_\text{n}$, $k_\alpha = m\,\omega_\text{n}^2$, $k_\beta = k_\gamma\, k_\alpha$.

p_0	k_γ	$\tilde{\mathrm{u}}_8(t)$	$\tilde{\mathrm{u}}_{10}(t)$	$\tilde{\mathrm{u}}_{12}(t)$	$\tilde{\mathrm{u}}_{14}(t)$
1.0	1.0	11.995	2.221	1.004 E−1	5.447 E−3
500.0	1.0	9.332	1.764	8.541 E−2	2.001 E−3
1.0	50.0	9.547	1.923	9.141 E−2	3.112 E−3
500.0	50.0	7.844	1.188	7.844 E−2	1.012 E−3

quires significant resources especially for $\tilde{\mathrm{u}}_{14}(t)$ and larger terms. But as stated for the results in Table 4.3, once the closed-form analytical approximation expression is obtained its evaluation needs only very little effort using the appropriate software. A comparison of both tables 4.5 and 4.4 shows quite significant differences between the quality of approximation with (4.96) demanding far more terms than the scheme in Table 4.3. This must be attributed to the fact that the first accounts for a solution involving non-zero initial conditions which result in more complex time-history response function.

A plot of the normalised response values for displacement, velocity and acceleration together with the respective error yields graphs very similar to Fig. 4.15 shown for the $f_\text{I}(u)$ restoring force system but have been omitted here.

4.5 Comparison to direct numerical integration methods

The main purpose of this section is to relate the accuracy, quality and computational cost of various analytical approximations derived in this chapter to solutions generically obtainable using numerical direct integration algorithms, so-called explicit first-order ODE solvers.[21] The mathematical background of the most simplest of these routines dates back to Newton, Euler and Gauss who used them for root-finding and the solution of nonlinear algebraic equation systems [245,246]. Building on these ideas, by considerably improving accuracy and stability, and establishing new methods which are significantly faster and more accurate while at the same time making optimal use of available computational resources, a large number of algorithms are readily accessible today. An overview of state-of-the-art implementations is given in [304,305]. Concerning the methods used for comparison to analytical solutions in this work the MATLAB® reference manual [294] and the well-known routines of Press *et al* [159] are important sources.

Throughout the preceding sections of this chapter newly derived solutions and numerical data have already been compared on various occasions. However, little has been said so far about their individual implementation in order to procure results having the anticipated or required accuracy.

[21] Although briefly mentioned in equation (3.5) implicit problems are not considered in this work.

Given the fact that all differential problems in here are neither implicit nor stiff,[22] it is possible to choose from a wide range of suitable routines. In fact, for the special system of two autonomous first-order equations (3.15) algorithms in [159] are very similar to MATLAB® implementations and therefore only the latter ones are considered in what follows.

The initial value problem can be solved using one of three different routines on offer.[23] Firstly, `ode45`, a (4,5)-pair embedded Runge-Kutta (RK) algorithm implemented according to Dorman and Prince, see [156, 157]. Secondly, `ode23`, its (2,3)-pair equivalent after Bogacki-Schampine, and thirdly, `ode113`, a variable order (1.-13.) predictor-corrector (PECE) Adams-Bashforth-Moulton solver. With `ode45` being the general purpose method, the pair in `ode23` is orders too low to yield accurate enough results for the problem under consideration and has therefore been discharged. Similarly, with `ode113` giving results only one order of magnitude more accurate than `ode45`, but significantly increasing calculation time, the (4,5) pair RK routine was the solver of choice.

Calculating average and total error of the RK time series system response using Eqs.(4.46) and (4.48) it is possible to compare the effects of various error tolerance settings for `ode45` with data obtained from the analytical approximations presented in this chapter. Due to the fact that first-order solver routines give only displacement and velocity but both e_{av} and e_{tot} require also acceleration-time history, numerical differentiation must be used. At this point it is important to mention that internal MATLAB® routines are completely insufficient for this task and a five-point numerical differentiating algorithm using local cubic polynomial fit[24] was employed.

The `ode45` solver algorithm provides essentially two control parameters in order to influence the solution accuracy. Firstly, the relative error tolerance `RelTol` with the default value of 10^{-3} applies to all components of the solution vector $\mathbf{u}(t) = \{u(t),\ \dot{u}(t)\}^{\mathrm{T}}$. Colloquially speaking, it is a measure of the error relative to the size of each part of $\mathbf{u}(t)$. The second parameter is the absolute error tolerance `AbsTol` which is set to 10^{-6} by default. It applies to the individual components of $\mathbf{u}(t)$ and can be seen as threshold below which the value of the parts u_i, $\dot{u}_i$ of $\mathbf{u}$ at the discretised time point t_i becomes unimportant. Roughly expressed, `AbsTol` determines the accuracy when the solution approaches zero. Bearing in mind these interrelations between `RelTol` and `AbsTol` it becomes apparent that significant gains in solution accuracy can only be achieved by simultaneously decreasing values for both tolerances.

Results for the Duffing system (3.181) with hardening-type stiffness $k_\alpha > 0, k_\beta > 0$ are listed in table 4.6 and must be compared to Fig. 4.3 and 4.4. Clearly, for `ode45` for default recom-

[22] A system of ordinary differential equations is said to be 'stiff' if during the numerical integration process, after a period of slow changes, large and sudden changes in the solution vector occur despite continuous use of small time steps. Any attempt to increase the integration step in order to reduce calculation time results in a sharp increase in the error. However, specially developed solver algorithms can obtain high-accuracy solutions while maximising the step size during appropriate time intervals. For autonomous system there exist a number of criterions in order to determine whether a differential system is stiff [297].

[23] MATLAB® v.7.0.4 build number 29-01-2005.

[24] The code `nd5p.m` from the MATLAB CENTRAL file exchange server has been used. The author is Dr. YangQuan Chen. See `http://www.mathworks.com/matlabcentral/fileexchange/`.

Table 4.6 – Duffing system $f_2(u) = k_\alpha\, u + k_\beta\, u^3$ - nonlinear hardening spring $k_\alpha > 0, k_\beta > 0$: Average e_{av} and total error e_{tot} in percent for MATLAB® ODE solver `ode45`. System parameters: $f_{\text{n}} = 0.5\,\text{Hz}$, $m = 0.3\,\text{kg}$, $\omega_{\text{n}} = 2\pi f_{\text{n}}$, $k_\alpha = m\,\omega_{\text{n}}^2$, $k_\beta = k_\gamma\, k_\alpha$. Default error tolerances: `RelTol` = 1.0E−3, `AbsTol` = 1.0E−6.

RelTol	AbsTol	p_0 =1.0 N, k_γ =1.0 N/m^2		p_0 =500 N, k_γ =50 N/m^2	
		e_{av} [%]	e_{tot} [%]	e_{av} [%]	e_{tot} [%]
1.0E−3	1.0E−6	1.025E−2	3.116E−2	1.565E−2	2.932E−2
1.0E−5	1.0E−8	2.292E−4	1.335E−3	1.895E−4	9.221E−4
1.0E−7	1.0E−10	7.132E−7	3.039E−5	6.995E−7	3.001E−5
1.0E−9	1.0E−12	4.664E−8	7.094E−6	2.445E−8	2.221E−6

mended values of `RelTol` and `AbsTol` the analytical approximation in (4.41) yields more accurate results than the MATLAB® routine. Even for moderate tolerances such as `RelTol` = 1.0E−5 and `AbsTol` = 1.0E−8 the total error $e_{\text{tot}} = 9.221\,\text{E}{-4}$ for $k_\beta = 50\,\text{N/m}^2$ and $p_0 = 500\,\text{N}$ is significantly higher than shown in Fig. 4.4. It is only for stringent tolerance values, and therefore a noticeable increase in calculation time, that results using the numerical RK algorithm give distinctive lower average and total errors.

Similar conclusions can be drawn by analysing results for $f_1(u)$ restoring force systems in Table 4.7. Compared to Table 4.4 showing error values for various orders of the Picard iteration series, e_{av} and e_{tot} from `ode45` with default settings for `RelTol` and `AbsTol` are up to four orders of magnitude higher than obtained from the analytical approximation. Moreover, by setting both tolerances in the numerical routine to their smallest possible value of 2.2E−14 and 1.0E−35, respectively, `ode45` arrives at its limits for calculating the average and total errors. No significant improvement beyond these values is possible. Interesting enough, results for the total error e_{tot} of both methods differ in this case in relative value[25] only marginally. But with having included only 14 terms in the Picard series, the analytical approximation holds a huge potential for even higher accuracy.

A final comment regarding the above presented comparison between the two methods must be made. It is evidently that purely numerical algorithms are able to obtain results with an accuracy far beyond the reach of any of the single-term trial functions and, even in case of Picard-iteration, RK can surpasses analytical approximate results with appropriate error tolerance settings as seen in both tables 4.6 and 4.7. Although, in theory, the Picard-method is guaranteed to approach the exact solution, hence leaving zero average and total errors, its practical usability for the two SDOF systems having $f_1(u)$ and $f_2(u)$ restoring force is limited to less than 12 terms in the approximation series if average computational resources are assumed.[26] However, the absolute error plot shown in figure 4.15 clearly indicates that for a 10-term analytical approximation with

[25] Compared in an absolute-value sense both numbers give a difference of almost 5.6E−5. However, normalised to the response functions of displacement, velocity or acceleration this value is significantly smaller.

[26] Generic PC modelling environment with single-core Pentium 4 processor or equivalent.

Table 4.7 – Restoring force $f_1(u) = k_\beta \operatorname{sgn}(u) |u|^b$: Average e_{av} and total e_{tot} error (4.82) in percent for the nonlinear oscillator in (3.78) using the MATLAB® ODE solver `ode45`. System parameter values: $f_{\text{n}} = 0.5\,\text{Hz}$, $m = 0.3\,\text{kg}$, $\omega_{\text{n}} = 2\pi f_{\text{n}}$, $k_\beta = m\omega_{\text{n}}^2$, and $p_0 = 0.1\,\text{N}$. Default error tolerances: `RelTol` = 1.0E−3, `AbsTol` = 1.0E−6.

RelTol	AbsTol	$b \equiv 0.6$		$b \equiv 8$	
		e_{av} [%]	e_{tot} [%]	e_{av} [%]	e_{tot} [%]
1.0E−3	1.0E−6	9.673E−3	5.677E−2	4.931	7.985
1.0E−5	1.0E−8	5.241E−4	9.232E−4	3.759E−2	5.492E−1
1.0E−7	1.0E−10	5.676E−5	1.853E−4	1.033E−5	1.078E−3
1.0E−9	1.0E−12	5.287E−6	9.583E−5	3.242E−8	5.141E−5
2.2E−14	1.0E−35	5.239E−6	9.367E−6	1.101E−12	2.446E−5

$e_{\text{av}} \approx e_{\text{tot}} = 5.013\,\text{E}{-2}$ the values for the displacement-time history differ at a single point by less than 2.0E−4 % compared to numerically obtained data, which is, in this case, a high-precision simulation with MATHEMATICA® giving a total error of $e_{\text{tot}} = 1.32\,\text{E}{-35}$ and can therefore be regarded as exact solution. Despite the evidently large differences for e_{av} and e_{tot} between the two solutions the approximate results are more than satisfactory. Although explicit plots have been omitted, very similar statements can be made for the single-term analytical approximations in section 4.3.

4.6 Summary

Extreme response values for two nonlinear SDOF systems with polynomial-type restoring forces $f_1(u) = k_\beta \operatorname{sgn}(u) |u|^b$ and $f_2(u) = k_\alpha u + k_\beta u^3$, respectively, subjected to different forms of time-independent transient loading have been obtained for all feasible sets of system parameters in the previous chapter. By employing this combination of partially well-known and partially novel results, new time-domain analytical exact and closed-form high-accuracy approximations were derived in this chapter.

It has been shown in section 4.2.1 that only one elliptic function is required for exactly satisfying the governing differential equation of both hardening and softening Duffing systems clearly disproving recently published results [295]. Furthermore, the very same was demonstrated for the snap-through system despite the complicacy that the oscillator exhibits significant qualitative differences in its response depending on the initial energy input level. Although a few exact solutions for $u_0 \neq 0$ and $\dot{u}_0 \equiv 0$ initial conditions are well established in the literature for the Duffing system, a previously unpublished rigorous mathematical approach has been presented between the newly defined more general solutions and specific domains of stability, as well as precisely described invariant sets of energy entirely depending on genuine system parameters and initial conditions.

Application of Eq.(3.49), which allows one to rewrite a Dirac-δ impulse excitation as nonzero initial velocity condition even in the case of strongly nonlinear restoring force, makes it crucial to

obtain solutions for the Duffing system subjected to $u_0 \equiv 0$, $\dot{u}_0 \neq 0$. Following a similar approach as for nonzero initial displacement, the nonlinear oscillation frequency ω_J must be obtained from an implicit quartic equation for which an explicit solution can be retrieved using standard textbooks. The derived exact analytical solution is valid for all three instances of the oscillator and not restricted to any constraints other than stability.

Combining the results of both section 4.2.1 and 4.2.2, a new closed-form solution for the impulse excited Duffing system subjected to general nonzero initial values has been presented in 4.2.3 rendering both previously obtained solutions, including those for any linear systems, as special cases.

It has been shown throughout the current chapter that finding exact analytical expressions for *homogeneous* general nonlinear systems can be very difficult, sometimes even impossible[27] Attempts of establishing closed-form solutions for the oscillator's response parameters $u(t)$, $\dot{u}(t)$ and $\ddot{u}(t)$ for the same system in its *nonhomogeneous* form leads very often nowhere. It is therefore of vital importance to establish analytical approximations modelling the exact, but unknown, solution of the system as accurately as possible and, ideally, over the entire range of feasible system parameters and initial conditions. Since there are various mathematical approaches possible, single-term solutions presented in section 4.3 should be seen as a realisable and a beneficial first step on the way towards a more general class of nonlinear systems approximations.

Various different displacement trial functions have been suggested for the incomplete Duffing oscillator in section 4.3.1, originating from the fact that all three instances of the polynomial restoring force $f_2(u)$ show large qualitative differences in their response behaviour. Some of the trial functions are only capable of delivering reasonable results for narrow ranges of k_α, k_β and p_0, whereas others do not have any restrictions apart from ensuring global stability of the dynamical system when selecting the system parameters. A complete mathematical definition of the error introduced by the trial function enables rigorous checks of the approximation quality to be made. Subsequent comparison of these error measures, with results obtained from high-accuracy direct numerical integration procedures, show very good performance of the newly proposed approximate solutions.

Due to the fact that no suitable displacement modelling function was found for the $f_1(u)$ oscillator, section 4.3.2 successfully introduced an equivalently efficient approximation procedure. Instead of trying to match the displacement $u(t)$ and bearing the risk of failing to accurately render higher-order derivatives, the system's acceleration was chosen directly for modelling. Although this results in the lack of closed-form solutions being available for either velocity or displacement, the procedure can be regarded as important in approximating experimentally obtained acceleration data. A comprehensive numerical analysis clearly shows that only small approximation errors exist for vast ranges of system parameters.

The main objective of section 4.4 is the significant improvement of the system's approximate response solutions for those parameter combinations which render application of the single-term

[27] A good example is the SDOF oscillator with $f_1(u)$ as restoring force. It is only for very few selected cases such as $b = 2$, 3 or 5 that analytical solutions can be obtained if the system possess a zero right-hand side [43].

trial function unsuitable. By employing a nonlinear least-square method derived from a modified Galerkin approach, together with the previously obtained single-term function as a fundamental approximation, the average and total error measures are substantially reduced. An additionally introduced weighting function emphasises regions within the single-oscillation cycle time-domain interval which show the largest error levels when using the one-term approximation only, thus making the method more efficient than a conventional variational approach [96, 97, 300, 306].

An entirely independent method is given with the Picard iteration procedure in section 4.4.2. Although it is for the $f_1(u)$ restoring force systems only, applicable to cases where the displacement function is single-signed, closed-form analytical series expressions are obtained converging towards the exact solution of the nonlinear problem. The procedure proves more versatile in the case of Duffing systems. The fact that the equation of motion integrals of the step-excited $f_2(u)$ oscillator are easier to solve than for $f_1(u)$ systems allows for inclusion of nonzero initial conditions of displacement and velocity. Given the very good agreement with results obtained from conventional high-accuracy direct numerical integration, the entire approach has the only disadvantage of requiring powerful algebraic manipulation software in order to explicitly solve the integral series expressions.

It is important to note that all of the approximation methods introduced in this chapter are applicable to a wide range of similar, polynomial-type nonlinear restoring forces. The fact that certain procedures are only used in conjunction with either $f_1(u)$ or $f_2(u)$ is dictated by the need of avoiding unnecessary repetition.

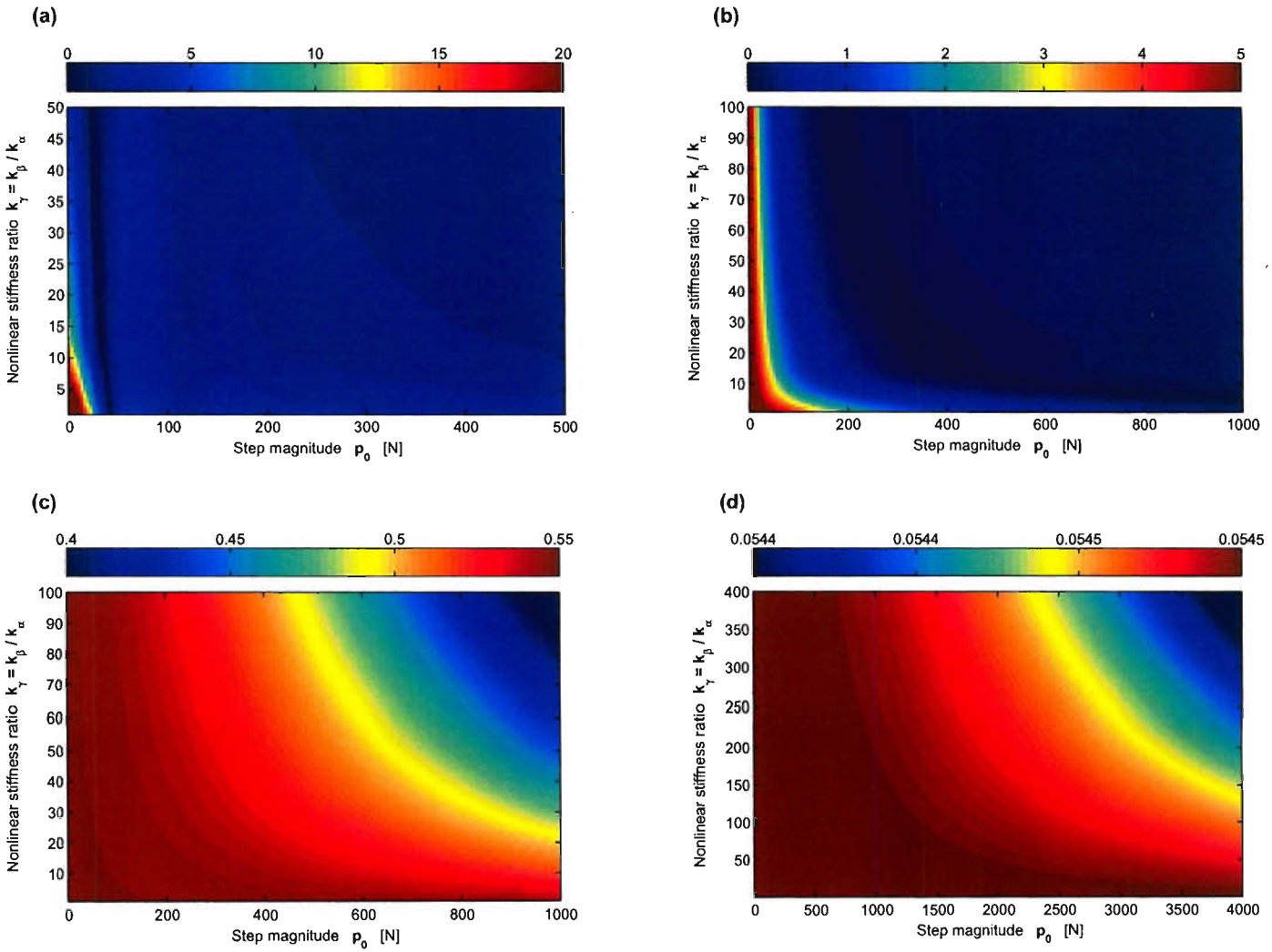

Figure 4.1 – Nonlinear hardening spring ($k_\alpha, k_\beta > 0$): **Method 1 - average error** e_{av} in percent for different linear stiffness coefficients $k_\alpha = 4\pi^2 f_n^2 m$ of the constant excitation force approximation. **(a)** $f_n = 0.5$ Hz, **(b)** $f_n = 5$ Hz, **(c)** $f_n = 50$ Hz, **(d)** $f_n = 500$ Hz. Parameter values: mass $m = 0.3$ kg.

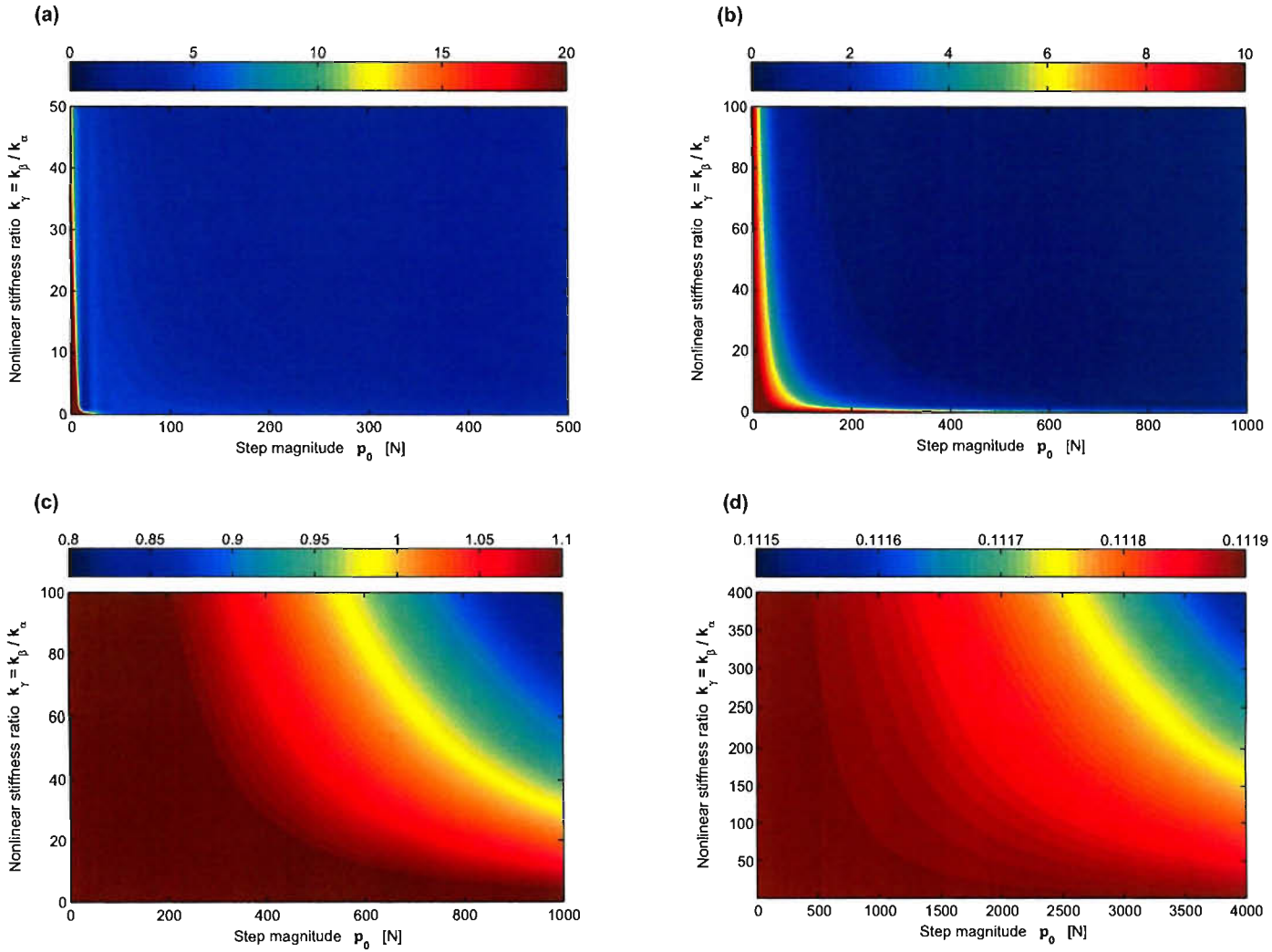

Figure 4.2 – Nonlinear hardening spring ($k_\alpha, k_\beta > 0$): **Method 1 - total error** e_{tot} in percent for different linear stiffness coefficients $k_\alpha = 4\pi^2 f_n^2 m$ of the constant excitation force approximation. **(a)** $f_n = 0.5$ Hz, **(b)** $f_n = 5$ Hz, **(c)** $f_n = 50$ Hz, **(d)** $f_n = 500$ Hz. Parameter values: mass $m = 0.3$ kg.

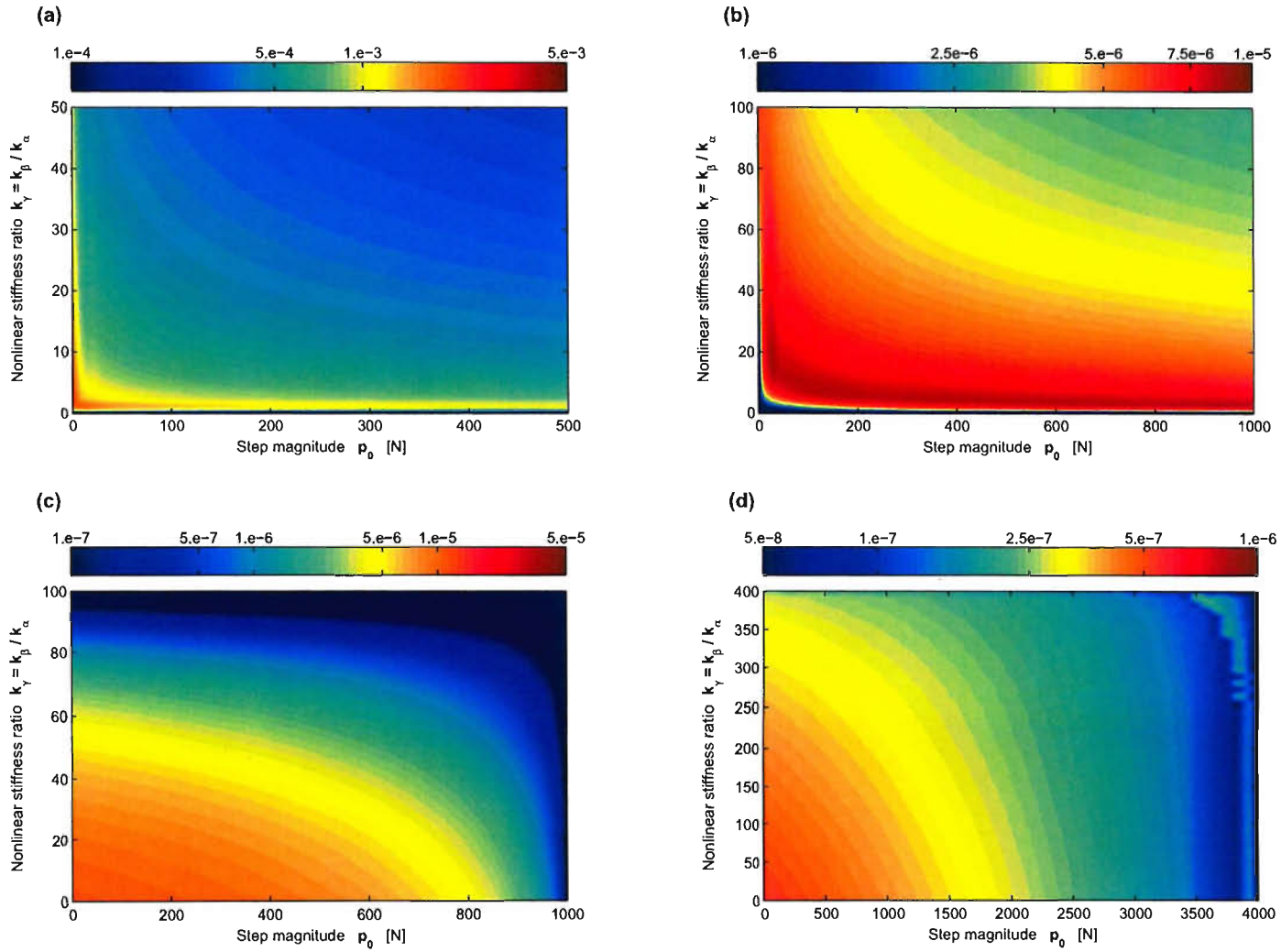

Figure 4.3 – Nonlinear hardening spring ($k_\alpha, k_\beta > 0$): **Method 2 - average error** e_{av} in percent for different linear stiffness coefficients $k_\alpha = 4\pi^2 f_n^2 m$ of the constant excitation force approximation. **(a)** $f_n = 0.5$ Hz, **(b)** $f_n = 5$ Hz, **(c)** $f_n = 50$ Hz, **(d)** $f_n = 500$ Hz. Parameter values: mass $m = 0.3$ kg.

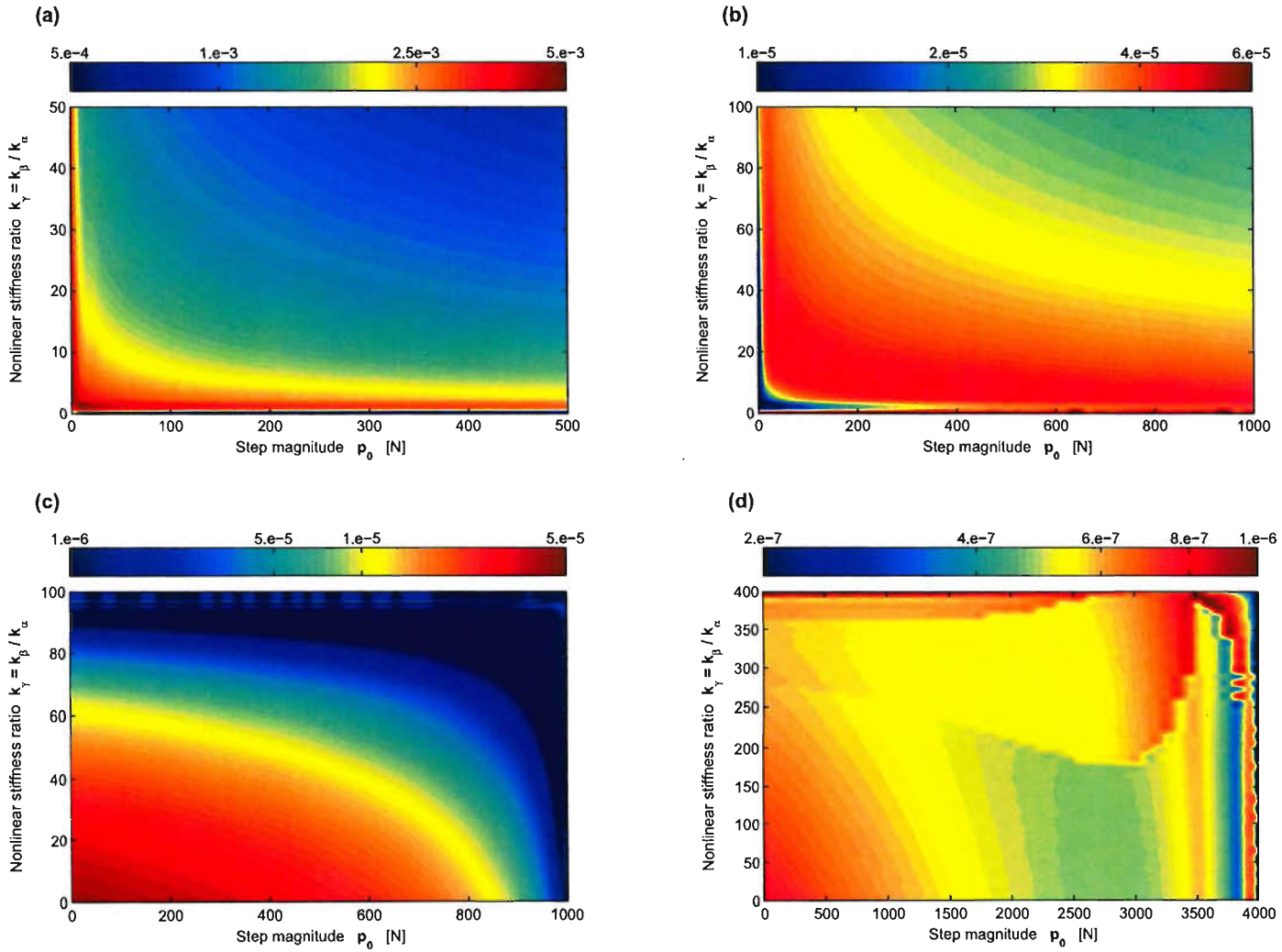

Figure 4.4 – Nonlinear hardening spring ($k_\alpha, k_\beta > 0$): **Method 2 - total error** e_{tot} in percent for different linear stiffness coefficients $k_\alpha = 4\pi^2 f_n^2 m$ of the constant excitation force approximation. **(a)** $f_n = 0.5$ Hz, **(b)** $f_n = 5$ Hz, **(c)** $f_n = 50$ Hz, **(d)** $f_n = 500$ Hz. Parameter values: mass $m = 0.3$ kg.

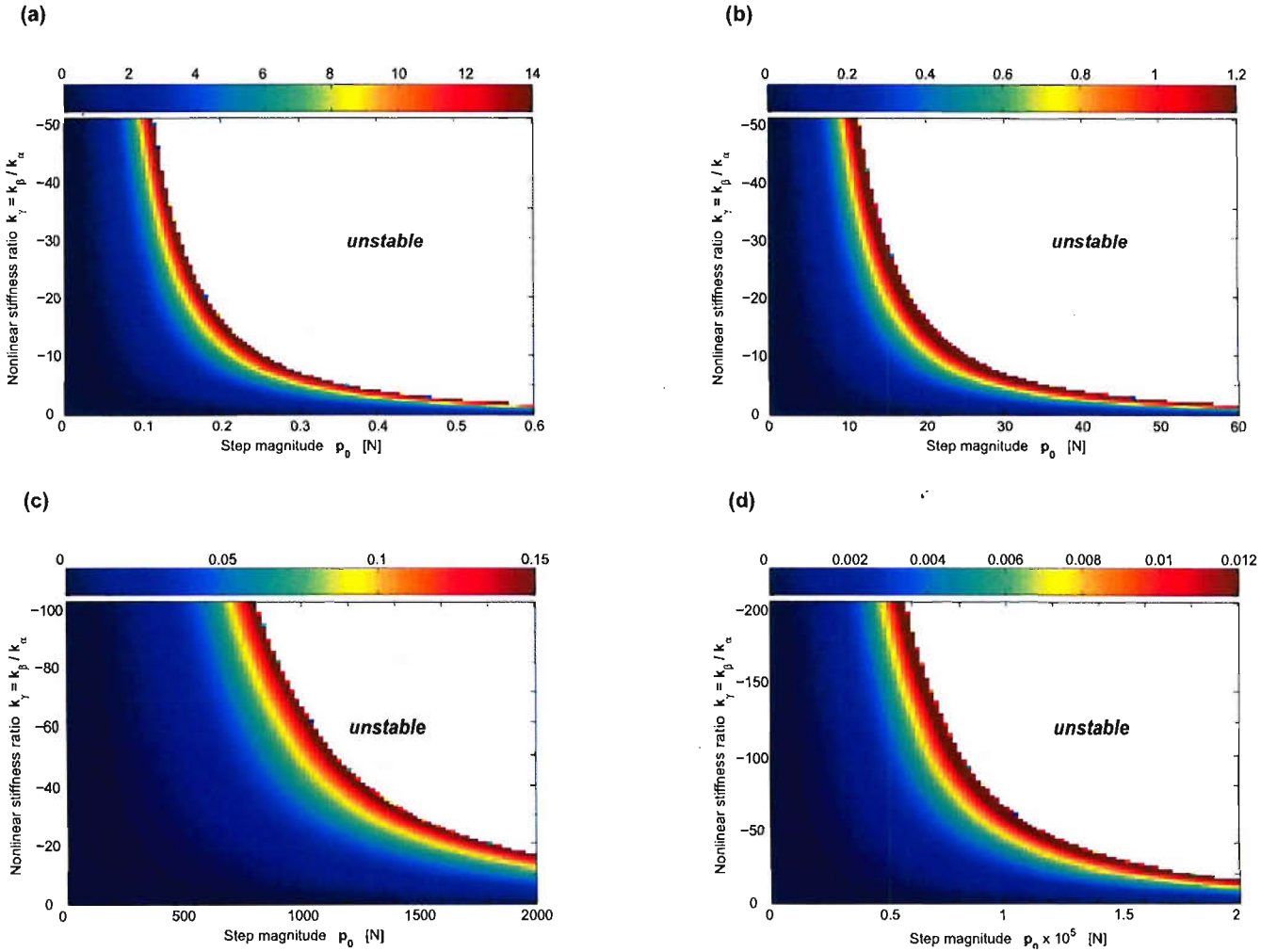

Figure 4.5 – Nonlinear softening spring ($k_\alpha > 0, k_\beta < 0$): **Method 1 - average error** e_{av} in percent for different linear stiffness coefficients $k_\alpha = 4\pi^2 f_n^2 m$ of the constant excitation force approximation. **(a)** $f_n = 0.5$ Hz, **(b)** $f_n = 5$ Hz, **(c)** $f_n = 50$ Hz, **(d)** $f_n = 500$ Hz. Parameter values: mass $m = 0.3$ kg.

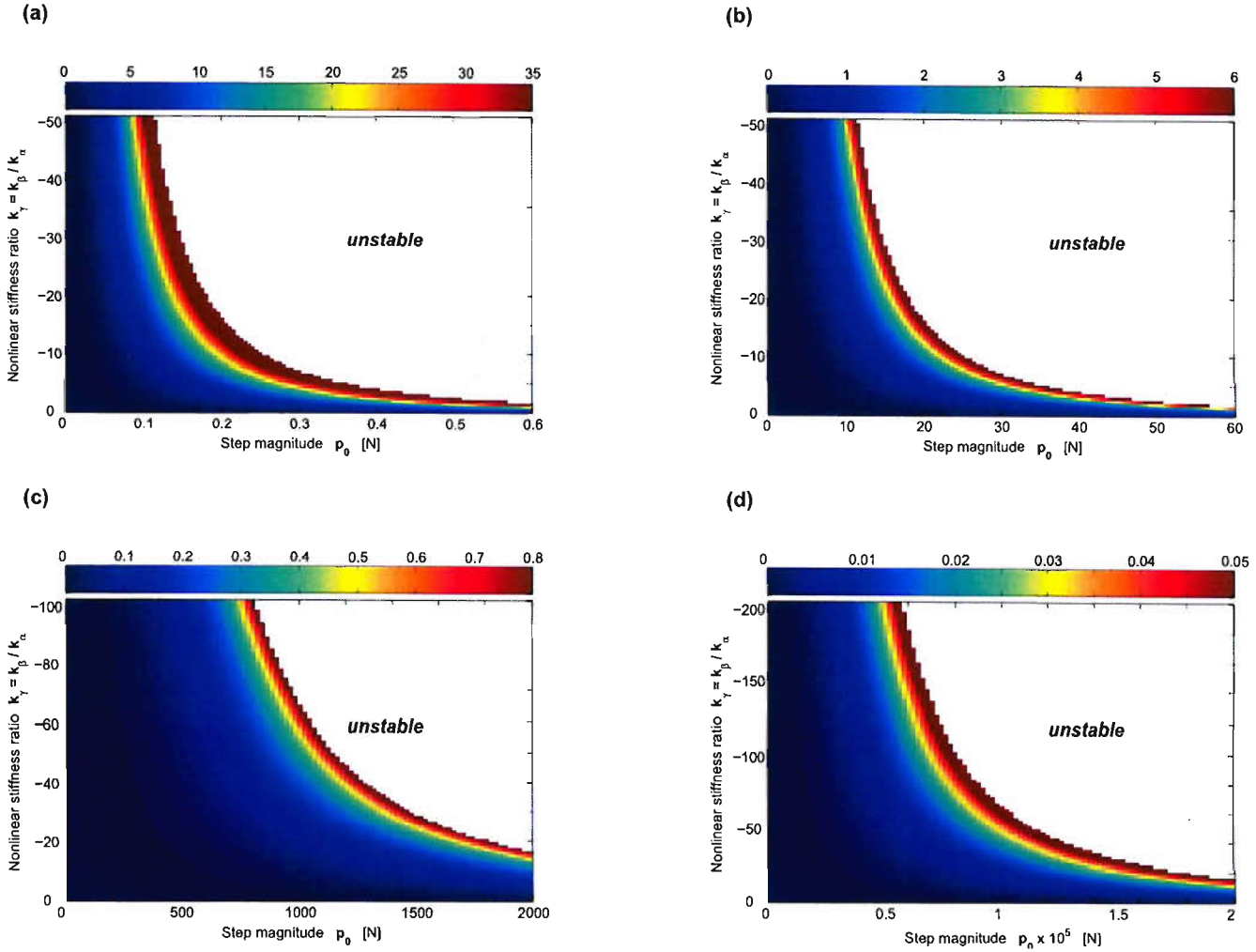

Figure 4.6 – Nonlinear softening spring ($k_\alpha > 0, k_\beta < 0$): **Method 1 - total error** e_{tot} in percent for different linear stiffness coefficients $k_\alpha = 4\pi^2 f_n^2 m$ of the constant excitation force approximation. **(a)** $f_n = 0.5$ Hz, **(b)** $f_n = 5$ Hz, **(c)** $f_n = 50$ Hz, **(d)** $f_n = 500$ Hz. Parameter values: mass $m = 0.3$ kg.

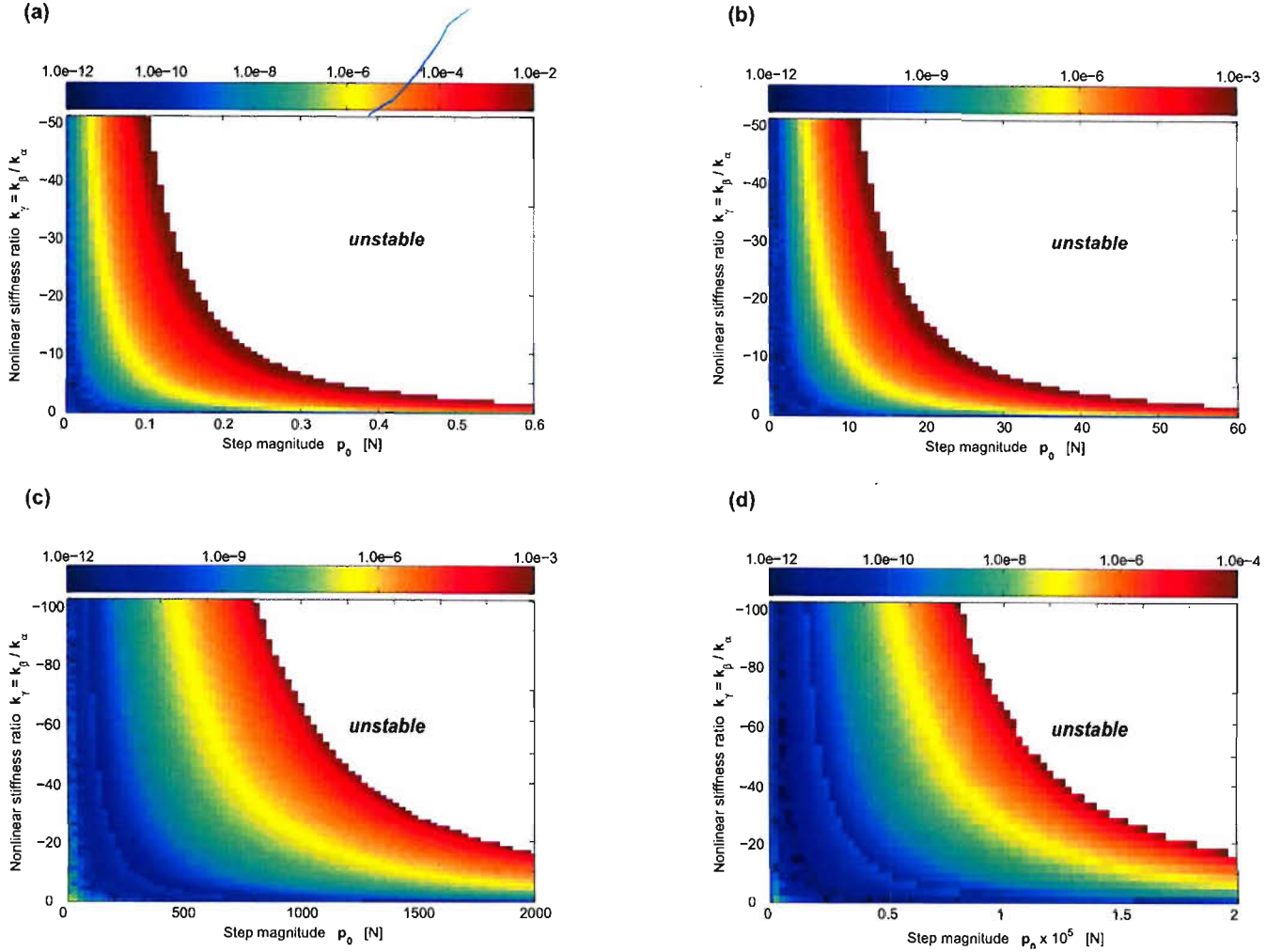

Figure 4.7 – Nonlinear softening spring ($k_\alpha > 0, k_\beta < 0$): **Method 2 - average error** e_{av} in percent for different linear stiffness coefficients $k_\alpha = 4\pi^2 f_n^2 m$ of the constant excitation force approximation. **(a)** $f_n = 0.5$ Hz, **(b)** $f_n = 5$ Hz, **(c)** $f_n = 50$ Hz, **(d)** $f_n = 500$ Hz. Parameter values: mass $m = 0.3$ kg.

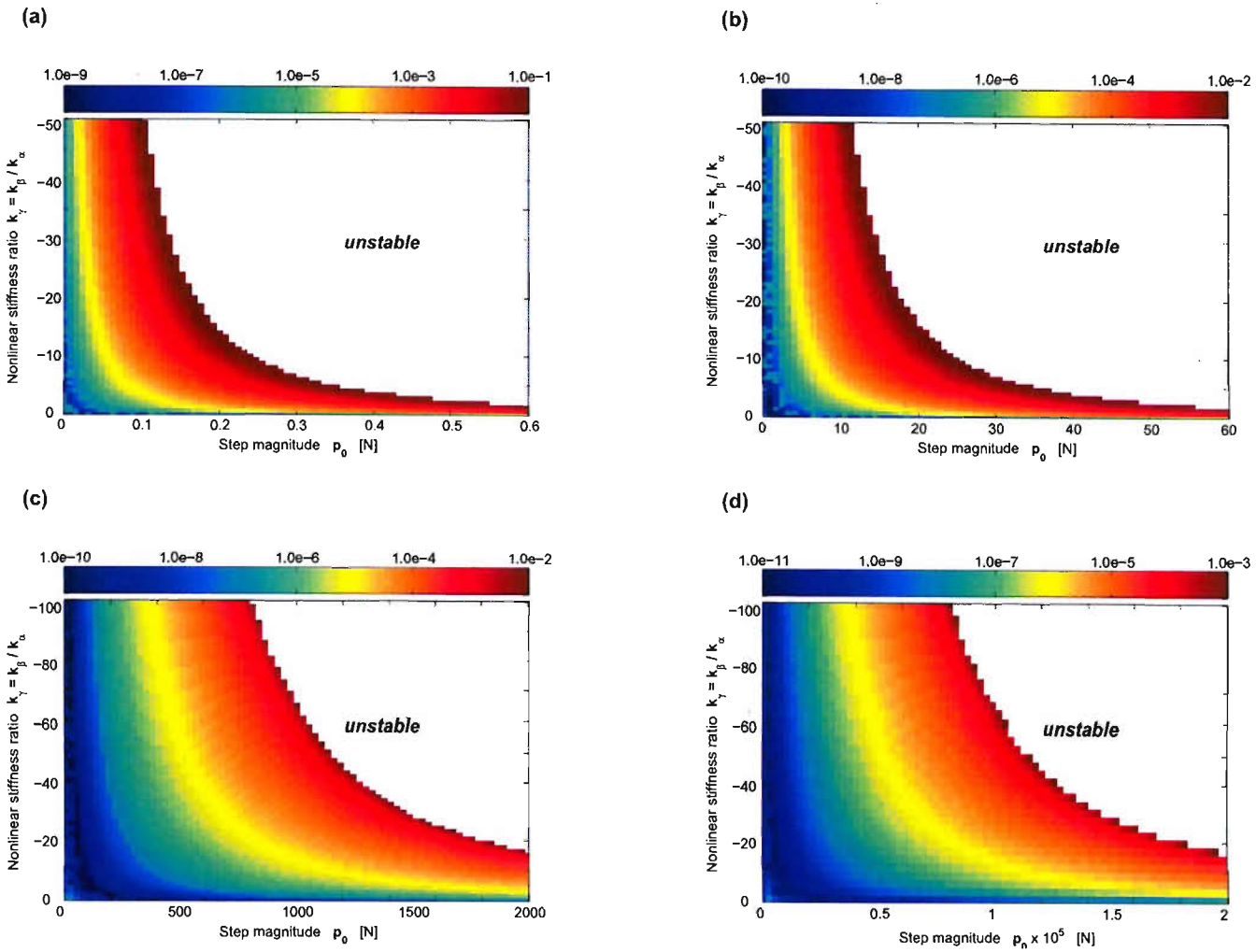

Figure 4.8 – Nonlinear softening spring ($k_\alpha > 0, k_\beta < 0$): **Method 2 - total error** e_{tot} in percent for different linear stiffness coefficients $k_\alpha = 4\pi^2 f_n^2\, m$ of the constant excitation force approximation. **(a)** $f_n = 0.5$ Hz, **(b)** $f_n = 5$ Hz, **(c)** $f_n = 50$ Hz, **(d)** $f_n = 500$ Hz. Parameter values: mass $m = 0.3$ kg.

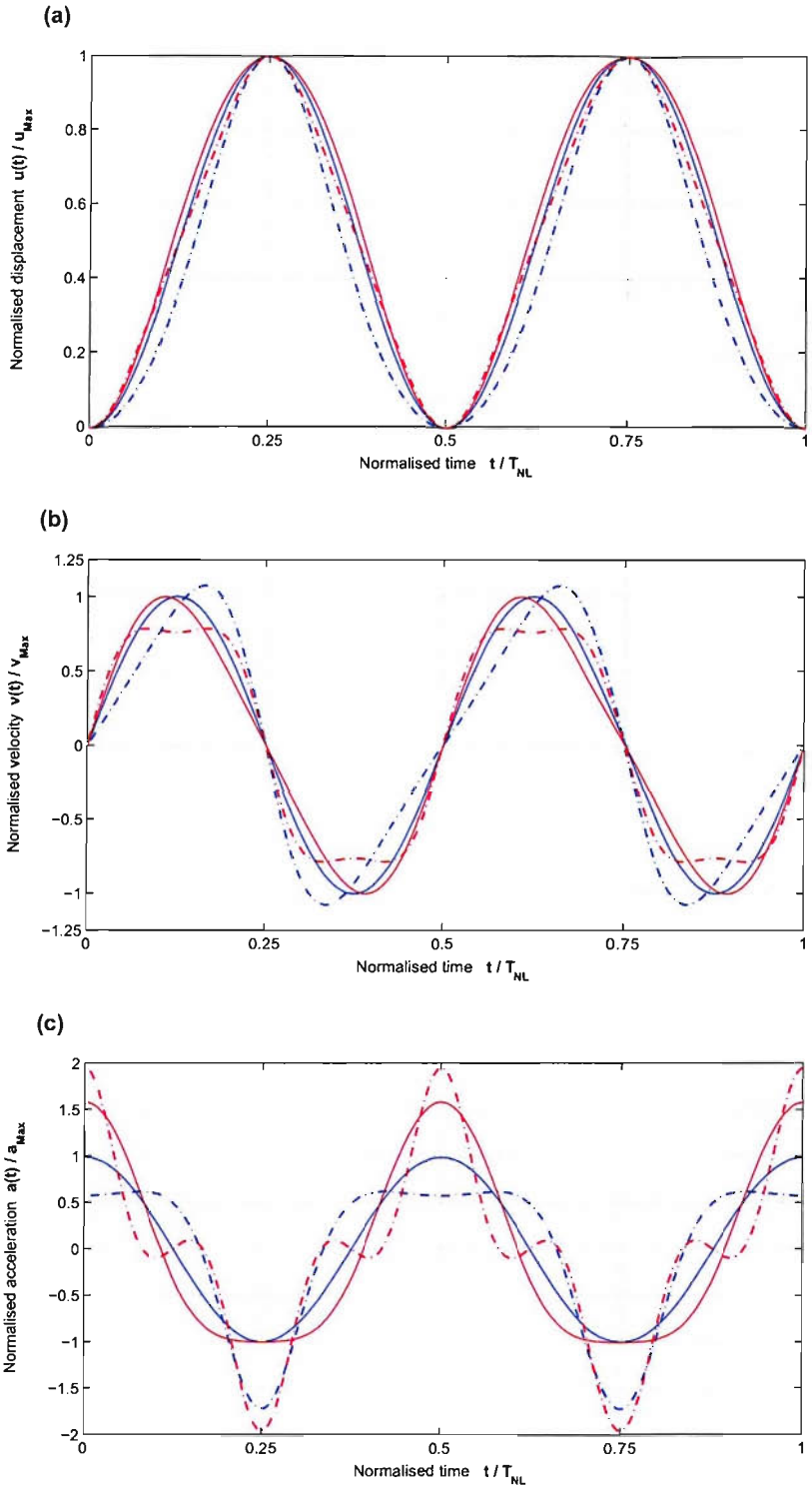

Figure 4.9 – Direct comparison of exact numerical solution (Runge-Kutta) and single-term approximation using **method 1** for maximum levels of average and total error. *Hardening-type* system: $e_{av} = 15.7\%$, $e_{tot} = 24.9\%$. *Softening-type* system $e_{av} = 14.5\%$, $e_{tot} = 35.8\%$. Line types: —— exact, – · – · – single-term. Normalised response for **(a)** displacement, **(b)** velocity, **(c)** acceleration. Parameters: $f_n = 0.5\,\text{Hz}$, $k_\alpha = 4\,m\,\pi^2\,f_n^2$ and $m = 0.3\,\text{kg}$. **Blue** lines: *hardening-type* spring with $p_0 = 0.1\,\text{N}$, $k_\gamma = 3\,\text{m}^2$. **Red** lines: *softening-type* spring with $p_0 = 0.2\,\text{N}$, $k_\gamma = -16\,\text{m}^2$.

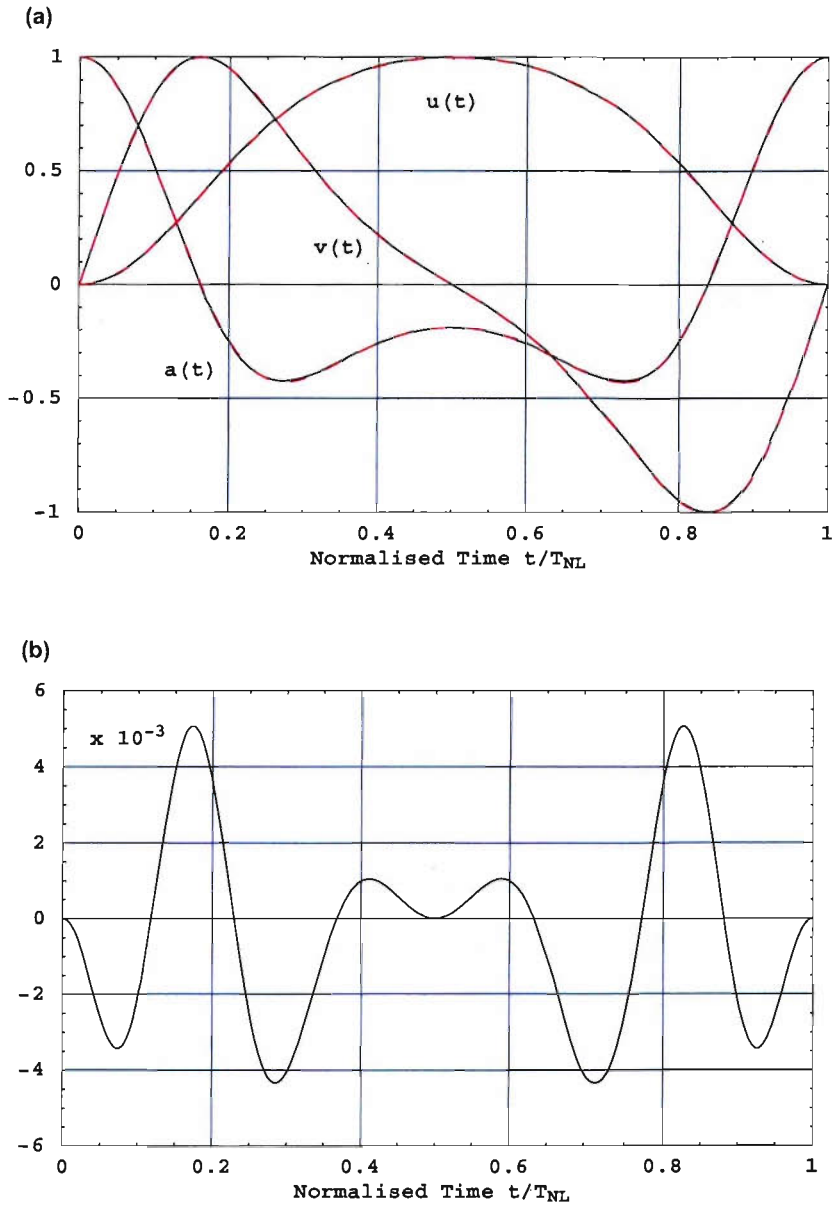

Figure 4.10 – Direct comparison of exact numerical solution (Runge-Kutta) and single-term approximation using **method 2** for maximum levels of average and total error, $e_{av} = 0.0098\%$ and $e_{tot} = 0.11\%$, respectively. **(a)** Normalised response for displacement, velocity, and acceleration. Line types: —— exact, – – – single-term. **(b)** Time-varying residue $R(t)$ of the approximation. Parameters: $f_n = 0.5\,\text{Hz}$, $k_\alpha = 4\,m\,\pi^2 f_n^2$ and $m = 0.3\,\text{kg}$. *Softening-type* spring with $p_0 = 0.2\,\text{N}$, $k_\gamma = -16\,\text{m}^2$.

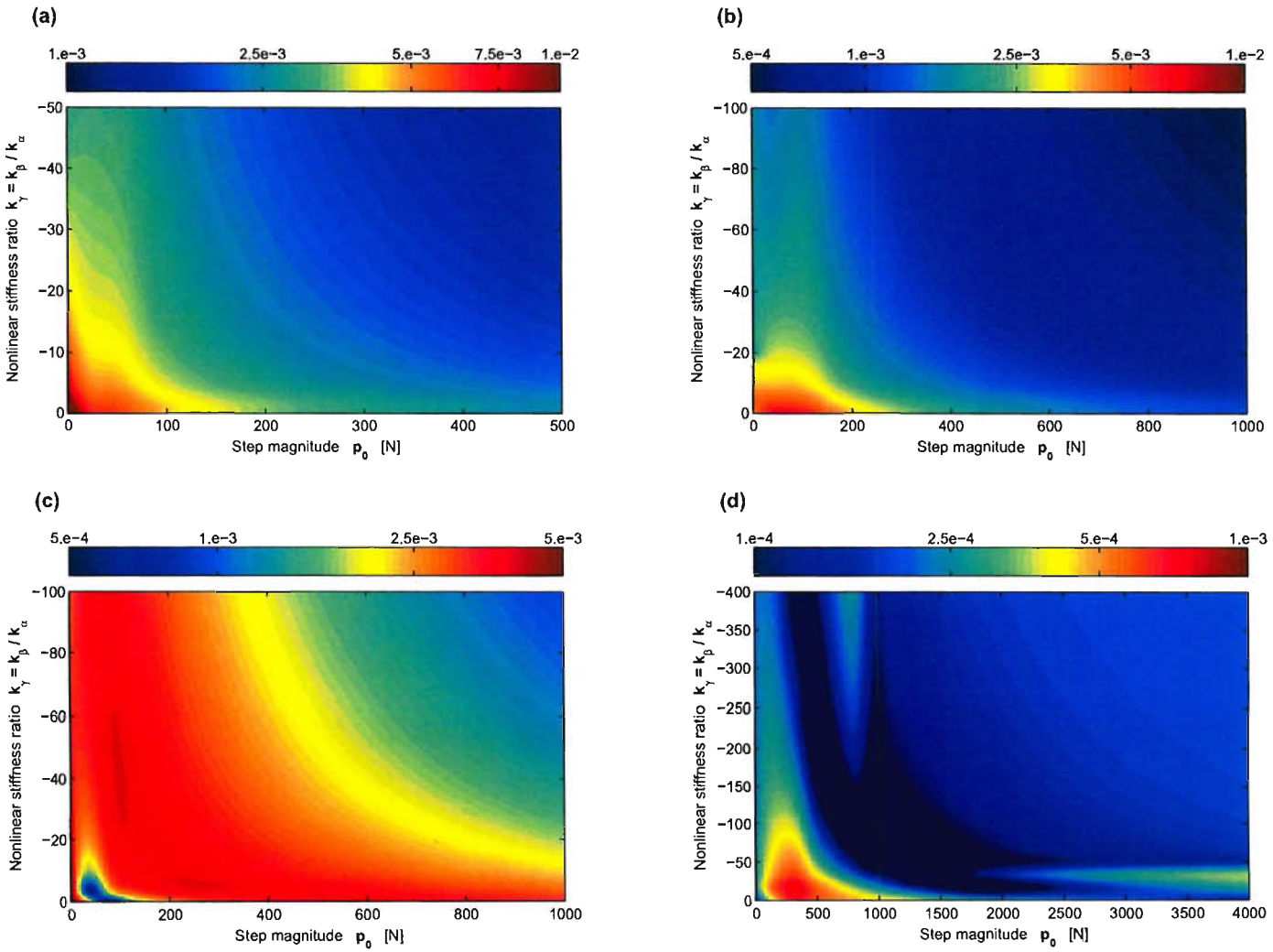

Figure 4.11 – Nonlinear snap-through spring ($k_\alpha < 0, k_\beta > 0$): **Method 2 - average error** e_{av} in percent for different linear stiffness coefficients $k_\alpha = 4\pi^2 f_n^2 m$ of the constant excitation force approximation. **(a)** $f_n = 0.5$ Hz, **(b)** $f_n = 5$ Hz, **(c)** $f_n = 50$ Hz, **(d)** $f_n = 500$ Hz. Parameter values: mass $m = 0.3$ kg.

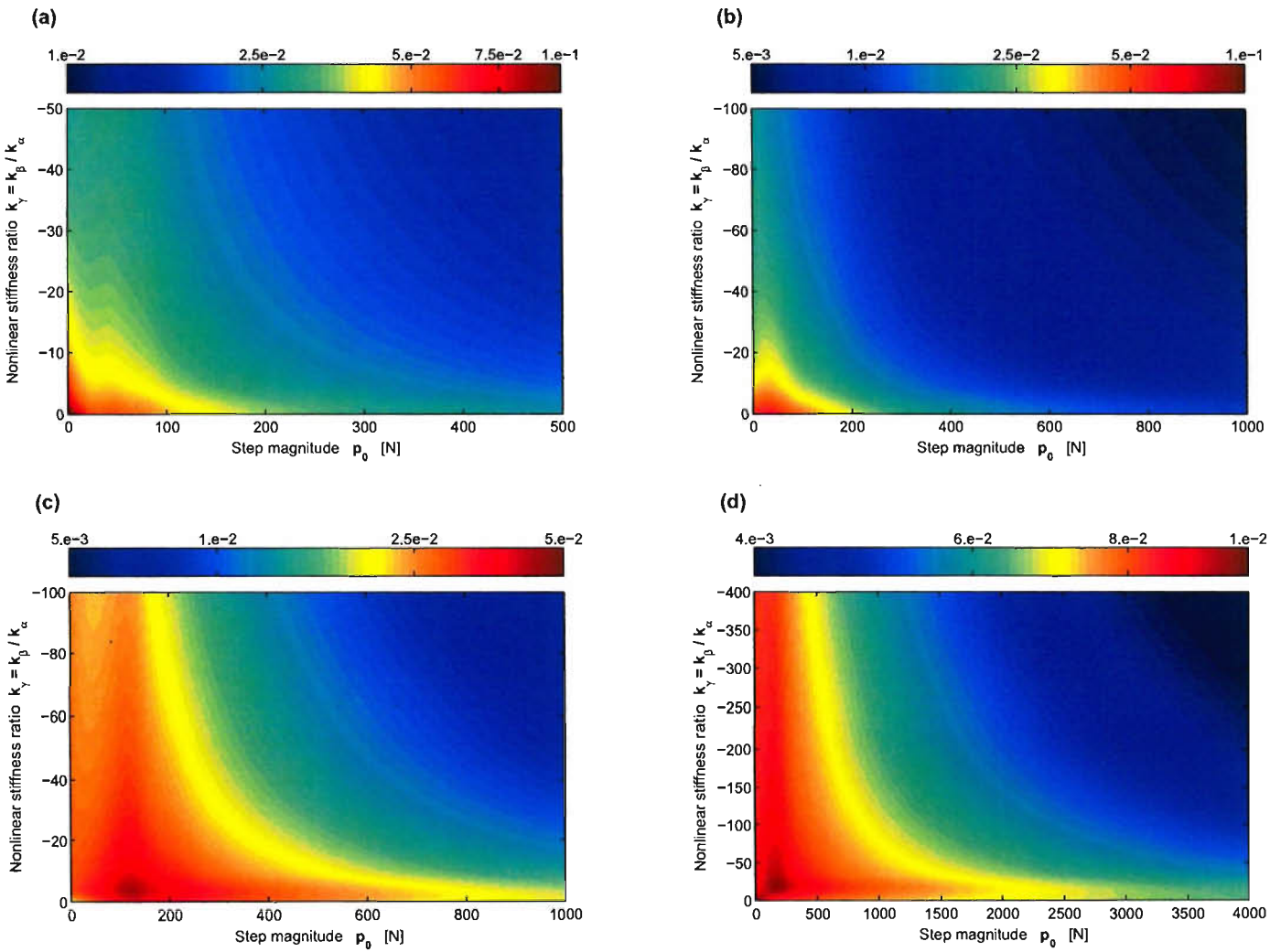

Figure 4.12 – Nonlinear snap-through spring ($k_\alpha < 0, k_\beta > 0$): **Method 2 - total error** e_{tot} in percent for different linear stiffness coefficients $k_\alpha = 4\pi^2 f_n^2 m$ of the constant excitation force approximation. **(a)** $f_n = 0.5$ Hz, **(b)** $f_n = 5$ Hz, **(c)** $f_n = 50$ Hz, **(d)** $f_n = 500$ Hz. Parameter values: mass $m = 0.3$ kg.

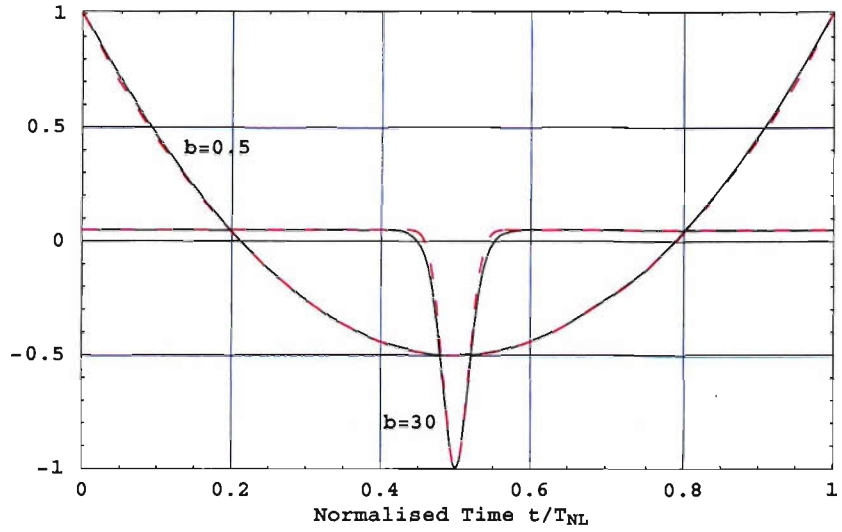

Figure 4.13 – Direct comparison of exact numerical solution (Runge-Kutta) and single-term **acceleration approximation** using equation (4.70) for maximum levels of average and total acceleration error. *Normalised acceleration* $\ddot{u}(t)/\ddot{u}_{\max}$. Cases: $b = 0.5$ with $e_{\text{av,a}} = 8.45\,\text{E}-1$ and $b = 30$ with $e_{\text{av,a}} = 8.26$. Line types: —— exact, – – – single-term. Parameter values: $f_{\text{n}} = 5$ Hz, $m = 0.3$ kg, $\omega_{\text{n}} = 2\pi f_{\text{n}}$, $k_\beta = m\,\omega_{\text{n}}^2$, and $p_0 = 200$ N.

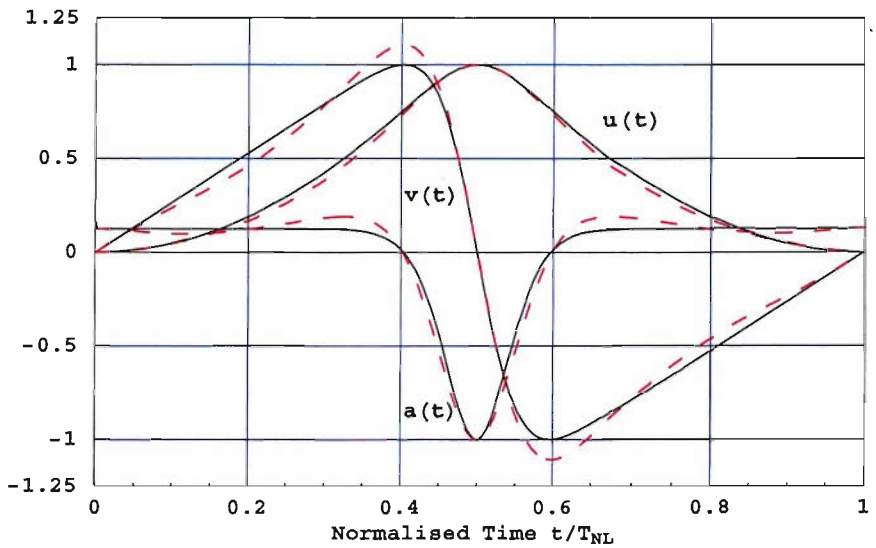

Figure 4.14 – Direct comparison of exact numerical solution (Runge-Kutta) and single-term **displacement approximation** for the system in (3.78) with $b \equiv 8$ using equation (4.61) for maximum levels of average and total error according to table 4.2, $e_{\text{av}} = 14.61\%$ and $e_{\text{tot}} = 135.9\%$, respectively. *Normalised response for displacement* $u(t)/u_{\max}$, *velocity* $\dot{u}(t) = v(t)/\dot{u}_{\max}$, and *acceleration* $\ddot{u}(t) = a(t)/\ddot{u}_{\max}$. Line types: —— exact, – – – single-term. Parameter values: $f_{\text{n}} = 0.5$ Hz, $m = 0.3$ kg, $\omega_{\text{n}} = 2\pi f_{\text{n}}$, $k_\beta = m\,\omega_{\text{n}}^2$, and $p_0 = 0.1$ N.

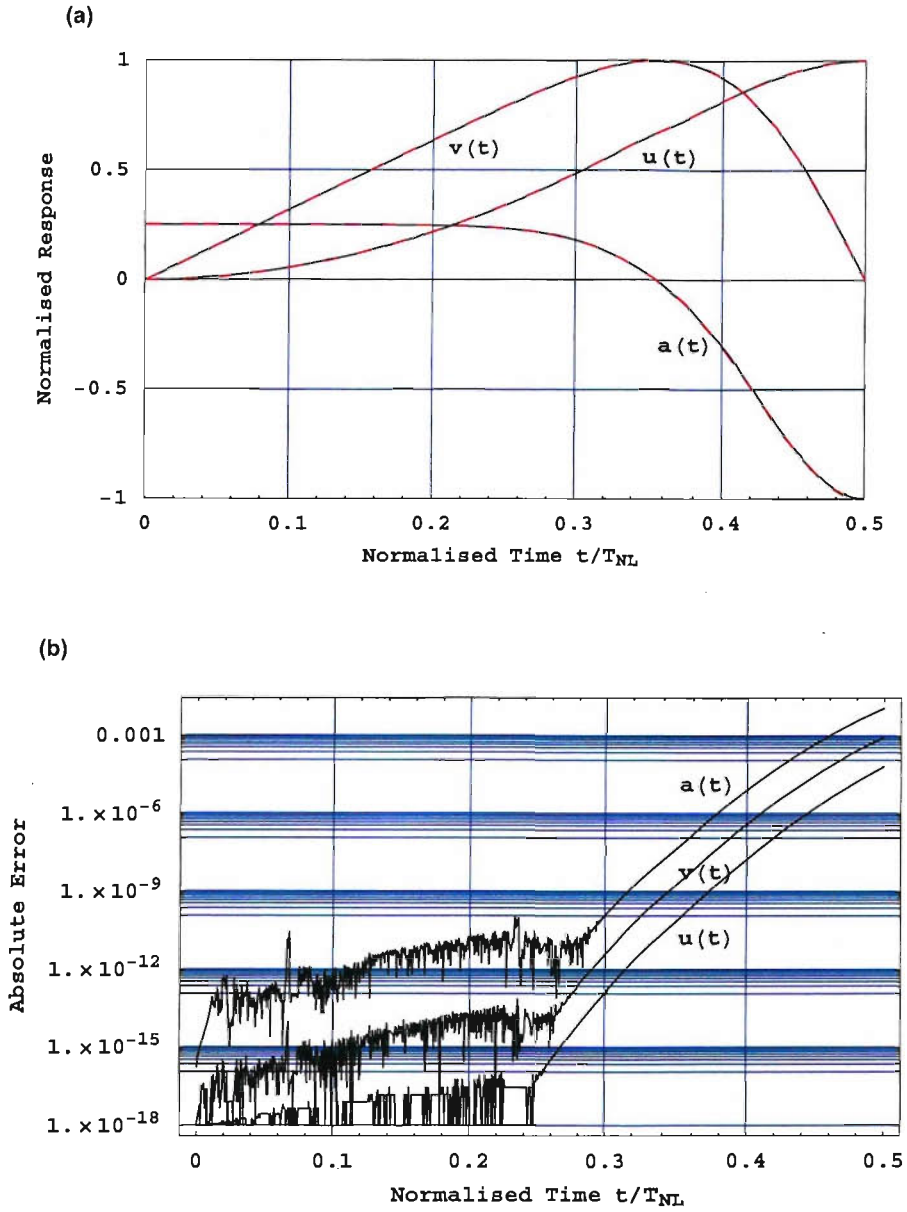

Figure 4.15 – Direct comparison of exact numerical solution (Runge-Kutta) and **10-term Picard iteration** summation for the system in (3.78) with $b \equiv 8$ using the iteration procedure in table 4.3 for maximum levels of average and total error according to table 4.4, $e_{\,\mathrm{av}} \approx e_{\mathrm{tot}} = 5.013\,\mathrm{E}{-2}\,\%$. (a) *Normalised response for displacement* $u(t)/u_{\max}$, *velocity* $\dot{u}(t) = v(t)/\dot{u}_{\max}$, and *acceleration* $\ddot{u}(t) = a(t)/\ddot{u}_{\max}$. Line types: —— exact, – – – single-term. (b) Absolute error for displacement $u(t) - \widetilde{u}(t)$, velocity $\dot{u}(t) - \dot{\widetilde{u}}(t)$ and acceleration $\ddot{u}(t) - \ddot{\widetilde{u}}(t)$. System parameter values: $f_{\mathrm{n}} = 0.5\,\mathrm{Hz}$, $m = 0.3\,\mathrm{kg}$, $\omega_{\mathrm{n}} = 2\pi f_{\mathrm{n}}$, $k_\beta = m\,\omega_{\mathrm{n}}^2$, and $p_0 = 0.1\,\mathrm{N}$.

CHAPTER 5

NONLINEAR NONAUTONOMOUS SDOF SOLUTIONS

5.1 Introduction

The previous chapter clearly revealed that complete analytical solutions for the Duffing system can only be found under special circumstances such as total energy conservation and periodic oscillation.[1)] Moreover, in case of the restoring force $f_1(u)$ it was completely impossible to obtain a closed form solution expression even under such stringent specifications. To the authors knowledge no such expressions have been published elsewhere yet.[2)] The promising attempt of integral approximation series given in section 4.4 quickly produces expressions too difficult to solve if employed for more general conditions such as damped oscillation or time-dependent applied forcing. Although the method is determined to converge to the exact solution of the linear or nonlinear system, its practical use is of limited value and confined to only a very small number of special cases.

This makes it necessary to derive a more generalised mathematical method which efficiently solves a large variety of nonlinear problems and is not restricted to extensively simplified, special cases. It would be desirable if the method would be applicable to high-order differential equations and first-order systems alike. In the very likely circumstance it cannot produce closed-form solutions, the approximate expression should ideally converge to the exact solution of the problem. Furthermore, it would be especially advantageous if the method is analytical or at least semi-analytical in nature, thus providing ways of analysing the problem with a unique mathematical insight. This presents a comprehensive list of essential requirements which seem hard to satisfy by

[1)] This does *not* exclude transient forced systems. It has been shown in section 3.3 that an ideal impulse excitation can be modelled using modified initial conditions and thus resulting in periodic response behaviour. However, the autonomy of the oscillator is essential.

[2)] Only for the special case of $b \equiv 2$ exists an analytical solution for a SDOF system [43].

a single method. However, an extensive literature research suggested that the Taylor Differential Transformation (TDT) might represent such a versatile approach.

The method furnishes an analytical-approximate way of solving systems of differential equations[3] using simple transformation laws, avoiding the necessity of directly finding a solution for the original linear or nonlinear problem. The equations of the physical system are rewritten as a functional series, which approaches the exact solutions as the number of terms in the series tends towards infinity. All unknown series coefficients are determined by differential spectra obtained from basic domain transformations of the original differential equation considering initial or boundary conditions. In this chapter the TDT is applied to nonlinear first and higher order systems similar to equation (3.15) having either $f_1(u)$ or $f_2(u)$ as the restoring force. Additionally, viscous damping and transient external forcing are considered. The application to first-order systems exploits a more generic adaption of the approach especially with respect to solving MDOF systems. In comparison, as will be seen in what follows, treatment of ordinary n-order differential equations can involve significantly more complex transformation operations. However, results are completely identical and both versions of the TDT are easily implemented in machine executable routines, but in terms of computational efficiency, using the n-order system transformation significantly speeds up calculations.

In order to explicitly show accuracy and efficiency of the new method, when compared to established but purely numerical solution algorithms, the conservative autonomous Duffing system is analysed since this allows for direct verification with exact closed-form solutions from chapter 4. However, it will also be shown that an equally effective error analysis methods exist by simply substituting the system's response parameters back into the governing differential equation and calculating a time varying residue. Since displacement, velocity, and acceleration obtained by a N-term TDT are not the exact values, the size of the residue indicates the absolute error of the approximation. Although this requires an accurate expression for the second time derivative of the unknown parameter,[4] the method is easily applicable to the majority of nonlinear cases where no exact solutions can be obtained and reliable error estimation tools are lacking. However, it will be shown in section 5.2.1 that even if an analytical expression exist, round-off and approximation series representation errors can have tremendous negative effects on the numerical implementation accuracy.[5] This can lead to a wrong relative error between 'exact' and analytically approximated results and subsequently to a biased judgement of the approximate solution performance. Using the newly proposed residue method instead such a situation cannot arise, since all response data is of equal absolute numerical error and the residue must always tend towards zero.

Rewriting the coupled system of n first-order differential equations as a single ODE of order n significantly reduces calculation time of the TDT implementation, additionally performance is gained by deriving a time-step normalised version of the new method. Although the procedure is

[3] Application to higher-order differential problems is automatically ensured since every n-order equation can be rewritten as a system of n first-order equations [235].

[4] In case of displacement as obtained from structural oscillation this is the acceleration $\ddot{u}(t) = \partial^2 u(t)/\partial t^2$.

[5] This refers to the specific example of the recursive Laden-Transformation [109, 288] in MATLAB® [294] for approximating Jacobian elliptic functions and values of elliptic integrals.

not as easily applicable to MDOF systems as the transformation of n coupled equations, it presents a remarkable increase in computational speed for the solution of the simple SDOF oscillator.

By extending the TDT to dissipative, linear and nonautonomous SDOF systems reveals significant advantages of the method over currently available numerical routines such as embedded Runge-Kutta and Adam-Bashford predictor-corrector algorithm [294]. The linear oscillator has been chosen for performance and accuracy comparison, since its highly transient response behaviour can be described using a closed-form analytical expression [270].

Finally, section 5.2.3 combines all previously derived results of the chapter to obtain novel expressions for the response prediction of highly transient, dissipative, nonlinear SDOF and MDOF oscillatory systems. Since no exact analytical solution exists, both methods namely Runge-Kutta and Taylor Differential Transformation are compared using the earlier introduced residue approach.

5.2 Application of the Taylor Differential Transformation (see also Appendix C)

Considering equation (3.15) with $f(u_1) \equiv f_1(u_1)$ and $p_0 \equiv 0$, the first-order system equations are

$$\begin{Bmatrix} \dot{u}_1 \\ \dot{u}_2 \end{Bmatrix} = \begin{Bmatrix} u_2 \\ -\omega_\alpha^2 u_1 - \omega_\beta^2 u_1^3 \end{Bmatrix} . \tag{5.1}$$

Analytical exact solutions for the autonomous conservative oscillator (5.1) are available in chapter 4. Every term of the first-order differential systems (5.1) can be transformed into a discrete-valued spectral domain, the so-called K-domain, employing the rules of the Taylor Differential Transformation in table C.1. Thus,

$$\begin{aligned} &\mathcal{D}\{u_1\} = U_1(k),\ \mathcal{D}\{u_2\} = U_2(k),\ \mathcal{D}\left\{\omega_\alpha^2 u_1\right\} = \omega_\alpha^2 U_1(k),\ \mathcal{D}\left\{\omega_\beta^2 u_1^3\right\} = \omega_\beta^2 U_1^{\{3\}}(k), \\ &\mathcal{D}\{\dot{u}_1\} = (k+1)\,U_1(k+1),\ \mathcal{D}\{\dot{u}_2\} = (k+1)\,U_2(k+1)\,, \end{aligned} \tag{5.2}$$

where $\mathcal{D}\{...\}$ is the differential transformation operator from (C.2b). Dividing the time interval of interest in $i = 1, 2, ..., n$ sub-intervals according to figure C.1, hence $h_i \in [t_0, t_0 + H]$ where $t_{i-1} \le t \le t_i$, leads for the differential system in (5.1) to the following coupled algebraic equations in the associated K-domain

$$\begin{Bmatrix} U_{1,i}(k+1) \\ U_{2,i}(k+1) \end{Bmatrix} = \frac{1}{k+1} \begin{Bmatrix} U_{2,i}(k) \\ -\omega_\alpha^2 U_{1,i}(k) - \omega_\beta^2 U_{1,i}^{\{3\}}(k) \end{Bmatrix} , \quad \text{for} \quad k = 0, 1, 2, ..., \infty , \tag{5.3a}$$

with the initial conditions $U_{1,1}(0) \equiv u_0$ and $U_{2,1}(0) \equiv \dot{u}_0$. In a more compact notation this gives

$$\mathbf{U}_i(k+1) = \frac{1}{k+1}\, g\Big(\mathbf{U}_i(k)\Big) , \qquad \text{where} \qquad \mathbf{U}_1(0) \equiv \mathbf{u_0} , \tag{5.3b}$$

and $g\big(\mathbf{U}_i(k)\big)$ is a function of $U_{1,i}(k)$ and $U_{2,i}(k)$. Both mass-normalised stiffness constants $\omega_\alpha = \sqrt{k_\alpha/m}$, $\omega_\beta = \sqrt{k_\beta/m}$ have previously been introduced and $U_{1,i}(k)$, $U_{2,i}(k)$ are the K-domain transformations of displacement $u_1(t)$ and velocity $u_2(t)$, respectively, for every time-step i according to the basic mathematical operations in table C.1. The expression $U_{1,i}^{\{3\}}(k)$ denotes a triple convolution and is obtained as

$$U_{1,i}^{\{3\}}(k) = U_{1,i}(k) \otimes U_{1,i}(k) \otimes U_{1,i}(k) = U_{1,i}(k) \otimes \sum_{p=0}^{k} U_{1,i}(p)\, U_{1,i}(k-p)$$

$$= U_{1,i}(k) \otimes U_{1,i}^{\{2\}}(k) = \sum_{q=0}^{k} U_{1,i}(q)\, U_{1,i}^{\{2\}}(k-q)\,. \tag{5.4}$$

Together with (C.4b) the exact analytical solution in the i-th time step h_i for the original problem in (3.15) is given as

$$\mathbf{u}_i(t) = \sum_{k=0}^{N=\infty} (t-t_i)^k\, \mathbf{U}_i(k) \qquad \text{where} \qquad t = [t_{i-1}, t_i]\ . \tag{5.5a}$$

Obeying the condition for the initial values at every interval h_i, see equation (C.4c), the solution for system (3.15) at each grid point $t_i = \sum_{j=0}^{i} h_j$ is obtained from

$$\mathbf{u}_i(t = t_i) = \mathbf{u}_{i+1}(t \equiv t_i) = \sum_{k=0}^{N=\infty} h_i^k\, \mathbf{U}_i(k)\,, \qquad h_i = t_i - t_{i-1}\,. \tag{5.5b}$$

Finally, the closed-form overall solution for $t \in [t_0, t_0 + H]$ is the set of n sub-interval solutions

$$\mathbf{u}(t) = \left\{ \mathbf{u}_i(t_i) \;\middle|\; \forall\, t = t_i \in \left[t_0 + \sum_{j=0}^{i-1} h_j,\ t_0 + \sum_{j=0}^{i} h_j \right],\ i = 1, 2, \ldots, n \right\}. \tag{5.6}$$

Both, efficiency and accuracy of the new TDT method if compared to well-established purely numerical approaches such as embedded Runge-Kutta (RK) algorithms [1,2,156,157,307] can be examined in two possible ways. Obviously, if exact analytical solutions for the differential system under study are available, it is straightforward to directly compare dynamic response results produced by the different algorithms. But without a closed-form solution such an explicit course is not possible. Moreover, for nonconservative systems a total energy comparison strategy as performed in the previous chapters cannot be applied. Instead the fact is used that all data obtained from either TDT or RK must still satisfy the differential equations, from which they have been obtained, for all time t within the solution interval $t \in [t_0, t_0 + H]$. Thus, reinserting displacement, velocity and acceleration derived for the structural system in (3.15) back into the governing second-order differential equation (4.1) will yield a residue $R(t) \neq 0$, since results from both TDT and RK do not coincide with the exact solutions. Clearly, the method which produces the smallest absolute $R(t)$ must be the more accurate one.

Unfortunately, a major disadvantage arises when using this approach with the system of two

coupled, first-order equations as given in (5.3), since verification of results by reinserting them into (4.1) requires a solution for the SDOF acceleration $\ddot{u}(t)$. One way of obtaining $\ddot{u}(t)$ is a straightforward numerical differentiation of the $u_2(t)$ data from (5.3a). This, however, is very prone to numerical errors. Satisfactory results of equal accuracy as the time histories for $u_1(t)$ and $u_2(t)$, directly obtained from the differential transformation, can only be achieved by high-order interpolation and very small time-stepping of the discrete numerical values solution vector for $u_2(t)$. A second and more accurate way of obtaining $\ddot{u}(t)$ follows from incorporating all three response parameters, namely displacement, velocity and acceleration into the solution of the differential system. Although, to the authors knowledge, this simple yet efficient method of comparison has not been used in literature so far, results obtained compare excellently to analytically derived data[6)] Thus, the second-order equation (4.1) is once more differentiated with respect to time, yielding

$$\dddot{u}(t) + \omega_\alpha^2\,\dot{u}(t) + 3\,\omega_\beta^2\,\dot{u}(t)\,u^2(t) = 0 \tag{5.7a}$$

with an additional, third initial condition

$$\ddot{u}(t \equiv 0) = \ddot{u}_0 = -\,\omega_\alpha^2\,u_0 - \omega_\beta^2\,u_0^3 \tag{5.7b}$$

given that $p_0 \equiv 0$. Rewriting (5.7a) as coupled first-order system is straightforward

$$\begin{Bmatrix} \dot{u}_1 \\ \dot{u}_2 \\ \dot{u}_3 \end{Bmatrix} = \begin{Bmatrix} u_2 \\ u_3 \\ -\omega_\alpha^2\,u_2 - 3\,\omega_\beta^2\,u_2\,u_1^2 \end{Bmatrix}, \tag{5.8}$$

with $u_1(t \equiv 0) = u_0$, $u_2(t \equiv 0) = \dot{u}_0$, and $u_3(t \equiv 0) = \ddot{u}_0$ and has $u_p(t)$ with $p = 1, 2, 3$ as solutions. Together with the governing equation the residue $R(t)$ is then obtained as

$$R(t) = u_3(t) + \omega_\alpha^2\,u_1 + \omega_\beta^2\,u_1^3\,. \tag{5.9}$$

Transformation of system (5.8) into the TDT K-domain, see appendix C, gives for the i-th interval $t_{i-1} \le t \le t_i$ with $i = 1, 2, ..., n$ along the time grid the following algebraic system

$$\begin{Bmatrix} U_{1,i}(k+1) \\ U_{2,i}(k+1) \\ U_{3,i}(k+1) \end{Bmatrix} = \frac{1}{k+1} \begin{Bmatrix} U_{2,i}(k) \\ U_{3,i}(k) \\ -\omega_\alpha^2\,U_{2,i}(k) - 3\,\omega_\beta^2\,U_{1,i}^{\{3\}}(k) \end{Bmatrix}, \qquad k = 0, 1, 2, ..., \infty\,, \tag{5.10a}$$

with the convolution

$$U_{1,i}^{\{3\}}(k) = U_{2,i}(k) \otimes U_{1,i}^{\{2\}}(k) = \sum_{q=0}^{k} U_{2,i}(q)\,U_{1,i}^{\{2\}}(k-q)\,, \tag{5.10b}$$

and the expression $U_{1,i}^{\{2\}}(k)$ from equation (5.4). The initial conditions are given as $U_{1,1}(0) \equiv u_0$,

[6)] In those rare cases where closed-form solutions are available. However, the method works for all differential systems, either linear or nonlinear, independent of the analytical or numerical solution procedure.

$U_{2,1}(0) \equiv \dot{u}_0$, and $U_{3,1}(0) \equiv \ddot{u}_0$, thus rewriting (5.10a) in a more compact form similar to (5.3b) above leads to

$$\mathbf{U}_i(k+1) = \frac{1}{k+1}\, g\Big(\mathbf{U}_i(k)\Big)\,, \qquad \text{where} \qquad \mathbf{U}_1(0) \equiv \mathbf{u_0}\,. \tag{5.10c}$$

For the unforced Duffing oscillator[7] with general initial conditions

$$u_{01} = u_0 \neq 0\,, \quad u_{02} = \dot{u}_0 \neq 0\,, \tag{5.11}$$

and thus $\ddot{u}_0 \neq 0$, a closed-form solution has been derived in equation (4.25). Inserting these expressions into (5.9) leads to $R(t) = 0$ for all $t = [t_0, t_0 + \Delta T]$ where ΔT is the time interval of interest. In practice, due to numerical errors, this is not always the case and the accuracy with which $R(t)$ for the analytical solution can be established heavily depends on the computational environment.[8] This fact reveals the two significant advantages of using the residue from (5.9) as a benchmark for comparing both methods TDT and RK instead of solely examining the error between the exact analytical and approximate solution:

(1) The residue of the governing differential equation can always be obtained, independent of whether exact analytical solutions are available or not.

(2) Calculating the exact solution, if it exists, at discrete time-points is subject to round-off errors. Therefore, subtracting from it the approximate solution results produces an error indicator which is biased twice as much by numerical errors than the residue of the associated differential equation. The theoretical value of $R(t)$ is fixed to zero for all $t \in [t_0, t_0 + \Delta T]$ regardless of the computational precision of the environment.

An important remark must be made here regarding the above concept. If the differential system satisfies the Lipschitz condition in (3.13), or the condition applied to (3.133) resulting from theorem 4 and 5 in chapter 3 for non-Lipschitzian oscillators, then there is no possibility that the approximating method, either TDT, RK or others, diverts to a non-unique branch of the n-dimensional solution space of the differential system, which might satisfy the equation for $R(t)$ but is not feasible. In other words, if the system possesses a unique analytical solution, although it cannot be obtained, the numerical approximation will follow exactly the same solution trajectory in the corresponding n-dimensional phase space with n being the number of unknown state variables. This follows directly from basic principles of existence and uniqueness [234] and bifurcation theory [125].

5.2.1 Nonlinear autonomous systems

The error between the exact analytical solution from equation (4.25) and a MATLAB® variable order predictor-corrector (PECE) Adams-Bashforth-Moulton routine (`ode113`) is given in figure 5.1(b) for all three response variables, namely displacement $u_1(t)$ – (○), velocity $u_2(t)$ – (□)

[7] Zero right-hand side. The case of Dirac-delta excitation is included in the analytical solution.

[8] This has been discussed to some extent in chapter 4.

and acceleration $u_3(t)$ – ($\Diamond$). The distance between two identical symbols marks the size of a time step used in the adaptive algorithm. For a time interval of $\mathcal{T}_{\mathsf{NL}} = [0, 0.1469\,\mathrm{s}]$ marking exactly one oscillation cycle 292 steps have been used. Smallest, largest and average step size are 3.141 E–10, 5.929 E–4, and 5.047 E–4 seconds, respectively. Calculation time on an almost idle 64-bit AMD Athlon 3.2 Ghz cluster node was on average 0.56 s for the system of three coupled, first-order differential equations in (5.8).

Figure 5.1(a) shows the corresponding time history for one oscillation cycle with normalised magnitude obtained from the exact analytical solution in (4.25). The far greater distance between identical symbols originates from the adaptive differential transformation approach for the system of three algebraic equations in (5.10). The error of the method compared to the exact solution is given in figure 5.2(a). Clearly, for the same interval $\mathcal{T}_{\mathsf{NL}}$ of 0.1469 s only 11 steps were necessary with an average of 1.341 E–2 seconds. Smallest and largest time step were 5.911 E–3 and 1.648 E–2 seconds, respectively, with the first one due to the fact that the computation was restricted to $0 \leq t \leq \mathcal{T}_{\mathsf{NL}}$, and not due to accuracy iterations as in the RK routine. Although 110 terms have been used in the algebraic-approximate solution series (5.5a), computation time was on average only 0.24 s, 43% of the time required for the RK solver. Furthermore, accuracy of the new TDT approach is orders of magnitude higher if compared to RK by using either the exact solution shown in Fig. 5.2(a) or the governing ODE residue $R(t)$ from Eq.(5.9) in 5.2(b). A closer examination of both graphs (a) and (b) in figure 5.2 reinforces the application of the residue method as a valuable accuracy benchmark. While the error in Fig. 5.2(a) appears to increase linearly, figure (b) suggests the contrary: data from the TDT algorithm in the last quarter of the normalised one-cycle time interval $0 \leq t/\mathcal{T}_{\mathsf{NL}} \leq 1$ satisfies (5.9) more accurately than the numerical approximation of the exact analytical solution. A direct comparison of obtained data within the scalable working precision environment of MATHEMATICA® shows that, due to the limited floating-point arithmetics threshold of MATLAB®, results for Jacobian elliptic function approximations do not coincide with more exact data derived using MATHEMATICA® algorithms.[9] Therefore, in numerical computation one should not expect the anticipated 'exact' solution to be the definite benchmark.

The differential transformation method with the spectrum defined in (C.2b), inverse transformations according to (C.3) and subintervals from (C.4a) has recently been used by a number of authors [217, 219, 220] to solve first-order differential systems and the procedure has been implemented in this work for the autonomous Duffing oscillator in equations (5.3b), (5.5) and (5.6) solving the system in (5.8). However, given the definition of the time interval $h_i = t_i - t_{i-1}$ in (C.4) and the resulting fact that all spectra at t_i are obtained according to (5.5b), lets $\mathbf{U}(k) \to \infty$ if k approaches values significantly larger than 1. This is easily demonstrated supposing h_i =0.002 s, thus, with k =110 the expression h_i^k from (5.5b) yields 1.298 E–297, which is just above the value of 2.225 E–308, the smallest positive floating-point number obtainable in MATLAB® [294]. Unfortunately, the number of terms in the approximation series (5.5) is therefore restricted due to the resource limits of the computational environment.

This can easily be avoided by normalising each time interval to $t_i \in [0, h_i]$. The spectra from

[9] See the discussion in chapter 4.

(C.2b) are then defined as

$$\mathbf{U}_i(k) = \frac{h_i^k}{k!}\left[\frac{\partial^k \mathbf{u}(t)}{\partial t^k}\right]_{t=t_0} \equiv \mathcal{D}\left\{\mathbf{u}_i(t)\right\}, \tag{5.12a}$$

and the time-domain solution is obtained from

$$\mathbf{u}_i(t) = \sum_{k=0}^{N}\left(\frac{t_i}{h_i}\right)^k \mathbf{U}_i(k) \equiv \mathcal{D}^{-1}\left\{\mathbf{U}_i(k)\right\} \qquad \text{where} \qquad t_i = [0, h_i], \tag{5.12b}$$

thus

$$\mathbf{u}_i(h_i) = \sum_{k=0}^{N}\mathbf{U}_i(k), \tag{5.12c}$$

and the response parameters $\mathbf{u}_i$ along the time grid in Fig. C.1 are simply a summation of the K-domain spectra $\mathbf{U}_i(k)$ for every time step h_i. Furthermore, with $h_i \leq 1$ equation (5.12a) assures that all $\mathbf{U}_i(k)$ approach zero as $k \to \infty$. With a new definition for the K-domain spectra, transformation rules given in table C.1 are no longer valid. Since the time t is now normalised with respect to the upper limit of the interval, i.e. t/h_i, the time step h_i must under specific circumstance be included in the transformation process. Table 5.1 shows the basic mathematical operations for the spectra defined in (5.12) and should be compared to table C.1.

Finally, both equations (5.12a) and (5.12b) require the algebraic system given in (5.10c) to be changed into

$$\mathbf{U}_i(k+1) = \frac{h_i}{k+1}\, g\Big(\mathbf{U}_i(k)\Big), \qquad \text{where} \qquad \mathbf{U}_1(0) \equiv \mathbf{u_0}, \tag{5.12d}$$

and the step size control condition in (C.10) must be adjusted by replacing the spectra vector $\mathbf{X}_i(N+s)$ with

$$\frac{\mathbf{U}_i(N+s)}{h_i^{(N+s)}}. \tag{5.13}$$

The significant difference of the new formulation compared to (5.5) is shown in Fig. 5.2(b). Not only is the ODE residue up to one order of magnitude smaller, the entire interval has been calculate using only 6 time steps instead of 11 and therefore at about 70 % of the time required for the method using non-normalised spectra C.2. However, this can still be improved as will be seen in the next paragraph.

The purpose of rewriting (5.7) as a system of three differential equations was to demonstrate the ability of the TDT method to solve MDOF systems which cannot be reduced to single n-order differential equation. However, in dealing with SDOF systems additional computation time can be saved in directly transforming the n-order differential equation into the K-domain and solving only one algebraic equation instead of n. Application of table 5.1 to the third-order equation in

Table 5.1 – Basic differential transformation relations between the two domains for the interval time normalised spectra definitions in equation (5.12) [216].

Original function $g(t)$	Transformed function $G(k) = \mathcal{D}\{g(t)\}$
1	$\delta(k) = \begin{cases} 1 & \text{if} \quad k = 0 \\ 0 & \text{if} \quad k \neq 0 \end{cases}$
t	$h_i\,\delta(k-1)$
t^r	$h_i^r\,\delta(k-r)\,, \qquad r \in \mathbb{Z}$
$x(t) \pm y(t)$	$X(k) \pm Y(k)$
$ax(t)$	$aX(k)$
$x(t)\,y(t)$	$X(k) \otimes Y(k) = \sum_{l=0}^{k} X(l)\,Y(k-l)$
$\frac{x(t)}{y(t)}$	$\frac{X(k)-X(k)\otimes Y(k)}{Y(0)} = \frac{X(k)-\sum_{l=0}^{k} X(l)\,Y(k-l)}{Y(0)}$
$\left.\frac{\mathrm{d}^\nu x(t)}{\mathrm{d}t^\nu}\right\|_{t\in[0,h_i]}$	$\frac{(k+\nu)!}{h_i^\nu\,k!}\,X(k+\nu)$
$\mathrm{e}^{\lambda t}$	$\frac{(\lambda\,h_i)^k}{k!}$

(5.7a) results together with the new definition from (5.12) in

$$U_i(k+3) = -\frac{h_i^3\,k!}{(k+3)!}\left[\omega_\alpha^2\,\frac{k+1}{h_i}\,U_i(k+1) + 3\,\omega_\beta^2\left(\frac{k+1}{h_i}\,U_i(k+1)\right) \otimes \left(U_i^{\{2\}}(k)\right)\right] \tag{5.14a}$$

where $U_i^{\{2\}}(k)$ is obtained in a similar way as in (5.4). An explicit expression for the convolution is given by

$$\left(\frac{k+1}{h_i}\,U_i(k+1)\right) \otimes \left(U_i^{\{2\}}(k)\right) = \frac{1}{h_i}\sum_{q=0}^{k}(k-q+1)\;U_i(k-q+1)\,U_i^{\{2\}}(q)\,, \tag{5.14b}$$

and initial values for the spectra U_1 in the first time step if $k \equiv 0$ are obtained using the differentiation rule in table 5.1, thus

$$U_1(0) = u_0\,, \quad U_1(1) = h_1\,\dot{u}_0\,, \quad U_1(2) = \frac{h_1^2}{2}\,\ddot{u}_0\,. \tag{5.14c}$$

However, a serious problem arises in accurately determining the initial conditions for all subsequent intervals h_i with $i = 2, 3, \ldots$ due to the fact that the inverse transformation (5.12b) delivers only the zeroth derivative of the governing equation. In case of (5.7a) this is the displacement $u_i(t)$, which at the end of each step h_i is obtained from (5.12c), hence $U_2(0) \equiv u_1\,(h_1)$. However, $U_2(3)$ in (5.14a) if $k \equiv 0$ also depends on $U_2(1)$ for which no initial values are available. The op-

tion of numerical differentiation of the data for $u_1(t)$ must be ruled out due to accuracy issues.[10] It should be noted that if the approach is used for a single time step $h_i \equiv H$ covering the entire interval of interest, the problem does not arise. Chen and Wu [214], for example, have transformed the simpler second-order equation (4.1) and derived results for response using 12 elements and one single time step. Unfortunately, the authors have not compared their results to the available exact solution and significant discrepancies remain unnoticed. Jang *et al* [216] have used the approach for multiple time steps, but fail to derive an exact solution on how to obtain the initial conditions for every step h_i.

In order to overcome the lack of initial values for each subsequent time step h_i, it is therefore suggested to directly differentiate the time-domain solution in (5.12b) with respect to t, thus

$$\frac{\partial}{\partial t} u_i(t_i) = \frac{1}{h_i} \sum_{k=0}^{N} k \left(\frac{t_i}{h_i}\right)^{k-1} U_i(k), \quad \frac{\partial^2}{\partial t^2} u_i(t_i) = \frac{1}{h_i^2} \sum_{k=0}^{N} k(k-1) \left(\frac{t_i}{h_i}\right)^{k-2} U_i(k), \tag{5.15a}$$

and to obtain the initial conditions for each interval h_i from

$$\dot{u}_i(t_i = 0) = \dot{u}_{i-1}(t_{i-1} = h_{i-1}) = \frac{1}{h_{i-1}} \sum_{k=0}^{N} k\, U_{i-1}(k), \qquad \text{and}$$

$$\ddot{u}_i(t_i = 0) = \ddot{u}_{i-1}(t_{i-1} = h_{i-1}) = \frac{1}{h_{i-1}^2} \sum_{k=0}^{N} k(k-1)\, U_{i-1}(k), \tag{5.15b}$$

respectively. Implementation of Eqs.(5.12) to (5.15) is straightforward. The accuracy of the results obtained with (5.14a) remains unchanged compared to the coupled algebraic system in (5.10), but overall computational time for one oscillation decreases significantly from 0.168 s to 0.075 seconds, a speed increase by more than 200 %. Compared to the variable order Runge-Kutta algorithm `ode113()` solving the first-order system in (5.8) means the routine with equation (5.14) requires less than 15 % of the time needed by the MATLAB® predictor-corrector algorithm. A brief summary is given in table 5.2.

5.2.2 *Linear nonautonomous systems*

Results of the previous section clearly show the good performance of the TDT in modelling the steady-state response behaviour of autonomous nonlinear systems when compared to conventionally employed, purely numerical algorithms. In order to examine the capability of the method in dealing with highly transient external forcing, a linear SDOF system subjected to blast wave loading [308–311] is chosen. Results from the TDT method will be compared to a recently published analytical solution for linear systems by the present author [270]. Despite the fact that a SDOF oscillator is investigated and (5.15) would be most suitable, the third-order governing equation will be rewritten as a system of coupled first-order equations, since accuracy of both approaches

[10] This would imply extensive data re-sampling with a large number of equally spaced points in order to achieve reasonable accuracy.

Table 5.2 – Efficiency comparison of different routines for solving the third-order differential equation (5.7) for the system values given in both figure 5.1 and 5.2. Algorithm parameters and error tolerances are identical.

Algorithm	`ode113`	Eqs.(5.10)/(C.2)	Eqs.(5.10)/(5.12)	Eqs.(5.14)/(5.12)
Time Steps	296	11	6	6
Total Time	0.563 s	0.243 s	0.168 s	0.075 s
% of `ode113`	100 %	43 %	30 %	13 %

in (5.8) and (5.14) are identical, provided that in both cases the newly defined normalised spectra (5.12) are used.[11] Thus, with $k_\gamma \equiv 0$ and the time-domain excitation function of a typical Friedlander blast profile [311]

$$p(t) = p_0 \left(1 - \frac{t}{t_d}\right) \mathrm{e}^{-\frac{\alpha}{t_d} t}, \quad \rightarrow \quad \frac{\partial}{\partial t} p(t) = \dot{p}(t) = \frac{p_0}{t_d} \left[1 + \alpha \left(1 - \frac{t}{t_d}\right)\right] \mathrm{e}^{-\frac{\alpha}{t_d} t}, \tag{5.16}$$

equation (5.8) is rewritten in its nonconservative version

$$\begin{Bmatrix} \dot{u}_1 \\ \dot{u}_2 \\ \dot{u}_3 \end{Bmatrix} = \begin{Bmatrix} u_2 \\ u_3 \\ \frac{\widehat{p}_0}{t_d} \left[\alpha(t-1) - 1\right] \mathrm{e}^{-\frac{\alpha}{t_d} t} - 2\,\xi\omega_\alpha\, u_3 - \omega_\alpha^2\, u_2 \end{Bmatrix}, \mathbf{u}_0 = \begin{Bmatrix} u_1(0) \\ u_2(0) \\ u_3(0) \end{Bmatrix} \equiv \begin{Bmatrix} 0 \\ 0 \\ \frac{p_0}{m} \end{Bmatrix}. \tag{5.17}$$

with $\widehat{p}_0 = p_0/m$ as mass-normalised force magnitude, the damping ratio $\xi = c/2\sqrt{k\,m}$ and the constant c as viscous damping coefficient [228]. It is worth noting that both initial values for displacement and velocity do not need to be zero in order to be able to apply the TDT. This limitation is only necessary for the exact closed-form solution of (5.17) by means of solving its second-order counterpart [270]. Using the fundamental operations from table 5.1, the differential system (5.17) is subjected to a transformation for every interval $t_i \in [0, h_i]$ according to the definition of the spectra in (5.12), and thus is piecewise defined in its original time-domain. Unfortunately, this is not the case for the excitation function $p(t)$ and its derivative $\dot{p}(t)$ but can be accomplished by rewriting (5.16)

$$p_i\,(t_i) = p_0 \left[1 - \frac{t_i + \sum_{j=1}^{i} h_{j-1}}{t_d}\right] \mathrm{e}^{-\frac{\alpha}{t_d}\left(t_i + \sum_{j=1}^{i} h_{j-1}\right)} \tag{5.18a}$$

[11] The only difference between both approaches lies in the computational speed as can be seen in table 5.2.

leading for the first derivative to

$$\frac{\partial p_i\,(t_i)}{\partial t_i} = \dot{p}_i(t) = \frac{p_0}{t_d^2}\, \mathrm{e}^{-\frac{\alpha}{t_d}\left(t_i+\sum_{j=1}^{i} h_{j-1}\right)} \left[\alpha\left(t_i + \sum_{j=1}^{i} h_{j-1}\right) - t_d(1+\alpha)\right]$$
$$= \frac{p_0}{t_d^2}\left[z_{1,i}\,(t_i)\, z_{2,i}\,(t_i)\right] . \tag{5.18b}$$

Clearly, if $t_i \equiv 0$ Eq.(5.18a) gives the force magnitude at the time point $t = h_1 + \ldots + h_{i-1}$, and if $t_i \equiv h_i$ then (5.18a) becomes $p(t) = p\,(t = h_1 + \ldots + h_i)$. Transformation of (5.18b) into the spectral domain using table 5.1 is rather straightforward

$$\dot{P}_i(k) = \mathcal{D}\left\{\dot{p}_i\,(t_i)\right\} = \frac{p_0}{t_d^2}\left(Z_{1,i}(k) \otimes Z_{2,i}(k)\right) , \tag{5.19a}$$

where

$$Z_{1,i}(k) = \mathcal{D}\left\{\mathrm{e}^{-\frac{\alpha}{t_d}\left(t_i+\sum_{j=0}^{i} h_{j-1}\right)}\right\} = \frac{\mathrm{e}^{-\frac{\alpha}{t_d}\sum_{j=1}^{i} h_{j-1}}}{k!}\left(-\frac{\alpha}{t_d}\, h_i\right)^k , \tag{5.19b}$$

and

$$Z_{2,i}(k) = \mathcal{D}\left\{\alpha\, t + \alpha \sum_{j=1}^{i} h_{j-1} - t_d(1+\alpha)\right\}$$
$$= \alpha\, h_i\, \delta(k-1) + \left(\alpha \sum_{j=1}^{i} h_{j-1} - t_d(1+\alpha)\right)\delta(k) , \tag{5.19c}$$

thus

$$Z_{1,i}(k) \otimes Z_{2,i}(k) = \sum_{q=0}^{k}\left[\frac{\mathrm{e}^{-\frac{\alpha}{t_d}\sum_{j=1}^{i} h_{j-1}}}{q!}\left(-\frac{\alpha}{t_d}\, h_i\right)^q\right]\left[\alpha\, h_i\, \delta(k-q-1)\right.$$
$$\left. + \left(\alpha \sum_{j=1}^{i} h_{j-1} - t_d(1+\alpha)\right)\delta(k-q)\right] . \tag{5.19d}$$

Together with (5.19) the differential system in (5.17) is rewritten in the K-domain

$$\begin{Bmatrix} U_{1,i}(k+1) \\ U_{2,i}(k+1) \\ U_{3,i}(k+1) \end{Bmatrix} = \frac{h_i}{k+1}\begin{Bmatrix} U_{2,i}(k) \\ U_{3,i}(k) \\ \widehat{P}_i(k) - 2\,\xi\omega_\alpha\, U_{3,i}(k) - \omega_\alpha^2 U_{2,i}(k) \end{Bmatrix} , \quad \widehat{\dot{P}_i}(k) = \frac{\dot{P}_i(k)}{m} , \tag{5.20}$$

and initial conditions are given as $\mathbf{U}_1(0) \equiv \mathbf{u}_0$. Solving (5.20) leads together with definition (5.12b) to the time-domain solution for displacement, velocity and acceleration as shown in figure 5.3(a). The error when comparing the exact analytical solution for the nonconservative system [270] with the MATLAB® RK routine `ode113` is given in Fig. 5.3(b) and for the approximate

analytical TDT approach above in figure 5.4(a). With only 7 time steps and a total calculation time of 0.172 s the TDT delivers with more than twice the speed results which are up to 2 orders of magnitude more precise than compared to the `ode113` RK method (0.351 s). Indeed, figure 5.4(b) clearly indicates that solutions from Eq.(5.20) satisfy the governing differential equation with equal accuracy as the exact closed-form expression [270] provided the number of terms in series (5.12b) is large enough.

5.2.3 *Nonlinear nonautonomous systems*

So far the Taylor Differential Transformation has been successfully applied to strongly nonlinear, autonomous systems in section 5.2.1 and linear but nonautonomous, highly transient coupled differential equations in section 5.2.2. By appropriately combining the expressions derived in both sections it is possible to obtain analytically approximate solutions for the response behaviour of transient, nonlinear, dissipative SDOF and MDOF systems.

The differential equation under consideration is given by the generalised version of the nonlinear oscillator (5.8) having the arbitrary restoring stiffness force $f(u_1)$, and the nonautonomous, viscously damped system in (5.17), thus

$$\begin{Bmatrix} \dot{u}_1 \\ \dot{u}_2 \\ \dot{u}_3 \end{Bmatrix} = \begin{Bmatrix} u_2 \\ u_3 \\ \widehat{p}(t) - 2\,\xi\omega_\alpha\, u_3 - \frac{1}{m}\frac{\partial}{\partial t} f(u_1) \end{Bmatrix}, \qquad \widehat{p}(t) = \frac{1}{m}\frac{\partial}{\partial t} p(t) \tag{5.21a}$$

subjected to the general initial conditions

$$\mathbf{u}_0 = \begin{Bmatrix} u_1(0) & u_2(0) & u_3(0) \end{Bmatrix}^{\mathrm{T}} \equiv \begin{Bmatrix} u_0 & \dot{u}_0 & \widehat{p}(0) + \ddot{u}_0 \end{Bmatrix}^{\mathrm{T}} . \tag{5.21b}$$

In case of the Duffing oscillator $f(u_1) \equiv f_2(u) = k_\alpha\, u(t) + k_\beta\, u^3(t)$ the first derivative of the stiffness restoring force equates to the expression from (5.7a)

$$\frac{1}{m}\frac{\partial}{\partial t} f_2(u) = \omega_\alpha^2\, \dot{u}(t) + 3\,\omega_\beta^2\, \dot{u}(t)\, u^2(t) . \tag{5.22}$$

Similar, for $f(u_1) \equiv f_1(u) = k_\beta\, \mathrm{sgn}(u)\, |u|^b$ this results together with equation (3.82) in

$$\frac{1}{m}\frac{\partial}{\partial t} f_1(u) = \omega_\beta^2\, b\, \dot{u}(t)\, |u(t)|^{b-1} . \tag{5.23}$$

Based on definition (5.12) for the time step normalised spectra, the K-domain transformed system of (5.21) is given as

$$\begin{Bmatrix} U_{1,i}(k+1) \\ U_{2,i}(k+1) \\ U_{3,i}(k+1) \end{Bmatrix} = \frac{h_i}{k+1} \begin{Bmatrix} U_{2,i}(k) \\ U_{3,i}(k) \\ \widehat{P}_i(k) - 2\,\xi\omega_\alpha\, U_{3,i}(k) - \frac{k+1}{h_i}\, \mathcal{D}\left\{ f_{1/2}(u) \right\} \end{Bmatrix}, \tag{5.24a}$$

together with the mass-normalised force from (5.21a)

$$\widehat{P_i}(k) = \frac{k+1}{h_i}\,\mathcal{D}\left\{\hat{p}(t)\right\} = \frac{k+1}{h_i}\,\mathcal{D}\left\{\frac{1}{m}\frac{\partial}{\partial t}p(t)\right\}, \tag{5.24b}$$

which equates in the special case of the Friedlander blast profile (5.16) to $\widehat{P_i}(k)$ from (5.20). The stiffness expressions from Eqs.(5.22) and (5.23) become

$$\mathcal{D}\left\{\frac{1}{m}\frac{\partial}{\partial t}f_2(u)\right\} = \omega_\alpha^2\,U_{2,i}(k) - 3\,\omega_\beta^2\,U_{1,i}^{\{3\}}(k)\,, \tag{5.24c}$$

and

$$\mathcal{D}\left\{\frac{1}{m}\frac{\partial}{\partial t}f_1(u)\right\} = b\,\omega_\beta^2\left(U_{2,i}(k)\otimes U_{1,i}^{\{b-1\}}(k)\right) = b\,\omega_\beta^2\sum_{q=0}^{k}U_{2,i}(q)\,U_{1,i}^{\{b-1\}}(k-q)\,, \tag{5.24d}$$

respectively, with $U_{1,i}^{\{3\}}(k)$ according to Eq.(5.10b) and the expression $U_{1,i}^{\{b-1\}}(k)$ derived from equation (5.23) as

$$\begin{aligned} U_{1,i}^{\{b-1\}}(k) &= |U_{1,i}(k)|\otimes U_{1,i}^{\{b-2\}}(k) = |U_{1,i}(k)|\otimes|U_{1,i}(k)|\otimes U_{1,i}^{\{b-3\}}(k)\,,\\ &= |U_{1,i}(k)|\otimes\ldots\otimes U_{1,i}^{\{b-r\}}(k)\,, \qquad 1\le r<b-1, \quad r\in\mathbb{N}\\ &= \prod_{r=1}^{b-1}|U_{1,i}(k)|^r\,. \end{aligned} \tag{5.24e}$$

Obviously, the force transformation in Eqs.(5.18), (5.19) and (5.24) are generalised cases of the more simple step function excitation presented so far in literature [216,217,220].

Normalised response parameters of (5.21) obtained from solving the algebraic system in equation (5.24a) with respect to the adaptive stepping condition in (C.10), including the normalisation from (5.13), are shown in both figures 5.5 and 5.7. Displacement and velocity in comparison with the time history of the blast excitation function are given in Fig. 5.5(a) and (b), respectively, were the dots (•) indicate time points t_i along the descritisation grid. Acceleration due to the highly transient forcing function (5.16) is shown in Fig. 5.7(a). With a total of 44 steps the TDT method took 1.04 seconds compared to 7491 steps and 2.23 seconds for the `ode113` RK routine. Clearly, as can be seen in Fig. 5.7(b), with less than half of the computation time and a fraction of required intervals the TDT delivers results two orders of magnitude more precise than the most accurate RK MATLAB® routine available.

It is necessary here to add one last final comment regarding accuracy and precision of the numerical implementation of the TDT algorithm. With an adaptive stepping technique, other than the method of calculating $h_{i,\mathrm{cr}}$ in equation (C.10), one can establish even more accurate results within the same precision environment, e.g. MATLAB®. The only reason for not increasing the number of series approximation terms N beyond a value of 75, in case of system (5.21) with the parameters in Figs. 5.5 and 5.7, are due to (C.10) in connection with the substitution from (5.13)

where the denominator of the term in brackets in equation (C.10) quickly exceeds the smallest double precision number possible in MATLAB®.[12)]

Introducing a different error prediction scheme it is possible to circumvent such memory allocation deficiency due to 16 bit data processing. One approach suggested here would be to calculate the spectra $U_{j,i}(k)$ for each time step h_i up to order $N + \Delta N$ where $\Delta N \ll N$ and obtain two different time-history approximation series according to (5.12b). Naturally, the $N + \Delta N$ results are more accurate and substitution of both solutions into the governing ODE indicates the error between both approximations. If the local error for the N-term series is greater than a globally specified tolerance ϵ, the time step h_i is adjusted. Since no information is given by how much the new time step must be changed, this is a rather crude technique which under special circumstances can significantly increase computational costs. On the other hand, results obtained with the stepping prediction in (C.10) are already very accurate within the MATLAB® environment, if one takes into account that the smallest possible difference between two floating-point values is always greater than 2.225 E – 16. Thus, errors below this margins cannot be accurately detected without a certain degree of randomness. Additionally, the TDT scheme presented above is optimised for minimum resource usage and versatility especially with its application to MDOF systems in mind. It exhibits a significant enhancement in computational speed while at the same time delivering results orders of magnitude more accurate than any other currently available routines.

5.3 Summary

Considerably modifying and extending a recently developed method, called the Taylor Differential Transformation (TDT), novel analytical-approximate solutions for various types of differential equations have been obtained in this chapter. The method was applied to the conservative autonomous Duffing oscillator which possess an exact closed-form solution derived in the previous chapter. Results of the TDT were found to be orders of magnitude more accurate than data obtained from widely spread, currently utilised but purely numerical approaches, while at the same time significantly reducing calculation time and computational resource usage. The very same conclusions can be drawn when applying the TDT algorithm to highly transient nonconservative systems, as shown for the linear SDOF subjected to blast excitation.

In order to be able to correctly assess performance and accuracy of any non-exact semi-analytical solution method for single or systems of differential equations, an error residue was defined as a simple time-varying remainder unequal to zero which left over from substituting all non-exact response parameter solutions back into the governing differential equation. The smaller the residue the more accurate the approximate solution. Employing this new benchmark was found to have several advantages than the more generally used direct comparison with analytical exact solutions. Its excellent versatility and content has been shown for the nonlinear conservative Duffing system as well as the linear viscously damped transient oscillator.

Extending the TDT method, new and previously unpublished semi-analytical time-domain

[12)] In general, this depends on the computer architecture. For a commonly used PC based environment this is given as 2.2251 E – 308, see the discussion in chapter 4.

solutions have been formulated for highly transient, nonconservative SDOF and MDOF systems possessing one of the two geometrical nonlinear restoring stiffness forces examined in this work. Due to the lack of closed form solutions for the systems the time dependent residue was used as benchmark. Compared to currently available routines the TDT method leads to results significantly more accurate and therefore closer to the exact solution, while at the same time notably reducing usage of computational resources.

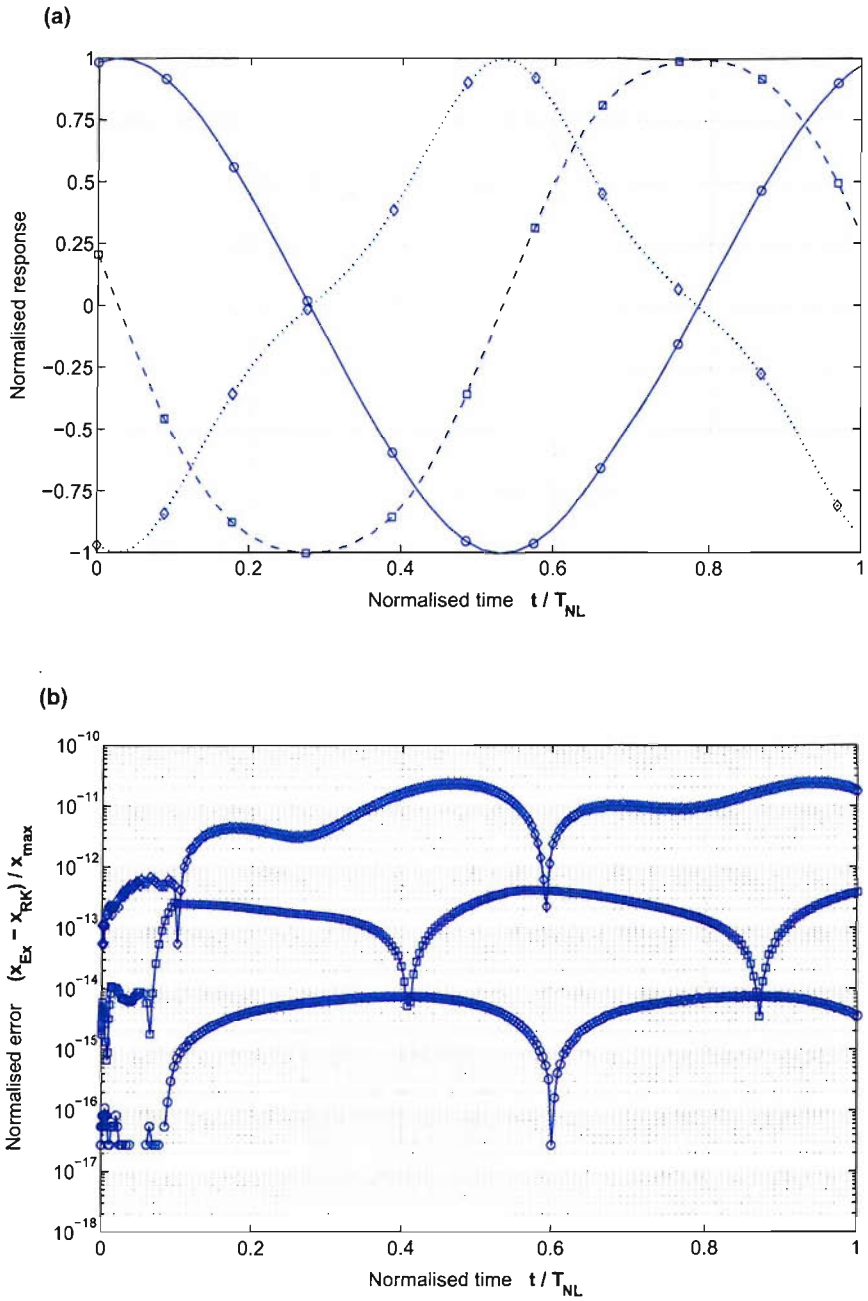

Figure 5.1 – Comparison between Runge-Kutta and Taylor Differential Transformation - *nonlinear autonomous system - Duffing oscillator:* **(a)** Analytical time-history solution of normalised response parameters $x_{\mathrm{Ex}}(t)/x_{\max}$. **(b)** Normalised absolute error $\left(x_{\mathrm{Ex}}(t) - x_{\mathrm{RK}}(t)\right)/x_{\max}$ for the RK algorithm `ode113` with `RelTol` = 1.0E−13 and `AbsTol` = 1.0E−15. The expression x stands for one of the response variables of the oscillator, either displacement $u(t)$, velocity $\dot{u}(t)$ or acceleration $\ddot{u}(t)$. Legend: o - $u(t)$, □ - $\dot{u}(t)$, and ◇ - $\ddot{u}(t)$. System parameters: mass $m = 0.3\,\mathrm{kg}$, $f_{\mathrm{n}} = 5\,\mathrm{Hz}$, $\omega_{\mathrm{n}} = 2\pi f_{\mathrm{n}}$, $k_\alpha = m\omega_{\mathrm{n}}^2$, $k_\gamma = 100\,\mathrm{N/m^2}$, $k_\beta = k_\gamma\, k_\alpha$. Initial values: $u_0 = 0.15\,\mathrm{m}$, $\dot{u}_0 = 1.25\,\mathrm{m/s}$.

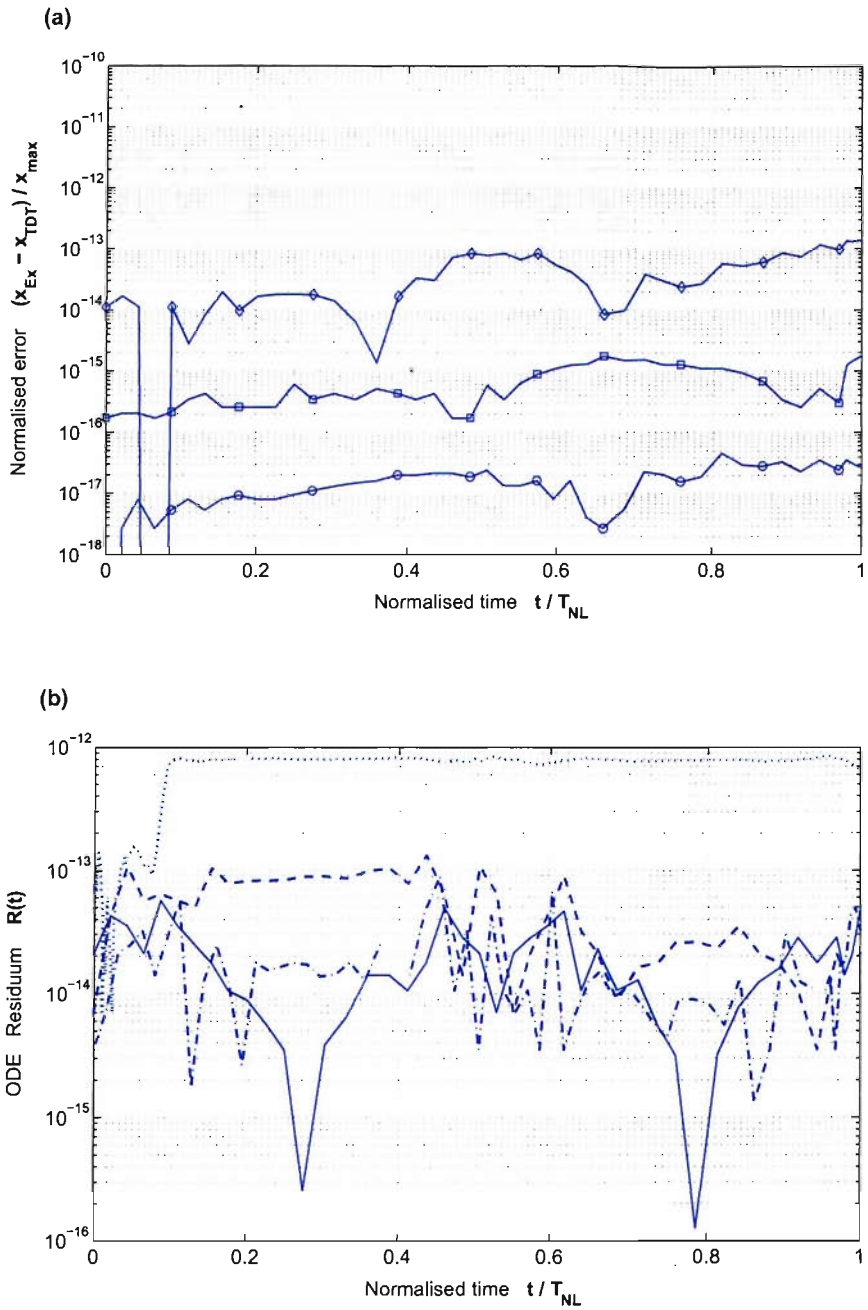

Figure 5.2 – Comparison between Runge-Kutta and Taylor Differential Transformation - *nonlinear autonomous system - Duffing oscillator:* **(a)** Normalised absolute error $(x_{\mathrm{Ex}}(t) - x_{\mathrm{TDT}}(t))/x_{\max}$ for the TDT algorithm using the algebraic system in Eq.(5.10). Transformation parameters: number of series elements $N = 110$, adaptive stepping tolerance according to Eq.(C.10) with $\epsilon = 1.0\,\mathrm{E}-50$. The expression x stands for one of the response variables of the oscillator, either displacement $u(t)$, velocity $\dot{u}(t)$ or acceleration $\ddot{u}(t)$. Legend: o - $u(t)$, □ - $\dot{u}(t)$, and ◊ - $\ddot{u}(t)$. **(b)** Governing differential equation residue $R(t)$ from (5.9). —— numerical implementation of exact analytical solution, – – – – TDT ($n = 11$), – · – · – TDT normalised ($n = 6$), · · · · RK ($n = 292$). System parameters: mass $m = 0.3\,\mathrm{kg}$, $f_{\mathrm{n}} = 5\,\mathrm{Hz}$, $\omega_{\mathrm{n}} = 2\pi f_{\mathrm{n}}$, $k_\alpha = m\omega_{\mathrm{n}}^2$, $k_\gamma = 100\,\mathrm{N/m^2}$, $k_\beta = k_\gamma\, k_\alpha$. Initial values: $u_0 = 0.15\,\mathrm{m}$, $\dot{u}_0 = 1.25\,\mathrm{m/s}$.

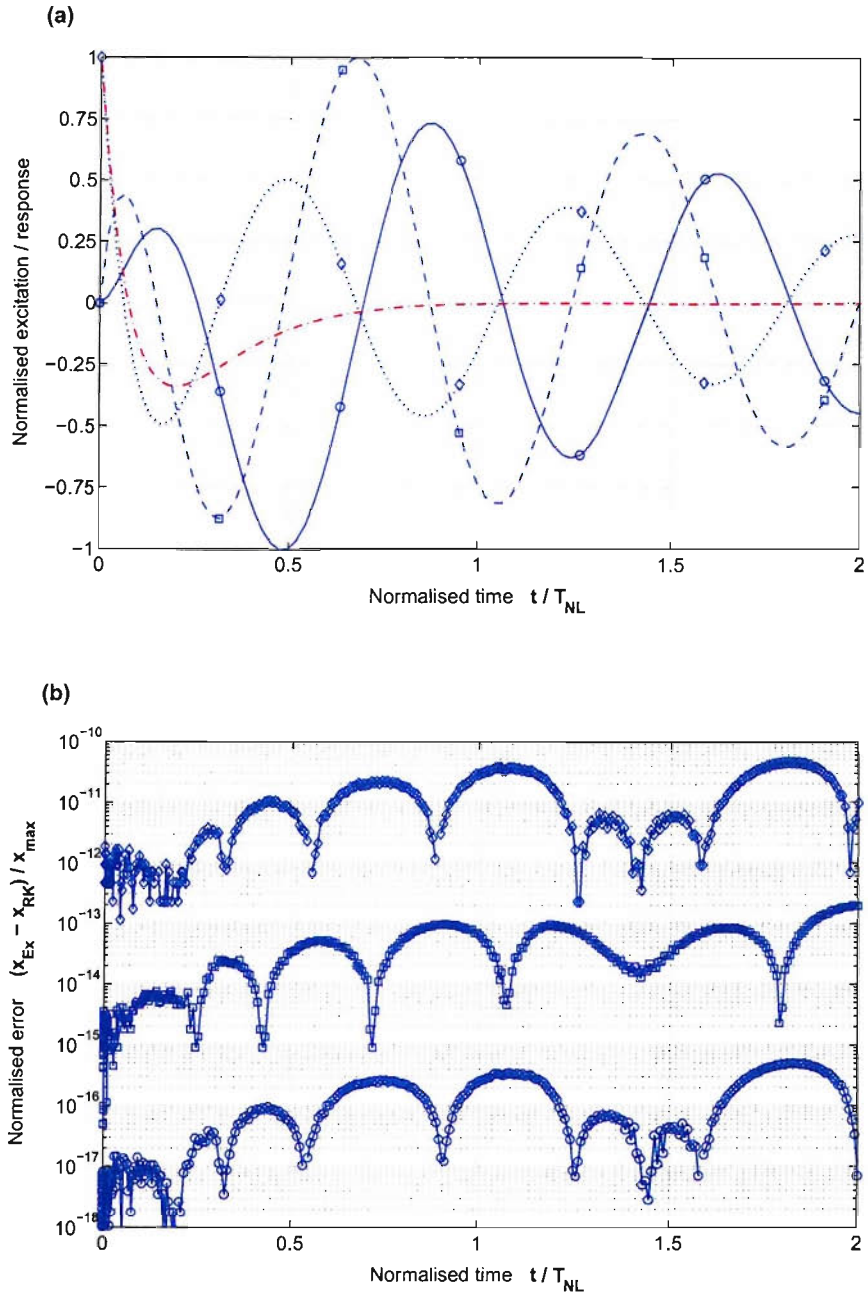

Figure 5.3 – Comparison between Runge-Kutta and Taylor Differential Transformation - *linear nonautonomous dissipative system - blast excitation:* **(a)** Analytical time-history solution of normalised response parameters $x_{\mathrm{Ex}}(t)/x_{\max}$. Normalised force function $-\cdot-\cdot-p(t)/p_0$. **(b)** Normalised absolute error $\left(x_{\mathrm{Ex}}(t) - x_{\mathrm{RK}}(t)\right)/x_{\max}$ for the RK algorithm `ode113` with `RelTol` = 2.3 E−14 and `AbsTol` = 2.25 E−16. The expression x stands for one of the response variables of the oscillator, either displacement $u(t)$, velocity $\dot{u}(t)$ or acceleration $\ddot{u}(t)$. Legend: o - $u(t)$, □ - $\dot{u}(t)$, and ◇ - $\ddot{u}(t)$. System parameters: mass $m = 0.3\,\mathrm{kg}$, $f_{\mathrm{n}} = 50\,\mathrm{Hz}$, $\omega_{\mathrm{n}} = 2\pi f_{\mathrm{n}}$, $k_\alpha = m\,\omega_{\mathrm{n}}^2$, $k_\gamma = k_\beta = 0$, $c = 10\,\mathrm{N}\cdot\mathrm{s}$. Initial values: $u_0 = \dot{u}_0 = 0$. Applied load: $p_0 = 1\,\mathrm{kN}$, $t_d = 1/(10\,f_{\mathrm{n}})\,\mathrm{s}$, $\alpha = 0.6$.

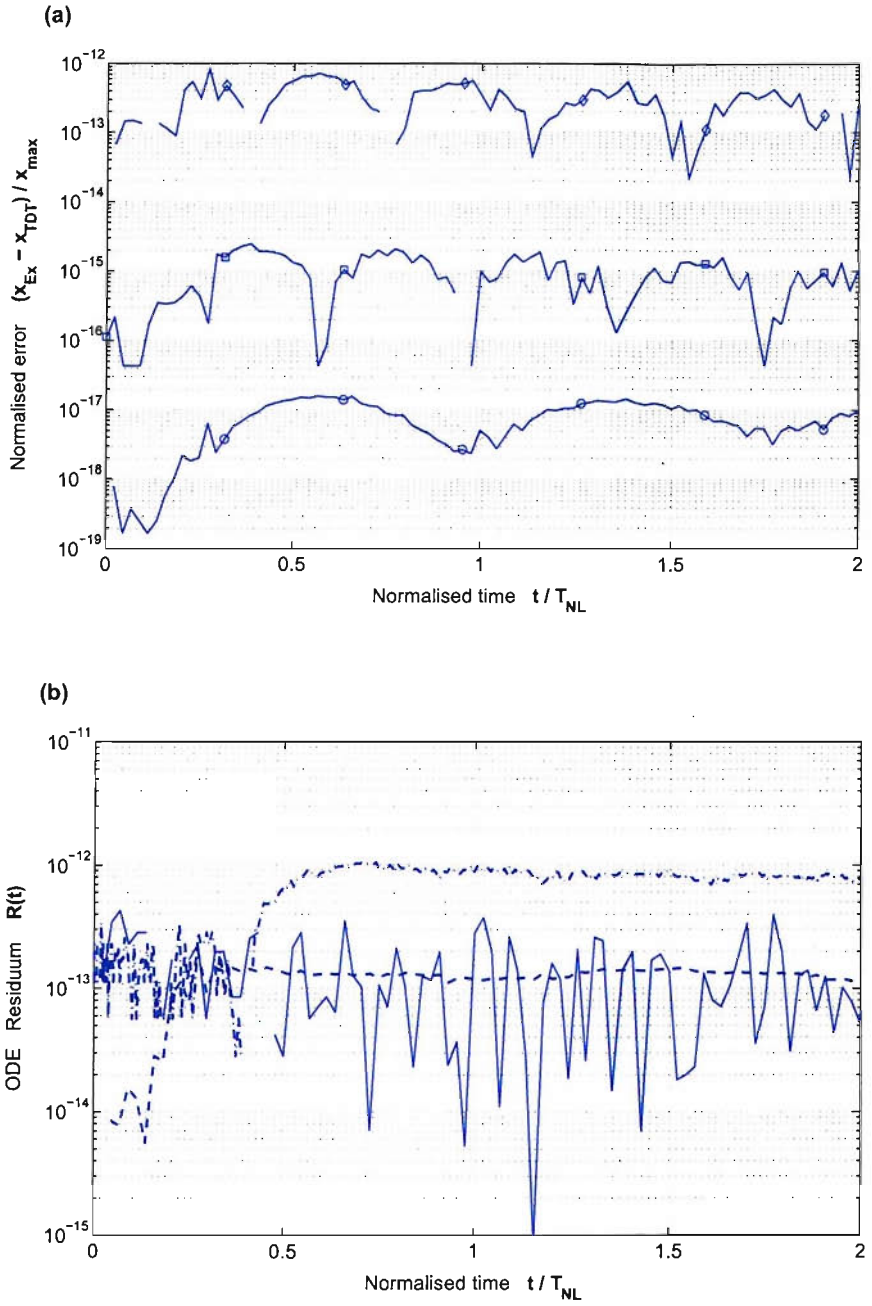

Figure 5.4 – Comparison between Runge-Kutta and Taylor Differential Transformation (TDT) - *linear nonautonomous dissipative system - blast excitation:* **(a)** Normalised absolute error $(x_{\mathrm{Ex}}(t) - x_{\mathrm{TDT}}(t))\,/x_{\max}$ for the TDT algorithm using the algebraic system in Eq.(5.20). Transformation parameters: number of series elements $N = 160$, adaptive stepping tolerance according to Eq.(C.10) with $\epsilon = 1.0\,\mathrm{E}-120$. The expression x stands for one of the response variables of the oscillator, either displacement $u(t)$, velocity $\dot{u}(t)$ or acceleration $\ddot{u}(t)$. Legend: o - $u(t)$, □ - $\dot{u}(t)$, and ◇ - $\ddot{u}(t)$. **(b)** Governing differential equation residue $R(t)$ from (5.9). —- numerical implementation of exact analytical solution, – · – · – TDT normalised ($n=7$), – – – – RK ($n=250$). System parameters: mass $m = 0.3$ kg, $f_{\mathrm{n}} = 50$ Hz, $\omega_{\mathrm{n}} = 2\pi f_{\mathrm{n}}$, $k_\alpha = m\omega_{\mathrm{n}}^2$, $k_\gamma = k_\beta = 0$, $c = 10\,\mathrm{N}\cdot\mathrm{s}$. Initial values: $u_0 = \dot{u}_0 = 0$. Applied load: $p_0 = 1$ kN, $t_d = 1/(10\,f_{\mathrm{n}})$ s, α =0.6.

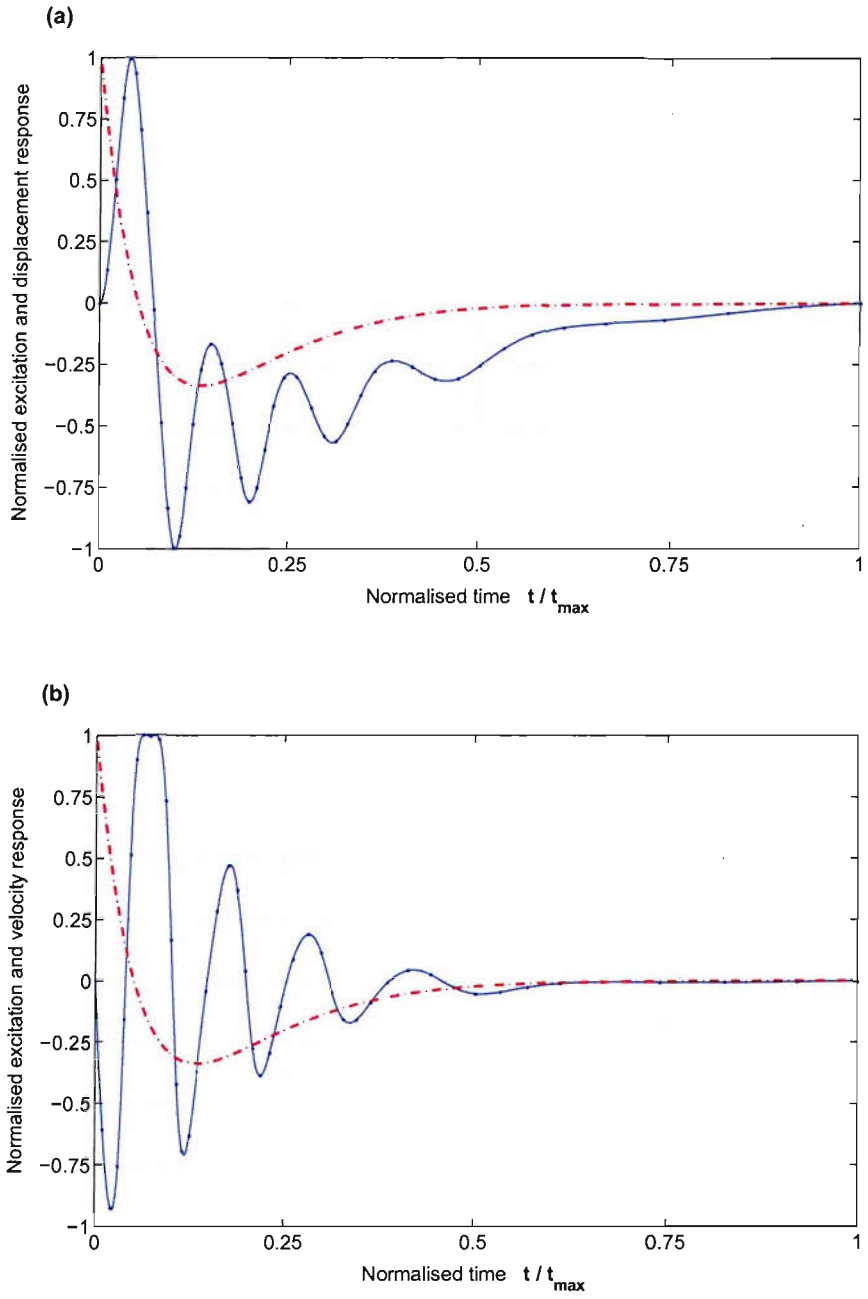

Figure 5.5 – Taylor Differential Transformation - *nonlinear, nonautonomous dissipative system - blast excitation:* Time history for TDT solution with adaptive stepping: n=44 time steps (•) h_i. ——— Blue lines: **(a)** Displacement. **(b)** Velocity. – · – · – Red line: Blast wave excitation. System parameters: mass $m = 0.3\,\text{kg}$, $f_\text{n} = 5\,\text{Hz}$, $\omega_\text{n} = 2\pi f_\text{n}$, $k_\alpha = m\,\omega_\text{n}^2$, $k_\gamma = 1000$, $k_\beta = k_\gamma\,k_\alpha$, $c = 10\,\text{N}\cdot\text{s}$. Initial values: $u_0 = \dot{u}_0 = 0$. Applied load: $p_0 = 1\,\text{kN}$, $t_d = 1/(10\,f_\text{n})\,\text{s}$, $\alpha = 0.6$.

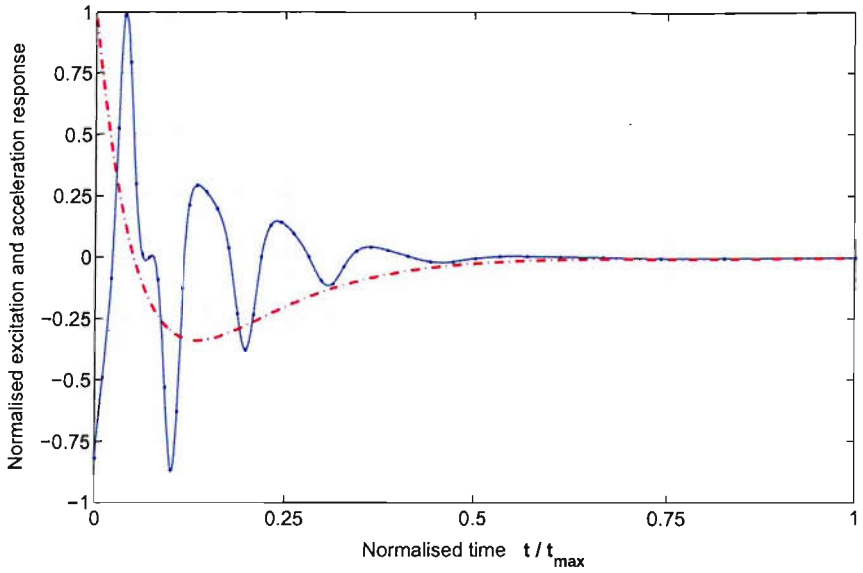

Figure 5.6 – Taylor Differential Transformation - *nonlinear, nonautonomous dissipative system - blast excitation:* Time history for TDT solution with adaptive stepping: $n=44$ time steps $(\bullet)\, h_i$. ——— Blue line: Acceleration. $- \cdot - \cdot -$ Red line: Blast wave excitation. System parameters: mass $m = 0.3\,\text{kg}$, $f_\text{n} = 5\,\text{Hz}$, $\omega_\text{n} = 2\pi f_\text{n}$, $k_\alpha = m\,\omega_\text{n}^2$, $k_\gamma = 1000$, $k_\beta = k_\gamma\, k_\alpha$, $c = 10\,\text{N}\cdot\text{s}$. Initial values: $u_0 = \dot{u}_0 = 0$. Applied load: $p_0 = 1\,\text{kN}$, $t_d = 1/(10\, f_\text{n})\,\text{s}$, $\alpha = 0.6$.

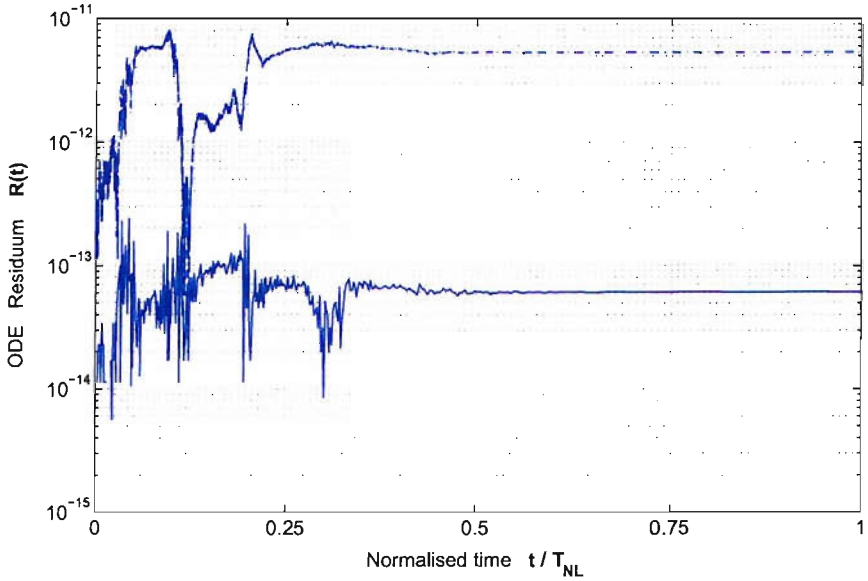

Figure 5.7 – Runge-Kutta and Taylor Differential Transformation comparison - *nonlinear, nonautonomous dissipative system - blast excitation:* Governing differential equation residue $R(t)$ from Eq.(5.9). Transformation parameters: number of series elements $N = 75$, adaptive stepping tolerance according to Eq.(C.10) with $\epsilon = 1.0\,\text{E}-25$. RK algorithm `ode113` with `RelTol` $=2.3\,\text{E}-14$ and `AbsTol` $=2.25\,\text{E}-16$. —— TDT normalised ($n=44$), $- - - -$ RK ($n=7491$). System parameters: mass $m = 0.3\,\text{kg}$, $f_\text{n} = 50\,\text{Hz}$, $\omega_\text{n} = 2\pi f_\text{n}$, $k_\alpha = m\,\omega_\text{n}^2$, $k_\gamma = 1000\,\text{m}^{-2}$, $k_\beta = k_\gamma\, k_\alpha$, $c = 10\,\text{N}\cdot\text{s}$. Initial values: $u_0 = \dot{u}_0 = 0$. Applied load: $p_0 = 1\,\text{kN}$, $t_d = 1/(10\, f_\text{n})\,\text{s}$, $\alpha = 0.6$.

CHAPTER 6

CONCLUSIONS AND FUTURE RESEARCH

6.1 Conclusions

This work has been aimed at gaining increased understanding of the complex dynamical processes involved in describing the response of geometrically nonlinear structural oscillators, by employing and appropriately modifying established concepts of nonlinear dynamical system theory. Based on well-known results for the extreme response prediction of two polynomial-type restoring forces, namely $f_1(u) = k_\beta \operatorname{sgn}(u) |u|^b$ and $f_2(u) = k_\alpha u + k_\beta u^3$, new expressions for a wide range of Hamilton systems under more general conditions regarding initial values and applied excitation have been derived. These new results have been employed for simple shock response spectra, which can immediately be deployed for practical response prediction. Novel formulations for the autonomous SDOF oscillator produced new analytical results for the problem of multiple harmonic oscillation frequency components, previously obtained by numerical Fourier transform and reported elsewhere.

Both systems investigated were subjected to a comprehensive uniqueness and stability investigation. Employing conventional methods of nonlinear dynamical system analysis, it has been shown that similar to the association of an hyperbola with the canonical form of a planar Hamilton system in the vicinity of an unstable equilibrium point, the eigenvectors of the linearised system at a stable fixed point corresponds to the slope of diameters of an ellipse which is equivalent to the invariant integral manifold of the Hamiltonian system.

The first restoring force $f_1(u)$ being single-term and of polynomial nature, with a real but positive exponent b, fails to satisfy the Lipschitz criteria for $0 < b < 1$. This interesting but rare phenomena has not received much attention in literature and no results existed for the restoring force considered here. Using two independent approaches, uniqueness of the non-trivial solutions for $f_1(u)$ was established. The first method adopted Picard iteration combined with recently pub-

lished results for so-called terminal systems. The important difference, however, lies in the fact that Peano's theorem was found to be sufficient in order to establish a valid uniqueness condition. Previously, the system had to be brought into a form such that the j-th derivative of the phase flow satisfies the Lipschitz theorem. For an autonomous conservative oscillator having $f_1(u)$ this is impossible. Clearly, the approach suggested here avoids this problem.

Recently published results predicting steady-state, nondissipative time domain behaviour for the Duffing-type restoring force $f_2(u)$ have been corrected and generalised. It was shown that for the autonomous SDOF system only a single one-term expression containing Jacobi elliptic functions is necessary in order to account for the response behaviour exhibited by the entire range of possible restoring forces, e.g. stiffening, softening and snap-through. Newly introduced closed-form approximate solutions modelling the steady-state time domain response of both systems, either single or multiple term, produce excellent results if compared to generally employed Runge-Kutta (RK) direct numerical integration schemes. Accuracy of the new solutions is good even for tight error tolerances of the numerical algorithm. Although these improvements are eventually outperformed by RK routines, if admissible error limits in the numerical computation are set to the feasible minimum values the novel analytical expressions provide valuable tools for studying the complex response behaviour of nonlinear systems, since they allow for a unique mathematical insight.

By adopting a modified Galerkin approach results of these newly introduced single-term expressions were considerably improved, especially for ranges of parameter combinations exhibiting unacceptable large approximation errors. Despite containing an empirically derived element, thus lacking consistent mathematical robustness, the new variational solutions are easily applicable while at the same time the error decreases by a factor of almost 2. A second method for obtaining explicit time-domain solutions for autonomous systems having either $f_1(u)$ or $f_2(u)$ is based on Picard iteration. Unfortunately, for $f_1(u)$ it is only possible to establish a limited number of terms in the approximation series, thus not significantly improving results obtained from the modified Galerkin algorithm. The reason for this constraint lies in the fact that even powerful algebraic manipulation software cannot solve the complex and difficult integral expressions arising from the iteration scheme. Contrary, for the Duffing-type oscillator circumstances were more promising and previously obtained results from a variational approach were substantially improved using Picard iteration.

A significant step towards adequate analytical-approximate solutions for highly transient, nonautonomous dissipative SDOF and MDOF systems has been introduced with the extension of a differential transformation technique, called the Taylor Differential Transformation (TDT). This exact solution method has been applied to blast wave excited systems to yield previously unpublished structural response results for both restoring forces $f_1(u)$ and $f_2(u)$. Two slightly different variants of the method were presented, allowing either for easy augmentation to MDOF systems or considerably increasing computational performance of the solution algorithm. Comparison to established Runge-Kutta procedures shows clear advantages of TDT routines with respect to both accuracy of results and speed of computation.

6.2 Future research

It certainly comes at no surprise that despite the modest range of newly introduced and generalised solutions, significant improvements for a number of aspects remain. Considerable effort is required to verify whether the proposed method of establishing uniqueness for non-Lipschitzian systems, which uses Peano's theorem, is also appropriate for other than polynomial nonlinear restoring forces exhibiting singularities of the phase flow's first derivative at stable equilibrium points. Furthermore, it would be of interest whether application of the method to nonconservative systems, either dissipative or absorptive, leads to similarly well-defined results as in the case of Hamiltonian systems.

The advantages of single and multiple term time domain approximate solutions over generally employed numerical methods have clearly been highlighted. But ranges of parameter combinations exist, although small and isolated, which do not allow for application of these results. Future research can be targeted at identifying mathematical reasons for this shortcoming and, eventually, provide expressions which cover the entire domain of feasible system parameter values. Staying with Jacobian elliptic functions but introducing a time varying modulus $\kappa \equiv \kappa(t)$ might open new ways for predicting the response behaviour of conservative but nonautonomous systems. The very same method in connection with an exponentially decaying term can potentially be used for modelling the generally encountered nonlinear amplitude-frequency relationship, here in particular for 'simple' linearly nonconservative but autonomous oscillators.

The real potential of the Taylor Differential Method is still to be examined in current research. Previously unpublished results presented in this work for a large class of nonlinear, nonautonomous and dissipative systems significantly strengthens the method's reputation for nonlinear dynamic analysis. Very few results exist in the literature concerned with elementary forms of nonlinear damping for SDOF systems. Further research is necessary to deal with far more complex models of nonlinear stiffness and damping. New transformation rules must be established, allowing analysis of systems containing various advanced functions such as polynomials with non-integer exponents or fractional derivatives. Using the results given for SDOF systems here, the application of the TDT method to space-discretised MDOF systems is easily performed by simply extending the first-order differential system from 2 to n equations. The outlined transformation process is identical.

BIBLIOGRAPHY

[1] Runge, C., "Ueber die numerische Aufloesung von Differentialgleichungen," *Mathematische Annalen*, Vol. 3, No. 46, 1895, pp. 167–178.

[2] Kutta, W., "Beitrag zur naeherungsweisen Integration totaler Differentialgleichungen," *Zeitschrift fuer Mathematik und Physik*, Vol. 46, 1901, pp. 435–453.

[3] Timoshenko, S., Young, D., and Weaver, W., *Vibration Problems in Engineering*, John Wiley & Sons, New York, 4th ed., 1974.

[4] Duffing, G., *Erzwungene Schwingungen bei veränderlicher Eigenfrequenz und ihre technische Bedeutung*, Vieweg, Braunschweig, 1918.

[5] Ergin, E., "Transient response of a nonlinear system," *ASME J. Appl. Mech.*, Vol. 23, 1956, pp. 635–639.

[6] Thomson, W., "Shock spectra of nonlinear systems," *ASME J. Appl. Mech.*, Vol. 27, 1960, pp. 528–533.

[7] Bapat, V. and Srinivasan, P., "Response spectrum of nonlinear spring mass system subjected to transient disturbance," *J. Sound Vibr.*, Vol. 8, No. 3, 1968, pp. 482–487.

[8] Bapat, V. and Srinivasan, P., "Response of undamped non-linear spring mass systems subjected to constant force excitation," *J. Sound Vibr.*, Vol. 9, No. 1, 1969, pp. 53–58.

[9] Bapat, V. and Srinivasan, P., "Response of undamped non-linear spring mass systems subjected to constant force excitation," *J. Sound Vibr.*, Vol. 9, No. 3, 1969, pp. 438–446.

[10] Panovko, Y., "A review of the method of direct linearisation," *Applied Mechanical Proceedings, XI International Congress of Applied Mechanics*, Munich, 1964, p. 167.

[11] Bapat, V. and Srinivasan, P., "Approximate methods for step function response of undamped nonlinear spring mass systems with arbitrary hardening type spring characteristics," *J. Sound Vibr.*, Vol. 10, No. 3, 1969, pp. 430–443.

[12] Atkinson, C., "On a superposition method for determining frequencies of nonlinear systems," *Proceedings of the IV. U.S. National Congress of Applied Mechanics*, 1964, pp. 57–62.

[13] Bapat, V. and Srinivasan, P., "Step function response of nonlinear spring mass systems in the presence of Coulomb damping," *J. Sound Vibr.*, Vol. 13, No. 1, 1970, pp. 51–65.

[14] Hundal, M., "Response of shock isolators with linear and quadratic damping," *J. Sound Vibr.*, Vol. 76, No. 2, 1981, pp. 273–281.

[15] Tamura, H. and Matsuda, Y., "Exact solutions of the autonomous Duffing equation and their computation," *JSME Int. J.*, Vol. 30, No. 261, 1987, pp. 482–490.

[16] Tamura, H. and Li, X., "Exact solutions of the free vibration of a nonlinear system with a quadratic spring (expressions of the solution and trial methods for the Fourier coefficients)," *JSME Int. J. Ser. III*, Vol. 33, No. 4, 1990, pp. 506–512.

[17] Tamura, H., Okabe, T., and Sueoka, A., "Exact solutions of the free vibration of a system with asymetrical single-term cubic spring," *JSME Int. J. Ser. C*, Vol. 36, No. 1, 1993, pp. 26–34.

[18] Tamura, H., Okabe, T., and Sueoka, A., "Exact Solutions for free vibration in an asymetrical Duffing equation," *JSME Int. J. Ser. C*, Vol. 37, No. 2, 1994, pp. 260–268.

[19] Lin, J., "A new approach to Duffing equation with strong and high order nonlinearity," *Comm. Nonlin. Sc. & Numer. Simul.*, Vol. 4, No. 2, 1999, pp. 132–135.

[20] He, J., "Some new approaches to Duffing equation with strongly and high order nonlinearity - part (I) linearised perturbation technique," *Comm. Nonlin. Sc. & Numer. Simul.*, Vol. 4, No. 1, 1999, pp. 78–81.

[21] He, J., "Some new approaches to Duffing equation with strongly and high order nonlinearity - part (II) parameterised perturbation technique," *Comm. Nonlin. Sc. & Numer. Simul.*, Vol. 4, No. 1, 1999, pp. 81–83.

[22] He, J., "Variational iteration method - a kind of nonlinear method: some examples," *Int. J. Nonlinear Mech.*, Vol. 34, 1999, pp. 699–708.

[23] He, J., "Modified straightforward expansion," *Meccanica*, Vol. 34, No. 4, 1999, pp. 287–289.

[24] He, J., "A coupling method of homotopy technique and perturbation technique for nonlinear problems," *Int. J. Nonlinear Mech.*, Vol. 35, No. 1, 2000, pp. 37–43.

[25] He, J., "Modified Linstedt-Poincaré methods for some strongly nonlinear oscillatons. Part III: double series expansion," *Int. J. Nonlin. Sc. Numer. Simul.*, Vol. 2, No. 4, 2001, pp. 317–320.

[26] He, J., "Iteration perturbation method for strongly nonlinear oscillations," *J. Vibr. Control*, Vol. 7, No. 5, 2001, pp. 631–642.

[27] He, J., "Bookkeeping parameter in perturbation methods," *Int. J. Nonlin. Sc. Numer. Simul.*, Vol. 2, No. 3, 2001, pp. 257–264.

[28] He, J., "Modified Linstedt-Poincaré methods for some strongly nonlinear oscillations. Part I: expansion of a constant," *Int. J. Nonlinear Mech.*, Vol. 37, No. 2, 2002, pp. 309–314.

[29] He, J., "Modified Linstedt-Poincaré methods for some strongly nonlinear oscillations. Part II: a new transformation," *Int. J. Nonlinear Mech.*, Vol. 37, No. 2, 2002, pp. 315–320.

[30] He, J., "Preliminary report on the energy balance for nonlinear oscillations," *Mech. Research Comm.*, Vol. 29, 2002, pp. 107–111.

[31] Nayfeh, A., *Perturbation Methods*, Vol. 12 of *Pure and Applied Mathematics*, Wiley, New York, 1973.

[32] Ribeiro, P. and Petyt, M., "Non-linear vibration of beams with internal resonance by the hierarchical finite-element method," *J. Sound Vibr.*, Vol. 224, No. 4, 1999, pp. 591–624.

[33] Ribeiro, P. and Petyt, M., "Non-linear free vibration of isotropic plates with internal resonance," *Int. J. Nonlinear Mech.*, Vol. 35, No. 2, 2000, pp. 263–278.

[34] Ribeiro, P. and Petyt, M., "Nonlinear vibration of plates by the hierarchical finite element and continuation methods," *Int. J. Mech. Sc.*, Vol. 41, No. 4-5, 1999, pp. 437–459.

[35] Petyt, M. and Ribeiro, P., "Geometrical non-linear periodic vibration of plates," *ASME Journal, Applied Mechanics Division*, Vol. 238, 2000, pp. 61–68.

[36] Ribeiro, P. and Petyt, M., "Non-linear vibration of composite laminated plates by the hierarchical finite element method," *Composite Structures*, Vol. 46, No. 3, 1999, pp. 197–208.

[37] Ribeiro, P. and Petyt, M., "Geometrical non-linear, steady state, forced, periodic vibration of plates, part I: Model and convergence studies," *J. Sound Vibr.*, Vol. 226, No. 5, 1999, pp. 955–983.

[38] Ribeiro, P. and Petyt, M., "Geometrical non-linear, steady state, forced, periodic vibration of plates, part II: Stability study and analysis of multi-modal response," *J. Sound Vibr.*, Vol. 226, No. 5, 1999, pp. 985–1010.

[39] Tiwari, S., Rao, B., Swamy, N., Sai, K., and Nataraja, H., "Analytical study on a Duffing-harmonic oscillator," *J. Sound Vibr.*, Vol. 285, 2005, pp. 1217–1222.

[40] Mickens, R., "Mathematical and numerical study of the Duffing-harmonic oscillator," *J. Sound Vibr.*, Vol. 244, 2001, pp. 563–567.

[41] Ehrich, F. and Abramson, H., *Shock and Vibration Handbook*, chap. Nonlinear Vibration, McGraw-Hill, New York, 3rd ed., 1988, pp. 4.1–4.47.

[42] Mickens, R. and Semwogerere, D., "Fourier analysis of a rational harmonic balance approximation for periodic solutions," *J. Sound Vibr.*, Vol. 195, 1996, pp. 528–530.

[43] Cveticanin, L., "Vibrations of the nonlinear oscillator with quadratic nonlinearity," *Physica A*, Vol. 341, 2004, pp. 123–135.

[44] He, J., "A new perturbation technique which is also valid for large parameters," *J. Sound Vibr.*, Vol. 225, 2000, pp. 1257–1263.

[45] He, J., "Determination of limit cycles for strongly nonlinear oscillators," *Phy. Rev. Lett.*, Vol. 197, No. 17, 2003, pp. Art.No. 174301.

[46] Rajendran, S., Pandey, S., and Lakshmanan, M., "Comment on 'Determination of limit cycles for strongly nonlinear oscillators'," *Phy. Rev. Lett.*, Vol. 93, No. 6, 2004, pp. 112–114.

[47] Sanchez, N., "A view to the new perturbation technique valid for large parameters," *J. Sound Vibr.*, Vol. 282, 2005, pp. 1309–1316.

[48] Lorenz, E., "Deterministic nonperiodic flow," *J. Athmos. Sc.*, Vol. 20, 1963, pp. 130–141.

[49] Diacu, F. and Holmes, P., *Celestial Encounters: The Origins of Chaos and Stability*, Princeton University Press, New Jersey, 1996.

[50] Zak, M., "The problem of irreversibility in Newtonian Dynamics," *Int. J. Theoretical Phy.*, Vol. 31, 1992, pp. 333–342.

[51] Dixon, D., Cummings, F., and Kaus, P., "Continuous chaotic dynamics in two dimensions," *Physica D*, Vol. 65, 1993, pp. 109–116.

[52] Zak, M., "Postinstability models in dynamics," *Int. J. Theoretical Phy.*, Vol. 33, 1994, pp. 1115–1180.

[53] Dixon, D., "Piecewise deterministic dynamics from the application of noise to singular equations of motion," *J. Phy. A*, Vol. 28, 1995, pp. 5539–5551.

[54] Zak, M., "Irreversibility in thermodynamics," *Int. J. Theoretical Phy.*, Vol. 35, 1996, pp. 347–382.

[55] Zak, M., "Non-Lipschitz approach to quantum mechanics," *Chaos, Solitons & Fractals*, Vol. 9, No. 7, 1998, pp. 1183–1198.

[56] Tabor, M., *Chaos and Integrability in Nonlinear Dynamics - An Itroduction*, John Wiley & Sons, New York, 1989.

[57] Ziblut, J., Dixon, D., and Zak, M., "Detecting singularities of piecewise deterministic (terminal) dynamics in experimental data," *Physics Letters A*, Vol. 304, 2002, pp. 95–101.

[58] Bronstein, I. and Semendjajew, K., *Taschenbuch der Mathematik (Handbook of Mathematical Formulas)*, Verlag Nauka, Moscow; B.G.Teubner Verlagsgesellschaft Stuttgart, 26th ed., 1992.

[59] Bhat, S. and Bernstein, D., "An example of indeterminacy in classical dynamics," *Proceedings of the American Control Conference*, AACC, Albuquerque, New Mexico, June 1997, pp. 3470–3472.

[60] Zak, M. and Meyers, R., "Non-Lipschitz dynamics approach to discrete event systems," *Proceedings of the 1995 International Symposium on Nonlinear Theory and its Applications*, Research Society of Nonlinear Theory and its Applications, IEICE, Las Vegas, Nevada, USA, December 10 – 14 1995, pp. 112–115.

[61] Strogatz, S., *Nonlinear Dynamics and Chaos*, Perseus Publishing, Cambridge, Ma., 1994.

[62] Roska, T., "On the uniqueness of solutions of nonlinear dynamic networks and systems," *IEEE Trans. Circuits Syst.*, Vol. CAS-25, No. 3, March 1978, pp. 161–169.

[63] Venkatasubramanian, V., Saberi, A., and Lin, Z., "A notion of solutions and equilibrium points for non-smooth systems," *Proceedings of the 32nd Conference on Decision and Control*, Vol. WA1-10:00, IEEE, San Antonio, Tx., Dec. 1993, pp. 1–7.

[64] Bernis, F. and Kwong, M., "A Picard method without Lipschitz continuity for some ordinary differential equations," *Annales de la Faculté des Sciences de Toulouse*, Vol. 5, No. 4, 1996, pp. 577–585.

[65] Forti, M., Grazzini, M., Nistri, P., and Pancioni, L., "Generalized Lyapunov approach for convergence of neural networks with discontinuous or non-Lipschitz activations," *Physica D*, Vol. 214, 2006, pp. 88–99.

[66] Filippov, A., "Differential equations with discontinuous right-hand side," *Transl. Amer. Math. Soc.*, Vol. 42, No. 2, 1964, pp. 191–231.

[67] Agarwal, R. and Lakshmikantham, V., *Uniqueness and Nonuniqueness Criteria for Ordinary Differential Equations*, Vol. 6 of *Series in Real Analysis*, World Scientific, Singapore, 1993.

[68] Hartman, P., *Ordinary Differential Equations*, John Wiley & Sons, New York, 1964.

[69] Bo-hu, L., Yang, W., and Xin-an, Y., "An effective method for a system of ordinary differential equations with right hand side functions containing discontinuities," *10th IMACS World Congress on System Simulation and Scientific Computation*, Vol. 1, IMACS, Montreal, Que., Canada, 1982, pp. 6–9.

[70] Morozov, S. and Sumin, M., "Class of control prblems of dynamical systems with a discontinuous right hand side," *Cybernetics (English Translation of Kibernetika)*, Vol. 21, No. 3, May-June 1985, pp. 346–355.

[71] Paden, B. and Sastry, S., "A calculus for computing Filippov's differential inclusion with application to the variable structure control of robot manipulators," *IEEE Trans. Circuits Syst.*, Vol. CAS-34, No. 1, Jan. 1987, pp. 73–82.

[72] Filippov, A., *Differential Equations with Discontinuous Right Hand Sides*, Kluwer Academic Publishers, Boston, 1988.

[73] Zbilut, J., Huebler, A., and Webber Jr., C., *Fluctuations and Order: The New Synthesis*, Springer-Verlag, New York, 1996.

[74] Huebler, A., *Modelling of Complex Phenomena*, Springer-Verlag, New York, 1993.

[75] Zak, M., Zbilut, J., and Meyers, R., *From Instability to Intelligence: Complexity and Predictability in Nonlinear Dynamics*, Vol. 49 of *Lecture Notes in Physics*, Springer-Verlag, Berlin, 1997.

[76] Miller, R. and Michel, A., *Ordinary Differential Equations*, Academic Press, New York, 1982.

[77] Iggidr, A., Kalitine, B., and Vivalda, J.-C., "New Lyapunov-like theorems for non-Lischitz vector fields," *Proceedings of the 38th Conference on Decision & Control*, Vol. 5, IEEE, Phoenix, Az., Dec. 1999, pp. 5235–5237.

[78] Shevitz, D. and Paden, B., "Lyapunov Stability Theory of Nonsmooth Systems," *IEEE Transac. Autom. Contr.*, Vol. 39, No. 9, Sep. 1994, pp. 1910–1914.

[79] Lu, X.-Y. and Hedrick, J., "A new approach for asymptotic stability analysis in the case of discontinuous Lyapunov function derivative," *Proceedings of the 42nd IEEE Conference on Decision and Control*, Vol. 2, IEEE, Maui, Hawaii, Dec. 2003, pp. 5083–5085.

[80] Nowak, C. and Stettner, H., "Nonuniqueness results for ordinary differential equations," *Nonlinear Analysis, Theory, Methods & Application*, Vol. 30, No. 6, 1997, pp. 3935–3938.

[81] Guo, Z. and Li, X., "Solutions with isolated point ruptures for a semilinear elliptic equation in R^2 with a non-Lipschitz nonlinearity," *Appl. Math. Letters*, Vol. 17, 2004, pp. 519–526.

[82] Lou, C. and Sikarskie, D., "A New Type of Nonlinear Approximation with Application to the Duffing Equation," *Int. J. Nonlinear Mech.*, Vol. 9, 1974, pp. 179–191.

[83] Rahman, Z. and Burton, T., "Large Amplitude Primary and Superharmonic Resonances in the Duffing's Oscillator," *J. Sound Vibr.*, Vol. 110, No. 2, 1986, pp. 363–380.

[84] Giacaglia, G., *Perturbation Methods in Nonlinear Systems*, Allen and Unwin, London, 1972.

[85] Nayfeh, A., *Introduction to Perturbation Techniques*, Wiley Classic Library Ed., Wiley-Interscience, New York, 1993.

[86] Astashev, V., Babitsky, V., and Kolovsky, M., *Dynamics and Control of Machines*, Springer-Verlag, 2000.

[87] Zahavi, E. and Barlam, D., *Nonlinear Problems in Machine Design*, CRC Press, 2001.

[88] Tufillaro, N., Abbott, T., and Reilly, J., *An Experimental Approach to Nonlinear Dynamics and Chaos*, Studies in Nonlinearity, Addison-Wesley, Redwood City, Ca., 1992.

[89] Lalanne, C., *Mechanical Shock*, Taylor Francis, London, 2002.

[90] Nixon, F., *Handbook of Laplace Transformation : Fundamentals, Applications, Tables, and Examples*, Prentice-Hall, 1965.

[91] Detinko, F., "Application of Jacobian elliptic functions to the analysis of forced vibrations of a nonlinear conservative system," *Mech. Solids*, Vol. 31, No. 4, 1996, pp. 5–8.

[92] Urabe, M., *Nonlinear Autonomous Oscillations*, Vol. 34 of *Mathematics in Science and Engineering*, Academic Press, New York, London, 1967.

[93] Smith, D., *Singular-Perturbation Theory : An Introduction with Applications*, Cambridge University Press, Cambridge, 1985.

[94] Szulkin, P. and Kacprzyński, B., "Comparative analysis of approximate methods in vibration theory," *Bulletin de L'Academie Polonaise des Sciences - Série des sciences techniques*, Vol. III, No. 7, 1960, pp. 361–370.

[95] Becker, M., *The Principles and Applications of Variational Methods*, MIT Press, Cambridge, Mass., 1964.

[96] Reddy, J., *Energy Principles and Variational Methods in Applied Mechanics*, John Wiley & Sons, New York, 2nd ed., 2002.

[97] Boresi, A., Chong, K., and Saigal, S., *Approximate Solution Methods in Engineering Mechanics*, Wiley-IEEE, 2nd ed., 2003.

[98] Klotter, K. and Cobb, P., "On the use of nonsinusiodal approximation functions for nonlinear oscillation problems," *ASME J. Appl. Mech.*, Vol. 27, Sep. 1960, pp. 579–583.

[99] Reif, Z., "Effect of static deflection on the natural frequency of a system with hardening non-linear spring," *J. Mech. Engineering Sc.*, Vol. 9, No. 3, 1967, pp. 177–181.

[100] Ueda, T. and Matsuzaki, Y., "The method of weigthed residuals in the time domain applied to nonlinear vibrations," *Trans. Jap. Soc. Aeronaut. Space Sc.*, Vol. 22, No. 56, Aug. 1979, pp. 80–89.

[101] Huang, T., "Harmonic oscillations of nonlinear two-degree-of-freedom systems," *ASME J. Appl. Mech.*, Vol. 3, March 1955, pp. 107–110.

[102] Huang, T., "Harmonic oscillations of nonlinear two-degree-of-freedom systems," *ASME J. Appl. Mech.*, Vol. 3, Dec. 1955, pp. 602–603.

[103] Vito, R., "An approximate method of treating the nonlinear vibrations of certain two-dregrees-of-freedom systems," *ASME J. Appl. Mech.*, Vol. 39, No. 2, June 1972, pp. 620–621.

[104] Shaw, S. and Pierre, C., "Normal modes for nonlinear vibratory systems," *J. Sound Vibr.*, Vol. 164, No. 1, 1993, pp. 85–124.

[105] Bailey, C., "The method of Ritz applied to the equation of Hamilton," *Comp. Meth. Appl. Mech. Engineering*, Vol. 7, 1976, pp. 235–247.

[106] Scharle, P., "On the relationship between different approximating methods," *Acta Technica Academiae Scientarium Hungaricae*, Vol. 82, No. 1-2, 1976, pp. 53–59.

[107] Bal, D., "Modified least square method: an application to a class of nonlinear vibration problems," *AMSE Review*, Vol. 6, No. 1, 1987, pp. 47–57.

[108] Groves F.R., J., "Numerical solution of nonlinear differential equations using computer algebra," *Int. J. Comp. Math.*, Vol. 13, 1983, pp. 301–309.

[109] Abramowitz, M. and Stegun, I., *Handbook of Mathematical Functions*, Dover, New York, 7th ed., 1968.

[110] Denman, H. and Howard, J., "Application of ultraspherical polynomials to nonlinear oscillations. Part I: free oscillations of the pendulum," *Quart. Appl. Math.*, Vol. 21, 1964, pp. 325–330.

[111] Denman, H. and Liu, Y., "Application of ultraspherical polynomials to nonlinear oscillations. Part II: free oscillations," *Quart. Appl. Math.*, Vol. 22, 1965, pp. 273–292.

[112] Liu, Y., "Application of ultraspherical polynomials to nonlinear forced oscillations," *J. Appl. Math.*, Vol. 34, 1967, pp. 223–226.

[113] Garde, R., "Application of Gegenbauer polynomials to nonlinear damped systems," *J. Sc. Engineering Res.*, Vol. 11, 1967, pp. 157–166.

[114] Anderson, G., "An approximate analysis of nonlinear, nonconservative, systems using orthogonal polynomials," *J. Sound Vibr.*, Vol. 29, 1973, pp. 463–474.

[115] Sinha, S. and Srinivasan, P., "Application of ultraspherical polynomials to nonlinear autonomous systems," *J. Sound Vibr.*, Vol. 18, No. 1, 1971, pp. 55–60.

[116] Rangacharyulu, M. and Srinivasan, P., "A note on the ultrasherical polynomial approximation method of averaging," *J. Sound Vibr.*, Vol. 53, No. 1, 1977, pp. 63–69.

[117] Rangacharyulu, M., Srinivasan, P., and Dasarathy, B., "Transient response of coupled nonlinear nonconservative systems," *J. Sound Vibr.*, Vol. 37, No. 4, 1974, pp. 467–473.

[118] Rangacharyulu, M., Srinivasan, P., and Dasarathy, B., "Approximate analysis of coupled nonlinear nonconservative systems subjected to step function excitation," *J. Sound Vibr.*, Vol. 37, No. 3, 1974, pp. 359–366.

[119] Srirangarajan, H. and Dasarathy, B., "Decoupling in nonlinear systems with two degrees of freedom," *J. Sound Vibr.*, Vol. 38, No. 1, 1975, pp. 1–8.

[120] Rangacharyulu, M. and Dasarathy, B., "Nonlinear systems with quadratic and cubic damping - an analytical approach," *J. Sound Vibr.*, Vol. 38, No. 1, 1975, pp. 9–13.

[121] Srirangarajan, H. and Srinivasan, P., "The transient response of certain third-order nonlinear systems," *J. Sound Vibr.*, Vol. 29, No. 2, 1973, pp. 215–226.

[122] Rangacharyulu, M., "Response of nonlinear nonconservative systems of two degrees of freedom to transient excitations," *J. Sound Vibr.*, Vol. 91, No. 1, 1983, pp. 45–56.

[123] Tamura, H. and Tsuda, Y. Sueoka, A., "Higher approximation of steady oscillations in nonlinear systems with single degree of freedom - Suggested multiharmonic balance method," *Bulletin of the JSME*, Vol. 24, No. 195, Sep. 1981, pp. 1616–1625.

[124] Diaz Bejarano, J. and Martin Sanchez, A., "Generalized Fourier series for nonlinear systems," *J. Sound Vibr.*, Vol. 134, No. 2, 1989, pp. 333–341.

[125] Nayfeh, A. and Balachandran, B., *Applied Nonlinear Dynamics*, Wiley Series in Nonlinear Science, Wiley-Interscience, John Wiley & Sons, Inc., New York, 1995.

[126] Hayashi, C., *Nonlinear Oscillations in Physical Systems*, McGraw-Hill, New York, 1964.

[127] Holmes, M., *Introduction to Perturbation Methods*, Vol. 20 of *Texts in Applied Mathematics*, Springer-Verlag, New York, Berlin, 1995.

[128] Awrejcewicz, J., "An analytical method for detecting Hopf bifurcation solutions in nonstationary nonlinear systems," *J. Sound Vibr.*, Vol. 129, No. 1, 1989, pp. 175–178.

[129] Bravo Yuste, S. and Diaz Bejarano, J., "Extension and improvement of the Krylov-Bogoliubov methods using elliptic functions," *Int. J. Control*, Vol. 49, 1989, pp. 1127–1141.

[130] Bravo Yuste, S. and Diaz Bejarano, J., "Improvement of a Krylov-Bogoliubov method that uses Jacobi elliptic functions," *J. Sound Vibr.*, Vol. 139, No. 1, 1990, pp. 151–163.

[131] Bravo Yuste, S., "Quasi-pure-cubic oscillatiors studied using a Krylov-Bogoliubov method," *J. Sound Vibr.*, Vol. 158, No. 2, 1992, pp. 267–275.

[132] Bravo Yuste, S. and Diaz Bejarano, J., "Construction of approximate analytical solutions to a new class of nonlinear equations," *J. Sound Vibr.*, Vol. 110, 1986, pp. 347–350.

[133] Garcia-Margallo, J. and Diaz Bejarano, J., "A generalization of the method of harmonic balance," *J. Sound Vibr.*, Vol. 116, No. 3, 1987, pp. 591–595.

[134] Mickens, R., "A generalization of the method of harmonic balance," *J. Sound Vibr.*, Vol. 111, No. 3, 1987, pp. 515–518.

[135] Diaz Bejarano, J., "Generalized Fourier series for nonlinear quantum mechanics," *Bull. Amer. Phys. Soc.*, Vol. 33, 1988, pp. 669.

[136] Garcia-Margallo, J., Diaz Bejarano, J., and Bravo-Yuste, "Generalized Fourier series for the study of limit cycles," *J. Sound Vibr.*, Vol. 125, No. 1, 1988, pp. 13–21.

[137] Garcia-Margallo, J. and Diaz Bejarano, J., "Generalized Fourier series and limit cycles of generalized van der Pol oscillators," *J. Sound Vibr.*, Vol. 136, No. 3, 1990, pp. 453–466.

[138] Chen, S., Yang, X., and Cheung, Y., "Periodic solutions of strongly quadratic nonlinear oscillators by the elliptic perturbation method," *J. Sound Vibr.*, Vol. 212, No. 5, 1998, pp. 771–780.

[139] Bender, C., Mitlon, K., Pinsky, S., and Simmons, L. J., "A new perturbative approach to nonlinear problems," *J. Math. Phy.*, Vol. 30, No. 7, June 1989, pp. 1447–1455.

[140] Belhaq, M. and Lakrad, F., "The elliptic multiple scales method for a class of autonomous strongly nonlinear oscillators," *J. Sound Vibr.*, Vol. 234, No. 3, 2000, pp. 547–553.

[141] Senator, M. and Bapat, C., "A perturbation technique that works even when the nonlinearity is not small," *J. Sound Vibr.*, Vol. 164, No. 1, 1993, pp. 1–27.

[142] Jones, S., "Remarks on the perturabtion process for certain conservative systems," *Int. J. Nonlinear Mech.*, Vol. 13, 1978, pp. 125–128.

[143] Eminhizer, C., Helleman, H., and Montroll, E., "On a convergence nonlinear perturbation theory without small denominators or secular terms," *J. Math. Phy.*, Vol. 17, 1976, pp. 121–140.

[144] Chen, S. and Cheung, Y., "A modified Linstedt-Poincaré method for a strongly nonlinear two degree-of-freedom system," *J. Sound Vibr.*, Vol. 193, No. 4, 1996, pp. 751–762.

[145] Yang, C., Zhu, S., and Chen, S., "A modified elliptic Linstedt-Poincaré method for certain strongly nonlinear oscillators," *J. Sound Vibr.*, Vol. 273, 2004, pp. 921–932.

[146] Sotiropoulou, A. and Panayotounakos, D., "On the reduction of some second-order nonlinear ODEs in physics and mechanics to first-order nonlinear integrodifferential and Abel's classes of equations," *Theoretical and Applied Fracture Mechanics*, Vol. 40, 2003, pp. 255–270.

[147] Cveticanin, L., "An approximate solution for a system of two coupled differential equations," *J. Sound Vibr.*, Vol. 152, 1992, pp. 375–380.

[148] Cveticanin, L., "Approximate analytical solutions to a class of nonlinear equations with complex functions," *J. Sound Vibr.*, Vol. 157, 1992, pp. 289–302.

[149] Cveticanin, L., "An approximate solution of a coupled differential equation with variable parameters," *ASME J. Appl. Mech.*, Vol. 60, 1993, pp. 214–217.

[150] Cveticanin, L., "Analytical methods for solving strongly nonlinear differential equations," *J. Sound Vibr.*, Vol. 214, No. 2, 1998, pp. 325–338.

[151] Cveticanin, L., "The conservation laws and the exact solutions for the singular nonlinear oscillator," *J. Sound Vibr.*, Vol. 224, No. 5, 1999, pp. 952–960.

[152] Cveticanin, L., "Analytical solutions of the system of two coupled pure cubic nonlinear oscillators equations," *J. Sound Vibr.*, Vol. 245, No. 3, 2001, pp. 571–580.

[153] Cveticanin, L., "The motion of a two-mass system with nonlinear connection," *J. Sound Vibr.*, Vol. 252, No. 2, 2002, pp. 361–369.

[154] Cveticanin, L., "Analytic solution of the system of two coupled differential equations with the fifth-order nonlinearity," *Physica A*, Vol. 317, 2003, pp. 83–94.

[155] Bathe, K. and Wilson, E., "Stability and accuracy analysis of direct integration methods," *Earthqu. Engineering Struct. Dyn.*, Vol. 1, 1973, pp. 283–291.

[156] Dorman, J. and Prince, J., "A family of embedded Runge-Kutta formulae," *J. Comp. App. Math.*, Vol. 6, 1980, pp. 19–26.

[157] Dorman, J. and Prince, J., "High order embedded Runge-Kutta formulae," *J. Comp. App. Math.*, Vol. 7, 1981, pp. 67–75.

[158] Xie, Y., "An assessment of time integration schemes for nonlinear dynamic equations," *J. Sound Vibr.*, Vol. 192, No. 1, 1996, pp. 321–331.

[159] Press, W., Flannery, B., Teukolsky, S., and Vetterling, W., *Numerical Recipes in C: The Art of Scientific Computing.*, Cambridge University Press, 1992, http://www.nr.com.

[160] Stroud, K., *Further Engineering Mathematics*, Springer-Verlag, Heidelberg, 2nd ed., 1990.

[161] Chan, H., Chung, K., and Xu, Z., "A perturbation-iterative method for determining limit cycles of strongly nonlinear oscillators," *J. Sound Vibr.*, Vol. 183, 1995, pp. 707.

[162] Chan, H., Chung, K., and Xu, Z., "A perturbation-incremental method for strongly nonlinear oscillators," *Int. J. Nonlinear Mech.*, Vol. 31, No. 1, 1996, pp. 59–72.

[163] Lau, S. and Cheung, Y., "Amplitude incremental variational principle for nonlinear vibration of elastic systems," *ASME J. Appl. Mech.*, Vol. 48, 1981, pp. 959.

[164] Lau, S. and Yuen, S., "Solution diagram of nonlinear dynamic systems by the IHB method," *J. Sound Vibr.*, Vol. 167, 1993, pp. 303.

[165] Chung, K., Chan, C., Xu, Z., and Xu, J., "A perturbation-incremental method for strongly nonlinear non-autonomous oscillators," *Int. J. Nonlinear Mech.*, Vol. 40, 2005, pp. 845–859.

[166] Wu, B. and Lim, C., "Large amplitude nonlinear oscillations of a general conservative system," *Int. J. Nonlinear Mech.*, Vol. 39, 2004, pp. 859–870.

[167] Wu, B. and Li, A., "A method for obtaining approximate analytical periods for a class of nonlinear oscillators," *Meccanica*, Vol. 36, 2001, pp. 167.

[168] Lim, C., Wu, B., and He, L., "A new approximate analytical approach for dispersion relation of the nonlinear Klein-Gordon equation," *Chaos*, Vol. 11, 2001, pp. 843.

[169] Qaisi, M., "Analytical solution of the forced Duffing's oscillator," *J. Sound Vibr.*, Vol. 194, No. 4, 1996, pp. 513–520.

[170] Li, P. and Wu, B., "An iteration approach to nonlinear oscillations of conservative single-degree-of-freedom systems," *Acta Mechanica*, Vol. 170, 2004, pp. 69–75.

[171] Lim, C. and Wu, B., "A modified Mickens procedure for certain nonlinear-linear oscillators," *J. Sound Vibr.*, Vol. 257, 2002, pp. 202–206.

[172] Maccari, A., "Nonlinear oscillations with multiple resonant or non-resonant forcing terms," *Int. J. Nonlinear Mech.*, Vol. 34, 1999, pp. 27–34.

[173] Cai, J., Wu, X., and Li, Y., "An equivalent nonlinearistaion method for strongly nonlinear oscillations," *Mechanics Research Communications*, Vol. 32, 2005, pp. 553–560.

[174] Ge, Z.-M. and Ku, F.-N., "Subharmonic Melnikov functions for strongly odd nonlinear oscillators with large perturbations," *J. Sound Vibr.*, Vol. 236, No. 3, 2000, pp. 554–560.

[175] Melnikov, V., "On the stability of the center for time periodic perturbations," *Transactions of the Moscow Mathematical Society*, Vol. 12, 1963, pp. 1–57.

[176] Holmes, P. and Marsden, J., "Partial differential equation with infinitely many periodic orbits: chaotic oscillations of forced beam," *Archive for Rational Mechanics Analysis*, Vol. 76, 1981, pp. 135–166.

[177] Mandal, S., "The approximate solution of a classical quartic anharmonic oscillator with periodic force: a simple analytical approach," *Comm. Nonlin. Sc. & Numer. Simul.*, Vol. 10, 2005, pp. 341–352.

[178] He, J., "A review on some new recently developed nonlinear analytical techniques," *Int. J. Nonlin. Sc. Numer. Simul.*, Vol. 1, 2000, pp. 57–71.

[179] Granas, A., Frigon, M., and Sabidussi, G., editors, *Topological Methods in Differential Equations and Inclusions*, Vol. 472 of *NATO ASI Series C: Mathematical and Physical Science*, Kluwer, Dordrecht, The Netherlands, 1995.

[180] Shafarevich, I., *Algebraic geometry I : Algebraic Curves, Algebraic Manifolds and Schemes*, Vol. 23 of *Encyclopaedia of Mathematical Sciences*, Springer-Verlag, 1994.

[181] Liao, S. and Chwang, A., "Application of homotopy analysis method in nonlinear oscillations," *ASME J. Appl. Mech.*, Vol. 65, 1998, pp. 914–922.

[182] Adomian, G., "A review of the decomposition method in applied mathematics," *J. Math. Anal. and Appl.*, Vol. 135, 1988, pp. 501–544.

[183] Wazwaz, A., "A reliable modification of Adomian's decomposition method," *Appl. Math. & Comput.*, Vol. 92, 1998, pp. 1–7.

[184] Lipscomb, T. and Mickens, R., "Exact solution to the antisymmetric, constant force oscillator equation," *J. Sound Vibr.*, Vol. 169, No. 1, 1994, pp. 138–140.

[185] Potti, P. and Sarma, M., "On the exact periodic solution for $\ddot{x} + \text{sign}(x) = 0$," *J. Sound Vibr.*, Vol. 220, 1999, pp. 380–383.

[186] Kreyszig, E., *Advanced Engineering Mathematics*, John Wiley & Sons, New York, 8th ed., 1999.

[187] Pilipchuck, V., "An explicit form general solution for oscillators with a non-smooth restoring force $\ddot{x} + \text{sign}(x)\, f(x) = 0$," *J. Sound Vibr.*, Vol. 226, No. 4, 1999, pp. 795–798.

[188] Pilipchuck, V., "Analytical study of vibrating systems with strong nonlinearities by employing saw-tooth time transformation," *J. Sound Vibr.*, Vol. 192, No. 1, 1996, pp. 43–64.

[189] Awrejcewicz, J. and Andrianov, I., "Oscillations of nonlinear systems with restoring force close to $\text{sign}(x)$," *J. Sound Vibr.*, Vol. 252, No. 5, 2002, pp. 962–966.

[190] Ariaratnam, S., "Response of a nonlinear system to pulse excitation," *J. Mech. Engineering Sc.*, Vol. 6, 1964, pp. 26–31.

[191] Bauer, H., "The response of a nonlinear system to pulse excitation," *Int. J. Nonlinear Mech.*, Vol. 1, 1966, pp. 267–282.

[192] Bauer, H., "The response of a nonlinear n-degree-of-freedom system to pulse excitation," *Int. J. Nonlinear Mech.*, Vol. 3, 1968, pp. 157–171.

[193] Bauer, H., "Nonlinear response of elastic plates to pulse excitation," *Int. J. Appl. Mech.*, Vol. 35, 1968, pp. 47–52.

[194] Bauer, H., "Vibrational behaviour of nonlinear systems to pulse excitations of finite duration," *Int. J. Nonlinear Mech.*, Vol. 6, 1971, pp. 529–543.

[195] Srirangarajan, H. and Srinivasan, P., "The pulse response of nonlinear systems," *J. Sound Vibr.*, Vol. 44, No. 3, 1976, pp. 369–377.

[196] Sinha, S. and Srinivasan, P., "An aproximate analysis of nonlinear nonconservative systems subjected to step function excitation," *J. Sound Vibr.*, Vol. 22, No. 2, 1972, pp. 211–219.

[197] White, R., "Effects of nonlinearity due to large deflections in the derivation of frequency response data from the impulse response of structures," *J. Sound Vibr.*, Vol. 29, No. 3, 1973, pp. 295–307.

[198] Anderson, G., "Application of ultraspherical polynomials to nonlinear, nonconservative systems subjected to step function excitation," *J. Sound Vibr.*, Vol. 32, No. 1, 1974, pp. 101–108.

[199] Beshai, M. and Dokainish, M., "The transient response of a forced nonlinear system," *J. Sound Vibr.*, Vol. 41, No. 1, 1975, pp. 53–62.

[200] Schetzen, M., *The Volterra and Wiener Theories of Nonlinear Systems*, Wiley & Sons, New York, 1980.

[201] Sato, A. and Asada, K., "Laplace transform transient analysis of a nonlinear system," *J. Sound Vibr.*, Vol. 121, No. 3, 1988, pp. 473–479.

[202] Hosono, T., "Numerical inversion of Laplace transform and some applications to wave optics," *Radio Science*, Vol. 16, 1981, pp. 1015–1019.

[203] Chandra Shekar, N., Hatwal, H., and Mallik, A., "Response of nonlinear dissipative shock isolators," *J. Sound Vibr.*, Vol. 214, No. 4, 1998, pp. 589–603.

[204] Abbasov, T. and Bahadir, A., "The investigation of the transient regimes in the nonlinear systems by the generalized classical method," *Math. Problems Engineer.*, Vol. 2005, No. 5, 2005, pp. 503–519.

[205] Zhou, J., *Differential Transformation and its Application for Electrical Circuits*, Huazhong University Press, Wuhan, P.R. China, 1986, (in Chinese).

[206] Pukhov, G., *Taylor Transformation and its Applications for Electrotechnics and Elektronics*, Naukova Dumka, Kiev, 1978, (in Russian).

[207] Pukhov, G., *Differential Transforms, Functions and Equations*, Naukova Dumka, Kiev, 1980, (in Russian).

[208] Pukhov, G., *Differential Analysis of Electrical Circuits*, Naukova Dumka, Kiev, 1982, (in Russian).

[209] Chen, C.-K. and Ho, S.-H., "Application of differential transformation to eigenvalue problems," *Appl. Math. Computation*, Vol. 79, 1996, pp. 173–188.

[210] Bert, C., "Application of differential transform method to heat conduction in tapered fins," *ASME J. Heat Transfer*, Vol. 124, Feb. 2002, pp. 208–209.

[211] Yu, L. and Chen, C., "Application of Taylor transformation to optimize rectangular fins with variable thermal parameters," *Appl. Math. Modelling*, Vol. 22, 1998, pp. 11–21.

[212] Chen, C.-K. and Ju, S.-P., "Application of differential transformation to transient advective-dispersive transport equation," *Appl. Math. Computation*, Vol. 155, 2004, pp. 25–38.

[213] Kóksal, M. and Herdem, S., "Analysis of nonlinear circuits by using differential Taylor transfrom," *Comp. Electrical Engineer.*, Vol. 28, 2002, pp. 513–525.

[214] Chen, C.-J. and Wu, W.-J., "Application of the Taylor differential transformation method to viscous damped vibration of hard and soft spring systems," *Comp. Struct.*, Vol. 59, No. 4, 1996, pp. 631–619.

[215] Chen, C.-L., Lin, S.-H., and Chen, C.-K., "Application of Taylor transformation to nonlinear predictive control problem," *Appl. Math. Modelling*, Vol. 20, 1996, pp. 699–710.

[216] Jang, M.-J. and Chen, C.-L., "Analysis of the response of a strongly nonlinear damped system using a differential transformation technique," *Appl. Math. Computation*, Vol. 88, 1997, pp. 137–151.

[217] Hassan, I.-H., "Differential transformation technique for solving higher-order initial value problems," *Appl. Math. Computation*, Vol. 154, 2004, pp. 299–311.

[218] Jang, M.-J., Chen, C.-L., and Liy, Y.-C., "On solving the initial-value problems using the differential transformation method," *Appl. Math. Computation*, Vol. 115, 2000, pp. 145–160.

[219] Kurnaz, A. and Oturanc, G., "The differential transform approximation for the system of ordinary differential equations," *Int. J. Computer Math.*, Vol. 82, No. 6, 2005, pp. 709–719.

[220] Chen, C.-K. and Chen, S.-S., "Application of the differential transformation method to a nonlinear conservative system," *Appl. Math. Computation*, Vol. 154, 2004, pp. 431–441.

[221] Kurnaz, A., Oturanç, G., and Kiris, M., "N-dimensional differential transformation method for solving PDEs," *Int. J. Computer Math.*, Vol. 82, No. 3, 2005, pp. 369–380.

[222] Efimov, I., "Exactitude of the electronic device analysis by differential transformation methods," *4th Siberian-Russian Workshop and Tutorials EDM*, Vol. Section II, 1-4 July 2003, pp. 150–151.

[223] Golovin, E. and Stoukatch, O., "Usage of orthogonal polynomials at calculation of transfer processes in electric circuits with variable parameters using differential transformations," *4th Siberian-Russian Workshop and Tutorials EDM*, Vol. Section II, 1-4 July 2003, pp. 152–157.

[224] Golovin, E. and Stoukatch, O., "The use of orthogonal polynoms in the differential transformations," *Modern Techniques and Technologies*, Vol. Section IV: Electrical material science, IEEE, 2001, pp. 105–107.

[225] Golovin, E. and Stoukatch, O., "Modelling accuracy of technical systems using the differential transformation method," *Modern Techniques and Technologies*, Vol. Section II: Instrument making, IEEE, 2000, pp. 62–64.

[226] Harris, C., *Shock and Vibration Handbook*, McGraw-Hill, New York, 3rd ed., 1988.

[227] Warburton, G., *The Dynamical Behaviour of Structures*, Structures and Solid Body Mechanics, Pergamon Press, Oxford, 2nd ed., 1976.

[228] Rao, S., *Mechanical Vibrations*, Addison-Wesley, Reading, Mass., 3rd ed., 1995.

[229] Ribeiro, P., "The Second Harmonic and the Validity of Duffing's Equation for Vibration of Beams with Large Displacement," *Comp. Struct.*, Vol. 79, 2001, pp. 107–117.

[230] Arnold, V., *Ordinary Differential Equations*, MIT Press, Cambridge, Massachusetts, 1973.

[231] Verhulst, F., *Nonlinear Differential Equations and Dynamical Systems*, Springer-Verlag, Berlin, Heidelberg, 1980.

[232] Goos, G., Hartmanis, J., and Leeuwen, J., editors, *Symbolic and Numerical Scientific Computation: Second International Conference - Snsc 2001*, Springer-Verlag, Berlin, Heidelberg, 2003.

[233] Davis, H. T., *Introduction to nonlinear differential and integral equations*, Dover Publications, 1962.

[234] Sastry, S., *Nonlinear Systems - Analysis, Stability, and Control*, Vol. 10 of *Interdisciplinary Applied Mathematics*, Springer, New York, Berlin, 1999.

[235] Coddington, E. and Levinson, N., *Theory of Ordinary Differential Equations*, McGraw-Hill, New York, 1955.

[236] Hale, J., *Oscillations in Nonlinear Systems*, McGraw-Hill, New York, 1963.

[237] Thompson, J. and Stewart, H., *Nonlinear Dynamics and Chaos*, John Wiley & Sons, Chichester, 2nd ed., 2002.

[238] Wiggins, S., *Global Bifurcation and Chaos - Analytical Methods*, Vol. 73 of *Applied Mathematical Sciences*, Springer-Verlag, New York, 1988.

[239] Meirovitch, L., *Elements of Vibration Analysis*, McGraw-Hill Book Company, New York, 2nd ed., 1986.

[240] Jackson, E., *Perspectives of Nonlinear Dynamics*, Vol. 1, Cambridge University Press, Cambridge, New York, 1991.

[241] Glendinning, P., *Stability, Instability and Chaos: An Introduction to the Theory of Nonlinear Differential Equations*, Cambridge Texts in Applied Mathematics, Cambridge University Press, Cambridge, 1994.

[242] Hale, J. and Kocak, H., *Dynamics and Bifurcations*, Vol. 3 of *Texts in Applied Mathematics*, Springer-Verlag, Berlin, Heidelberg, 1991.

[243] Burns, K. and Gidea, M., *Differential Geometry and Topology : With a View to Dynamical Systems*, Chapman & Hall, Boca Raton, Fla., London, 2005.

[244] Khalil, H., *Nonlinear Systems*, Prentice Hall, 2002.

[245] Corduneanu, C., *Principles of Differential and Integral Equations*, Chelsea Publishing Company, The Bronx, New York, 2nd ed., 1977.

[246] Matheij, K. and Molenaar, J., *Ordinary Differential Equations in Theory and Practice*, Vol. 43 of *Classics in Applied Mathematics*, SIAM, Philadelphia, PA., 2002.

[247] Arnold, V., *Geometrical Methods in the Theory of Ordinary Differential Equations*, Springer-Verlag, New York, 1988.

[248] Lyapunov, A., Fuller, A., Smirnov, V., and Barrett, J., *The general problem of the stability of motion*, Taylor & Francis, London, 1992.

[249] Guckenheimer, J. and Holmes, P., *Nonlinear Oscillations, Dynamical Systems, and Bifurcation of Vector Fileds*, Springer-Verlag, New York, 1983.

[250] Kapitaniak, T., *Chaotic Oscillators : Theory and Applications*, World Scientific, Singapore, 1991.

[251] Ueda, Y., "Randomly transitional phenomena in the system governed by Duffing's equation," *J. Stat. Phy.*, Vol. 20, 1979, pp. 181–196.

[252] Ueda, Y., *Steady motions exhibited by Duffing's equation: a picture book of regular and chaotic motion*, Vol. 42 of *New Approaches to Nonlinear Problems in Dynamics*, Society of Industrial and Applied Mathematics (SIAM), Philadelphia, PA., 1980.

[253] Ueda, Y., *The Road to Chaos*, Aerial Press, Santa Cruz, 1992.

[254] Moon, F., *Chaotic Vibrations*, John Wiley & Sons, 1987.

[255] Davis, J., *Differential Equations with Maple: A Intercative Approach*, Birkhaeuser, Boston, 2001.

[256] Krasovskii, N., *Stability of Motion*, Stanford University Press, Stanford, CA., 1963.

[257] Jackson, E., *Perspectives of Nonlinear Dynamics*, Vol. 2, Cambridge University Press, Cambridge, New York, 1991.

[258] Rosenberg, R., *Analytical Dynamics of Discrete Systems*, Vol. 4 of *Mathematical Concepts and Engineering Methods in Science and Engineering*, Plenum Press, New York, 1977.

[259] LaSalle, J., "The Stability of Dynamical Systems," *Regional Conference Series in Applied Mathematics*, Society for Industrial and Applied Mathematics (SIAM), 1976, pp. 112–119.

[260] Perko, L., *Differential Equations and Dynamical Systems*, Vol. 7 of *Texts in Applied Mathematics*, Springer, New York, Berlin, 3rd ed., 2001.

[261] Bullo, F. and Lewis, A., *Geometric Control of Mechanical Systems*, Vol. 49 of *Texts in Applied Mathematics*, Springer-Verlag, New York, Berlin, 2004.

[262] Barbashin, E., *Introduction into Stability Theory*, Nauka, Moscow, 1967.

[263] Greenwood, D., *Advanced Dynamics*, Cambridge University Press, Cambridge, UK, 2003.

[264] Ruelle, D., *Elements of Differentiable Dynamics and Bifurcation Theory*, Academic Press, New York, 1989.

[265] Lakshmikantham, L. and Lakshmikantham, V., *Trends in Theory and Practice of Nonlinear Differential Equations*, Vol. 90 of *Lecture Notes in Pure and Applied Mathematics*, Marcel Dekker, New York, 1984.

[266] Seydel, R., *Practical Bifurcation and Stability Analysis - From Equilibrium to Chaos*, Vol. 5 of *Interdisciplinary Applied Mathematics*, Springer, Berlin, Heidelberg, 2nd ed., 1994.

[267] Merkin, D., *Introduction to the Theory of Stability*, Vol. 24 of *Texts in Applied Mathematics*, Springer, New York, Berlin, 1997.

[268] Zubov, V., *Methods of A.M.Lyapunov and their Application*, Noordhoff, Groningen, The Netherlands, 1964.

[269] Brannan, D., Esplen, M., and Gray, J., *Geometry*, Cambridge University Press, Cambridge, UK, 5th ed., 2003.

[270] Schaedlich, M. and Ferguson, N., "Blast Induced Shock Waves in Structures - Part I," ISVR Technical Memorandum 936, Institute of Sound and Vibration Research, University of Southampton, June 2005.

[271] Kanwal, R., *Generalized Functions: Theory and Applications*, Birkhaeuser, Boston, 3rd ed., 2004.

[272] Simmonds, J. and Mann, J., *A First Look at Perturbation Theory*, Dover Publications, New York, 2nd ed., 1998.

[273] Bogaevski, V., *Algebraic Methods in Nonlinear Perturbation Theory*, Vol. 88 of *Applied Mathematical Sciences*, Springer-Verlag, New York, 1991.

[274] Mladenov, V., Hegt, H., and Van Roermund, A., "Terminal dynamics approach to cellular neural networks," *ISCAS 2001. The 2001 IEEE International Symposium on Circuits and Systems*, Vol. 3, IEEE, Sydney, NSW, Australia, May 2001, pp. 97–100.

[275] Vanden-Eijnden, W., "A note on generalized flows," *Physica D*, Vol. 183, 2003, pp. 159–174.

[276] Bhat, S. and Bernstein, D., "Geometric homogeneity with applications to finite-time stability," *Math. Control Signals Sys.*, Vol. 17, May 2005, pp. 101–127.

[277] Krastanov, M., Malisoff, M., and Wolenski, P., "On the strong invariance property for non-Lipschitz dynamics," *Comm. Pure Appl. Analysis*, Vol. 5, No. 1, March 2006, pp. 107–124.

[278] Jiang, M.-Y., "Periodic Solutions of Second Order Differential Equations with Discontinuous Nonlinearities," Tech. rep., LMAM, School of Mathematical Sciences, Peking University, Beijing, 100871, P.R. China, Dec. 2005.

[279] Jiang, M.-Y., "Periodic solutions of second order differential equations with an obstacle," *Nonlinearity - Institute of Physics Publishing*, Vol. 19, 2006, pp. 1165–1183.

[280] Robinson, J., "Solutions of continuous ODEs obtained as the limit of solutions of Lipschitz ODEs," *Nonlinearity*, Vol. 12, 1999, pp. 555–561.

[281] Rios, V. and Wolenski, P., "A characterization of strongly invariant systems for a class of non-Lipschitz multifunctions," *Proceedings of the 42nd IEEE Conference on Decision and Control*, Vol. 3, IEEE, Maui, Hawaii, Dec. 2003, pp. 2593–2596.

[282] Zeidler, E., *Nonlinear Functional Analysis and its Application: Fixed Point Theorems*, Vol. 1, Springer-Verlag, Berlin, 1986.

[283] Mantri, R., Venkatasubramanian, V., and Saberi, A., "An investigation of simple nonsmooth power systems models," *Proceedings of the 3rd Conference on Decision and Control*, Vol. WM4-2:50, IEEE, Lake Buena Vista, Fl., Dec. 1994, pp. 619–642.

[284] Köksal, M., "On the state equations of nonlinear networks and the uniqueness of their solutions," *IASTED Measurement and Control Symposium*, Proceedings of the IASTED Measurement and Control Symposium, Istanbul, Turkey, July 1986, pp. 141–147.

[285] Parker, T. and Chua, L., "Chaos: A tutorial for engineers," *Proceedings of the IEEE*, Vol. 75, No. 8, August 1987, pp. 982–1008.

[286] Venkatasubramanian, V., Mantri, R., and Saberi, A., "On the existence and uniqueness of solutions for nonsmooth systems," *Proceedings of the 32nd Conference on Decision and Control*, Vol. 3, IEEE, Seattle, Wa., June 1995, pp. 1811–1815.

[287] Marques, H., *Nonlinear Control System - Analysis and Design*, Wiley Interscience, Hoboken, New Jersey, 2003.

[288] Byrd, P. and Friedman, M., *Handbook of Elliptic Integrals for Engineers and Physicists*, Vol. LXVII of *Die Grundlehren der Mathematischen Wissenschaften*, Springer-Verlag, Berlin, Heidelberg, 2nd ed., 1972.

[289] Wolfram, S., *The Mathematica Book*, Cambridge University Press, 4th ed., 1999.

[290] Gradshteyn, I. S., Ryzhik, I. M., Jeffrey, A., and Zwillinger, D., *Table of Integrals, Series, and Products*, Academic Press, London, 4th ed., 1980.

[291] Hancock, H., *Elliptic Integrals*, Dover Publications, New York, 1958.

[292] Groebner, W. and Hofreiter, N., *Integraltafeln - Erster Teil: Unbestimmte Integrale*, Vol. 1, Springer-Verlag, Wien and Innsbruck, 2nd ed., 1957.

[293] Jones, N., *Structural Impact*, Cambridge University Press, Cambridge, U.K., 1997.

[294] *Matlab 7 Reference*, 3 Apple Hill Drive, Natick, MA 01760-2098, vers. 6/7 ed., 2005.

[295] Chen, S. and Cheung, Y., "An elliptic perturbation method for certain strongly nonlinear oscillators," *J. Sound Vibr.*, Vol. 192, No. 2, 1996, pp. 453–464.

[296] Faulkner, L. and Logan, E., *Handbook of Machinery Dynamics*, Marcel Dekker, 2000.

[297] Hazewinkel, M., *Encyclopaedia of Mathematics*, Springer Verlag, Berlin, Heidelberg, 2002.

[298] Schaedlich, M. and Ferguson, N., "Analysis of the nonlinear transient response of simple structures to shock excitation," *Proceedings of the XXIII International Modal Analysis Conference - IMAC 2005*, Vol. 1, IMAC, Orlando, Fl., 31 January - 4 February 2005, pp. 234–241.

[299] Paz, M. and Leigh, W., *Structural Dynamics*, Springer, 2003.

[300] Vainberg, M., *Variational Methods and Methods of Monotone Operators in the Theory of Nonlinear Equations*, Wiley & Sons, New York, 1973.

[301] Atkinson, K. and Han, W., *Theoretical Numerical Analysis: A Functional Analysis Framework*, Vol. 39, Springer-Verlag, New York, 2001.

[302] Betounes, D., *Theory of Differential Equations*, Springer-Verlag, New York, 2001.

[303] "Encyclopædia Britannica 2006," Encyclopædia Britannica Online, September 29 2006, http://www.britannica.com/eb/article-9059897/Charles-Emile-Picard.

[304] Shampine, L., *Numerical Solution of Ordinary Differential Equations Volume IV*, CRC Press, Boca Raton, FL., USA, 1994.

[305] Agarwal, R., editor, *Contributions in Numerical Mathematics*, World Scientific, Singapore, 1993.

[306] Lemons, D. S., *Perfect Form: Variational Principles, Methods, and Applications in elementary Physics*, Princeton University Press, 1997.

[307] Cash, J. and Karp, A., "A Variable Order Runge-Kutta Method for Initial Value Problems with Rapidly Varying Right-Hand Sides," *ACM Transactions on Mathematical Software*, Vol. 16, No. 3, 1990, pp. 201–222.

[308] Baker, W., *Explosion Hazards Evaluation*, Elsevier Scientific Publishing Co., 1983.

[309] Dyne, S., "The Prediction of the Response and Damage Potential of Structures under Shock Loading," Contract Report Ref.: D/ER1/9/4/2040/394-SAL 1053, Institute of Sound and Vibration, University of Southampton, 1985.

[310] Glasstone, S. and Dolan, P., *The Effects of Nuclear Weapons*, Castle House Publications Ltd., 3rd ed., 1980.

[311] Kinney, G. and Graham, K., *Explosive Shocks in Air*, Springer-Verlag, New York, 1985.

[312] Naval Surface Warfare Center, Engineering & Information Systems Dep., Dahlgren, VA, 22448-5000, USA, *NSWC - Naval Surface Warfare Center Mathematical Library*, 2005, http://www.csit.fsu.edu/~burkardt/f_src/nswc/nswc.html.

[313] The Scilab Consortium, *Scilab Scientific Software Package*, 2006, http://www.scilab.org/.

[314] MapleSoft, 615 Kumpf Drive, Waterloo, Ontario, Canada N2V 1K8, *Maple 10*, 2005, http://www.maplesoft.com.

[315] Carlson, B., "Computing elliptic integrals by duplication," *Numer. Math.*, Vol. 33, 1979, pp. 1–16.

[316] Morita, T., "Calculation of the complete elliptic integrals of the first and second kinds with complex modulus," *Numer. Math.*, Vol. 82, 1999, pp. 677–688.

[317] Morita, T., "Calculation of the complete elliptic integrals with complex modulus," *Numer. Math.*, Vol. 29, 1978, pp. 233–236.

[318] Enright, W., "A new error-control for initial value solvers," *Appl. Math. Computation*, Vol. 31, 1989, pp. 288–301.

[319] Higham, D., "Global Error versus Tolerance for Explicit Runge-Kutta Methods," *IMA J. Numer. Analysis*, Vol. 11, 1991, pp. 457–480.

[320] Shampine, L., "Local error control in codes for ordinary differential equations," *Appl. Math. Computation*, Vol. 3, No. 3, 1977, pp. 189–210.

[321] Atkinson, K. and Han, W., *Theoretical Numerical Analysis: A Functional Analysis Framework*, Vol. 39 of *Texts in Applied Mathematics*, Springer Verlag, 2nd ed., 2005.

[322] Gear, C., *Numerical Initial Value Problems in Ordinary Differential Equations*, Englewood Cliffs, New Jersey, USA, 1971.

APPENDIX A

ANALYTICAL ROOTS FOR HIGHER-ORDER POLYNOMIALS

A.1 Third-order polynomials

Only a limited number of procedures are available for solving cubic algebraic equations explicitly and analytically. A very robust and straightforward method is Cardan's algorithm described in [58]. A brief outline is given in what follows.

Making use of the substitution

$$y = x + \frac{r}{3} \tag{A.1a}$$

the general third-order equation

$$x^3 + r\,x^2 + s\,x + t = 0 \tag{A.1b}$$

is rewritten in its reduced form

$$y^3 + p\,y + q = 0 \tag{A.1c}$$

where

$$p = \frac{3\,s - r^2}{3}, \quad q = \frac{2\,r^3}{27} - \frac{r\,s}{3} + t, \qquad \text{and,} \qquad D_s = \left(\frac{p}{3}\right)^3 + \left(\frac{q}{2}\right)^2 \tag{A.1d}$$

with the sign of D_s and the nature of x (real or imaginary) determining the number of solutions of (A.1b) as shown in Table A.1. It becomes clear that Eq.(A.1c) has at least always one real solution

Table A.1 – Nature of possible solutions for y from equation (A.1c) depending upon the sign of D_s as given in Eq.(A.1d), see [58].

	$x \in \mathbb{R}$	$x \in \mathbb{C}$
$D_s > 0$	one real	one real, two conjugate complex
$D_s < 0$	three real	three real
$D_s = 0$	one real, two double real, or triple real (if $p = q = 0$)	one real, two double real, or triple real (if $p = q = 0$)

which is determined by

$$y_1 = w + v \tag{A.2a}$$

together with

$$w = \sqrt[3]{\frac{-q}{2} + \sqrt{D_s}} \qquad \text{and} \qquad v = -\frac{p}{3\,w}\,. \tag{A.2b}$$

The two remaining solutions, being complex in the case of $D_s > 0$, are obtained as

$$y_2 = -\frac{w+v}{2} + \frac{w-v}{2}\,\mathrm{i}\,\sqrt{3}\,, \qquad\qquad y_3 = -\frac{w+v}{2} - \frac{w-v}{2}\,\mathrm{i}\,\sqrt{3}\,, \tag{A.2c}$$

respectively. Worth noting here is the fact that for $D_s < 0$ Eq.(A.2b) seems to contradict Table A.1 since w becomes complex. However, this must be seen as an integral part of the solution process and can be circumvented by introducing [58]

$$\rho_p = \sqrt{-\frac{p}{27}} \qquad \text{and} \qquad \cos\varphi_p = -\frac{q}{2\,\rho_p} \tag{A.3a}$$

which leads to three real solutions for (A.1c) in the case of $D_s < 0$, given as

$$y_k = 2\sqrt[3]{\rho_p}\cos\left[\frac{1}{3}\left(\varphi_p + 2\,\pi(k-1)\right)\right]\,, \qquad \text{with} \qquad (k = 1, 2, 3)\,. \tag{A.3b}$$

The variation of y_k for $0 \leq \varphi_p \leq 2\pi$ is shown in Fig. A.1 and illustrates that the amplitude of any solution y_k is very much dependent upon φ_p, i.e. the ratio of q to p but, unfortunately, is not ordered by absolute size in any way with either increasing or decreasing index k.

Finally, rearranging the substitution made at the beginning in Eq.(A.1a) the solutions for the original problem (A.1b) are obtained as

$$x_j = y_j - \frac{r}{3}\,, \qquad (j = 1, 2, 3)\,. \tag{A.4}$$

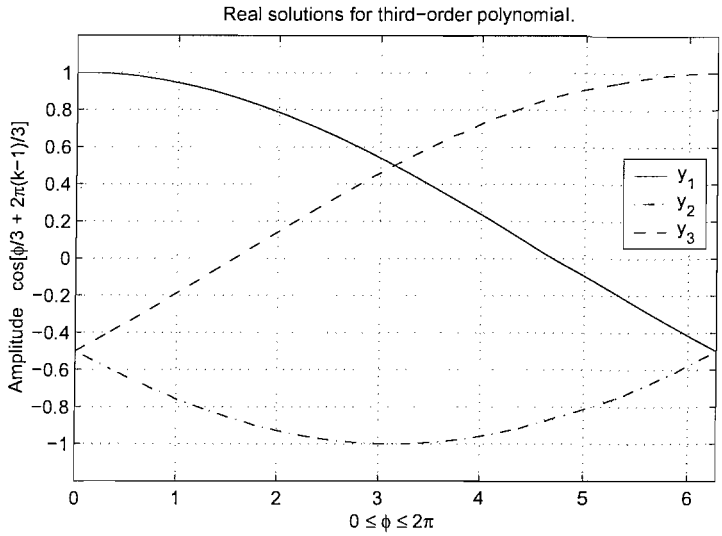

Figure A.1 – Oscillation of the solutions for y_k with $0 \leq \varphi_p \leq 2\pi$.

A.2 Fourth-order polynomials

A nonlinear fourth-order algebraic equation

$$a\,x^4 + b\,x^3 + c\,x^2 + d\,x + e = 0\,, \qquad a, b, c, d, e \in \mathbb{R}\,;\;\; a \neq 0 \tag{A.5a}$$

can be rewritten in its reduced form

$$y^4 + p\,y^2 + q\,y + r = 0 \tag{A.5b}$$

using the substitution [58]

$$y = x + \frac{b}{4\,a}\,. \tag{A.5c}$$

Table A.2 – Nature of possible solutions for y depending upon the solution of the cubic resolving term, see [58]. According to Vieta's theorem the product of $z_1 z_2 z_3 = q^2$ of all roots z_1, z_2, z_3 must be positive.

cubic resolving term	fourth-order equation
all roots real and positive	four real roots
all roots real, one positive, two negative	two pairs of conjugate complex roots
one root real, two conjugate complex	two real, two conjugate complex roots

The nature of all solutions of (A.5b) depend upon the solution behaviour of the equivalent *cubic resolving term* [58]

$$z^3 + 2\,p\,y^2 + \left(p^2 - 4\,r\right) y - q^2 = 0\,, \tag{A.6}$$

which can be solved for using Eq.(A.1c) to (A.4). The solutions to (A.5b) are subsequently obtained with

$$\begin{aligned} y_1 &= \frac{1}{2}\left(\sqrt{z_1} + \sqrt{z_2} - \sqrt{z_3}\right)\,, & y_2 &= \frac{1}{2}\left(\sqrt{z_1} - \sqrt{z_2} + \sqrt{z_3}\right)\,, \\ y_3 &= \frac{1}{2}\left(-\sqrt{z_1} + \sqrt{z_2} + \sqrt{z_3}\right)\,, & y_4 &= \frac{1}{2}\left(-\sqrt{z_1} - \sqrt{z_2} - \sqrt{z_3}\right)\,. \end{aligned} \tag{A.7}$$

It should be noted here that in addition to the signs given in (A.7) all roots $\sqrt{z_i}$ have to be chosen in a manner to comply with Vieta's Lemma [58]

$$z_1\,z_2\,z_3 = q^2\,. \tag{A.8}$$

APPENDIX B

ELLIPTIC INTEGRALS AND RELATED FUNCTIONS

B.1 Hypergeometric and Gamma functions

The Gauss' hypergeometric function ${}_2\mathsf{F}_1(\ldots)$ has a series expansion of the form [58]

$$ {}_2\mathsf{F}_1(a,b;c;x) = \sum_{k=0}^{\infty} \frac{a_k\, b_k}{c_k\, k!} x^k \tag{B.1} $$

and is a special case of the generalised hypergeometric series [109]

$$ {}_v\mathsf{F}_w(a_1, a_2, \ldots, a_v; c_1, \ldots, c_w; x) = \sum_{m=0}^{\infty} \frac{x^m}{m!} \frac{(a_1)_m \ldots (a_v)_m}{(c_1)_m \ldots (c_w)_m} \,. \tag{B.2} $$

The series in (B.1) satisfies the differential equation

$$ x(1-x)y''(x) + [c - (a+b+1)x]\, y'(x) = ab\, y(x) \tag{B.3} $$

and terminates if either a or b is equal to a negative integer or zero. For the case of

$$ \Re\{a+b-c\} < 0\,, \tag{B.4} $$

(B.1) converges absolutely throughout the entire unit circle [290], i.e. a solution to the specific problem exists. The function ${}_2\mathsf{F}_1(\ldots)$ can be written in terms of an integral representation [289]

$$ {}_2\mathsf{F}_1(a,b;c;x) = \frac{\Gamma(c)}{\Gamma(b)\,\Gamma(c-b)} \int_0^1 \xi^{b-1} (1-\xi)^{c-b-1} (1-\xi x)^{-a}\, \mathrm{d}\xi \,, \quad (c > a > 0) \tag{B.5} $$

where $\Gamma(\ldots)$ is the Gamma function defined as [58]

$$\Gamma(x) = \lim_{n\to\infty} \frac{n!\, n^{x-1}}{x(x+1)(x+2)\ldots(x+n)}\,, \qquad \begin{array}{l} x \in \mathbb{R}\,, \\ x \notin \{0, -1, -2, -3, \ldots\}\,. \end{array} \tag{B.6}$$

In the special case of $x > 0$ this simplifies to

$$\Gamma(x) = \int_0^\infty \mathrm{e}^{-\vartheta} \vartheta^{x-1}\, \mathrm{d}\vartheta\,. \tag{B.7}$$

For a certain range of specific values of a, b and c the hypergeometric function in Eq.(B.5) can be represented in terms of elementary functions [290], for example

$${}_2\mathsf{F}_1\left(\frac{1}{2}, \frac{1}{2}; \frac{3}{2}; \frac{x^2}{a}\right) = \frac{\sqrt{a}}{x} \arcsin(x)\,. \tag{B.8}$$

B.2 Legendre form

Any third-order algebraic polynomial equation

$$-x^3 + A\,x^2 + B\,x + C = \mathcal{P}^{[3]} \tag{B.9}$$

can be transformed into Legendre's canonical form [58]

$$\mathcal{P}^{[3]} = (a - x)(x - b)(x - c) \tag{B.10a}$$

with

$$\begin{aligned} A &= (a + b + c) \\ B &= -a(b + c) - b\,c \\ C &= a\,b\,c\,, \end{aligned} \tag{B.10b}$$

and $a, b, c \in \mathbb{R}$ are the roots of the equation $\mathcal{P}^{[3]} \equiv 0$. In case this yields only one real-valued and two conjugate complex roots, (B.9) is rewritten as

$$\mathcal{P}^{[3]} = (a - x)\Big[(x - c_1)^2 + c_2^2\Big]\,, \qquad a \in \mathbb{R}\,, \quad b, c \in \mathbb{C} \tag{B.11a}$$

with

$$c_1 = \frac{b + c}{2}\,, \qquad \text{and} \qquad c_2^2 = -\frac{(b - c)^2}{4}\,. \tag{B.11b}$$

Similarly, a fourth-order polynomial

$$-x^4 + A\,x^3 + B\,x^2 + C\,x + D = \mathcal{P}^{[4]} \tag{B.12}$$

can be transformed into

$$\mathcal{P}^{[4]} = (a-x)(x-b)(x-c)(x-d)\,, \tag{B.13a}$$

where

$$\begin{aligned} A &= a+b+c+d \\ B &= -a\,(b+c+d) - b\,(c+d) - c\,d \\ C &= a\,(b\,c+b\,d+c\,d) + b\,c\,d \\ D &= -a\,b\,c\,d\,, \end{aligned} \tag{B.13b}$$

and a, b, c, d are the roots of (B.12), thus $\mathcal{P}^{[4]} \equiv 0$. If

$$x^4 + A\,x^3 + B\,x^2 + C\,x + D\,, \tag{B.14a}$$

then

$$\begin{aligned} A &= -a-b-c-d \\ B &= a\,(b+c+d) + b\,(c+d) + c\,d \\ C &= a\,(-b\,c-b\,d-c\,d) - b\,c\,d \\ D &= a\,b\,c\,d\,. \end{aligned} \tag{B.14b}$$

Both transformations assume four real-valued roots of $\mathcal{P}^{[4]}$. For the case of $a, b \in \mathbb{R}$ and $c, d \in \mathbb{C}$, i.e. two real and two conjugate complex solutions of $\mathcal{P}^{[4]} \equiv 0$, equation (B.12) is rewritten as

$$\mathcal{P}^{[4]} = (x-a)(x-b)\Big[(x-c_2)^2 + c_1^2\Big] \equiv (x-a)(b-x)\Big[(x-c_2)^2 + c_1^2\Big] \tag{B.15a}$$

with

$$c_1^2 = -\frac{1}{4}\,(c-d)^2 \qquad \text{and} \qquad c_2 = \frac{1}{2}\,(c+d)\,. \tag{B.15b}$$

B.3 Elliptic integrals and Jacobian elliptic functions

The integral [58]

$$I = \int R\left(x, \left[a_0\,x^4 + a_1\,x^3 + a_2\,x^2 + a_3\,x + a_4\right]^{\frac{1}{2}}\right) \tag{B.16}$$

is called an elliptic integral[1)] if the equation

$$a_0\,x^4 + a_1\,x^3 + a_2\,x^2 + a_3\,x + a_4 = 0\,, \qquad (a_0\,, a_1 \neq 0) \tag{B.17}$$

[1)]The name originates from a special example where an integral of this type occurs in the rectification of the arc of an ellipse, see [288].

has no multiple roots and if R is a rational function of x and the square root

$$\sqrt{a_0\,x^4 + a_1\,x^3 + a_2\,x^2 + a_3\,x + a_4}\,. \tag{B.18}$$

Using different methods of substitution it is always possible to express a very few types of equation (B.16) in terms of elementary functions[2)] but certainly all variants of (B.16) in terms of three fundamental integrals [288], the so-called incomplete (or normal) elliptic integrals of first $\mathsf{F}(\phi,\kappa)$, second $\mathsf{E}(\phi,\kappa)$ and third $\mathsf{P}(\phi,n,\kappa)$ kind in Legendre's canonical form [58]. The inversion of the first kind of elliptic integrals leads to the elliptic functions of Abel, Jacobi and Weierstrass [109].

Because of the various definitions established in literature, and the resulting incompatible conversions of the three forms of $\mathsf{F}(\phi,\kappa)$, $\mathsf{E}(\phi,\kappa)$ and $\mathsf{P}(\phi,n,\kappa)$, a brief overview of elliptic integrals and Jacobian elliptic functions as used in this work is given in what follows. The employed versions represent the most commonly used forms found in numerous standard reference books [58, 109, 288, 292],

$$\mathsf{F}(\phi,\kappa) = \int_0^y \frac{\mathrm{d}\,x}{(1-x^2)\,(1-\kappa^2x^2)} = \int_0^\phi \frac{\mathrm{d}\,\vartheta}{\sqrt{1-\kappa^2\sin^2(\vartheta)}} \tag{B.19a}$$

$$\mathsf{E}(\phi,\kappa) = \int_0^y \frac{\left(1-\kappa^2x^2\right)\,\mathrm{d}\,x}{\sqrt{(1-x^2)\,(1-\kappa^2x^2)}} = \int_0^\phi \sqrt{1-\kappa^2\sin^2(\vartheta)}\,\mathrm{d}\,\vartheta \tag{B.19b}$$

$$\mathsf{P}(\phi,n,\kappa) = \int_0^y \frac{\mathrm{d}\,x}{(1+nx^2)\sqrt{(1-x^2)\,(1-\kappa^2x^2)}} = \int_0^\phi \frac{\mathrm{d}\,\vartheta}{\left(1+n\sin^2(\vartheta)\right)\sqrt{1-\kappa^2\sin^2(\vartheta)}} \tag{B.19c}$$

with the modulus κ usually defined between $0 < \kappa < 1$. The transition from the form with x to $\sin\phi$ is done using the substitution $x = \sin\phi$. For $\varphi = \pi/2$ all three expressions in equation (B.19) simplify to their associated *complete form*, thus

$$\mathsf{F}(\pi/2,\kappa) = \mathsf{K}(\kappa)\,, \qquad \mathsf{E}(\pi/2,\kappa) = \mathsf{E}(\kappa)\,, \qquad \text{and} \qquad \mathsf{P}(\pi/2,n,\kappa) = \mathsf{P}(n,\kappa)\,. \tag{B.20}$$

The reversed problem of (B.19) was studied by Jacobi and Abel, who defined the inverse functions

$$y = \sin(\phi) = \mathrm{sn}(\mathsf{F},\kappa) \qquad \text{and} \qquad \phi = \mathrm{am}(\mathsf{F},\kappa) \tag{B.21}$$

as *sine amplitude* F and *amplitude* F. Similarly, two other functions are derived as *cosine amplitude*

[2)] Elementary functions are algebraic, trigonometric, inverse trigonometric, logarithmic and exponential functions.

$y = \cos(\phi) = \mathrm{cn}(\mathsf{F}, \kappa)$ and *delta amplitude* $\sqrt{1 - \kappa^2 \sin^2(\phi)} = \mathrm{dn}(\mathsf{F}, \kappa)$, see [288,290] for details. The quotients and reciprocals of sn, cn and dn used in here follow Glaisher's notation [233]

$$\mathrm{ns} \equiv \frac{1}{\mathrm{sn}}, \qquad \mathrm{nc} \equiv \frac{1}{\mathrm{cn}}, \qquad \mathrm{nd} \equiv \frac{1}{\mathrm{dn}}, \tag{B.22a}$$

$$\mathrm{sc} \equiv \frac{\mathrm{sn}}{\mathrm{cn}}, \qquad \mathrm{cs} \equiv \frac{\mathrm{cn}}{\mathrm{sn}}, \qquad \mathrm{ds} \equiv \frac{\mathrm{dn}}{\mathrm{sn}}, \tag{B.22b}$$

$$\mathrm{sd} \equiv \frac{\mathrm{sn}}{\mathrm{dn}}, \qquad \mathrm{cd} \equiv \frac{\mathrm{cn}}{\mathrm{dn}}, \qquad \mathrm{dc} \equiv \frac{\mathrm{dn}}{\mathrm{cn}}, \tag{B.22c}$$

where all expressions have argument F and modulus κ. This gives in total twelve Jacobian elliptic functions.

Against common belief, the modulus κ must not necessarily lie between zero and one. All three integrals (B.19) are also defined for negative real and even complex-valued κ. However, various numerical software packages and general available algorithms are only capable of handling both, elliptic integrals and elliptic functions for $0 < \kappa < 1$. Typical examples include freely available routines [312,313] as well as commercially maintained programs, most notably MATLAB®, see [294], and algorithms given in [159]. Two applications which can be used to obtain results for (B.19) and (B.22) if $\kappa \in \mathbb{C}$ are MAPLE® [314] and MATHEMATICA® [289], with the latter one being extensively employed here.

It is usually possible to transform an elliptic function expression having a purely imaginary modulus $\mathrm{i}\,\kappa$ with $\kappa \in \mathbb{R}$ into an equivalent elliptic expression with real-valued modulus κ_1 [109, 288,290]. For the elliptic integral of the first-kind, repeatedly employed throughout this work, a suitable relation for such a modulus transformation is given as equation *(160.02)* in [288]

$$\mathsf{F}(\varphi, \mathrm{i}\kappa) = \kappa_1' \mathsf{F}(\beta, \kappa_1) \tag{B.23a}$$

where

$$\sin(\beta) = \left[\frac{\sqrt{1+\kappa^2}}{\sqrt{1+\kappa^2 \sin^2 \varphi}} \sin\varphi \right], \qquad \kappa_1 = \frac{\kappa}{\sqrt{1+\kappa^2}}, \qquad \kappa_1' = \sqrt{1-\kappa_1^2}. \tag{B.23b}$$

By setting $\varphi \equiv \pi/2$, which leads to $\beta = \pi/2$, the associated complete integral is derived as

$$\mathsf{K}(\mathrm{i}\kappa) = \kappa_1' \mathsf{K}(\kappa_1) \,. \tag{B.23c}$$

In fact, there are two transformations contained in (B.23). First, the factor $1 \leq \kappa < \infty$ of the imaginary unit $\mathrm{i} = \sqrt{-1}$ is changed into $0 \leq \kappa_1 < 1$. Secondly, the argument $\mathrm{i}\kappa_1$ is transformed into the real-valued κ_1 with the elliptic integral function being adjusted accordingly by multiplication with the complementary modulus κ_1'.

Unfortunately, for the more general case of a complex-valued modulus $\kappa_\mathrm{C} = \kappa_\mathrm{R} + \mathrm{i}\,\kappa_\mathrm{I}$ where $\kappa_\mathrm{R}, \kappa_\mathrm{I} \in \mathbb{R}$ no such transformation is possible and values for both elliptic integrals and Jacobian functions must be obtained using series approximation. Very few articles exist regarding the imple-

mentation of these approximations for elliptic integrals [315–317], but to the author's knowledge none were obtainable for Jacobian elliptic functions. Figure B.1 shows real and imaginary parts of the complex valued complete elliptic integral $\mathsf{K}(\kappa_\mathrm{C})$ whereas B.2 shows the real-valued complete integral for real and imaginary modulus κ and $\mathrm{i}\kappa$, respectively, according to (B.23c).

B.3.1 Addition formulas

Together with the addition formulas in [109, 288] the Jacobian sine function having the argument $x - \mathsf{K}(\kappa)$ is expressed as

$$\mathrm{sn}(x - \mathsf{K}(\kappa)\,, \kappa) = \mathrm{sn}(x - \mathsf{K}) = \frac{\mathrm{sn}(x)\,\mathrm{cn}(\mathsf{K})\,\mathrm{dn}(\mathsf{K}) - \mathrm{sn}(\mathsf{K})\,\mathrm{cn}(x)\,\mathrm{dn}(x)}{1 - \kappa^2\,\mathrm{sn}^2(x)\,\mathrm{sn}^2(\mathsf{K})} \tag{B.24a}$$

which simplifies using the special values $\mathrm{sn}(\mathsf{K}) = 1$, $\mathrm{cn}(\mathsf{K}) = 0$ and $\mathrm{dn}(\mathsf{K}) = \left(\kappa_1'\right)^2$ to

$$= \frac{-\,\mathrm{cn}(x)\,\mathrm{dn}(x)}{1 - \kappa^2\,\mathrm{sn}^2(x)} \tag{B.24b}$$

and the denominator together with $\mathrm{sn}^2(x) = 1 - \mathrm{cn}^2(x)$ and $\mathrm{dn}^2(x) - \kappa^2\,\mathrm{cn}^2(x) = \left(\kappa_1'\right)^2$ can be rewritten to yield

$$= \frac{\mathrm{cn}(x)}{\mathrm{dn}(x)} = -\,\mathrm{cd}(x)\,. \tag{B.24c}$$

A similar addition formula gives for the cosine function

$$\mathrm{cn}(x - \mathsf{K}(\kappa)\,, \kappa) = \sqrt{1 - \kappa^2}\;\mathrm{sd}(x, \kappa)\;. \tag{B.25}$$

B.3.2 Imaginary modulus transformation

For a purely imaginary modulus $\kappa_\mathrm{C} = \mathrm{i}\kappa$, $\kappa \in \mathbb{R}$ the following transformation formulas for the basic Jacobian functions can be given [288, 290]

$$\mathrm{sn}(x, \mathrm{i}\kappa) = \kappa_1'\,\mathrm{sd}\left(x\sqrt{1 + \kappa^2}, \kappa_1\right)\,, \qquad \mathrm{cn}(x, \mathrm{i}\kappa) = \mathrm{cd}\left(x\sqrt{1 + \kappa^2}, \kappa_1\right)\,, \tag{B.26a}$$

and

$$\mathrm{dn}(x, \mathrm{i}\kappa) = \mathrm{nd}\left(x\sqrt{1 + \kappa^2}, \kappa_1\right)\,, \tag{B.26b}$$

with κ_1 and κ_1' from (B.23b). This leads for the extended function sd from (B.22) to

$$\mathrm{sd}(x, \mathrm{i}\kappa) = \kappa_1'\,\frac{\mathrm{sd}}{\mathrm{nd}} = \kappa_1'\,\mathrm{sn}\left(x\sqrt{1 + \kappa^2}, \kappa_1\right)\,. \tag{B.27}$$

B.3.3 Derivatives

Differentiation of Jacobian functions is usually straightforward except for inverse problems. Important references are [109, 233, 288, 290, 292] which cover almost all possible cases. The trial function in (4.70) is not particular difficult but laborious. With

$$\frac{\mathrm{d}\ddot{\tilde{u}}(t)}{\mathrm{d}t} = \dddot{\tilde{u}}^{(1)} = \frac{A\,\nu\,\omega_\mathrm{J}}{\mathrm{sd}}\left(\sqrt{1-\kappa^2}\,\mathrm{sd}\right)^{\nu}\mathrm{cn}\,\mathrm{dn} = \frac{\varrho\,\omega_\mathrm{J}}{\mathrm{sd}}\,\mathrm{cn}\,\mathrm{dn} \tag{B.28a}$$

as the first derivative, where all Jacobian functions have argument $\omega_\mathrm{J}\,t$ and modulus κ, the second, third and fourth derivative of the approximate acceleration are given as

$$\ddot{\tilde{u}}^{(2)} = \frac{\varrho\,\omega_\mathrm{J}^2}{\mathrm{sd}^2\,\mathrm{dn}^4}\left[\left(\kappa^2\,\mathrm{sn}^2+\nu-1\right)\mathrm{cn}^2+\left(\kappa^2-1\right)\mathrm{sn}^2\right] \tag{B.28b}$$

$$\begin{aligned}\ddot{\tilde{u}}^{(3)} = \frac{\varrho\,\omega_\mathrm{J}^3\,\mathrm{cn}}{\mathrm{sn}^3\,\mathrm{dn}^3}\Big[&4\kappa^2\left(\kappa^2-1\right)\mathrm{sn}^4+(3\,\nu-2)\left(\kappa^2\,\mathrm{cn}^2+\kappa^2-1\right)\mathrm{sn}^2\\ &+(\nu-2)\,(\nu-1)\,\mathrm{cn}^2\Big],\end{aligned} \tag{B.28c}$$

$$\begin{aligned}\dddot{\tilde{u}}^{(4)} = \frac{\varrho\,\omega_\mathrm{J}^4\,\mathrm{cn}}{\mathrm{sn}^4\,\mathrm{dn}^4}\Big\{&\Big[\kappa^2\,(3\nu-2)\,\mathrm{sn}^4+2\,(\nu-1)(3\nu-4)\kappa^2\,\mathrm{sn}^2+(\nu-3)(\nu-2)(\nu-1)\Big]\mathrm{cn}^4\\ &+2\left(\kappa^2-1\right)\mathrm{sn}^2\left(2\kappa^4\,\mathrm{sn}^4+\kappa^2\,(11\,\nu-4)\,\mathrm{sn}^2+3\,\nu^2-7\,\nu+4\right)\mathrm{cn}^2\\ &+\left(\kappa^2-1\right)^2\mathrm{sn}^4\left(4\,\kappa^2\,\mathrm{sn}^2+3\,\nu-2\right)\Big\},\end{aligned} \tag{B.28d}$$

respectively.

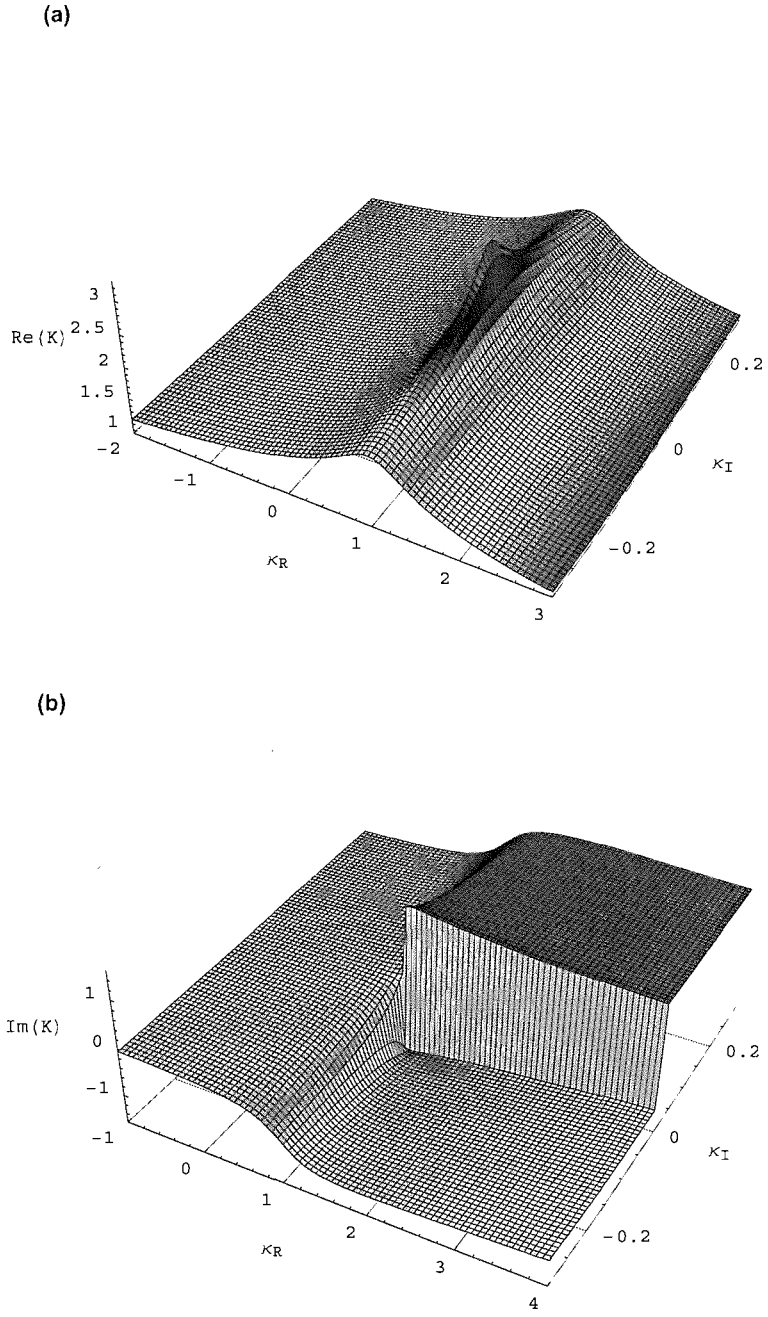

Figure B.1 – Complete elliptic integral of the first kind with complex modulus: $\mathsf{K}(\kappa_{\mathrm{R}} + \mathrm{i}\,\kappa_{\mathrm{I}})$. **(a)** Real part, **(b)** imaginary part.

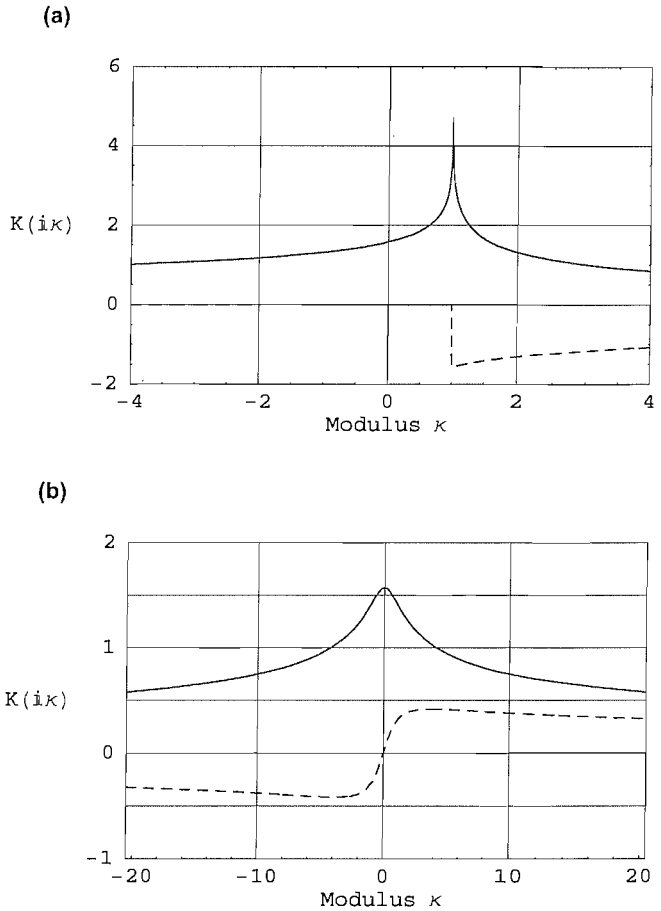

Figure B.2 – Real-valued complete elliptic integral of the first kind for real and imaginary modulus. **(a)** $\mathsf{K}(\kappa)$, **(b)** $\mathsf{K}(\mathrm{i}\kappa)$.

APPENDIX C

DIFFERENTIAL TRANSFORMATION METHODS

C.1 Taylor Differential Transformation

If $x(t)$ is an analytical function in the time domain interval $I_T = [T_0,\ T_1]$, then it will be continuously differentiable with respect to t

$$\frac{\partial^k x(t)}{\partial t^k} = \vartheta(t,k) \qquad \forall \quad t \in I_T \tag{C.1a}$$

for all $t \equiv t_i$ with $i = 1, 2, ..., \infty$, thus $\vartheta(t,k) = \vartheta(t_i,k)$, where k belongs to a set of nonnegative integers, denoted as the K domain [213]

$$K = \{k \in \mathbb{N} : 0 \leq k \leq \infty\}\ . \tag{C.1b}$$

Defining the spectrum [208]

$$X(k) = M(k)\left[\frac{\partial^k\, q(t)x(t)}{\partial t^k}\right]_{t=t_0} \tag{C.1c}$$

makes is possible to express $x(t)$ as an exact analytical series at the point t_0

$$x(t) = \frac{1}{q(t)}\sum_{k=0}^{\infty}\frac{(t-t_0)^k}{k!}\frac{X(k)}{M(k)}\,, \qquad q(t) \neq 0,\ M(k) \neq 0\,, \tag{C.1d}$$

where $q(t)$ is the kernel corresponding to $x(t)$ and $M(k)$ takes the role of a weighting factor [214]. For the purpose the differential transformation is used in this thesis both parameters are set to $q(t) \equiv 1$ and $M(k) \equiv H^k/k!$, respectively, with H designating the upper bound of the time interval of interest $[t_0, t_0 + H]$. Combining (C.1c) and (C.1d) gives the inverse transformation from

Table C.1 – Basic differential transformation relations between the two domains if spectra definitions according to (C.2) are used [213].

Original function $g(t)$	Transformed function $G(k) = \mathcal{D}\{g(t)\}$
1	$\delta(k) = \begin{cases} 1 & \text{if} \quad k = 0 \\ 0 & \text{if} \quad k \neq 0 \end{cases}$
t	$\delta(k-1)$
t^r	$\delta(k-r), \qquad r \in \mathbb{Z}$
$x(t) \pm y(t)$	$X(k) \pm Y(k)$
$ax(t)$	$aX(k)$
$x(t)\,y(t)$	$X(k) \otimes Y(k) = \sum_{l=0}^{k} X(l)\,Y(k-l)$
$\frac{x(t)}{y(t)}$	$\frac{X(k)-X(k)\otimes Y(k)}{Y(0)} = \frac{X(k)-\sum_{l=0}^{k} X(l)\,Y(k-l)}{Y(0)}$
$\frac{\mathrm{d}^\nu x(t)}{\mathrm{d}t^\nu}$	$\frac{(k+\nu)!}{k!}\,X(k+\nu)$
$\mathrm{e}^{\alpha t}$	$\frac{\alpha^k}{k!}$

the K-domain back into the domain of the original problem[1)]

$$x(t) = \sum_{k=0}^{\infty} \frac{1}{k!} \left[\frac{\partial^k x(t)}{\partial t^k}\right]_{t=t_0} (t-t_0)^k = \sum_{k=0}^{\infty} X(k)\,(t-t_0)^k \;\equiv\; \mathcal{D}^{-1}\{X(k)\} \tag{C.2a}$$

with a modified spectra from (C.1c)

$$X(k) = \frac{1}{k!} \left[\frac{\partial^k x(t)}{\partial t^k}\right]_{t=t_0} \;\equiv\; \mathcal{D}\{x(t)\}\;. \tag{C.2b}$$

The unknown function $x(t)$ can then be obtained as finite-term Taylor series approximation

$$x(t) = \sum_{k=0}^{N} X(k)\,(t-t_0)^k + R_{\mathrm{DT}}(t)\,, \tag{C.3}$$

where the number of terms N is sufficiently large so that the reminder $R_{\mathrm{DT}}(t)$ of order $N+1$ can be neglected, thus $R_{\mathrm{DT}}(t) \approx 0$. Table C.1 lists the fundamental relations between the domain of the differential problem and spectral domain K.

For most practical applications the interval $[t_0, t_0 + H]$ is not necessarily small and a satisfying approximation around the point t_0 for the entire interval requires a large value for N in (C.3). It is computational more effective [222–225][2)] to split the entire domain $I_T = [t_0, t_0 + H]$ into n

[1)]It is easy to see that Taylor differential transformation is not limited to problems in the time domain. The independent variable of the original differential problem can belong to any domain. Examples for space descritisation are given in [209, 210, 219].

[2)]For highly transient response behaviour as exhibited by a shock excited system, the base polynomial transforma-

sub-intervals as shown in figure C.1. For all time t in every interval $I_T(i)$

$$t \subset I_T(i) = \left[t_0 + \sum_{j=0}^{i-1} h_j,\ t_0 + \sum_{j=0}^{i} h_j \right] \qquad \text{with} \qquad i, j = 1, 2, 3, \ldots, n \tag{C.4a}$$

there exists a solution $x_i(t_i) \subset x(t)$ for every interval $h_i = t_i - t_{i-1}$

$$x(t) \simeq x_i(t_i) = \sum_{k=0}^{N} (t - t_i)^k X_i(k) \qquad \text{where} \qquad t = I_T(i)\,. \tag{C.4b}$$

The end conditions of the actual i interval are the initial conditions of the $i+1$ time interval with $t_i \leq t \leq t_{i+1}$

$$x_{i+1}\left(t \equiv t_i\right) = x_i\left(h_i\right) = \sum_{k=0}^{N} h_i^k X_i(k)\,. \tag{C.4c}$$

The overall solution function $x(t)$ for the entire interval $I_T = [t_0, t_0 + H]$ is an ordered set of all sequentially obtained $x_i\left(t_i\right)$ such that

$$x(t) = \left\{ x_1\left(t_1\right), x_2\left(t_2\right), \ldots, x_i\left(t_i\right), \ldots, x_n\left(t_n\right)\ ;\ i \in \mathbb{N} \right\}\,. \tag{C.4d}$$

Instead of defining a fixed time step h_i, accuracy and speed of the method can be both significantly increased by introducing adaptive stepping techniques. Several different implementations for various numerical time-stepping schemes such as Runge-Kutta or Adam-Bashford algorithms exist [156, 318–320], all using the same approach of keeping the local error in each time step below permissible bounds and thus minimising the global error of the entire computation. Although in general the global error of a numerical method cannot be determined [159, 304], both local and global errors are strongly related to each other [321]. Following Jang *et al* [218], Chen *et al* [215] and introducing an ideal difference equation

$$g_{i+1}\left(t_{i+1}\right) = g_i\left(t_i\right) + h_i\, \Phi\left(t_i, g_i, h_i\right) \tag{C.5}$$

where g_i is the approximation of the unknown function $g(t)$ in the i-th time interval, h_i is the step size and $\Phi\left(t_i, g_i, h_i\right)$ is an increment function solely defined in terms of t_i, g_i and h_i and has the property that for any given tolerance $\epsilon > 0$ a minimum value for h_i is used ensuring the global error does not exceed ϵ. In order to expand the idea of [215, 218] it is now assumed that both g and x_i are vector functions with m elements. Thus,

$$\mathbf{g}_i\left(t_i\right) = \left\{ g_{i,1} \quad g_{i,2} \quad \ldots \quad g_{i,l} \quad \ldots \quad g_{i,m} \right\}^{\mathrm{T}}, \mathbf{x}_i\left(t_i\right) = \left\{ x_{i,1} \quad x_{i,2} \quad \ldots \quad x_{i,l} \quad \ldots \quad x_{i,m} \right\}^{\mathrm{T}}, \tag{C.6}$$

tion suggested by Golovin and Stoukatch [223] does not yield significant improvement and is certainly not worth the additional computational effort. However, for rather slowly varying systems the method works well.

leading to

$$\max_{0\leq i\leq n} \|\mathbf{x}_i - \mathbf{g}_i\| < \epsilon\,. \tag{C.7}$$

where $n \in \mathbb{N}$ from equation (C.4a) stands for the number of time domain sub-intervals. It is well known from the error estimation of the Taylor method that under suitable differentiability conditions the method of order p has local error $O\left(h_i^{p+1}\right)$ and global error $O\left(h_i^{p}\right)$ [76, 322]. With two separate differential transformations of $\mathbf{x}_i$ only distinguished by their approximation error

$$\mathbf{x}_{i+1}\left(t_{i+1}\right) = \mathbf{x}_i\left(t_i\right) + h_i\,\mathbf{\Phi}\left(t_i, \mathbf{x}_i, h_i\right) + O\left(h_i^r\right)\,, \qquad \text{with} \quad r = \begin{cases} p+1, \\ p+q+1 \end{cases} \tag{C.8}$$

two inequalities can be formulated

$$\left\| \mathbf{x}_i\left(t_i\right) - \mathbf{g}_i\left(t_i\right) \right\| \leq Q_p\, h_i^{p+1}\,, \quad \text{and} \quad \left\| \mathbf{x}_i\left(t_i\right) - \mathbf{g}_i\left(t_i\right) \right\| \leq Q_{pq}\, h_i^{p+q+1}\,, \tag{C.9}$$

depending on whether $r = p+1$ or $r = p+q+1$, respectively. Both equations in (C.9) are satisfied for all relevant time steps h_i^r but only specific values of $Q_{p/qp}$. Expressing the factor Q_p as function of the truncation error resulting from the $p+q+1$ approximation and the exact approximate solution $\mathbf{g}_i$ gives the result of [218] generalised to a system of functions

$$h_{i,\mathrm{cr}} < \left[\frac{\epsilon}{\max_{1\leq l\leq m} \left\| \sum_{s=1}^{W} \mathbf{X}_i(N+s)\, h_i^{s-1} \right\|} \right]^{\frac{1}{N}} \tag{C.10}$$

where $\mathbf{X}_i(k)$ is the K-domain spectrum vector of the continuous-time vector function $\mathbf{x}_i\left(t_i\right)$ at the i-th subinterval. Although satisfactory results can be obtained by setting the arbitrary constant $W \equiv 1$, see [217, 218], the iteration process for finding the critical time step $h_{i,\mathrm{cr}}$ it is computational more efficient if

$$W > \frac{N}{10}\,, \qquad W \in \mathbb{N}\,. \tag{C.11}$$

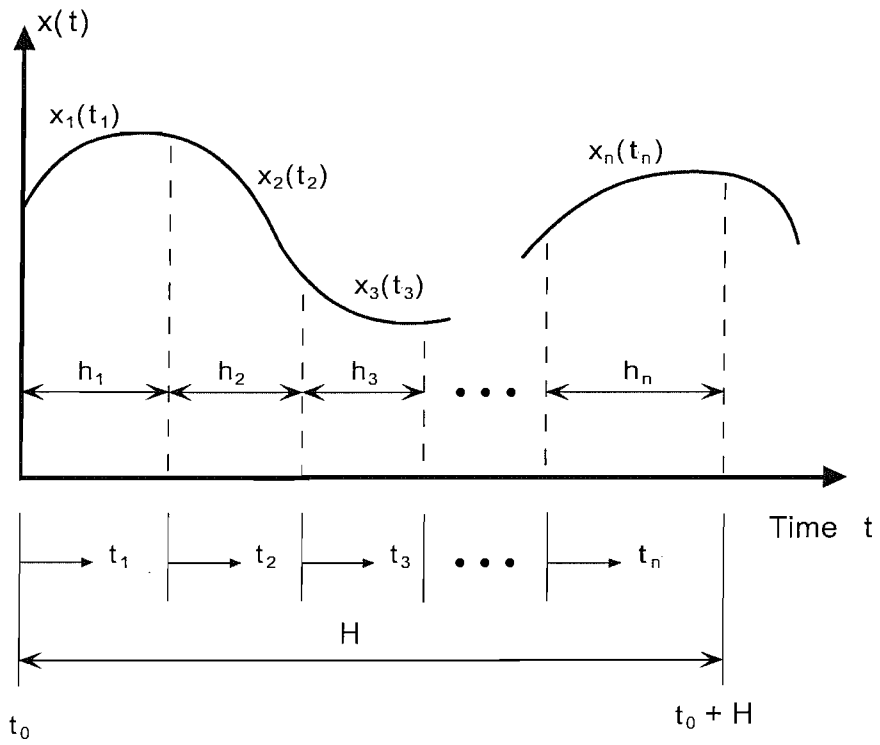

Figure C.1 – Subintervals of time domain H.